IDENTIFICATION OF MRSA-SPECIFIC PEPTIDES AND EXPRESSION OF PEPTIDE CONTAINING RECOMBINANT PROTEINS FOR TARGETED PHOTODYNAMIC THERAPY

THESIS SUBMITTED FOR THE DEGREE OF DOCTOR OF PHILOSOPHY

Rebecca Vince, BSc

Biological Sciences,
University of Hull,
September 2009

DECLARATION

I declare that the content of this thesis have not been submitted in whole or part for any other academic award at the University of Hull or any other institution.

Rebecca Vince,
September 2009

ACKNOWLEDGEMENTS

Firstly I would like to thank my supervisor Professor John Greenman for all of his continued help and support throughout the duration of my PhD. I would also like to thank Dr Tim Paget for all of his valuable assistance and useful conversations and additionally Smith & Nephew for financial support, in particular to Dr Martin Todman. I would also like to express my deep gratitude to Dr Leigh Madden for constant technical advice, laboratory support and wisdom. Also, many thanks to all members of the MRL, BRL and Biological Sciences, past and present who have made my experience thoroughly enjoyable.

Thanks also, to Rhonda Green, for careful proofreading of the manuscript and good advice over the past years. Also many thanks to Cath Wadforth for letting me 'borrow' numerous things over the years and suggesting the 'One shot', without which I may never have made my protein!

Additionally, I would also like to thank Huguette Savoie for keratinocyte cell line maintenance and cytotoxicity assays. Additional thanks to Dr Ross Boyle for lots of useful advice and Dr Cristina Alonso for providing the porphyrin, thank you all in the Chemistry department for always being so friendly. Thanks also to Dr Bill Hutchinson for DNA sequencing advice and Dr Frank Voncken for providing a competent cell line.

Finally, eternal thanks to my family, Mum, Dad and Carly, whose constant support and belief in me has always helped me to achieve my goals.

PRESENTATIONS IN SUPPORT OF THIS THESIS

Vince, RV, Todman, M, Greenman, J and Paget, T. Identification of peptides which bind to MRSA. 2007. Immunology 120 (Suppl. 1) p75.

Vince, RV, Paget, T, Todman, M and Greenman J. Identification of novel peptides from a random display library for bacterial targeting. 2008. Society for General Microbiology Annual Meeting Abstract Booklet, p76.

For Mum and Dad

ABSTRACT

Staphylococcus aureus (*S. aureus*) is an opportunistic pathogen capable of causing infection at multiple sites and is one of the predominant organisms found in chronic wounds, such as venous ulcers. Furthermore, there is an ever-increasing prevalence of multi-drug resistant strains, such as methicillin-resistant *S. aureus* (MRSA) that can contribute to the non-healing and infection of wounds as well as other life-threatening complications. The increase in bacterial resistance necessitates the development of alternative modes of bacterial targeting and elimination whilst avoiding collateral damage to host cells and commensal bacteria. One such modality is photodynamic therapy (PDT), whereby the activation of a photosensitiser by light in the presence of oxygen produces reactive oxygen species to elicit bacterial cell death. PDT has previously been shown to be effective against a wide range of Gram-positive and Gram-negative bacteria and furthermore selective targeting of the photosensitiser directly to the pathogenic bacteria is likely to improve the efficacy of this treatment.

The FliTrx™ bacterially-displayed random peptide library (Invitrogen), displaying 12-mer peptides in a conformationally constrained manner on the surface of *E. coli* was screened by panning against UV-inactivated MRSA. Panning was also performed against *S. aureus* and *S. epidermidis* in a similar manner. Clones (n = 20) were then randomly selected, DNA sequenced and peptide sequences analysed. No obvious consensus sequence or repeat sequences were observed. Two peptides selected from panning against MRSA were commercially synthesised (peptide19 and peptide12) as both cyclic and linear constructs with N-terminal biotin for characterisation of binding by flow cytometry. Furthermore, one peptide (peptide12) was synthesised as both a cyclic and linear construct replacing the biotin with C-terminal FITC for direct characterisation of peptide binding by flow cytometry. Binding of the cyclic construct was observed against 3 different strains of MRSA, with the greatest binding observed against the strain of MRSA originally panned against. No binding of the linear construct was observed. Low/no reactivity was observed with other *Staphylococcal* sp, Gram-negative bacteria and a mammalian cell line demonstrating apparent specificity for MRSA.

Peptide sequences of interest were also cloned in-frame, situated within the full length thioredoxin sequence, so as to reflect the original display format, into an *E. coli* based

expression vector. Recombinant protein expression was optimised and the protein extracted, purified and characterised by Western blotting. The porphyrin photosensitiser (5-(4-isothiocyanatophenyl)-10,15,20-tris-(4-*N*-methylpyridiniumyl) porphyrin trichloride) was conjugated to recombinant protein P12 at a molar ratio of 5:1 and the *in vitro* cytotoxic effect of the resulting bioconjugate was determined against MRSA, *E. coli* and keratinocytes. Pilot data demonstrated a 66% reduction in MRSA growth following incubation and irradiation with the bioconjugate in comparison to non-irradiated control cells. The conjugated porphyrin gave higher levels of cytotoxicity than equivalent concentrations of unconjugated capped porphyrin. No toxicity of the conjugate or the capped porphyrin against MRSA was observed when light of the correct wavelength was not given. Additionally no/little cytotoxic effect against *E. coli* or mammalian keratinocytes was observed.

Additionally, binding of two other purified recombinant proteins (P5 and P19) to MRSA, *E. coli* and keratinocytes was assessed by flow cytometry. Both recombinant proteins were observed to bind MRSA in comparison to *E. coli* and keratinocytes. Furthermore, one sequence (P5) was expressed as an additional GFP fusion protein construct to allow direct characterisation of recombinant protein binding. A very small increase in binding was observed with an increasing concentration of recombinant protein against MRSA, *E. coli* and keratinocytes.

In summary, this thesis has described a system to isolate and characterise novel peptides with binding specificity against MRSA. Furthermore, it has demonstrated the feasibility of expressing recombinant proteins and conjugation to a porphyrin photosensitiser for targeted PDT against pathogenic bacteria whilst limiting damage to the host, providing an alternative to antibody-based targeting in microbiology.

T**ABLE OF CONTENTS**

LIST OF FIGURES

CHAPTER FOUR

CHAPTER FIVE

LIST OF TABLES

ARREVIATIONS

aTc	anhydrotetracycline
CA-MRSA	community-acquired methicillin resistant *Staphylococcus aureus*
CGPC	Cys-Gly-Pro-Cys
EMRSA	epidemic methicillin resistant *Staphylococcus aureus*
FACS	fluorescence activated cell sorting
FBS	foetal bovine serum
FITC	fluorescein isothiocyanate
FliC	flagella filament protein
*fli*C	flagellin gene
GFP	green fluorescent protein
HA-MRSA	hospital-acquired methicillin resistant *Staphylococcus aureus*
HRP	horse radish peroxidase
IMAC	immobilised metal affinity chromatography
MF	mean fluorescence
MRSA	methicillin resistant *Staphylococcus aureus*
MRSE	methicillin resistant *Staphylococcus epidermidis*
MSCRAMMs	microbial surface components recognising adhesive matrix molecules
MSSA	methicillin sensitive *Staphylococcus aureus*
NAG	N-acetylglucosamine
NAM	N-acetyl muramic acid
NCS	reactive isothiocyanate group
OMP	outer membrane proteins
PBP	penicillin-binding protein
PCR	polymerase chain reaction
PDT	photodynamic therapy
PI	propidium iodide
ROS	reactive oxygen species

S.N.A.P. ™	simple nucleic acid prep
SAP	shrimp-alkaline phosphatase
SCC*mec*	staphylococcal cassette chromosome
TSST-1	toxic shock syndrome toxin
VISA	vancomycin intermediate *Staphylococcus aureus*
VRE	vancomycin resistant *Enterococci*
VRSA	vancomycin resistant *Staphylococcus aureus*

CHAPTER ONE
Introduction

1.2 General introduction

The increasing prevalence of bacterial resistance has led to new alternative methods of bacterial elimination to be required. The majority of wounds are contaminated and/or colonised with bacteria (Filius and Gyssens, 2002), although these do not always illicit a host response (e.g. inflammation) or impede wound healing. However, microbial 'critical colonisation' describes a condition whereby bacteria multiply and adversely affect the healing of the wound in the absence of an immune response (White and Cutting, 2006). This condition can be an important factor for the invasion and proliferation of potentially pathogenic organisms that can have a major impact on the infection and non-healing of the wound.

Within chronic wounds the normal response to wound healing is altered and can result in prolonged inflammation, abnormal wound matrix and deficient regeneration of epithelial cells and remodelling (Herrick et al., 1992). In addition these chronic wounds such as venous, arterial and diabetic foot ulcers that are infected with resistant organisms can be frequently more difficult to treat, resulting in increased cost, prolonged treatment and increased trauma to the patient.

Peptide display technology may represent an alternative modality for identification of ligands with potential pathogen specific targeting and diagnostic properties that could be utilised in the treatment of chronic wounds whilst minimising damage to surrounding host tissue. In this thesis, venous ulcers will be used as a wound model to discuss the potential utility of novel peptide targeting strategies for the treatment of chronic wounds. This wound model was utilised because approximately 70% of ulcers are of venous origin and also due to the prevalence, which is an estimated 1% at some point in the lifetime of the adult population in developed countries that increases with age (O'Meara et al., 2008). MRSA was used as a target organism due to its increased prevalence within chronic wounds (Valencia et al., 2004) and also the threat of increasing resistance to 'last line of defence' antibiotics, such as vancomycin, has led to an urgent need for new strategies of MRSA targeting and elimination.

1.2.1 Venous ulcers

Venous ulcers are common chronic wounds that arise due to venous insufficiency, often occurring due to obstruction or valve incompetence. The resulting congestion causes venous hypertension and leakage of fluid from blood vessels into the extravascular space, resulting in oedema (Bjarnsholt et al., 2008). The decreased tissue perfusion results in impeded transportation of oxygen and nutrients resulting in ischaemic damage and build up of waste products. Not only is the prevalence of venous ulcers high, but venous ulcers are often recurrent and are therefore costly to the patient in terms of immobility, pain and distress but are also a financial burden on the NHS. The estimated cost of treatment is approximately £400 million per year, or 1-2% of total health care costs (Ruckley, 1997).

1.1.2 Microorganisms associated with venous ulcers

Venous ulcers are good examples of a chronic wound that is frequently of a polymicrobial nature. Of the diverse bacteria isolated, *S. aureus* is the predominant organism isolated in numerous studies investigating the bacteriology of venous ulcers (Gjodsbol et al., 2006, Lim et al., 2006, Valencia et al., 2004, Bowler and Davies, 1999, Brook and Frazier, 1998, Halbert et al., 1992). Additional aerobic bacteria frequently associated include *Pseudomonas* sp, *Streptococci*, coagulase-negative *Staphylococci*, *Enterobacteriaceae*, *Proteus* sp and *Enterococci* (Gjodsbol et al., 2006, Brook and Frazier, 1998) indicating the diverse aerobic ecology within the wound. However, it is not surprising that these organisms frequently feature, as *S. aureus* is carried innocuously by approximately 30% of the population and many other organisms frequently isolated contribute to the normal cutaneous/oral flora, nasal passages or mucous membranes without clinical consequence, although have pathogenic potential to cause infection within a wound environment.

The wound environment usually presents a combination of aerobic and anaerobic species. Anaerobes commonly found within the wound environment include *Peptostreptococcus* sp, *Propionibacterium* sp, *Bacteriodes* sp, and pigmented and non-pigmented *Provotella* sp, presumably of cutaneous origin, or as part of the normal faecal or oral flora that may also impact on wound healing (Stephens et al., 2003, Bowler and Davies, 1999, Brook and Frazier, 1998). For example, Bowler and Davies

(1999) isolated a significantly greater mean number and higher proportion of anaerobic bacteria from infected leg ulcers when compared with uninfected wounds, suggesting that anaerobes are potentially key factors involved in pathogenesis of infection. However, although anaerobes commonly feature, and may be detrimental to wound healing, they are frequently overlooked in a wound management setting probably due to lengthy culture and isolation time, and increased expense.

Due to the diverse microbiology of venous ulcers, investigations into the bacteriology are conflicting not only in species identification but also in the varying number of species isolated within the wound. For example, Brook and Frazier (1998) demonstrated the presence of between 1 and 5 bacterial isolates with approximately 25% presenting only a single organism isolated from 43 samples derived from 41 patients. This is in contrast to Gjodsbol et al (2006) who analysed 342 samples derived from 46 patients, detecting more than one bacterial species in all chronic ulcers with a mean number of 6.3 species per wound, which is likely to be an underestimate as all anaerobes were represented as a single species. In addition, resident colonising species (i.e. bacterial species present in all or all but one sample taken over the 8 week duration) were found in all 46 ulcers, most commonly *S. aureus* (n = 32) and *P. aeruginosa* (n = 17). The differences in number of bacterial species isolated in these studies may be due to different patient cohorts with different exclusion criteria, but moreover is likely to be due to the different methodologies of sampling and processing; with particular reference to anaerobic species, and also the infection status of the ulcer and duration of the studies. Methods of sampling of wounds with swabs or biopsies to determine the bacteriology of chronic wounds also remains debatable as such methods may not cause a representative spread of organisms capable of causing infection to be isolated. For example, Stephens et al (2003) isolated bacterial species from surface swabs compared with deep tissue biopsies from 18 patients with non-infected refractory chronic venous ulcers of at least 24 months duration that were resistant to conventional treatment. The study found that although many bacterial species detected on the swab were also present in the biopsy, a greater number of bacterial strains were isolated from the deep tissue biopsies and suggested that the presence of Gram-positive anaerobes such as *Peptostreptococci* may impair cell-mediated wound healing in *in vitro* assays (Stephens et al., 2003). Therefore tissue biopsies may provide a greater insight into the presence of

bacteria especially the presence of anaerobes, that routine diagnostic techniques would have overlooked (Stephens et al., 2003).

Lim et al (2006) demonstrated that although bacteria isolated from swab and punch biopsies of chronic lower limb ulcers from 39 patients (20 were of venous origin) were often in agreement (46%), 28% showed no similarity between the bacterial species isolated. Additionally, when analysing the microbiology of chronic ulcers this group advocated taking biopsies instead of swabs due to increased sensitivity and specificity and also to rule out ulcer malignancy by histopathology. However, Bjarnsholt et al (2008) indicated that bacteria within the wound can exist as a biofilm in infected wounds, unevenly distributed in microcolonies, and therefore a swab or biopsy may not accurately depict the total bacterial load within the wound. Nonetheless, although difficulties with bacterial sampling exist, it is worth noting that the majority of sources of bacterial wound contaminants are endogenous to the host and therefore those found on devitalised sloughy superficial tissue will also comprise those that have disseminated deeper into tissue and more likely associated with infection (Bowler and Davies, 1999).

Furthermore, owing to the increased prevalence of bacterial resistance, there is an increased risk of chronic wounds becoming infected with resistant organisms, in particular with methicillin-resistant *S. aureus* (MRSA). A study evaluating the microbiology of leg ulcers over a decade, of which the majority (29/72; 40%) were of venous origin, found that *S. aureus* was isolated in 67% of isolates from leg ulcers of which three quarters were MRSA in 2001, an increase from 50% in 1996 and 26% in 1992 (Valencia et al., 2004). Additionally, this study also highlighted the increasing trend in quinolone-resistant *P. aeruginosa* isolates from leg ulcers: this increased from 19% in 1992, to 36% in 1996 and 56% in 2001, a further reason for concern over bacterial resistance.

It seems apparent that difficulties arise in comparative assessment of bacteria involved in venous ulcers. Although single or multiple species may colonise the wound, it is not necessarily indicative of infection and furthermore the presence of specific strains of bacteria within infected ulcers may not necessary be contributing to the infected phenotype. Nonetheless, colonised bacteria remain in the wound and colonisation of potentially pathogenic bacteria is an essential factor in invasion and the progression to

infection, and therefore knowledge of the microbiology of the wound may assist future treatment options. Additionally, determination of the presence of drug resistant pathogens is also crucial to deliver optimal treatment regimens.

1.1.3 Impact of organisms on wound healing

The significance of specific organisms within the wound and their adverse effect on wound healing has been subject to much debate. Although little attention has been paid to anaerobic organisms, various groups have suggested that *S. aureus, P. aeruginosa,* and beta-haemolytic *Streptococci* within the wound are associated with delayed healing and infection (Gjodsbol et al., 2006, Danielsen et al., 1998, Madsen et al., 1996, Halbert et al., 1992, Schraibman, 1990). However although *S. aureus* is a common isolate associated with persistent colonisation and/or infection within the wound, Bowler and Davies (1999) failed to show a clear correlation between the presence of facultative pathogens such as *S. aureus* and *P. aeruginosa* and wound infection. This group instead suggested that the significant diversity of bacteria and presence of anaerobes, particularly in infected ulcers, and aerobic/anaerobic synergy as of potentially greater clinical significance impacting on wound healing. For example, wounds are often hypoxic environments as a result of tissue necrosis and the oxygen consumption/metabolism by host cells, and as such aerobic bacteria provide an ideal environment for the proliferation and virulence of anaerobic microorganisms (Bowler et al., 2001).

In addition, Trengove et al (1996) demonstrated that no single or group of causative species, including aerobes and anaerobes, were detrimental to wound healing. These researchers suggested that it was the presence of 4 or more bacterial species in combination which was associated with delayed healing, therefore indicating that microbial synergy may induce a greater pathogenic potential. For example, the production of essential growth factors by specific bacteria, which are often unidentified, can enable growth of more fastidious organisms that may enable enhanced virulence and increased pathogenicity of bacteria within the wound (Bowler et al., 2001, Bowler and Davies, 1999). Additionally, a critical microbial load, greater than 10^5 bacteria per gram of tissue, has also been cited as a potential cause of infection and non-healing (Howell-Jones et al., 2005, Halbert et al., 1992).

As has been mentioned previously, bacteria can survive within wounds as biofilms. These are complex structures consisting of aggregations of bacteria growing on a solid surface. In addition to bacterial synergy, the polymicrobial nature of the wound milieu can also enhance genetic exchange between bacteria, further contributing to the increasing problem of bacterial resistance (Howell-Jones et al., 2005). The formation of biofilms and bacterial synergy can offer some bacterial protection from the host immune response and can also offer bacterial protection from antimicrobial therapy, contributing to non-healing of the wound (Stephens et al., 2003, Wall et al., 2002). The reduced susceptibility of bacteria in biofilms to antimicrobials requires higher concentrations of these drugs in order to treat bacteria present in biofilms (Dissemond, 2009, Reichenberg and Davis, 2005, Anwar et al., 1990).

In summary, chronic wounds are complex in nature and the impact on wound healing and infection is likely to be multifaceted involving the bacteria, their virulence determinants and the host response. The potential microbial factors that, either independently or collectively, can contribute to non healing/wound infection are summarised in Figure 1.1. The effect of wound infection and non-healing may result in prolonged incapacity and increased trauma to the patient which can impact on quality of life. Additionally, the presence of resistant pathogens may result in infections that are difficult to treat resulting in longer hospital stays, increased patient distress and greater risk of colonisation and transmission. Therefore prompt identification and effective appropriate treatment is imperative.

1.1.4 Treatment of venous ulcers

Venous ulcers pose an increasing problem in the Industrialised World owing to an ageing population, an increase in obesity and related diseases such as diabetes, venous hypertension, cardiovascular disease and an increase in the immunocompromised population (e.g. AIDS or cancer therapy) all lead to a larger patient group susceptible to the development of chronic wounds (Bjarnsholt et al., 2008, Bowler et al., 2001). Compression bandages or stockings are the mainstay of treatment in the treatment of venous ulcers to increase blood flow by reducing venous stasis and oedema. Additionally, debridement which involves the removal of devitalised or contaminated tissue to expose healthier tissue achieved either through surgical, mechanical, autolytic

or enzymatic methods can enhance wound closure. Debridement can be of particular benefit in the treatment of venous ulcers to remove damaged tissue, as bacteria favour growth on necrotic tissue, and furthermore may aid physical removal of biofilms that affect the utility of topical or systemic antibiotic therapy (Reichenberg and Davis, 2005). Additionally, the application of 'maggot therapy', an alternative but not new form of debridement overlooked due to the development of antibiotics, has also proved successful in the management of chronic wounds and has been demonstrated to show antimicrobial activity in the treatment of MRSA-infected wounds (Nigam et al., 2006).

Broad-spectrum systemic and topical antimicrobial agents and antiseptics to reduce microbial load are frequently used in the management of chronic wounds and are essential in the management of infected wounds (Howell-Jones et al., 2005, Bowler et al., 2001). Empirical broad-spectrum treatment, prior to organism identification and sensitivity testing, includes the use of penicillin, macrolide and quinolone antibiotics (Grey et al., 2006). However, various groups have highlighted the possible clinical and cost ineffectiveness in the treatment of non-healing venous ulcers without infection with antimicrobials; supporting antimicrobial therapy only when there are clinical signs or symptoms of infection (Howell-Jones et al., 2005, Bowler et al., 2001, Kac et al., 2000). Administration of antimicrobials should take into account the presence of aerobes, anaerobes and drug resistant bacterial species to ensure the correct targeting of pathogens. In addition to appropriate antimicrobial prescribing practices, good infection control procedures (handwashing, gloves, gowns, cleaning, use of disposable devices), screening for colonised patients/staff, patient isolation/decontamination, education and rapid detection should all be employed to reduce the risk of bacterial transmission as many pathogenic bacteria are easily spread through either infection or colonisation reservoirs (Valencia et al., 2004, Kac et al., 2000, Carbon, 1999).

The impact of infection, particularly with resistant organisms, may result in an increase in morbidity, mortality and cost to both the healthcare system and trauma to the patient. It is therefore essential that new methods of appropriate detection and elimination of bacteria for treatment of venous ulcers and other chronic wounds that avoid the advancement of bacterial resistance are developed to enable more effective wound healing. Current alternative treatment strategies in development have explored the use of new antimicrobial therapies such as bactericidal antimicrobial peptides, hyperbaric

oxygen therapy or photodynamic therapy (PDT) to target and kill bacterial pathogens (reviewed later in the chapter section 1.5).

1.2 *Staphylococcus aureus*

S. aureus is a Gram-positive spherical bacterium, often considered an opportunistic pathogen. This bacterium is a frequent cause of superficial and serious skin and soft tissue infections such as infected ulcers, cellulitis, furuncles and impetigo, but can invade surgical and other wounds and cause bone and joint infections through contamination in orthopaedic surgery (Livermore, 2000). These bacteria are facultative anaerobes that grow rapidly by aerobic respiration or by fermentation. They are non-motile, non-spore forming and although considered potential human pathogens can also comprise part of the normal bacterial flora without detriment in healthy humans.

1.2.1 Cell wall structure and virulence factors

The cell wall of *S. aureus* is composed mainly of peptidoglycan (up to 90% dry weight of Gram-positive bacteria) that is approximately 15 to 30 nm thick. Peptidoglycan is a continuous polymer that confers shape and rigidity to the cell providing protection from the environment and preventing osmotic lysis. It is composed of interlocking glycan chains of alternate monomers N-acetylglucosamine (NAG) and N-acetyl muramic acid (NAM) cross-linked by pentapeptide bridges from the NAM composed of L-Ala-D-Gln-L-Lys-D-ala-D-ala (Fig 1.2). Additionally to peptidoglycan, the bacterial cell wall is composed of covalently bound teichoic, teichuronic and lipoteichoic acid associated with the cell membrane to provide rigidity, and wall-associated surface proteins to promote attachment to the host (Fig 1.3).

Aside from resistance determinants, *S. aureus* possesses a number of virulence factors, many of which are not possessed, or only produced in small amounts by coagulase-negative *Staphylococci* such as *S. epidermidis*, a common skin commensal, and may help to explain the enhanced virulence and capacity for infection. Virulence determinants of *S. aureus* are summarised in Fig 1.4. Adhesion of pathogenic bacteria to host tissues is an essential step in bacterial colonisation and the initiation of infectious disease and an important part of pathogenesis. Bacteria need to adhere to epithelial

surfaces in order to colonise tissue and avoid the clearing defence mechanisms of the host (Westerlund-Wikstrom et al., 1997). *S. aureus*, amongst other bacterial species, possess adhesins known as microbial surface components recognising adhesive matrix molecules (MSCRAMMs) that mediate cell anchorage in the infection process by binding to collagen, fibrinogen and fibronectin and other host extracellular matrix components (Foster and Hook, 1998). Protein A on the bacterial cell surface binds IgG molecules by their Fc region hence enabling an immunological disguise from the host, inhibiting phagocytic engulfment. Coagulase also protects against phagocytosis and immune recognition by catalysing the formation of fibrin around the cell (Dissemond, 2009). Invasins such as kinases and hyaluronidase aid bacterial invasion and spread. *S. aureus* strains also secrete toxins that cause membrane damage to host cells such as toxic shock syndrome toxin (TSST-1), enterotoxins, α-Toxin and leukocidins (Dissemond, 2009). Additionally, growth of *S. aureus* and other colonists within biofilms pose further problems in that these bacteria have increased protection from host defences and also exhibit enhanced resistance to antibiotics.

1.2.2 Mechanisms of bacterial resistance

Bacterial resistance to antibiotics has continued to increase with time and the extensive use of these agents. Resistance can emerge not only due to overuse and misuse of antibiotics but also due to treatment regimens of too short a duration or ineffective concentrations of the antibiotics at the site of infection. Prior to the discovery and development of antibiotics, infections caused by *S. aureus* and *S. pneumoniae* were often fatal (Trias and Gordon, 1997). Although *Staphylococci* are inherently susceptible to most antibiotics they remain a frequent cause of morbidity and mortality, owing to an adept capacity for the development of resistance to antimicrobial agents (Livermore, 2000). Development of drug resistance in *S. aureus* and other bacterial species is achieved either via mutation in chromosomal genes and selection of resistant strains, or more commonly due to the acquisition of resistance genes via DNA transfer between bacteria. Bacterial resistance can arise either from a single genetic mutation whilst resulting in no detrimental effect to the pathogenicity or viability of a strain, or mutations may change an existing resistance mechanism to confer a broader spectrum of activity (Gold and Moellering, 1996).

Antimicrobial agents have been developed against a range of bacterial targets including cell wall synthesis, protein synthesis at 50S and 30S ribosomal subunits, blocking nucleotide and mRNA synthesis, blocking DNA topoisomerases and disruption of membranes displaying bactericidal or bacteriostatic effects (Walsh, 2003). However, an equally diverse range of resistance mechanisms have been utilised by bacteria including, efflux mechanisms, modified target, inactivation of the antibiotic, bypass of metabolic pathways and modified permeability (Dzidic et al., 2008). For example, *Enterococcal* resistance to aminoglycosides is conferred by production of aminoglycoside modifying enzymes to inactivate the drugs but can also be due to decreased permeability of the bacterial cell or alterations in the ribosome binding site (Chow, 2000). Resistance to tetracyclines and quinolones is often conferred by efflux mechanisms that have been identified in both Gram-positive and Gram-negative bacteria (Jayaraman, 2009). Additionally numerous target mutations in bacteria exist, for example, alterations of RNA polymerase in order to confer rifampicin resistance in *Mycobacterium tuberculosis* (Telenti et al., 1993) and alterations in penicillin-binding proteins in pneumococci resulting in penicillin resistance (Nagai et al., 2002).

1.2.3 Methicillin resistant *Staphylococcus aureus*

MRSA is a significant nosocomial pathogen. Following the introduction of penicillin in 1944, a β-lactam antibiotic that inhibits cell wall synthesis by inhibition of peptidoglycan cross-linking, nearly all isolates were susceptible; however, resistant strains of *S. aureus* began to develop quickly and synthetic drugs including methicillin were introduced to combat their emergence. Unsurprisingly, methicillin resistance in a clinical *S. aureus* isolate was first reported in 1961, the year of the drug's launch (Jevons, 1961), from which five major genetic lineages of MRSA have evolved with strains resistant to all β-lactams.

Epidemic MRSA strains (EMRSA) are defined as those that have spread to two or more patients at two or more hospitals and since the emergence of MRSA, EMRSA strains -1, -3, -15 and -16 have been prominent in the UK; the latter strains account for the majority of isolates sent annually for epidemiological typing to the Laboratory of Hospital Infection (Livermore, 2000). Additionally, *S. aureus* is not only an important nosocomial pathogen but is becoming increasingly worrying as an important frequent

cause of infection in the community. Community-acquired (CA) MRSA is genetically distinct from hospital-acquired (HA) MRSA and can also differ in the antibiotic susceptibility profile (Ma et al., 2002). However, CA-MRSA can be highly virulent and is increasing in prevalence being often associated with skin and soft tissue infections, although the distinction between CA- and HA- MRSA infections is becoming more difficult due to CA-MRSA crossover into hospitals and healthcare setting causing HA-infections (Elston, 2007, O'Brien et al., 1999).

1.2.3.1 Mechanism of MRSA resistance

Methicillin resistance is commonly mediated by the presence of the *mecA* gene within the staphylococcal chromosome in a discrete region called the staphylococcal cassette chromosome (SCC*mec*) that is related to the production of a modified penicillin-binding protein (PBP), PBP2' or 2a, a fifth PBP in addition to the four others found in all strains of *S. aureus* (Hiramatsu et al., 2001). Variants of the SCC*mec* have been identified that vary not only in size and organisation but also differ in different genes that they carry other than *mecA* (Hiramatsu et al., 1999). PBPs are essential enzymes involved in cell wall synthesis and are the targets for β-lactam antibiotics. Production of PBP2a specifies a reduced affinity for binding methicillin and other β-lactam antibiotics such as cephalosporins, monobactams and carbapenems to strains of MRSA conferring resistance against these antibiotics allowing maintenance of cellular homeostasis.

The expanding use of antimicrobials including methicillin has led to strains of MRSA that are multi-resistant to nearly all classes of antibiotics (e.g. macrolides, lincosamides, tetracyclines, aminoglycosides, quinolones, trimethoprim and sulphonamides), excluding the glycopeptides (e.g. vancomycin and teicoplanin) to which strains of MRSA remain susceptible (Trias and Gordon, 1997). However, conjugative transfer of vancomycin resistance from *Enterococcus faecalis* to *S. aureus* via a *vanA*- containing plasmid has been demonstrated *in vitro* and *in vivo* (Noble et al., 1992). In addition, horizontal transfer of the *vanA* gene from *Enterococcus faecalis* has been shown to confer high levels of vancomycin resistance in clinical isolates of *S. aureus* (Chang et al., 2003). Since the first clinical isolate of *S. aureus* with intermediate vancomycin resistance (VISA) was reported from Japan in 1997 (Hiramatsu et al., 1997), other VISA and vancomycin resistant *S. aureus* (VRSA) cases have subsequently been

reported in numerous countries. This potential threat of increasing bacterial resistance is cause for serious concern in that the antibiotic therapies currently utilised may no longer prove effective in the treatment of certain infections. If increased resistance continues, there is a possibility that infections caused by *S. aureus* could potentially revert back to a preantibiotic era (Trias and Gordon, 1997). Therefore there is a need for new alternate treatment options to those provided by antibiotics that are not hindered by resistance.

1.3 Display technology

Various display and screening methodologies using phage, yeast, ribosomal, synthetic and bacterial display systems have been developed that enable libraries consisting of a large number of individual peptides and proteins to be expressed on their surface that can be screened to select ligands against specific targets. Libraries are synthesised so that each individual display vehicle from the library contains a single, different, DNA or RNA coding sequence, each representing a specific clone of the library; although each sequence will be present in numerous copies (Mersich and Jungbauer, 2008). Screening of libraries for clones of interest allows identification of a link between a specific gene and not only the protein it codes for, but also allows analysis of the function of that protein. Furthermore, the expanding prevalence of genomics and proteomics has led to the complete or partial sequencing of many bacterial and human genomes (currently over 5500 species identified in Genbank; http://www.ncbi.nlm.nih.gov/sites/entrez?db=genome) (Information, 2009) that allow comparison of genes and gene products previously uncharacterised, to gain insight into homology and unknown function. These technologies have emerged as powerful tools for the exploration of protein-protein interactions, protein identification and mapping, receptor-ligand interactions and drug discovery offering many important applications in targeted diagnostic and therapeutic technology. One of the first display technologies was phage display, from which antibodies have been selected that currently have FDA approval or are in clinical trials for the treatment of a variety of diseases (Brekke and Loset, 2003).

1.3.1 Phage display

Phage display, originally described by Smith (1985) is a technique whereby proteins are displayed on the surface of bacteriophage. Various strains of phage including M13, f1

and fd and also T7 and λ have been used that consist of single stranded DNA surrounded by several coat proteins (Azzazy and Highsmith, 2002). Foreign DNA sequences are inserted into filamentous phage genome and expressed as a fusion product with one of the phage coat proteins on the surface of phage, usually pIII or pVIII (Azzazy and Highsmith, 2002). Numerous foreign proteins including peptides (El Zoeiby et al., 2003), antibody fragments (Fab (de Haard et al., 1999) and scFv (Nissim et al., 1994)), enzymes (McCafferty et al., 1991), enzyme inhibitors (Huang et al., 1998), hormones (Sidhu et al., 2000), cytokines (Buchli et al., 1997) and also cDNA (Somers et al., 2002) have all been displayed on the surface of phage thus showing the enormous diversity and potential of this selection technique.

Isolation of phage that bind to a target of interest usually utilises a technique known as affinity selection (or panning); this method allows selection of molecules against a target by screening and amplification to select specific binders from an excess of non-binders. Briefly, the phage library is allowed to bind to the target of interest, non-binding phage are removed by washing, and the remaining phage are eluted and amplified in *E. coli* that are infected by phage using the F-pili as receptors. Successive rounds of panning allow amplification and enrichment of specific clones that bind to the target. Following panning, DNA sequencing of the clones and translation allows deduction of the protein sequence.

Phage display technology is advantageous in that it offers high-throughput screening and has had enormous successes in selecting phage particles displaying biologically active ligands with the unique, desired, binding specificities, having been routinely used against a wide range of targets. One of the most investigated applications of phage display has been in the selection of antibodies or antibody fragments (especially Fab or scFv) that recognise specific antigens. In addition to the isolation of recombinant antibodies, phage display has also been utilised for receptor-ligand isolation, selection of enzyme substrates, drug discovery/screening, identification of novel therapeutic targets, epitope mapping and recovered proteins may also have potential as novel vaccine candidates, diagnostic or prognostic markers (Mullen et al., 2006, Azzazy and Highsmith, 2002, Benhar, 2001).

Peptide phage display has emerged as a powerful complement to antibody display that can generate reagents with similar binding affinities to those of antibodies, with the advantage that peptides are easier to produce in large quantities. One particular application of phage display is the emergence of this technology as a promising tool for the detection and generation of novel therapeutics against pathogens. For example, Carnazza et al (2008) identified a 9-mer cationic peptide that binds highly selectively to the cell surface of *P. aeruginosa*. These peptides, selected from rounds of whole cell panning against *P. aeruginosa,* have enormous potential to act as biosensors/diagnostic tools against this frequent human pathogen, and most importantly this technology is applicable to a range of clinically relevant microorganisms (Carnazza et al., 2008). Furthermore, a peptide that specifically binds to *Mycoplasma arginini* infected pancreatic β cells and not other *Mycoplasma* strains or non-infected cell lines was isolated from phage peptide display; clearly demonstrating the widespread use of this technology as detection and purification reagents and even drug delivery vehicles (De et al., 2005), in a similar manner to those employed in the field of cancer. Interestingly, unlike the peptide sequences derived against *P. aeruginosa* (Carnazza et al., 2008), the peptides derived against *M. arginini* were synthesised and shown to retain binding potential in the absence of the phage vehicle (De et al., 2005). Furthermore, tetramerisation of the peptide was shown to increase its binding affinity for the target, presumably because multivalent display is more similar to the original phage configuration whereby 3-5 copies are presented on the phage surface (De et al., 2005). The specific targeting potential of ligands isolated from phage display indicates the possible utility of phage to act as carrier systems as drug delivery vehicles, which may have important applications in infection and disease states to deliver drugs directly to the target of interest. Phage display has been employed not only to identify *S. aureus* specific peptides, but also phage were conjugated to chloramphenicol through a labile linker to deliver controlled release of chloramphenicol whilst retaining binding specificity (Yacoby et al., 2006). This work showed that growth obstruction of *S. aureus* using the targeting conjugate was as efficient as administration of a 20-fold higher concentration of free chloramphenicol and importantly, the equivalent concentration of free chloramphenicol to that conjugated to the phage did not obstruct bacterial growth (Yacoby et al,. 2006). Cell specific delivery of therapeutic agents is therefore expected to improve the efficacy of the drugs, decrease unwanted side effect and reduce the

concentration required for treatment thus reducing the possibility of drug resistance development (Yacoby et al., 2006, De et al., 2005).

1.3.2 Bacterial display libraries

Bacterially-displayed libraries have emerged as a viable alternative platform to phage display technology. Bacterial libraries have been generated in both Gram-negative species, including *E. coli* and *Salmonella* sp, and Gram-positive bacteria such as *Staphylococci* and *Streptococci* that display peptides and proteins on the bacterial surface expressed on a range of outer membrane proteins (OMP). Peptides or proteins are expressed on the microbial cell surface by fusion with an anchoring motif via N- or C-terminal, or more commonly sandwich fusion depending on the characteristics of the display/carrier proteins (Lee et al., 2003). Early work established that peptides could be expressed on the bacterial cell surface of recombinant *E. coli* as fusions such as OmpA (Freudl et al., 1986), LamB (Charbit et al., 1988), and PhoE (Agterberg et al., 1990). However, in most applications these carrier systems were not permissive for the display of large proteins on the cell surface (Mersich and Jungbauer, 2008, Tommassen et al., 1993). This is presumably because regions at the N- and C- termini are required unaltered for efficient outer membrane targeting of most OMP (Georgiou et al., 1997) and therefore lateral fusion of a polypeptide end to end is not possible without interference with membrane insertion thus allowing only display of peptides and not full-length proteins within integral OMP (Chen and Georgiou, 2002). This indicates that the positioning and length of the peptide as well as choice of carrier protein are important factors that influence efficient peptide display (Nakajima et al., 2000). To circumvent these limitations the Lpp-OmpA system was constructed utilising *E. coli* lipoprotein and OmpA to display full length heterologous protein (Francisco et al., 1992). Furthermore, ice nucleation protein is an OMP found in *Pseudomonas*, amongst other species, that has an internal repeated domain that is adjustable in-frame in length allowing successful expression of foreign proteins as large as 60kDa (Lee et al., 2003).

Bacterial display libraries have also been successfully generated for display on lipoproteins, S-layer proteins and extracellular appendages, such as flagella, fimbriae and pili. In addition to the display of peptides, bacterial display technology has also been utilised for the display of antibodies (Gunneriusson et al., 1996, Fuchs et al.,

1996), enzymes (Strauss and Gotz, 1996, Francisco et al., 1992) on both Gram-positive and Gram-negative bacteria and also human cDNA library in *E. coli* for high-throughput screening of recombinant human proteins (Bussow et al., 2000). However, the more rigid structure of Gram-positive cells walls makes them generally more suitable for the development of whole cell catalysts/adsorbants (Lee et al., 2003). One of the most common applications of microbial cell surface display has been the development of live vaccine delivery by displaying heterologous immunogenic epitopes to induce an antibody response in the host (Lee et al., 2000). Additionally, bacterial display systems for environmental applications such as bioremediation purposes for removal of heavy metals have also been utilised. For example, insertion of yeast and mammalian metallothioneins, cellular metal sequestering peptides, into Omp LamB and expressed in *E. coli* demonstrated a twenty-fold increase in its natural $Cd^{(2+)}$ accumulation ability (Sousa et al., 1998).

One important feature of bacterial display is that it allows libraries to be screened by fluorescence activated cell sorting (FACS) enabling a high-throughput process of quantitative screening and direct functional analysis of clones avoiding lengthy immobilisation, elution and reinfection steps needed with phage technology (Dane et al., 2006, Chen and Georgiou, 2002). Furthermore, analysis of clones utilising FACS enables distinction of clones with different binding abilities, allowing selection of the 'better binders' or those against epitopes of varying density. Screening by FACS analysis is not often utilised using phage technology as phage are too small to be directly detected unless labelled with, for example, an antibody with a fluorescent tag. FACS using bacterial display libraries is emerging however as an important tool in the rapid isolation of clones with specific binding properties. Dane et al (2006) used fluorescent bacterial display libraries and FACS analysis, incorporating negative selection steps to remove clones that bound to healthy breast tissue, in order to identify peptides that bind to a human breast cancer cell line, with one identified clone displaying over 80-fold specificity for the tumour cell type relative to healthy breast cell lines (Dane et al., 2006). In addition to peptide display, flow cytometry has been used to screen cell surface expressed scFvs utilising the Lpp-OmpA system to select from a 10^5 excess of control bacteria (Francisco et al., 1993) and also been utilised for screening of enzyme libraries (Olsen et al., 2000).

Bacterial display libraries offer additional advantages over phage display counterparts. For example, a bacterial display library was successfully used for the identification of peptides that mediate entry into eukaryotic cells by using antimicrobial agents to eliminate extracellular bacteria, whereas this differentiation is not as easily achievable using phage technology due to the difficulties involved in the selective separation of intracellular and extracellular phage (Taschner et al., 2002). In general, the utilisation of bacterial display libraries is slightly simpler than that of phage in that it does not require separation and infection steps, and also that direct visualisation by microscopy can be used without the need for further labelling (Nakajima et al., 2000). Additionally the expression of large polypeptides, such as antibodies or antibody fragments, by phage display is not usually permissive as fusions to pVIII, and therefore expression as fusions to pIII is usually adopted (Benhar, 2001). However, a phage particle only expresses 3-5 copies of pIII as compared with 2,700 copies of pVIII. The low expression of phage coat protein genes and the usual unconstrained nature of peptides is often disadvantageous, particularly in structural studies of isolated peptides, whereas constrained peptides offer advantages in the identification of structural epitopes (Lu et al., 1995). Microbial surface display also offers an advantage in that it enables surface expression of larger proteins than is typically permitted by phage display (Lee et al., 2003). However, the diversity of peptides that can be displayed is usually lower in bacterially displayed libraries, whereas phage display libraries are frequently created displaying diversities as high as 10^{10} (Willats, 2002, Nakajima et al., 2000).

1.4 Flagella peptide display

The bacterial flagellum is the organelle associated with motility consisting of a filament, hook and basal body (Fig 1.5). FliC (flagella filament protein) is the major structural component of the *E. coli* flagellum. The filament is made by polymerisation of approximately 20,000 FliC molecules that assemble at the distal end of the filament, and extends from the cell surface that is capped with five FliD molecules (Majander et al., 2005). The N- and C- termini of FliC proteins are highly conserved whereas the central region is highly variable (Westerlund-Wikstrom, 2000). Flagella display is based on insertion of foreign DNA into this variable region of FliC, displayed as fusion proteins in a functional form, and has been shown to permit the insertion of large peptides (up to 302 amino acids), although this may not represent the largest insert that could be

expressed (Westerlund-Wikstrom et al., 1997). Additionally, it has also been demonstrated that FliD can be used as a carrier of foreign peptides (Majander et al., 2005) but this is less common.

1.4.1 The FliTrx™ random peptide display library

The FliTrx™ random peptide library is based on research carried out by Lu et al (1995). This group demonstrated that the entire thioredoxin gene can be inserted into the non-essential region of the flagellin gene (*fli*C) and the resulting fusion proteins are efficiently transported and assembled into partially functional flagella on the cell surface. The random dodecapeptides are inserted in-frame into the active site loop of thioredoxin, that is itself contained within the non-essential region of the *fli*C gene. Subsequent analysis demonstrated the display of constrained peptides on the flagella of *E. coli*. More than 90% of the flagella were functional, and can accumulate up to 20% of total cellular protein (Lu et al., 1995).

The library contains an estimated 1.77×10^8 individual 12-mer peptides that are flanked by Cys-Gly-Pro and Gly-Pro-Cys sequences at the N and C terminus, respectively. These sequences form a disulfide loop which displays the peptide on the cell surface in a conformationally constrained manner, making peptides easily accessible to ligands for binding (Fig 1.6). For expression of the library, the plasmid, pFliTrx^{TM}, propagated in *E. coli* G1820, uses the P_L promoter from bacteriophage λ to drive expression of the peptide fusion construct where the *c*I repressor gene is under control of the *trp* promoter (Xin et al., 2003). Expression of the fusion proteins is induced by the addition of tryptophan that blocks *c*I repressor synthesis, enabling transcription of the thioredoxin-flagellin fusion proteins. A schematic representation of expression of the peptide library is shown in Figure 1.7.

1.4.2 Applications of the FliTrx^{TM} peptide library

The previous applications of the FliTrx^{TM} library principally include the exploration of protein-protein interactions such as receptor-ligand binding and enzyme-substrate specificity. Antibody-antigen recognition studies using the library have been performed

by many groups based on epitope mapping, and various groups have highlighted the potential for use in vaccine development. Studies focussing on epitope mapping work as well as examples of other applications are shown in Table 1.1 to show the libraries versatility.

Interestingly, similar to phage display, the FliTrx™ library has also been utilised to screen against whole cells in order to identify novel targets for potential new diagnostic and therapeutic approaches. For example, Brown et al (2000) used the library to identify tumour vasculature binding peptides by panning against tumour-derived murine endothelial cells. This group applied a negative selection step to remove clones that bound non-specifically to cellular markers and generated tumour endothelial cell specific reagents, highlighting the potential of the library to be used for specific targeting (Brown et al., 2000). Similarly, Li et al (2008) have recently screened a normal liver cell line and a hepatoma cell line, again using negative selection, to identify tumour specific peptides. Yang et al (2008) have also screened the library with negative selection to identify a peptide that bound to a metastatic prostate cell line, with the synthetic peptide showing specificity for metastatic prostate, breast, lung and gastric cells both *in vitro* and *in vivo* but no reactivity against non-metastatic cells.

Additionally, Zitzmann et al (2005) identified specific peptides derived from panning against a human prostate carcinoma cell line that showed a reduced affinity to HUVECs and benign prostate cells. Peptides were radiolabelled with ^{125}-I or ^{131}-I and shown to bind tumour cell lines preferentially in *in vitro* studies. Biodistribution studies in a mouse model showed moderate tumour accumulation, identifying the possible utility of peptide technology for directing radioisotopes to tumours that may have the potential for tumour targeting and diagnostic/imaging purposes (Zitzmann et al., 2005). In summary, screening of display libraries has led to the identification of a vast array of proteins with unique binding applications. These libraries offer a great deal of potential for isolation of ligands that bind to specific targets enabling development of new systems for drug delivery or as diagnostic reagents.

1.5 Photodynamic therapy (PDT)

1.5.1 History of PDT

The antimicrobial effect of PDT was originally published in 1900 when Raab noted the toxicity of acridine hydrochloride when combined with certain wavelengths of light to *Paramecia cauatum* (Raab, 1900). Further to this, in 1904 Raab's tutor designated the phrase 'photodynamic reaction' (von Tappeiner, 1904). The discovery of many classes of antibiotics with the capacity for broad and effective killing of microbes resulted in the antimicrobial action of PDT not being fully investigated and utilised. However, the rise in bacterial resistance has led to alternative approaches of antimicrobial action to be researched and developed. The use of PDT as an alternative approach in this instance is particularly attractive as it is not hindered by bacterial resistance (Wainwright and Crossley, 2004).

1.5.2 Mechanism of action

PDT involves the administration of a photosensitiser that is activated by illumination with light of an appropriate wavelength and the presence of oxygen. The energy absorbed by the photosensitiser converts it from ground state into an excited singlet state and then to a more stable lower energy triplet state and reacts with oxygen. The activity of PDT is based on two photooxidative reactions: type I and type II (Maisch, 2007). In type I reactions, the photosensitiser reacts directly with substrates other than molecular oxygen via electron or hydrogen atom transfer to produce free radicals such as superoxide, hydrogen peroxide or hydroxyl radicals. In type II reactions the activated photosensitiser reacts with ground state molecular oxygen to produce highly reactive singlet oxygen, which is the main bactericidal species produced that reacts rapidly with the environment. A summary of antimicrobial PDT is summarised in Figure 1.8.

The lethal damage to bacteria following PDT can result in damage to either DNA and/or the cytoplasmic membrane that results in leakage of cellular contents, enzyme inactivation and non-functional membrane transport systems (Hamblin and Hasan, 2004). The different classes of compounds that show effective antimicrobial action are

summarised in Table 1.2, whereby methylene blue and toluidine blue have been used clinically for antimicrobial applications.

1.5.3 Photodynamic inactivation of bacteria

The application of PDT has been shown to be effective against a wide range of both Gram-positive and Gram-negative bacteria utilising a range of different photosensitisers and light sources. The differences in cell wall structure renders Gram-negative bacteria less susceptible to anionic and neutral photosensitisers than Gram-positive isolates due the negative charge conferred by lipopolysaccharides in the outer membrane (O'Riordan et al., 2005). However, other groups have demonstrated that addition of the nonapeptide polymyxin or EDTA resulted in greater membrane permeability thus allowing successful photoinactivation of Gram-negative bacteria utilising anionic photosensitisers (Nitzan et al., 1992, Bertoloni et al., 1990). In comparison, cationic photosensitisers have been utilised as compounds that are capable of photoinactivation of Gram-positive and Gram-negative species (Hamblin et al., 2002b, Segalla et al., 2002, Merchat et al., 1996, Minnock et al., 1996).

The penetration of light through the skin decreases with depth. Different classes of antimicrobial photosensitisers have varying absorption maxima depending on the molecular structure, generally within the 300-700 nm range (Wainwright, 1998) and diffusion of light through tissue increases with increasing wavelength within 400-700 nm (Maisch, 2007). Effective PDT requires delivery of light not only of the correct wavelength but also of sufficient intensity. Therefore penetration of light can be a problem at lower wavelengths and as such the PDT to kill pathogenic bacteria within wounds should consider the absorption spectrum of the photosensitiser and the penetration depth required (Maisch, 2007). Following accumulation of the photosensitiser, numerous light sources such as lasers or lamps of appropriate wavelengths can be utilised for PDT via either direct illumination of treatment site, fibre optics or bundles or implanted light emitting diodes (Hamblin and Hasan, 2004). The application of PDT for treatment of chronic wounds has some advantages; not only can the photosensitiser be directly placed on the affected area, but the light source used to activate the compound can also be accurately applied (Hamblin and Hasan, 2004).

PDT may also be effective as a treatment of bacteria present within biofilms. Wainwright et al (2002) demonstrated that treatment of a *P. aeruginosa* biofilm with new methylene blue caused both a bactericidal effect and breakdown of the extracellular polymeric substance that was superior to biofilm treatment with ampicillin. This technology has also been demonstrated to be effective in the treatment of oral biofilms (Zanin et al., 2006, Wilson et al., 1996). In addition, antimicrobial PDT has also been shown to reduce microbial virulence factors (lipopolysaccharide and proteases) that may contribute to the pathogenesis of infection (Komerik et al., 2000). Furthermore, Di Poto et al (2009) demonstrated that PDT was effective against *S. aureus* biofilms and that nearly complete eradication was observed when PDT was used in conjunction with either exposure to vancomycin or the phagocytic action of whole blood. Therefore, the bactericidal effect achieved with photodynamic therapy my be enhanced by being used in conjunction with antimicrobial therapy (Di Poto et al., 2009, Zolfaghari et al., 2009).

1.5.4 Photodynamic therapy of *S. aureus* and MRSA

Previous research has shown that numerous different photosensitisers have been shown to have a bactericidal effect on MRSA and drug sensitive *S. aureus* both *in vitro* and *in vivo*. A selection of these photosensitisers utilised over the last 15 years are characterised in Table 1.3, based on a search of Web of Knowledge and Pubmed, that are categorised according to the compound type and then reverse chronological order. Although many of these compounds have shown efficacy against various strains of *Staphylococci*, few/if any of these antimicrobial agents are in everyday use and therefore further work is needed to make this a real treatment option to eradicate bacteria present in wounds.

1.5.5 Conjugation of photosensitisers to biomolecules

The optimum photosensitiser used for effective antimicrobial PDT would be a compound that is localised to the bacteria causing the infection, whilst avoiding host cells or commensal bacteria (O'Riordan et al., 2005). Conjugation of the photosensitiser with a targeting moiety specifically for pathogens would be advantageous in that it would improve specificity of treatment without damaging normal tissue, and targeting may require lower drug doses. The different biomolecules that have been conjugated to

photosensitisers for targeting of MRSA and *S. aureus* are summarised in Table 1.4. Similarly, biomolecules have been used to target photosensitisers to other bacterial strains and are given in Table 1.5.

In addition to delivery of photosensitisers conjugated to biomolecules for specific bacterial targeting, other forms of improved photosensitiser delivery have been investigated. For example, Ferro et al (2006) demonstrated greater inactivation of MRSA when the photosensitiser (haematoporphyrin) was delivered by positively charged liposomes than was achieved with the free dye. A similar effect was also observed by Tsai et al (2009) whereby the concentration of liposome and micelle encapsulated haematoporphyrin required for *S. aureus* and MRSA eradication was lower than that of the free form, presumably by reducing photosensitiser aggregation thus limiting the quenching potential of the photosensitiser and an increase in reactive oxygen species (ROS) production.

1.5.6 Other applications of PDT

PDT has been used clinically for many years for the treatment of age-related macular degeneration (Bressler and Bressler, 2000) and recently for cancer (Brown et al., 2004). However, PDT has successfully been applied to the treatment of skin diseases including psoriasis (Boehncke et al., 2000) and acne (Hongcharu et al., 2000) and also against oral pathogenic bacteria (Chan and Lai, 2003).

In addition to utilisation against bacteria, PDT has also been applied to the inactivation of viruses, mainly for sterilisation of blood components (Santus et al., 1998), and against parasites (Grellier et al., 1997). Furthermore, PDT has shown promise in the treatment of fungi (Calzavara-Pinton et al., 2005), such as *Candida* sp (Bliss et al., 2004), and the protection/decontamination of food (Kreitner et al., 2003) and disinfection of water (Kuznetsova et al., 2007, Alouini and Jemli, 2001). In summary, PDT has shown potential in many disease states, the most useful clinically being age-related macular degeneration, however for widespread use in microbiology there remains the problems of specificity and effectiveness.

1.6 Aims

The overall aim of this thesis was to identify novel peptides with MRSA binding specificity that may prove useful in targeted PDT of chronic wounds. These could provide new modes of targeting bacteria that are not hindered by the development of bacterial resistance. The main objectives of this study were:

1. Identification of MRSA-specific peptides derived through panning of the FliTrx™ bacterially display random peptide library. Following DNA sequencing of positive clones, peptides were synthesised and binding characterised by flow cytometry against a range of Gram-positive and Gram-negative species.
2. Expression, purification and characterisation of recombinant proteins containing the specific peptides sequences of interest. Recombinant proteins were also expressed as green fluorescent protein (GFP) fusion proteins to allow direct assessment of recombinant protein binding.
3. Analysis of recombinant protein binding and functional effects, followed by conjugation to a porphyrin for cytotoxicity assays against MRSA, *E. coli* and keratinocytes.

CHAPTER TWO
Materials and methods

2.1 Materials

2.1.1 Bacterial strains and keratinocyte cell line

Three strains of MRSA (MRSA1, MRSA2 and MRSA3), *S. aureus*, *S. epidermidis*, *E. coli* and *P. aeruginosa* used in this study were community-acquired samples obtained from Hull Royal Infirmary. The NCTC2544 human keratinocyte cell line was kindly provided and maintained by Huguette Savoie.

2.1.2 Bacterial cell lines

- *E. coli* GI826: F^-, *lac*I^q, *amp*C:: P_{trp} *c*I, Δ*fli*C, Δ*mot*B, *eda*::Tn*10* (Flitrx™ library strain, Invitrogen, Paisley, UK)
- *E. coli* DH10B: F– *mcr*A Δ(*mrr-hsd*RMS-*mcr*BC) Φ80*lac*ZΔM15 Δ*lac*X74 *rec*A1 *end*A1 *ara*D139 Δ(*ara leu*) 7697 *gal*U *gal*K *rps*L *nup*G λ– (Cloning strain, kindly provided by Dr Frank Voncken, University of Hull)
- *E. coli* JM109: *end*A1, *rec*A1, *gyr*A96, *thi, hsd*R17 (r_k^-, m_k^+), *rel*A1, *sup*E44, Δ(*lac- pro*AB), [F´ *tra*D36, *pro*AB, *laq*I^qZΔM15] (Cloning strain, Promega, Southampton, UK)
- *E. coli* BL21: F- ompT $hsdS_B(r_B^- m_B^-)$ gal dcm tonA (Cloning strain, Sigma Chemical Company Ltd., Poole, UK
- *E. coli* GC10: F- mcrA Δ(mrr-hsdRMS-mcrBC) Φ80dlacZΔM15 ΔlacX74 endA1 recA1 Δ(ara, leu)7697 araD139 galU galK nupG rpsL λ- T1R (Cloning strain, Sigma)

2.1.3 Vectors

- pPROTet (Clontech, Saint-Germain-en-Laye, France)
- pFlitrx™ (Invitrogen)

2.2 Methods

2.2.1 Bacterial cell culture

MRSA, *S. aureus* and *S. epidermidis* were cultured in nutrient broth ('Lab-Lemco' powder 1 g/L, yeast extract 2 g/L, peptone 5 g/L and sodium chloride 5 g/L; Oxoid, Basingstoke, UK) in 250 ml Erlenmeyer flasks. *E. coli* and *P. aeruginosa* were cultured in Luria-Bertani (LB) medium (yeast extract 5 g/L, tryptone 10 g/L and NaCl 10 g/L). All media was made with dH_20 and autoclaved at 121°C for 15 min. Bacterial cultures were grown at 30ºC with shaking and subcultured aseptically using a 1% (v/v) inoculum every 24 h. Cultures were plated out onto nutrient broth or LB plus agar (15 g/L; Oxoid) in 90 mm Petri dishes and incubated at 30ºC. For glycerol stocking, cultures were centrifuged at 2,000 x g for 20 min at 4°C and the bacterial pellets resuspended in 1 ml phosphate buffered saline (PBS; 0.01M phosphate buffer, 0.0027 M KCl, 0.137 M NaCl, pH 7.4 and autoclaved; Sigma) supplemented with 15% (v/v) glycerol and stored at –80ºC until required. New aliquots of bacteria taken from glycerol stocks were used every 1-2 weeks in order to maintain genotype and phenotype.

2.2.2 Determining the presence of MRSA

Selective mannitol broth (Oxoid), originally described by Gurran et al (2002), was used in order to determine the presence of MRSA. A 50 µl sample of bacterial culture was used to inoculate 5 ml selective mannitol broth and incubated overnight at 30ºC. Presence of MRSA is confirmed by fermentation of mannitol that acidifies the medium as denoted by a colour change from red to yellow. Similarly, the presence of MRSA was confirmed by plating out a bacterial culture suspension onto chromogenic MRSA agar (Oxoid) used to detect phosphatase activity. Plates were incubated for 24-48 h at 30ºC and presence of MRSA determined by the presence of denim blue colonies, described by Macrae (2006).

2.3 Determination of optimal killing time of MRSA using UV radiation

The effect of UV radiation to kill MRSA cultures was first determined to ensure that the MRSA target cells were not able to compete with the *E. coli* expressed peptide library during the panning process. In preliminary investigations a 15 W 254 nm UV lamp was used to kill the bacteria. Bacterial cultures were grown to late log phase and a 10 ml sample was applied to 90 mm Petri dishes. The plates were subject to irradiation by UV-C exposure at 15 cm distance for 0-60 min and 100 µl samples extracted every 5 min and plated onto nutrient agar. The agar plates were incubated at 30ºC for 24-48 h and then inspected for bacterial growth.

Furthermore, a 40 ml overnight culture was centrifuged at 2,000 x g for 20 min at 4ºC. The pellet was resuspended in 20 ml PBS to concentrate the bacteria and 10 ml samples were applied to 90 mm Petri dishes. The plates were subject to irradiation and culture samples were taken every 5 min and plated out as described above. This method was also repeated utilising a new 15 W 254 nm lamp using the method described above except that the lamp was placed 10 cm distance from the plate prior to irradiation.

2.3.1 Confocal microscopy analysis

Bacterial viability was assessed utilising the LIVE/DEAD *Bac*Light Bacterial Viability kit (Invitrogen), a fluorescence-based assay that employs the use of two fluorescent dyes – SYTO 9 and propidium iodide (PI) that differ in their spectral characteristics and ability to penetrate healthy bacterial cells. The excitation/emission maxima are 480/500 nm for SYTO 9 and 490/635 nm for PI respectively. For STYO 9 and PI dye staining, two bacterial cultures (30 ml) were grown in nutrient broth to late log phase. One sample was UV irradiated using a 15 W 254 nm lamp at a 10 cm distance in order to effectively kill the bacteria (section 2.3). The MRSA cultures, both viable and irradiated, were concentrated by centrifugation at 10,000 x g for 15 min. The supernatants were removed and the pellets resuspended in 2 ml of 0.85% (w/v) sterilised NaCl. An aliquot (1 ml) of each suspension was added to centrifuge tubes containing 20 ml of 0.85% (w/v) NaCl and these were incubated for 1 h at room temperature (RT) mixing every 15 min to ensure thorough homogeneity. Samples were centrifuged at 10,000 x g for 15 min and the pellets washed using 20 ml 0.85% (w/v)

NaCl and re-centrifuged. Both pellets were resuspended in 10 ml 0.85% (w/v) NaCl. A 1 ml aliquot of bacterial suspensions was mixed with 3 µl of equal parts of SYTO 9 and PI, and incubated in the dark for 15 min. A 5 µl sample of stained bacterial suspension was used for confocal microscope analysis.

Samples were analysed on Biorad Radiance 2100 attached to a Nikon TE200 inverted microscope. Briefly, samples were placed on a slide, sealed with a coverslip and inverted for visualisation with the confocal microscope, the argon 488 nm laser line was used and fluorescent emission was collected in photomultiplier tubes 1 and 2 collecting light using a 515+/-30 (SYTO 9) and 570 long pass (PI) filters, respectively.

2.4 Bacterial immobilisation

Bacterial immobilisation assays were performed using 6-well pre-coated poly-D-lysine or collagen I plates (Nunclon® Delta, Nunc, Raskilde, Denmark) or 6-well plates coated in poly-L-lysine (Sigma). MRSA bacterial cultures (40 ml) were centrifuged at 2,000 x g for 20 min at 4ºC and resuspended in 20 ml PBS. One sample (10 ml) was UV irradiated using a 15 W 254 nm lamp at a 10 cm distance in order to kill the bacteria (section 2.3). A 2 ml aliquot of either live or dead/non-viable bacterial suspensions were added to each well, except for the control wells containing no bacteria, and the bacteria were left to adhere for 2 h at RT, 2 h at 4°C or overnight at 4ºC. The bacterial culture was carefully aspirated from the wells and the plates rinsed with PBS and bacterial immobilisation determined by light microscopy and visible examination of the plates to ensure plate coverage. All plates were washed 5 times with 2 ml wash solution used in the panning protocol (section 2.5.1) and vortexed for 30 s. Methylene blue (0.3% (w/v); 0.5 ml) was added to each well and incubated for 15 min. The plates were rinsed 5 times with 2 ml PBS and destained with ethanol and the absorbance of the stained bacteria was measured on a spectrophotometer (Pharmacia) at 668 nm.

2.5 Peptide display library

The FliTrx™ peptide library (Invitrogen) is a bacterially-displayed peptide library. The library displays random dodecapeptides on the surface of *E. coli* and has a diversity of 1.77×10^8 different specificities based on manufacturer's information. The peptides are

displayed within the active site loop of thioredoxin that is itself inserted into the dispensable region of the flagellin gene and are displayed on the surface within a conformationally constrained manner (section 1.4.1, Fig 1.6).

2.5.1 Growth media and solutions

5X M9 salts (1 L)

5 x M9 salts containing 200 mM Na_2HPO_4, 100 mM KH_2PO_4, 42.5 mM NaCl and 100 mM NH_4Cl (Sigma) were dissolved in 900 ml double distilled water (ddH_2O) and the pH adjusted to 7.4 with 10 M NaOH. Double distilled water was added up to 1 L and the solution autoclaved at 121ºC for 15 min.

Ampicillin stock

Ampicillin (Melford) was made at a 100 mg/ml stock solution in 0.2 µM filter sterilised (Millipore, Watford, UK) ddH_2O. Aliquots were stored at -20ºC.

L-tryptophan

L-tryptophan (Sigma) was made at a 10 mg/ml stock solution in 0.2 µM filter sterilised ddH_2O Aliquots were stored protected from light at 4ºC.

IMC medium (1L)

1 x M9 salts (40 mM Na_2HPO_4, 20 mM KH_2PO_4, 8.5 mM NaCl, 20 mM NH_4Cl, pH 7.4), 0.2% casamino acids, 0.5% glucose, 1 mM $MgCl_2$ containing 100 µg/ml ampicillin. Casamino acids were dissolved in 775 ml ddH_2O before autoclaving. After sterilisation, the solution was left to cool to ~55ºC before aseptic addition of 5X M9 salts, $MgCl_2$, glucose and ampicillin. The solution was stored at 4ºC.

RM medium (1L)

1 x M9 salts, 2% casamino acids, 1% glycerol 1 mM $MgCl_2$ containing 100 µg/ml ampicillin. Casamino acids and glycerol were dissolved in 790 ml ddH_2O before autoclaving. After sterilisation, the solution was left to cool before aseptic addition of 5X M9 salts, $MgCl_2$ and ampicillin. The solution was stored at 4ºC.

RMG plates

1 x M9 salts, 2% casamino acids, 0.5% glucose, 1 mM $MgCl_2$, 100 μg/ml ampicillin supplemented with 1.5% agar. Casamino acids and agar were dissolved in 775 ml ddH_2O before autoclaving. When the solution had cooled to ~55ºC, 5X M9 salts, $MgCl_2$, glucose and ampicillin were added aseptically. The agar (approximately 25 ml aliquots) was poured into 90 mm Petri dishes and stored protected from light at 4ºC.

Blocking solution

IMC medium containing 100 μg/ml ampicillin supplemented with 1% non-fat dry milk, 150 mM NaCl and 1% α-methyl mannoside (Sigma)

Wash solution

IMC medium containing 100 μg/ml ampicillin supplemented with 1% α-methyl mannoside

2.5.2 Growth and induction of the peptide library

One vial of FliTrx™ peptide library was used to inoculate 50 ml IMC medium containing 100 μg/ml ampicillin. The culture was grown to saturation at 250 rpm for 15 h at 25ºC. Expression of the FliTrx™ library was induced by adding 1 x 10^{10} colonies of the overnight culture to 50 ml IMC medium containing 100 μg/ml ampicillin and 100 μg/ml tryptophan. The culture was grown for 6 h at 25ºC.

2.5.3 Immobilisation of bacteria onto culture plates as panning target

Tissue culture plates (60 mm; Nunclon®) were coated with 1 ml poly-L-lysine. The plate was gently rocked for 5 min, rinsed with 5 ml PBS and allowed to dry for 4 h. MRSA cultures (40 ml) at log phase were centrifuged at 2,000 x g for 20 min at 4ºC and the pellet resuspended in 20 ml PBS. Cultures (10 ml) were added to the plate and allowed to adhere overnight at 4ºC. The plate was then rinsed with 5 ml PBS and 10 ml blocking solution added and the plate gently agitated at 50 rpm for 1 h (Gyrorocker, Stuart). The blocking solution was decanted and the bacteria subject to UV irradiation at

254 nm for 5 min. This method of bacterial immobilisation prior to panning was also repeated using cultures of *S. aureus* and *S. epidermidis*.

2.5.4 Panning of the random peptide display library

Following 6 h growth of the FliTrx culture, a mixture of 0.1g non-fat dry milk, 300 µl 5M NaCl and 500 µl 20% (w/v) α-methyl mannoside were added to sterile, conical centrifuge tubes. A 10 ml aliquot of the induced culture was added to each tube and gently mixed. The library cultures were added to the plates onto which the target bacteria had been immobilised (section 2.5.3). The plates were gently agitated at 50 rpm on a shaker for 1 min and then incubated at RT for 1 h to allow library clones to bind.

The bacterial cultures were decanted and the plates then washed by gentle rotation with 5 ml wash solution (section 2.5.1) at 50 rpm for 5 min. The wash procedure was repeated four more times to remove non-specific or weakly bound clones. The fifth wash was decanted and the plates vortexed for 30 s to elute the bound bacteria. IMC medium (10 ml) containing 100 µg/ml ampicillin was added to each plate and transferred to culture flasks. The cultures were grown at 250 rpm for 15 h at 25ºC. The same selection procedure was performed in four subsequent rounds of panning. After the fifth round of panning against the target bacteria, overnight cultures were streaked onto RMG plates and incubated overnight at 30ºC. After each round of panning, the *E. coli* library and MRSA cultures were plated out onto agar to ensure that there was no contamination of cultures and cultures were inoculated into oxoid selective mannitol broth to verify the presence of MRSA and ensure no contamination of the library (section 2.2.2). Glycerol was added to a final concentration of 20% (v/v) to the panned library and stored at –80ºC until required.

2.5.5 Negative panning step

Following 5 rounds of positive panning, bacterial stock cultures that were isolated from the final panning round were grown in 50 ml IMC medium containing 100 µg/ml ampicillin. The cultures were grown for 15 h at 250 rpm and 25ºC. The bacterial culture was induced by the addition of tryptophan (final concentration 100 µg/ml). The panning protocol was conducted in the same way as the previous method (section 2.5.4) except

that the induced culture was added to lysine only coated plates to remove clones which bound to lysine for 1 h before those clones that did not bind were transferred to the bacteria coated plates. The wash procedure was performed and isolation of positive clones performed according to the panning protocol.

2.6 Plasmid DNA isolation

Plasmid DNA was isolated from the panned library using the S.N.A.P. ™ (Simple Nucleic Acid Prep) Miniprep Kit (Invitrogen) and buffers supplied according to the manufacturer's instructions. Colonies were randomly selected from RMG plates and inoculated into 2 ml RM medium containing 100 μg/ml ampicillin to obtain high yields of plasmid DNA. Bacterial cultures were grown at 250 rpm for 16-24 h at 30ºC. Overnight cultures were pelleted by centrifugation at 2,000 x g for 10 min at 4ºC. The cell pellet was resuspended in 150 μl of resuspension buffer by vortexing. The cells were lysed to release the plasmid by the addition of 150 μl lysis solution. The lysate was gently mixed and incubated at RT for 3 min. A 150 μl aliquot of precipitation salt was added and the solution gently inverted 6-8 times to ensure thorough mixing. The solutions were centrifuged at 13,000 x g for 5 min at RT in order to precipitate the unwanted proteinaceous solution.

The supernatant was transferred into a 1.5 ml sterile microcentrifuge tube and 600 μl binding buffer added to the tubes and inverted 6 times. The plasmid containing solution was pipetted onto the S.N.A.P. ™ Miniprep Column that was then centrifuged at 3,000 x g for 30 s at RT. The column flow through was discarded and first washed with 500 μl of wash buffer. Columns were centrifuged at 3,000 x g for 30 s at RT and column flow through was discarded. A 900 μl aliquot of 1X final wash buffer was added and tubes centrifuged for 3,000 x g for 30 s at RT. The column was centrifuged at 13,000 x g for 1 min in order to dry the resin. To elute the plasmid DNA the columns were transferred to sterile 1.5 ml polypropylene microfuge tubes and 60 μl of sterile water was added directly to the resin. The tubes were incubated at RT for 3 min and centrifuged at 13,000 x g for 30 s at RT in order to elute the plasmid DNA from the column. Plasmid DNA was stored at -20ºC until required.

2.6.1 DNA quantification

The concentration and purity of the isolated DNA was determined spectrophotometrically by measuring the absorption of each sample at 260 and 280 nm. Distilled water was used as a reference to calibrate the spectrophotometer. The absorption was measured using a 6 µl aliquot of DNA diluted in 54 µl of distilled water or undiluted in a quartz cuvette. The concentration of DNA in each sample was calculated using the following formula:

DNA concentration (µg/ml) = A_{260} x dilution factor x Extinction Coefficient for DNA (50)

Assessment of the purity of the DNA in the samples was determined by measuring the A_{260} /A_{280} ratios. A ratio greater than 1.8 was considered acceptable and indicative of a relatively high purity of DNA (Maniatis et al., 1982).

2.7 Polymerase chain reaction (PCR) of plasmid preparations

PCR is an *in vitro* technique used to exponentially amplify sections of DNA and was performed to amplify the DNA sequence encoding the unknown peptide. DNA amplification was performed using Master Mix (Promega) that contains all the necessary components (*Taq* DNA polymerase, dNTPs and $MgCl_2$). The amplification reactions were performed in 50 µl reaction mixtures containing:

Plasmid DNA	1 µl
Master Mix	25 µl
FliTrx™ Forward Primer (200 ng/µl)	1 µl
FliTrx™ Reverse Primer (200 ng/µl)	1 µl
Nuclease free water	22 µl
Final volume	50 µl

Additionally, a negative control reaction containing no template DNA was included to ensure no PCR reagent contamination and amplification of the correct DNA. The reaction mixtures were cycled in a Thermal Cycler (Techne) using the programme

shown below in Table 2.1 under conditions described in the FliTrx™ manual (Invitrogen), except that the number of cycles was optimised to 35 cycles to increase the amount of amplified DNA.

Table 2.1: PCR programme

Phase	Temp	No. of cycles	Time	Event
DNA denaturation	94°C	1	2 min	Denaturation of DNA
PCR	94°C 55°C 72°C	35	1 min 1 min 1 min	Denature DNA strands Annealing of primers Extend DNA
Final extension	72°C 4°C	1	7 min	Final extension of unfinished strands Final hold

2.7.1 Agarose gel electrophoresis

Agarose gel electrophoresis was used to separate DNA fragments on the basis of their rate of movement through a gel under the influence of an electrical field. The PCR product (section 2.7) was visualised by gel electrophoresis. A 4.5% (w/v) Agarose-1000 (Invitrogen) gel was prepared in TBE buffer (90 mM Tris, 90 mM Boric acid, 2 mM EDTA) by heating in a microwave until the agarose had dissolved. After addition of 2 µl ethidium bromide (10 mg/ml; Sigma) to a final concentration of 0.2 µg/ml, the gel was poured into an electrophoresis tray with the appropriate comb and left to set for at least 30 min at 4°C. After setting, the combs were removed and the tray placed in an electrophoresis tank and covered with TBE buffer. A DNA ladder was prepared with 5 µl of a commercial 10 bp ladder (Invitrogen) and 10 µl 1X loading dye (0.25% (w/v)

bromophenol blue, 0.25% (v/v xylene cyanol FF and 30% (v/v) glycerol in dH_20. The PCR samples were loaded at a 1:1 ratio with loading dye (10 µl final volume). Samples were mixed by repeated pipetting and loaded into the wells. Electrophoresis was carried out at 100 V for 1 h or until the bands were 1 cm from the end of the gel. The DNA bands were visualised using a UV transilluminator (UVItec, Cambridge, UK) and photographed.

2.7.2 DNA sequencing of PCR products

DNA sequencing was performed using the dideoxy chain termination method developed by Sanger et al (1977). This technique uses a mixture of four specific terminator dideoxynucleotides (ddNTP) that are each labelled with a specific fluorescent dye, that stop chain elongation. Primers bind to the complementary section of DNA and the DNA chain extends linearly incorporating normal dNTPs into the chain until DNA polymerase, by chance, incorporates a ddNTP into the chain and elongation is terminated. Following elongation, the DNA fragments are sorted by size using capillary electrophoresis and a laser beam excites each different ddNTP to produce a different fluorescent colour that is translated into a DNA sequence.

DNA sequencing of PCR products was performed by MWG (Eurofins MWG Operon, Germany (MWG)). PCR products were purified and prepared for sequencing using exonuclease I, shrimp-alkaline phosphatase (SAP) (both GE Healthcare, Buckinghamshire, UK) and ethanol precipitation in order to concentrate the amount of DNA. A 1 µl aliquot of exonuclease I was mixed with 10 µl SAP. A 1.3 µl aliquot of this solution was added to 50 µl aliquots of PCR fragments. The samples were mixed, incubated at 37ºC for 15 min and heat inactivated for 15 min at 80ºC. Ethanol precipitation of purified PCR products was performed by mixing aliquots (50 µl) with 5 µl sodium acetate (3 M) and 165 µl ice cold ethanol and stored on ice for 30 min to precipitate the DNA. The samples were centrifuged at 12,000 x g for 30 min at 4ºC. The supernatant was discarded and the samples washed in 200 µl ice cold ethanol (70%) and centrifuged at 12,000 x g at 4ºC for 5 min. The wash step was repeated, the supernatant discarded and the samples air dried. All PCR fragments were sequenced in both directions.

2.8 Peptide synthesis

Following panning of the bacterial library against MRSA, DNA sequences of 20 peptide inserts were determined. Two peptides that shared similar homology with the other sequences (peptide12 and peptide19), but not overly similar to each other, were synthesised commercially (PeptideSynthetics, Fareham, UK). Peptides were synthesised with the N and C-terminal cysteine residues linked by a disulphide bridge in order to conformationally constrain the peptide and so retain its proposed binding motif as per panning. Additionally, peptides were synthesised as a linear construct in order to act as a comparison to assess binding ability. All peptides were synthesised with N-terminal biotin to allow subsequent characterisation of binding. Additionally, peptide12 was synthesised as a cyclic and linear construct with a C-terminal FITC instead of N-terminal biotin for direct assessment of binding.

2.8.1 Assessment of biotinylated peptide binding by flow cytometry

The binding of the peptides to both live and UV-inactivated MRSA stains (MRSA1, 2 &3), *S. aureus* and *S. epidermidis* were evaluated by flow cytometry. Bacterial cultures (40 ml) were centrifuged at 2,000 x g for 20 min at 4°C. The supernatant was discarded and the bacterial pellets were washed twice in 20 ml of filter sterilised (0.2 μM) PBS, that was used subsequently throughout the experiment, and the pellet resuspended finally in 10 ml PBS.

Bacterial suspensions (4 ml) were blocked with an equal volume of 2% (w/v) milk powder in PBS supplemented with 1% (w/v) bovine serum albumin (BSA; Sigma) by incubation for 30 min at 4°C. The bacteria were then centrifuged for 5 min at 2,000 x g, 4°C and the pellets resuspended in 4 ml PBS. An aliquot (2 ml) of each bacterial culture was subject to UV-C exposure, (15 W 254 nm) for 5 min in order to inactivate the bacteria. Live and UV irradiated bacterial cultures were adjusted with PBS to give a cell density of 1.67 x 10^7/ml. Preliminary data acquired by FACS and confocal analysis demonstrated that streptavidin FITC and streptavidin PE:Cy5 (both Serotec) alone are capable of binding to MRSA. In order to reduce the level of binding of streptavidin alone, peptide solutions were preincubated at a ratio of 5:1 with streptavidin-PE:Cy5 in

equal volumes (10 µl each) at 4°C for 30 min. An aliquot (20 µl) of each preincubated peptide: streptavidin PE:Cy5 solution was applied to 30 µl (5 x 10^5) bacteria and incubated at 4°C for 1 h ensuring gentle mixing every 15 min. Bacteria were washed by centrifugation at 6, 000 x g for 5 min at 4°C to remove excess, unbound peptide and the bacterial pellet resuspended in 300 µl with PBS and transferred to 75 x 12 mm polypropylene tubes (Sarstedt, Leicester, UK) prior to analysis by flow cytometry. A non-treated bacterial suspension, bacteria stained with SYTO 9 and bacteria labelled with streptavidin-PE:Cy5 for 1 h (all containing 5 x 10^5 cells) were used to determine parameters for FACS analysis.

Furthermore, biotin and unconjugated streptavidin (20 µl) were preincubated at a ratio of 5:1 and 50:1 for 30 min prior to initial incubation with blocked bacterial cells at 4°C for 30 min in order to saturate non-specific binding of biotin and/or streptavidin. Bacteria were washed as described above and then the preincubated peptide:streptavidin-PE:Cy5 complex (20 µl) was then added to the bacterial aliquots and incubated for 1 h at 4°C mixing gently every 15 min. Bacteria were washed again prior to flow cytometry analysis. Additionally, peptide solutions (10 µl) were preincubated at a molar ratio of 1:1 with an anti-biotin-Cy5 antibody (10 µl; Abcam) at 4°C for 30 min. Preincubated solutions were incubated with 30 µl (5 x 10^5) bacteria at 4°C for 1 h, mixing gently every 15 min. Bacteria were washed prior to analysis by flow cytometry.

2.8.1.2 Assessment of FITC-labelled peptide binding to bacteria and keratinocytes by flow cytometry

Binding of FITC-labelled peptides was assessed against 3 strains of MRSA (MRSA 1, 2 & 3) and also *S. aureus*, *S. epidermidis*, *E. coli*, *P. aeruginosa* and keratinocytes. Bacteria were prepared and blocked as described previously (section 2.8.1). Keratinocytes (grown to approximately 80% confluence) were detached from tissue culture flasks by cell scraping. Keratinocytes were washed in 5 ml PBS, centrifuged at 180 x g for 3 min, and resuspended in PBS. Bacteria (5 x 10^5 cells) and keratinocytes (1 x 10^5 cells) were incubated with 25 µl of peptide12 (previously diluted in PBS giving approximately 100,000 peptide molecules per cell). Following incubation for 30 min at

RT, bacteria and keratinocytes were washed and resuspended in 300 µl PBS prior to analysis by flow cytometry.

2.9 Cloning

2.9.1 Primer sequences and vector constructs

All of the primers (all synthesised by MWG) used subsequently for cloning experiments are shown below in Table 2.2. Primers are shown in the 5' to 3' direction. The appropriate primers were constructed to contain restriction sites, shown as underlined bases, to allow subsequent cloning into a vector for bacterial expression. Italicised bases are additional bases as flanking sequences to allow the relevant restriction enzyme to cut efficiently. A flow diagram demonstrating the overall cloning process is summarised in Figure 2.1 depicting cloning of thioredoxin containing peptides only (A) and also as a GFP fusion construct (B). The final overall thioredoxin/pPROTet (A) and thioredoxin/GFP/pPROTet (B) cloning vector constructs are shown in Figure 2.2.

2.9.2 Amplification of thioredoxin inserts containing individual peptide sequences by PCR

PCR was performed to amplify DNA from plasmid preparations (section 2.7) of samples that contained no stop codons following sequencing (section 2.7.2). PCR was performed using forward (ThioFor) and reverse (ThioRev) primers shown in Table 2.2 designed in order to amplify the entire thioredoxin gene containing the individual peptide sequences of interest. The entire thioredoxin sequence was amplified to allow greater stability of the 12-mer peptides and also to keep the same structural context from which the peptides were originally selected. The amplification reactions were performed in 50 µl reaction mixtures under similar conditions described previously (section 2.7). Amplification was performed similar to conditions described in Table 2.1 (section 2.7) except that the annealing temperature was changed to 69°C and the number of cycles to 30.

2.9.2.1 Optimisation of primers

Conjugation of photosensitisers to thioredoxin inserts requires the presence of lysine moieties. Although the thioredoxin sequence does contain lysine residues this was optimised by incorporation of a 15 lysine residue linker on the forward thioredoxin primer to allow multiple sites for the photosensitiser to be conjugated. Individual thioredoxin inserts containing the peptide inserts of interest were amplified again from plasmid DNA using a forward primer (ThioLysineFor; Table 2.2) to amplify thioredoxin containing a 15 lysine linker by PCR using the same conditions described in Table 2.1 in conjunction with the reverse ThioRev primer.

2.9.3 PCR product purification and quantification

PCR products were purified directly from the reaction samples using the NucleoSpin® Extract II kit (Macherey-Nagel GmbH & Co. KG, Germany) using buffers supplied to remove contaminants such as salts, dNTPs and unused primers, according to the manufacturer's instructions. Each PCR reaction (50 µl) was adjusted to 100 µl with nuclease free water and mixed with 200 µl diluted Buffer NT. Buffer NT was diluted with 4 volumes of distilled water, whereby the dilution of Buffer NT lowers the binding efficiency of smaller unwanted DNA fragments to the silica membrane that may interfere with subsequent cloning applications. The samples were loaded onto spin columns and centrifuged at 11,000 x g for 1 min to bind the DNA to the silica membrane. The column flow-through was discarded and the membrane washed with 600 µl ethanolic buffer, NT3, and centrifuged at 11,000 x g for 1 min to remove contaminants. The column flow through was discarded and the columns centrifuged at 11,000 x g for 2 min to dry the silca membrane. The columns were transferred to clean 1.5 ml polypropylene tubes and 28 µl Elution Buffer NE (5 mM Tris-HCl, pH 8.5) was added to the membrane, incubated at RT for 1 min, and centrifuged at 11,000 x g for 1 min to elute purified DNA. The concentrations of the purified PCR products were determined spectrophotometrically (section 2.6.1) using 5 mM Tris-HCl, pH 8.5 as a reference for calibration of the spectrophotometer. All samples were stored at -20°C.

2.9.3.1 Test gel of PCR products following clean-up

Agarose gel electrophoresis was used to analyse the size of PCR products following purification (section 2.7.1) on a 2% (w/v) Seakem gel (FMC Bioproducts) in 100 ml TBE buffer supplemented with 2 µl ethidium bromide to a final concentration of 0.2 µg/ml. Aliquots (3 µl) were mixed at a 1:1 ratio with loading dye and loaded into wells alongside 2-3 µl 100 bp ladder (Promega). Electrophoresis was carried out at 100 V for approximately 1 h. The DNA was visualised using a UV transilluminator and photographed.

2.9.4 DNA digestion of PCR products and pPROTet vector

The PCR products and the pPROTet bacterial expression vector (Clontech) were digested using *Sal*I and *Bam*HI restriction endonucleases (both NEB) in the appropriate buffer to cut the DNA at specific sites. Double digestion reactions were performed to digest an aliquot (25 µl) of each PCR product with 25 U (1.25 µl) *Sal*I and 25 U (1.25 µl) *Bam*HI in a reaction mixture containing 4 µl 10X buffer (NE Buffer 3), 0.4 µl 100X BSA and 8.1 µl nuclease free water. The samples were incubated at 37°C for 90 min and the reactions stopped by storage at -20°C. To optimise *Sal*I digestion a futher aliquot of 25U of *Sal*I was added halfway through the reaction. The pPROTet vector (2.5 µg) was digested with 25 U (1.25 µl) *Sal*I and 25 U (1.25 µl) *Bam*HI in a reaction mixture containing 4 µl 10X buffer, 0.4 µl 100X BSA and 28.1 µl nuclease free water at 37°C for 90 min and the reactions stopped by storage at -20°C.

2.9.4.1 Purification of digested DNA from agarose gel

The digested pPROTet vector (40 µl) and PCR products (40 µl) were purified by gel extraction using the NucleoSpin® Extract II kit according to the manufacturer's instructions. Samples were mixed with 10 µl of loading dye and applied to a 1.5% (w/v) low melting point gel (Seaplaque, Cambrex Bio Science) in 100 ml TBE buffer supplemented with a low concentration of ethidium bromide to minimise DNA damage (1 µl; final concentration 0.1 µg/ml) in order to facilitate the extraction and purification of the products without inducing mutation. An aliquot (2-3 µl) of 100 bp ladder (Promega) was used to analyse the size of the products. Electrophoresis was carried out

at 100 V for approximately 1 h. The DNA was visualised using a UV transilluminator, photographed and excised from the gel using a clean scalpel. The weight of each excised gel fragment was determined and 200 µl of Buffer NT was added per 100 mg of gel fragment. The gel fragments were incubated at 50°C until completely dissolved. Each sample was then loaded onto a spin column purified as previously described (section 2.9.3). The pPROTet vector was eluted in 48 µl elution buffer and the PCR products eluted in 25 µl elution buffer. Agarose gel electrophoresis was performed (section 2.9.3.1) to confirm the presence and size of purified DNA following extraction.

2.9.5 Ligation of PCR products into the pPROTet vector

Each ligation reaction was set up to join 150 ng of vector with a 25:1 molar ratio of PCR product insert to vector supplemented with 10X buffer (10% final volume) and DNA ligase (5% final volume; both NEB). Ligation reactions were incubated at room temperature for 3 h and the reactions stopped by storing at -20°C. Control ligation reactions were set up with cut plasmid and no insert DNA, replacing insert DNA with nuclease free water. Gel electrophoresis of ligation reactions was performed under similar conditions described previously (section 2.7.1) using a 0.7% (w/v) Seakem gel to analyse ligated vectors prior to transformation. Aliquots of ligation reactions (1 µl) mixed with 4 µl loading dye were loaded alongside 2-3 µl of 100 bp ladder (Promega) or 1 kb ladder (Fermentas, York, UK). Following electrophoresis, DNA was visualised and photographed.

2.9.6 Transformation of thioredoxin/pPROTet ligated vectors into *E. Coli* JM109

E. coli JM109 bacterial cells were thawed on ice, gently mixed and 50 µl per reaction transferred to chilled, sterile 75 x 12 mm polystyrene culture tubes (BD Biosciences). An aliquot (1 µl) of each ligated vector was added and the tube flicked quickly several times and incubated on ice for 10 min. The bacteria were subsequently heat-shocked at exactly 42°C for 45-50 sec and then returned to ice for 2 min. Following incubation, the bacteria were mixed with 900 µl of 4°C SOC medium (2% (w/v) tryptone, 0.5% (w/v) yeast extract, 10 mM NaCl, 2.5 mM KCL, 10 mM $MgSO_4$, 10 mM $MgCl_2$, 20 mM glucose) and incubated for 60 min with shaking (~225 rpm) at 37°C. Additionally, *E. coli* JM109 cells without an expression vector and also JM109 cells transformed with an

empty pPROTet vector were used as controls. Transformed cells (100 µl): neat, diluted 1:10 and 1:100 were plated on LB plates containing 34 µg/ml chloramphenicol to select for the pPROTet vector and incubated overnight at 37°C. Transformations were also attempted using *E. coli* GC10 and BL21 (both Sigma) to increase protein yield.

2.9.7 Colony PCR of transformants

Colony PCR was performed in order to confirm that individual transformants contained the thioredoxin insert in the correct orientation using a forward primer that anneals to the pPROTet vector (pPROTetFor; Table 2.2) and a reverse primer that anneals to the C-terminal of thioredoxin (ThioRev; Table 2.2). Additionally, competent cells alone and competent cells transformed with the empty expression vector were amplified by colony PCR using various paired primer combinations that anneal to the N- and C- termini of thioredoxin and the pPROTet vector (ThioFor, ThioLysineFor, pPROTetFor, ThioRev, pPROTetRev; Table 2.2). Amplification reactions were performed under similar conditions described previously (section 2.7) except that template DNA was obtained from individual colonies selected from each transformant plate with a sterile tip. Amplification was performed under similar conditions (section 2.7) except that the annealing temperature was 66°C for 26 cycles.

2.9.8 Bacterial culture and glycerol stocks of transformants

Glycerol stocks were made of transformants confirmed positive by colony PCR in order to have an continuous supply of bacteria for expression and purification of proteins. Individual colonies were inoculated into 7 ml LB medium supplemented with 34 µg/ml chloramphenicol to select for the pPROTet vector and grown overnight at 250 rpm at 37°C. Cultures were centrifuged at 2,000 x g for 10 min at 4°C and the bacterial pellets resuspended in 1 ml PBS supplemented with 15% (v/v) glycerol and stored at –80ºC until required.

2.9.9 Plasmid DNA extraction and DNA sequencing

Plasmid DNA was isolated from the transformants using the Nucleospin Plasmid (Macherey-Nagel) purification kit with buffers supplied, according to the manufacturer's instructions under to similar conditions described in section 2.6. Following plasmid purification, plasmid DNA was ethanol precipitated under similar conditions previously described (section 2.7.2) prior to DNA sequencing. Sequencing was conducted by MWG using primers pPROTetFor and pPROTetRev (Table 2.2).

2.10 Transformation of GFP and amplification by PCR

The GFP vector (Clontech) was transformed into JM109 *E. coli* competent cells (Promega; section 2.9.6). Individual colonies were screened for successful transformation of GFP using confocal microscopy (section 2.3.1). Single colonies that were confirmed to contain GFP were amplified in 7 ml LB supplemented with 50 µg/ml ampicillin and grown overnight at 37°C. Following culture, purified plasmid DNA was extracted from bacterial cultures and stored at -20°C. GFP was amplified by PCR from purified plasmid DNA using primers designed to amplify GFP retaining the natural stop codon of GFP, and alternatively a substitution to allow read through. The amplification reactions were performed in 50 µl reaction mixtures similar to that previously described (section 2.7) using GFPFor primer (Table 2.2) and GFPRev(WS) or GFPRev(NS) primer (Table 2.2). The reaction mixtures were amplified as described previously (section 2.7) except that the annealing temperature was 67°C and 25 amplification cycles were performed. Amplified PCR products were stored at -20°C.

2.10.1 Gel extraction of GFP PCR products

An aliquot (40 µl) was mixed with 10 µl of loading dye and separated on an 1.5% (w/v) low melting point agarose gel using a 100 bp ladder (Invitrogen) to analyse the size of the products then extracted and purified from the gel (section 2.9.4.1). Samples were eluted in 48 µl nuclease free water and stored at -20°C. Following purification, a test agarose gel was performed (section 2.9.3.1) to confirm the presence of DNA at the expected size following transformation. The concentration of the purified PCR products

were determined spectrophotometrically (section 2.6.1) using nuclease free water for calibration.

2.10.2 Digestion of PCR products and pPROTet vector

Amplified GFP PCR products and the pPROTet vector were digested using *Pst*I and *Pvu*I restriction enzymes (NEB). An aliquot (2.5 µg in 16.7 µl) of each PCR product was digested with 25 U (1.25 µl) *Pst*I and 25 U (2.5 µl) *Pvu*I in a reaction mixture containing 4 µl 10X buffer (NE Buffer 3), 0.4 µl 100X BSA and 15.15 µl nuclease free water. Similarly, 2.5 µg (5 µl) of the pPROTet vector was digested with 25 U (1.25 µl) *Pst*I and 25 U (2.5 µl) *Pvu*I supplemented with 4 µl 10X buffer, 0.4 µl 100X BSA and 26.85 µl nuclease free water. All samples were incubated at 37°C for 90 min and the reactions stopped by storage at -20°C. Digested DNA (20 µl pPROTet vector and 40 µl PCR products) were gel extracted and purified from a 1.5% (w/v) Seaplaque agarose gel supplemented with a low ethidium bromide concentration (1 µl; final concentration 0.1 µg/ml in TBE buffer (section 2.9.4.1). All samples were eluted in 48 µl nuclease free water. Agarose gel electrophoresis was performed (section 2.9.3.1) to confirm the presence and size of purified DNA following extraction.

2.10.3 Ligation of GFP PCR products into the pPROTet vector

Ligations reactions were set up to ligate each GFP PCR product both with and without a stop codon into 100 ng of the pPROTet vector at a molar ratio of 5:1 under similar conditions described in section 2.9.5. pPROTet plasmid DNA was incubated with the relevant PCR product in a reaction tube containing 10X Buffer, DNA ligase and nuclease free water alongside a negative control using nuclease free water in place of the insert. Each reaction was incubated at RT for 3 h and the reaction stopped by storing at -20°C. A test gel of ligation reactions was performed (section 2.9.5) to analyse ligated vectors prior to transformation on a 0.7% (w/v) Seakem gel by loading 1 µl of each ligation reaction in 4 µl loading dye.

2.10.4 Transformation of GFP/pPROTet ligated vectors

An aliquot (1.5 µl) of each ligated vector was transformed into DH10B *E. coli* competent cells under similar conditions described in section 2.9.6 except that bacteria were heat shocked at 42°C for 90 sec. Each aliquot was mixed with 300 µl of 4°C LB and incubated with shaking at 225 rpm for 1 h at 37°C. Transformed cells were plated out and incubated as previously described (section 2.9.6). Following transformation, single colonies were selected and confocal microscopy used to check transformants for the presence of GFP (section 2.3.1). Individual colonies that were confirmed positive to contain GFP by confocal microscopy were amplified, plasmid DNA isolated (section 2.6), and glycerol stocks were made (section 2.9.8) and stored at –80ºC until required.

2.10.5 GFP/pPROTet and thioredoxin insert digestion and purification

Purified GFP/pPROTet plasmid DNA (section 2.10.4) and thioredoxin PCR products amplified using thioredoxin forward and reverse primers (without the 15 lysine linker) (section 2.9.2) were digested using *Sal*I and *Bam*HI restriction enzymes. Double digestion reactions were performed to digest an aliquot (35 µl) of each PCR product with 20 U (1 µl) *Sal*I and 20 U (1 µl) *Bam*HI in a reaction mixture containing 4 µl 10X buffer and 0.4 µl 100X BSA. Aliquots of the purified GFP/pPROTet vectors (45 µl) were digested with 20 U (1 µl) *Sal*I and 20 U (1 µl) *Bam*HI in a reaction mixture containing 5 µl 10X buffer supplemented with 0.5 µl 100X BSA. All double digestion reactions were incubated at 37°C for 90 min and the reactions stopped by storage at -20°C. The digested GFP/pPROTet DNA and thioredodin PCR products were resolved by agarose gel electrophoresis and purified (section 2.9.4.1). Following purification, a test gel was performed (section 2.9.3.1) to ensure successful extraction and to confirm the size of the extracted PCR products and vectors.

2.10.6 Ligation of thioredoxin inserts into GFP/pPROTet vectors and transformation into *E. Coli* GC10

Ligation reactions were set up to ligate 100 ng of GFP/pPROTet vector at a 10:1 insert to vector molar ratio of thioredoxin inserts supplemented with the appropriate volumes of 10X buffer and DNA ligase (section 2.9.5). Control ligation reactions were set up

with cut plasmid and no insert DNA, replacing insert DNA with nuclease free water. A test gel of ligation reactions was performed (section 2.9.5) to analyse ligated vectors prior to transformation loading 1 µl of each ligation reaction in 4 µl loading dye. GC10 competent cells (Sigma) were thawed on ice and transformed with 1.5 µl of each ligation reaction or negative control under similar conditions described in section 2.9.6 except that bacteria were incubated on wet ice for 30 min prior to heat shock. Following incubation, cells were heat-shocked at 42°C for exactly 45 sec and returned to ice for 10 min. SOC media (450 µl) was added to each tube and the reactions transferred to sterile 75 x 12 mm polystyrene culture tubes and incubated at 37°C for 60 min with continuous shaking (~225 rpm). Transformed cells were plated out and incubated as previously described (section 2.9.6). Glycerol stocks were made of individual transformants (section 2.9.8). Following selection of single transformants, all other transformants were selected from whole plates and inoculated into 20 ml LB/chloramphenicol media and centrifuged at 2,000 x g for 20 min at 4°C. The bacterial pellets were suspended in 5 ml 15% glycerol in PBS and stored at -80°C as 1 ml aliquots.

2.10.7 PCR and DNA sequencing of transformants

Plasmid DNA was extracted from individual transformants (section 2.6) and analysed for the presence of thioredoxin and GFP inserts using the primers pPROTetFor and either GFPRev(WS or NS) primer or pPROTetRev primers (Table 2.2). Amplification reactions were performed and amplified under similar condition to those previously described (section 2.7), except that the annealing temperature was 57°C for 25 cycles. DNA was visualised by agarose gel electrophoresis (section 2.9.3.1) by mixing 5 µl of each PCR product with an equal volume of loading dye and loading onto a 2 % Seakem gel. All PCR products were stored at -20°C. Extracted plasmid DNA (section 2.6) was ethanol precipitated (section 2.7.2) and samples were sequenced commercially by MWG.

2.11 Determination of optimal protein induction and expression

Optimal protein induction and expression analysis was determined according to the manufacturer's instructions. Glycerol stocks of *E. coli* transformed with pPROTet vectors containing each thioredoxin insert were streaked onto LB/agar plates

supplemented with 34 µg/ml chloramphenicol and incubated at 37°C overnight. Single colonies were picked and inoculated into 5 ml LB media containing 34 µg/ml chloramphenicol and grown at 37°C overnight with shaking. An aliquot (2 ml) of the overnight culture was used to inoculate 100 ml LB/chloramphenicol media and grown at 37°C with shaking until the culture reached an OD_{600} of 0.5. This culture was used to start 5 x 20 ml cultures that were induced with varying concentrations (0-100 ng/ml) anhydrotetracycline (Clontech). The cultures were incubated at 37°C with shaking and at 0,2,4,6,7 and 24 h time points following induction, 1 ml samples were removed and diluted to give to a pre-induction OD_{600} of 0.5 to give the same concentration of bacteria. Bacteria were centrifuged at 13,000 x g to pellet the cells and these were stored at -20°C until analysis.

2.12 Sodium Dodecyl Sulphate Polyacrylamide Gel Electrophoresis (SDS-PAGE)

SDS-PAGE and Western blotting were used to ensure that the recombinant protein was expressed. SDS-PAGE was performed using 10% or 4-20% gradient precast gels (Pierce, Rockford, USA). The gels were placed into the electrophoresis tank covered in running buffer (100 mM Tris base, 100 mM HEPES, 0.3 mM SDS, pH 8.0 (all Melford) in dH_2O) ensuring that all air bubbles were removed from the wells. The bacterial pellets were resuspended in 100 µl sample buffer (13 ml 1M Tris-HCl (pH 6.8), 6.5 ml 20% (w/v) SDS, 5.2 ml 100% glycerol and 0.26 ml 0.5% (w/v) bromophenol blue). For reducing gels, beta-mercaptoethanol (β-ME 1.43M; Sigma) was added to 10% (v/v) final volume of loading buffer. The bacterial pellets were then boiled for 5 min to denature the proteins and centrifuged at 13,000 x g for 10 min. An aliquot (12 µl) of supernatant was loaded into each well alongside 15 µl Benchmark™ pre-stained protein ladder (Invitrogen) in order to determine protein size. The gel was subject to electrophoresis at 120 V for approximately 1 h or until the dye front had reached the bottom of the gel.

2.12.1 Coomassie staining

Coomassie staining was used to observe the induction of protein expression. Following electrophoresis, the stacking gel was removed and the gel rinsed with dH_2O to remove

residual SDS. The gel was stained with Coomassie (Severn Biotech) and incubated on a rocker at RT for 3 h or overnight at 4°C. The gel was destained by washing with dH_2O and visualised on a lightbox.

2.12.2 Western blotting

Following electrophoresis, the stacking gel was removed and the gel plus a sheet of nitrocellulose membrane were placed in transfer buffer at 4°C (25 mM Tris base, 25 mM bicine (Melford), 10% (v/v) methanol in dH_2O) and allowed to equilibrate for approximately 5 min. Proteins were transferred from the gel to the membrane by assembling a transfer unit consisting of a fibre pad, 2 sheets of wetted filter paper, the gel, the nitrocellulose membrane and 4 pieces of wetted filter paper. The transfer unit was placed in a Biorad cassette in the correct orientation in a tank of transfer buffer to transfer negatively charged proteins to the membrane. The proteins were transferred whilst stirring continuously at 100 V for 1 h or overnight at 30 V at 4°C.

Following transfer the membrane was blocked in 20 ml PBS supplemented with 2% (w/v) non-fat dry milk and 1% (w/v) BSA for 1 h at room temperature or overnight at 4°C. After blocking, the membrane was incubated with the primary antibody (Table 2.3) in the blocking buffer for 2 h at RT. The membrane was washed 3 times for 5 min each wash with PBS/0.05% (v/v) Tween 20 (Sigma) and then incubated with the relevant secondary antibody conjugated to horse radish peroxidase (HRP) (Table 2.3) in blocking buffer for 1 h at RT. Following a second wash to remove the unbound antibody the membrane was placed in equal volumes of ECL detection reagents (GE Healthcare) for 1 min ensuring complete coverage of the membrane before development.

Table 2.3: Antibodies used for Western blotting

Primary antibody	Dilution	Secondary antibody	Dilution
Rabbit anti-thioredoxin polyclonal antibody (Abcam)	1:1000	Sheep anti-rabbit IgG:HRP (Serotec)	1:4000
Rabbit anti-6xHN tag polyclonal antibody (Clontech)	1:1000	Sheep anti-rabbit IgG:HRP (Serotec)	1:4000

2.12.2.1 Development of the film

Following immersion in ECL detection reagents, the membrane was placed between an acetate sheet in the X-Omatic Fine Cassette (Kodak, Rochester, US) and exposed onto a film (Amersham) for between 1-30 min depending on the primary antibody used. Following exposure, the film was placed in developer (Sigma), rinsed in 1% (v/v) acetic acid and then fixed (Sigma). The film was rinsed with water and left to air dry.

2.12.2.2 Stripping and reprobing the membrane

Following development of the film the membrane was stripped with Restore™ PLUS stripping buffer (ThermoScientific) according to the manufacturer's instructions. The membrane was washed for 5 min in 20 ml PBS to remove all traces of the ECL detection reagent and 12 ml stripping buffer added to the membrane and incubated for 15 min at RT at 30 rpm. Following incubation, the membrane was washed 3 times with 20 ml PBS for 5 min. The membrane was blocked and probed with the secondary antibody and developed to ensure stripping of both the primary and secondary antibodies (section 2.12.2, 2.12.2.1). Following successful stripping, the membrane was washed and blocked again and incubated with the next primary antibody followed by the appropriate secondary and development (section 2.12.2.1).

2.13 Shake-flask expression and purification

2.13.1 Protein expression

LB/chloramphenicol media (100 ml) was subcultured with a 2% inoculum of an overnight culture of *E. coli* transformed with pPROTet expression plasmids and amplified with shaking at 37°C until an OD_{600} of 0.5 was reached. A 1 ml aliquot was removed from the culture and centrifuged at 13,000 x g and stored at –20°C as a representation of bacterial expression prior to induction. The bacterial cultures were induced by addition of anhydrotetracycline (final concentration: 0.1 ng/ml) and incubated for a further 2 h. A further 1 ml aliquot was stored following induction to confirm protein expression prior to purification.

2.13.2 Protein sample preparation

Protein samples of interest were purified using the TALON® metal affinity resin (Clontech) according to the manufacturer's instructions in order to isolate native proteins. The protocol was optimised to lyse bacteria using a One Shot Cell Disruptor (Constant Systems, Northants, UK) instead of sonication. The 150 ml cell culture was centrifuged at 2,000 x g for 15 min at 4°C. The cell pellet was resuspended in 4 ml chilled Equilibration/Wash buffer (50 mM Na_2HPO_4, 300 mM NaCl, pH 7.0) supplemented with 20 µl protease inhibitor cocktail set 3 (Calbiochem). Bacterial cultures were lysed by passage once through a One Shot Cell disruptor. The cell extract was centrifuged at 12,000 x g for 20 min at 4°C to pellet any insoluble material and the supernatant containing native proteins extracted. This method was repeated 6 times for each different recombinant protein of interest to produce sufficient amounts of recombinant protein for downstream applications.

2.13.3 Column purification

The following protocol was performed at 4ºC in order to decrease protein breakdown and loss. An aliquot (2 ml) of TALON® metal affinity resin (equal to 1 ml bed volume) was thoroughly resuspended per protein sample to be purified and centrifuged at 700 x g for 2 min to pellet the resin. The supernatant was discarded and 10 bed volumes of 1 x

Equilibration/Wash buffer was added and briefly vortexed to pre-equilibrate the resin. The resin was centrifuged for a further 2 min at 700 x g and washed with a further 10 bed volumes of 1 x Equilibration/Wash buffer. The supernatant was discarded and the clarified protein samples applied to the resin. Polyhistidine tagged proteins were bound to the pre-equilibrated resin by gently agitating the resin and extracted proteins on a platform shaker for 20 min at RT. Following incubation, the samples were centrifuged at 700 x g for 5 min and the supernatant removed. The resin was washed by adding 12 bed volumes of 1 x Equilibration/Wash buffer and agitated for 10 min. The suspension was centrifuged at 700 x g for 5 min and the supernatant discarded and the wash step repeated. The resin was resuspended by vortexing in one bed volume of 1 x Equilibration/Wash buffer and transferred to a 2 ml gravity flow column and allowed to settle out of suspension. The buffer was allowed to drain off until the top of the resin bed and then the column washed with 5 bed volume of 1 x Equilibration/Wash buffer. The polyhistidine tagged proteins were eluted by applying 5 bed volumes of 1 x Elution buffer (50 mM Na_2HPO_4, 300 mM NaCl and 150 mM imidazole, pH 7.0) to the column collecting the eluate in fractions.

2.13.4 Protein concentration

Following elution, protein samples were concentrated and the buffer exchanged to remove imidazole and elute proteins in the appropriate buffer for conjugation in spin columns with a 10,000 MWCO (Sartorius Stedim Biotech, France). Eluted proteins were applied to the concentrator and centrifuged at 3,000 x g in a swing bucket centrifuge for 10-30 min at 4ºC until the samples were concentrated from approximately 5 ml start volume to 0.5 ml final volume. The lower filtrate container was emptied and the concentrator refilled with 7 ml 0.05 M Na_2CO_3 buffer, pH 9.6 (Sigma) and the samples centrifuged again. Buffer exchange was completed following 2 further washes in Na_2CO_3 buffer for a total of 3 wash cycles.

2.13.5 Bradford assay

Extracted protein was quantified using a modified Bradford (1976) method. The method is based on the interaction of dye and protein producing a shift in absorbance that is correlated to the concentration of protein in the sample. A standard curve was prepared

using known concentrations of BSA (0-2,000 µg). Each BSA standard or sample (10 µl) was applied in triplicate to a 96-well flat-bottomed tissue culture plate and 300 µl Coomassie reagent (Pierce) added to each well. The samples were mixed for 30 s, incubated at RT for 10 min, and absorbance measured at 595 nm on a plate reader (Anthos 2010, SLS). Absorbance at 595 nm was used to calculate unknown protein concentration based on the standard curve.

2.13.6 SDS-PAGE and Western blotting

Purified proteins were analysed by SDS-PAGE using 4-20% gradient gels (section 2.12) and either stained with Coomassie (section 2.12.1) or subject to Western blotting (sections 2.12.2, 2.12.2.1) using antibodies shown in Table 2.3. An aliquot (30 µl) of each protein fraction was mixed with 20 µl sample loading buffer and boiled for 5 min. A 30 µl aliquot was loaded into each well of the gel alongside 15 µl Benchmark™ pre-stained ladder for comparison.

2.14 Bioconjugation of recombinant protein to porphyrin

2.14.1 Porphyrins

The porphyrin used in this study was kindly provided by Dr Ross Boyle and Dr Cristina Alonso (Department of Chemistry, University of Hull). The porphyrin structure (5-(4-isothiocyanatophenyl)-10,15,20-tris-(4-*N*-methylpyridiniumyl) porphyrin trichloride) is shown in Fig 2.3 (left hand side) with the NCS group able to react with lysine residues. The porphyrin was dissolved in anhydrous DMSO (Sigma) to a stock concentration of 5 mM prior to conjugation to the protein of interest. Additionally, a 5 mM stock solution of the same porphyrin was prepared in anhydrous DMSO except that the NCS group had been capped with an amino group, as shown in Fig 2.3 (right hand side), to use as a control in later toxicity assays.

Fig 2.3: Porphyrin structures

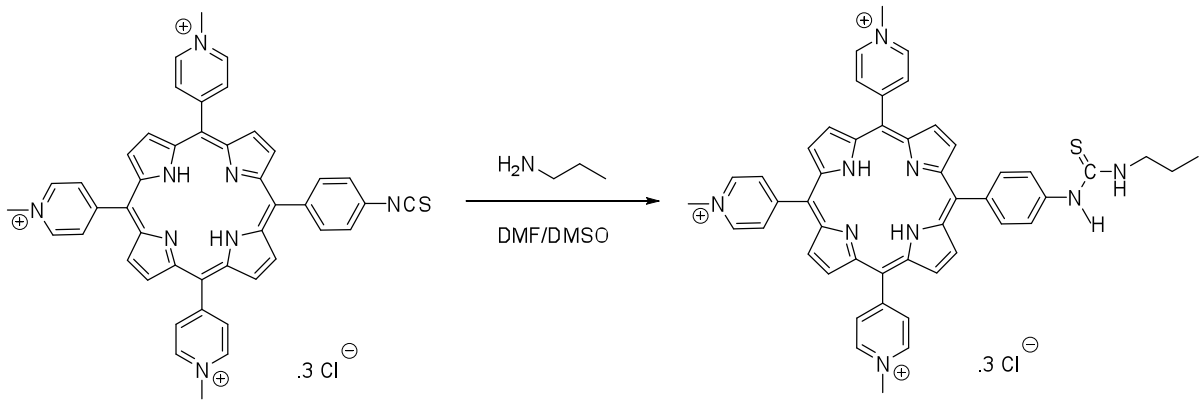

Fig 2.3: Structure of 5-(4-isothiocyanatophenyl)-10,15,20-tris-(4-*N*-methylpyridiniumyl) porphyrin trichloride.

2.14.2 Bioconjugation and purification procedure

Recombinant protein was conjugated to the porphyrin at a molar ratio of 5:1 porphyrin:protein by gentle agitation at RT for 1 h protected from light. Following conjugation, immediate purification of the conjugate was achieved through application onto a PD10 desalting column (GE Healthcare), according to the manufacturer's instructions, in order to remove unbound porphyrin. Briefly, the column storage solution was removed from the column and the column washed 4 times in 0.05M bicarbonate buffer (pH 9.6) discarding the column flow-through. Following equilibration, the conjugate was applied to the top of the column and the volume adjusted to 2.5 ml with bicarbonate buffer. The conjugate was eluted by addition of 3.5 ml bicarbonate buffer in seven 500 µl fractions and each eluate collected for analysis.

Fractions were characterised spectrophotometrically at 280 and 420 nm to monitor the protein and porphyrin respectively in order to determine which fractions contained the highest concentration of conjugate. Fractions containing the highest concentration, denoted by the highest absorbance readings (4 aliquots in total) were combined together and the absorbance at 260, 280, 320 and 420 nm determined in order to calculate the concentration of the protein/porphyrin and the degree of loading to calculate the moles of porphyrin per mole of protein. Conjugated protein and capped porphyrin were separated on a 4-20% gradient gel in order to visualise the conjugate using similar

methods to that described in sections 2.12. Following electrophoresis, the gel was illuminated with UV light to visualise the porphyrin and then stained with Coomassie in order to visualise the conjugated protein and porphyrin (section 2.12.1). The conjugate was stored protected from light at 4°C.

2.15 *In vitro* bacterial cytotoxicity assay

Cytotoxicity assays were performed against MRSA and *E. coli* based upon an optimised method established within our group (Hall, 2008). Bacterial cultures were adjusted with PBS to give a cell density of 1.11 x 10^7/ml. Bacterial aliquots (540 µl) were incubated with 540 µl P12 conjugated protein (final concentration; 1.25 µM). Additionally, bacteria (540 µl) were incubated with either 540 µl capped porphyrin to a final concentration of 1.25 mM or 54 µl capped porphyrin (final concentration; 12.5 µM) adjusted to a final volume of 1.08 ml with media. Bacteria only (540 µl) in 1.08 ml media and media only (1.08 ml) were also used as controls. Bacteria were allowed to incubate with the conjugate or capped porphyrin for 30 min at RT before centrifugation at 6,000 x g for 10 min to pellet the bacteria. The supernatant was carefully removed and discarded and each pellet resuspended in 1.08 ml fresh media. Aliquots (180 µl containing 1 x 10^6 cells) of each suspension were transferred in triplicate onto 2 separate 96-well flat bottomed plates. One plate (light plate) was irradiated with 40 J/cm^2 red light from a lamp at 633 nm (Omnilux EL1000A Phototherapeutics Ltd, Altrincham, UK) in a dark room to ensure light dose control and the other plate kept in the dark as a control (dark plate). Following irradiation, both plates were incubated for 30 min at 30°C at 225 rpm to replenish the oxygen levels. Once incubated, the light plate was further subject to irradiation with 40 J/cm^2 red light whilst the dark control plate remained in the dark. Both plates were incubated at 30°C overnight with shaking at 225 rpm. After incubation, the absorbance of each well was measured at 630 nm on an automated plate reader (Bio-tek Instruments) and the absorbance from triplicate wells averaged for data analysis. Cell growth (%) was determined in comparison to untreated control bacteria. Following overnight incubation, MRSA cultures from the light plate following incubation with the conjugate, capped porphyrin and bacteria only were serially diluted across the range of 10^{-3} to 10^{-7} in PBS and 100 µl plated out onto nutrient agar. The plates were incubated overnight at 30°C and bacterial colonies counted in order to determine the colony forming units (cfu)/ml.

2.15.1 *In vitro* keratinocyte cytotoxicity assay

Keratinocyte cytotoxicity assays were kindly performed by Huguette Savoie. Keratinocytes (1.11 x 10^6cells/ml) in supplemented media without foetal bovine serum (FBS) were incubated with conjugate, capped porphyrin (1.25 µM final concentration) or 10-fold excess of capped porphyrin (final concentration; 12.5 µM) in sterile 75 x 12 mm polystyrene tubes for 30 min at RT in the dark. Following incubation, keratinocytes were washed with 5 ml of supplemented media without FBS to remove unbound conjugate or porphyrin. The cells were centrifuged at 1,200 x g for 10 min and resuspended in serum free media. Aliquots (180 µl containing 1x10^5 keratinocytes) were plated out in triplicate onto two separate 96-well flat bottomed plates. One plate (light plate) was irradiated with 40 J/cm^2 whilst the other non-irradiated plate was kept in the dark. Both plates were incubated for 30 min at 37°C and the light plate irradiated for a further 40 J/cm^2. FBS (5 µl) was added to each well and each plate incubated overnight at 37°C.

An MTT assay was performed to determine the number of viable cells that utilise the tetrazolium salt (3-4, 5-dimethylthiazol-2-yl)-2, 5-diphenyltetrazolium bromide) that is reduced to formazan in the mitochondria of metabolically active cells. The greater the amount of formazan product produced the greater the cell growth which is therefore proportional to the amount of living cells. MTT reagent (10 µl; Sigma) was added to each well and incubated at 37°C to allow the colour to develop (~90 min). Following sufficient colour development, 150 µl MTT lysis solution (0.02 M isopropanol/HCl) was added to stop the reaction and dissolve the formazan product by vigorous pippetting. The plates were read at 630 nm using an automated plate reader.

2.16 Flow cytometric analysis of unconjugated purified proteins

Flow cytometric analysis was performed to characterise binding of purified unconjugated recombinant proteins P5 and P19 with proposed binding affinity for MRSA and also against *E. coli* and a human keratinocyte cell line for comparison. The concentration of P5 and P19 was determined by Bradford assay (section 2.13.5). Bacterial cultures (4 ml) were centrifuged at 2,000 x g for 10 min at 4°C. The supernatant was discarded and each pellet was resuspended in 4 ml filter sterilised (0.2

μM) PBS, used in all subsequent applications, supplemented with 2% milk powder and 1% BSA. The bacteria were incubated in blocking buffer for 30 min at 4°C and re-centrifuged and each pellet resuspended in 4 ml PBS. Individual bacterial aliquots of MRSA and *E. coli* (both 5 x 10^5) were incubated separately with 200 μl of P5 or P19 (final concentration 173 μg/ml) and the proteins were allowed to bind to the bacteria for 30 min at RT. Following incubation, bacterial suspensions were incubated with 10 μl of a rabbit anti-thioredoxin antibody (Abcam) (0.5 μg; 1:10 dilution in PBS) and incubated for 30 min at RT.

PBS (200 μl) was added and bacteria were centrifuged at 6,000 x g for 5 min and resuspended in 25 μl secondary sheep anti-rabbit:FITC (Serotec). The secondary antibody was incubated for 30 min at RT. PBS (400 μl) was added to each tube and then centrifuged for a further 6,000 x g for 5 min to wash the cells. The supernatant was discarded and each pellet was resuspended in 150 μl PBS for flow cytometric analysis. A non-treated bacterial suspension and also bacteria incubated individually with either the primary or secondary antibody or both antibodies without recombinant protein were used to define FACS analysis parameters. Furthermore, recombinant protein binding to a human keratinocyte cell line was also performed using the method described except that 1 x 10^5 cells were used. Keratinocytes were prepared for flow cytometry as described in section 2.8.1.2.

2.16.1 Determination of GFP tagged recombinant protein binding by flow cytometry

The binding ability of P5/GFP to MRSA, *E. coli* and keratinocytes was characterised by flow cytometry. Bacterial suspensions of MRSA and *E. coli* were blocked and resuspended in PBS, as described in section 2.16. Keratinocytes were prepared for flow cytometry under the same conditions as illustrated in section 2.8.1.2. The concentration of P5/GFP was determined by Bradford assay (section 2.13.5). Bacterial suspensions (5 x 10^5) or keratinocytes (1 x 10^5) were incubated with 0, 5, 25 and 50 μl (0 – 398 μg/ml) of P5/GFP at RT for 45 min. The cells were washed as described above in section 2.16 and each pellet resuspended in 150 μl of filtered PBS prior to flow cytometry analysis.

CHAPTER THREE

Identification and characterisation of novel peptide sequences derived from a MRSA-panned library

3.1 Introduction

Chronic wounds such as venous ulcers are frequently of a polymicrobial nature that usually includes a combination of aerobic and anaerobic bacterial species. However, although the bacteriology of venous ulcers is diverse, *S. aureus*, including drug resistant strains such as MRSA, is often one of the predominant organisms isolated from venous ulcers (Gjodsbol et al., 2006, Valencia et al., 2004). *S. aureus* can be carried innocuously by healthy people but is an important opportunistic pathogen capable of causing a wide range of superficial and serious skin and soft tissue infections at multiple sites (Livermore, 2000). Resistant strains of *S. aureus* quickly emerged following the introduction of penicillin, and furthermore to synthetic drugs such as methicillin, originally developed to combat the emergence of these resistant strains. MRSA has emerged not only as a significant nosocomial pathogen but also an important and frequent cause of community acquired infection. Bacterial resistance to antibiotics has continued to increase over time resulting from multiple factors including the extensive use of antibiotics, antibiotic misuse and ineffective treatment regimens. As a result, strains of MRSA have emerged that are multiply resistant to nearly all classes of antibiotics (Barrett, 2004).

Since the first display system, pioneered by Smith (1985) to display small peptide fragments on the surface of phage, the display of foreign peptides/proteins has been achieved utilising various display platforms which have identified ligands with high affinity and specificity that interact with target molecules. Display technologies can offer a high-throughput and relatively inexpensive methodology to identify a wide range of ligands with different binding specificities. Affinity selection, or panning, using display technologies involves the selection of 'binders' to a target of interest, from an excess of non-binders, that are then successively recovered and amplified through rounds of panning in order to enrich clones with specific, desired binding affinity.

Bacterial display in which proteins are displayed on the surface of bacteria have since emerged as a successful complement to phage display, although phage display remains the most described within the literature. Bacterial display offers an attractive alternative to phage display in that it can offer advantages including the potential of utilising flow cytometry for high throughput screening and direct microscopy without the need for additional phage labelling. The methodology also allows direct recovery of clones of interest from a self-replicating system without additional infection steps required with phage technology (Dane et al., 2006, Chen and Georgiou, 2002). Peptides, proteins, antibodies and enzymes have all been successfully displayed on the cell surface of both Gram-negative and Gram-positive species as either fusion proteins to outer membrane proteins, or displayed on surface appendages such as flagella or fimbriae. Bacterial display systems have been utilised to identify an array of ligands with specificities to numerous different targets including those with potential targeting/drug delivery properties, vaccine development and bioremediation applications (Wernerus and Stahl, 2004, Lee et al., 2003).

In this study the FliTrx ^{TM} bacterially-displayed random peptide library (Invitrogen), developed by Lu et al (1995), displaying 12-mer peptides in a conformationally constrained manner was screened in order to identify peptide sequences that bind to the surface of MRSA. Such MRSA-specific peptides could be of value in early detection of antibiotic-resistant isolates within a wound as well as having potential in targeted drug delivery. Peptides with proposed binding specificity to MRSA were selected by panning against MRSA. The DNA sequences of randomly selected clones following panning were determined and sequence homology compared. Peptides were synthesised and their binding ability characterised by flow cytometry to 3 different strains of MRSA and also against *S. aureus* and *S. epidermidis, P. aeruginosa, E. coli* and a mammalian keratinocyte cell line to evaluate specificity.

3.2 Methods

3.2.1 UV irradiation and fluorescent staining of MRSA

Bacterial cultures were grown to late log phase and subject to UV-C exposure. Bacterial aliquots were extracted and plated onto nutrient agar and inspected for bacterial growth

following incubation at 30ºC for 24-48 h (section 2.3). Bacterial viability following UV irradiation of MRSA was also assessed using a fluorescence-based assay utilising SYTO 9 and PI fluorescent dyes and confocal microscopy analysis to discriminate between viable and non viable cells (section 2.3.1).

3.2.2 Investigation of bacterial immobilisation

Immobilisation of both live and UV-inactivated MRSA was performed using 6-well plates coated with either poly-L-lysine, poly-D-lysine or collagen I (section 2.4) in order to simplify recovery of clones expressing the random peptides from the target cells. Bacteria were allowed to adhere overnight at 4°C and washed according to the panning protocol. The remaining immobilised bacteria were stained with methylene blue and measured spectrophotometrically (section 2.4).

3.2.3 Panning and DNA sequencing

The panning procedure was performed against MRSA adsorbed onto poly-L-lysine coated tissue culture plates (section 2.5.2, 2.5.3, 2.5.4). Both MRSA and *E. coli* library cultures were plated out onto nutrient agar following each round of panning to ensure that there was no contamination of bacterial cultures, and were used to inoculate oxoid mannitol broth to confirm the presence or absence of MRSA as appropriate (section 2.5.4). Following 5 successive rounds of panning, cultures were plated out onto RMG plates (section 2.5.4). A negative panning step was performed following the successive rounds of positive panning (section 2.5.5). Single colonies were then selected and grown in RM medium to obtain high yields of plasmid DNA. Plasmid DNA was extracted and quantified (section 2.6, 2.6.1). PCR was performed to amplify the insert (section 2.7) for subsequent sequencing reactions and analysed by electrophoresis (section 2.7.1). Following PCR clean-up, ethanol precipitation was performed prior to double stranded DNA sequencing (section 2.7.2).

3.2.4 Peptide synthesis

Two different peptides sequences were synthesised commercially with disulphide linked N- and C- terminal cysteines to retain the proposed binding structure as per panning,

and without this disulphide bond to give a linear construct for comparison. All peptides were synthesised with an N-terminal biotin (section 2.8). Additionally, one of these peptides was synthesised replacing the N-terminal biotin with a C-terminal FITC, in both the cyclic and linear constructs for assessment of binding directly, without the need for additional probes.

3.2.4.1 Assessment of binding of biotinylated and FITC-labelled peptides by flow cytometry

Cyclic and linear biotinylated peptides were assessed for binding potential to both live and UV-irradiated MRSA, *S. aureus* and *S. epidermidis* (section 2.8.1). Preincubated peptide: streptavidin-PE:Cy5 solutions were incubated with bacteria, washed and analysed by flow cytometry. Additionally, bacteria were incubated with biotin and unconjugated streptavidin to saturate non-specific binding sites prior to incubation with peptide: streptavidin-PE:Cy5 solutions for flow cytometric analysis (section 2.8.1). Cyclic and linear FITC-peptides were incubated with 3 different strains of MRSA and also *S. aureus*, *S. epidermidis*, *P. aeruginosa*, *E. coli* and keratinocytes and analysed by flow cytometry (section 2.8.1.2).

3.3 Results

3.3.1 Investigation of UV irradiation and fluorescent staining to determine optimal killing of MRSA cultures

The effect of UV irradiation to inactivate MRSA cultures was first determined so that the target cells (MRSA) were not able to compete with the *E. coli* peptide library, and therefore simplify the recovery of positive library clones. Preliminary investigation using a 15 W 254 nm UV lamp demonstrated that irradiation of a bacterial culture (10 ml) positioned 15 cm distance from the lamp, and irradiated for up to 30 min, had an effective bactericidal consequence, as determined by no growth on nutrient agar following overnight incubation. Furthermore, doubling the density of bacteria/ml (from 3.3×10^8 to 6.7×10^8/ml) in order to improve bacterial coverage of the plates for later immobilisation studies meant that 120 min of UV exposure at 15 cm distance using the 15 W lamp was required to kill the bacteria. Due to this lengthy killing time a new 15 W

254 nm UV lamp was installed. A maximum of 5 min of UV exposure of a 10 ml culture (6.7 x 10^8 bacteria/ml) that was 10 cm distance from the lamp was sufficient to kill the bacteria prior to each round of panning.

To confirm the effect of UV irradiation, visualisation of MRSA cultures by confocal microscopy utilising fluorescent dyes that differ in their ability to penetrate healthy cells was performed. Live MRSA cultures were dual stained with the fluorescent dyes SYTO 9 and PI and a different culture was stained following exposure to UV radiation. SYTO 9 stains both live and dead bacteria and fluoresces green. Whereas, PI penetrates only bacteria with damaged membranes and fluoresces red. Results indicated that overall, UV radiation is effective at killing MRSA (Fig 3.1). The non-irradiated cultures stained predominantly green, indicating healthy viable cells, although some were stained red denoting bacterial cell death. In contrast, UV irradiated bacteria were mainly stained red indicating cell death with only a small proportion of live bacteria present.

3.3.2 Investigation of bacterial immobilisation

The effect of MRSA immobilisation onto different substrates was investigated prior to panning experiments. Preliminary investigations showed that bacterial cultures left to adhere to wells overnight at 4°C resulted in greater bacterial adhesion than those left to adhere for 2 h at RT or 4°C. Furthermore, preliminary investigation into doubling the density of bacteria/ml and subsequent immobilisation of bacteria onto plates resulted in near maximal plate coverage as determined by light microscopy and visible examination of the plates. Following immobilisation, the wash procedures used in panning were performed in order to confirm that bacteria would remain adhered to the plate for the duration of the panning protocol. The greatest amount of bacterial immobilisation was observed using plates coated with collagen I as determined by staining the bacteria that had adhered with methylene blue and measuring the absorbance (A_{668} = 1.07) as shown in Figure 3.2. Plates coated in poly-L-lysine showed a reduction in bacterial adhesion compared with collagen I coated plates (A_{668} = 0.88) and a further decrease in bacterial adhesion was observed using plates coated in poly-D-lysine (A_{668} = 0.81) (Fig 3.2). Furthermore, staining of collagen I immobilised live bacteria demonstrated a greater than two-fold increase in absorbance than when using UV inactivated cells (A_{668} = 1.07 vs. 0.43), suggesting that the irradiation was inhibiting an active adhesion process. A

similar effect was observed when immobilising live bacteria compared with UV inactivated onto both poly-L-lysine (A_{668} = 0.88 vs. 0.42) and also poly-D-lysine (A_{668} = 0.81 vs. 0.38). This result was further supported by visualisation of the immobilised bacteria, demonstrating that near maximal plate coverage was still retained following washing according to the panning protocol (Fig 3.3).

3.3.3 Panning and DNA sequencing

The panning process was undertaken against MRSA, *S. aureus* and *S. epidermidis* to select for peptides with binding specificity for the desired target cell. No contamination of either the library of target bacterial cultures was observed from plating of cultures onto nutrient agar or utilising mannitol fermentation to confirm the presence/absence of MRSA in any round of panning. Following negative selection, sequencing of plasmid DNA from panned library cultures resulted in a low signal to noise ratio, whereby accurate determination of each individual DNA sequence was problematic. Subsequently PCR was performed to amplify the insert from plasmid DNA for DNA sequencing. Preliminary investigations were performed varying the number of cycles, in order to optimise the DNA amplification process, together with the type and percentage gel to be used to best visualise the inserts. It was determined that 35 cycles, and running the PCR products on a 4.5% (w/v) Agarose-1000 gel was most effective at amplifying and visualising the peptide inserts. Following PCR amplification and verification by agarose gel electrophoresis confirming a DNA fragment of 177 bp, the samples were sequenced. Further details of the molecular cloning of the thioredoxin moiety containing the selected peptides are given in detail in Chapter 4.

3.3.3.1 MRSA peptide sequence analysis

The amino acid sequences of 20 randomly selected peptides from the completed panning process against MRSA were determined and analysed for possible consensus sequences including criteria such as charge of the amino acid R-groups and repeats. The amino acid sequences of the selected peptides are shown in Figure 3.4. No obvious consensus sequence amongst these 20 peptide sequences was observed, and no clones of the same sequence were selected more than once. Additionally, no clear repeating sequences were observed.

The most frequently occurring amino acid was arginine accounting for 14.6% of residues from the 20 sequences. Other frequently occurring amino acids include alanine, glycine, valine and serine (9.2%, 9.2%, 7.9% and 6.7% of residues respectively). Analysis based on charge of the amino acid R-group also revealed no distinct patterns. However, nearly all of the peptides sequenced contained at least one charged residue with positively charged residues (15.8%) occurring slightly more frequently than negatively charged residues (11.3%), however one peptide sequence was composed entirely of neutral amino acids (peptide3). Surprisingly, eleven of the 20 randomly selected sequences contained in-frame stop codons.

3.3.3.2 *S. aureus* and *S. epidermidis* peptide sequence analysis

The amino acid sequences of randomly chosen peptides derived from panning against *S. aureus* and *S. epidermidis* are shown in Figures 3.5 and 3.6 respectively. Similarly to MRSA derived peptide sequences, no clear consensus sequences were observed for either set of sequence data. The predominantly occurring amino acids in the S. *aureus* derived sequences were arginine (14.8%), valine (13.9%), glycine (13%) and leucine (12%). Positively charged residues accounted for 18.5% of all amino acids and negatively charged residues accounted for 10.2%. Only 1 peptide sequence contained a stop codon and all sequences contained at least one charged residue.

Similarly to sequences derived against MRSA and *S. aureus*, arginine (23.5%) was the most predominant amino acid residue that occurred within the selected sequences against *S. epidermidis*. Serine (12.1%), glycine (10.6%), leucine and lysine (both 8.3%) also occurred frequently. Positively charged residues accounted for 31.8% of all amino acids sequenced whereas only 2.3% were negatively charged and charged residues were present in all of the derived sequences. One peptide sequence contained a stop codon.

3.3.4 Assessment of biotinylated peptide binding by flow cytometry

Two peptide sequences derived from panning (Fig 3.4; peptide19 and peptide12) that were not particularly similar to each other in sequence, but did share sequence homology with the other sequences selected against MRSA, were commercially

synthesised. Both peptides were synthesised as both linear and conformationally constrained structures with N-terminal biotin for characterisation of binding to bacteria.

This method was subject to extensive optimisation. Preliminary investigation by flow cytometry and confocal microscopy compared streptavidin FITC and streptavidin PE:Cy5 as detection molecules to assess peptide binding of the biotinylated peptides. Although both streptavidin FITC and streptavidin PE:Cy5 and biotin alone were demonstrated to be able to bind to the surface of bacteria, subsequent analysis was performed using streptavidin PE:Cy5 as this gave a brighter signal with flow cytometry and more stable signal with confocal microscopy.

Preliminary investigations to assess binding of freely available peptides in solution followed by secondary labelling with streptavidin PE:Cy5 demonstrated no clear peptide binding to the bacterial surface. Therefore, the peptides were preincubated with streptavidin at a molar ratio of 5:1 prior to binding to bacteria in order to saturate the biotin binding sites on the streptavidin with the intention of excluding any contribution to binding from streptavidin. Additionally, preliminary binding studies were performed using a range of serially diluted peptide concentrations and was optimised so that all binding studies were performed assuming that there were 100,000 targets/cell for the peptide to potentially bind to. Therefore all experiments were calculated to contain the same number of peptide molecules (100,000 peptides per bacteria) and the relative number of streptavidin PE:Cy5 molecules based on a ratio of 5:1, all in the same volume, in order to optimise peptide binding. The binding of the peptides to both live and UV-inactivated strains of MRSA1 is shown in Figure 3.7. The FSC/SCC (Panel A) of MRSA1 was used to identify the main bacterial population for analysis. No binding was observed for any peptide construct, demonstrated by no difference between the cyclic and linear constructs or compared with the streptavidin PE:Cy5 only as a negative control (Panels B-E; Fig 3.7). However, in both cases, binding of peptides and streptavidin PE:Cy5 was greater to live bacteria than binding to UV-inactivated bacteria (Fig 3.7). Furthermore, no binding of peptides was observed against two other strains of MRSA (MRSA2 & MRSA 3), *S. aureus* or *S. epidermidis*.

Due to the non-specific binding capability of streptavidin and biotin alone, attempts were made to block the bacteria with unconjugated streptavidin preincubated with

biotin, or a 10-fold excess of biotin in order to saturate non-specific binding before addition of peptides. Flow cytometry profiles characterising binding are shown in Figure 3.8. Bacterial populations were similarly identified based on FSC/SSC analysis for MRSA1 (Fig 3.8; Panel A). Binding of peptide12 and peptide19 to MRSA1 are shown in panels B-E. Mean fluorescence and the percentage of the gated marker are shown in Table 3.1. Generally, no binding of either peptide was observed in comparison to the streptavidin alone control (Fig 3.8, Table 3.1). A very small difference between the cyclic and linear constructs was observed with cyclic peptide19 binding slightly better to MRSA than the linear peptide19 construct, whereas the linear peptide12 appeared to bind better than cyclic peptide12 to MRSA (Table 3.1, Fig 3.8). However, in both cases there was a slight increase in mean fluorescence following preincubation with the biotin:unconjugated streptavidin complex (5:1) that was further increased following preincubation with the biotin:unconjugated streptavidin (50:1) complex compared with the negative control presumably due to non specific protein interactions (Table 3.1, Fig 3.8). A similar effect was observed following binding to a different strain of MRSA (MRSA2).

Due to streptavidin and biotin apparently binding to MRSA alone, an anti-biotin antibody conjugated to Cy5 was used to attempt to characterise peptide binding in a different way that did not involve streptavidin (Fig 3.9). Bacterial populations of MRSA1 and MRSA2 were selected based on FSC/SSC properties as before (Panels A and B respectively). Binding of cyclic and linear peptide19 and peptide12 to MRSA1 are shown in Panels C and D respectively. Panels E and F represent FACS profiles used to determine binding of both peptides (in both cyclic and linear constructs) to MRSA2. Overall, no peptide binding was observed against either strain of MRSA.

3.3.4.1 Characterisation of binding of FITC-labelled peptides by flow cytometry

Due to the difficulties associated with secondary labelling in order to assess peptide binding to bacteria, one of the peptides of interest was re-synthesised directly conjugated to a fluorophore (FITC). It was not considered possible to re-synthesise peptide19 to characterise binding due to the presence of a lysine residue within the sequence that would affect conjugation of the peptide to the fluorophore. The binding of FITC-labelled peptide12 alone in a cyclic and linear conformation against 3 strains of

MRSA was characterised by flow cytometry. FACS profiles used to determine peptide binding to MRSA are shown in Figure 3.10a. A typical FSC/SCC profile (Panel A) was used to identify the main bacterial population for analysis as described previously. Binding of the cyclic peptide12 to MRSA1 was demonstrated by an increase in fluorescence (Panel B - green; mean = 33.8, gated marker = 37.5%) compared to that of MRSA alone (mean = 19.5, gated marker = 8.3%). However, no binding of the linear construct was observed (Panel B - pink; mean = 9.2, gated marker = 3.7%). Similarly, an increase in fluorescence was observed denoting binding of the cyclic peptide12 (Panel C - green; mean = 20.6, gated marker = 34.2%) to MRSA2 alone (Panel C; mean = 8.7, gated marker = 8.5%). The linear peptide12 demonstrated no binding affinity (Panel C - pink; mean = 7.3, gated marker = 7.9%). Binding of the cyclic peptide12 was also observed to a different strain of MRSA (MRSA3) (Panel D - green; mean = 7.5, gated marker = 32.4%) in comparison to MRSA3 alone (mean = 4.0, gated marker = 8.7). Again, no binding of the linear construct was observed (Panel D - pink; mean = 3.8, gated marker = 10.9%).

Furthermore, peptide binding was also assessed against *S. aureus*, *S. epidermidis*, *P. aeruginosa*, *E. coli* and a mammalian keratinocyte cell line for comparison and to determine whether the peptide has any reactivity for a eukaryotic cell type (Fig 3.10b). Bacterial populations were determined based on FSC/SSC analysis shown previously. Panel A demonstrates binding of peptide12 to *S. aureus*. A limited amount of binding of the cyclic construct was observed (Panel A - green; mean = 3.4, gated marker = 30.1%) compared to *S. aureus* alone (mean = 2.0, gated marker = 8.5%). A very small increase in mean fluorescence was observed following incubation with the linear construct compared with control values (Panel A - pink; mean = 2.2, gated marker = 13.0%). Similarly, peptide12 (cyclic) showed a small level of binding to *S. epidermidis* (Panel B - green; mean = 3.7; gated marker = 45.0%) compared to *S. epidermidis* alone (mean = 1.6, gated marker = 8.8%) and peptide12 (linear) (Panel B - pink; mean = 2.9; gated marker = 35.4%). Binding of cyclic peptide12 was observed against *P. aeruginosa* (Panel D -green; mean = 6.1; gated marker = 49.6%) in comparison to the control (mean = 1.2, gated marker = 8.1%). The linear construct demonstrated a small degree of binding (Panel D- pink; mean = 2.1; gated marker = 29.7%). No binding was observed for either the cyclic or linear construct of peptide12 against *E. coli* (Panel C). Additionally, no binding was observed against a keratinocyte cell line (Panel E).

3.4 Discussion

Peptides with MRSA binding properties were selected through panning of a random peptide library and characterised by DNA sequencing. Two peptides were synthesised commercially and the ability of selected peptides to bind methicillin-sensitive and methicillin-resistant strains of *S. aureus* was assessed by flow cytometry. Additionally, one peptide was synthesised that was directly conjugated to a fluorophore for direct assessment of binding against *Staphylococci*, Gram-negative bacteria and a keratinocyte cell line by flow cytometry.

The effective UV inactivation of MRSA bacterial cultures prior to panning experiments was considered important in order to simplify the recovery of positive clones from the *E. coli* library culture to ensure that MRSA was not able to compete with the peptide library. The application of UV radiation in this investigation was successful in inactivating the MRSA cultures as no bacterial growth was observed on any occasion (n = 20) following 5 min UV exposure. The use of UV-C radiation (200-280 nm) has a lethal effect on bacteria whereby absorption by DNA causes genetic damage and inactivation of bacteria. The use of UV radiation has previously been shown to kill cultures of MRSA *in vitro* (Conner-Kerr et al., 1998) and reduce MRSA in chronic superficial wounds following a 180 second exposure (Thai et al., 2005). The use of fluorescence staining techniques further confirmed the bacterial death following UV exposure. Overall, live bacterial cultures of MRSA were mainly stained green indicating healthy viable cells, although some were stained red denoting bacterial cell death, presumably this being due to the sample preparation time of approximately 2 h. In contrast, >90% of UV-irradiated bacteria were stained red indicating cell death. However, although some bacteria may fluoresce green indicating an intact bacterial membrane, UV exposure was presumably sufficient to prevent growth in a nutrient medium.

Immobilisation of the MRSA onto tissue culture plates prior to panning was needed to enable simple recovery of positive library clones, whereby the unbound library without the desired binding abilities are washed away from the specifically bound clones. The library clones displaying peptides that bind MRSA can subsequently be eluted by mechanical shearing, amplified, and subject to successive rounds of panning in an

analogous fashion to epitope mapping using the FliTrx™ library (Ito et al., 2004, Lu et al., 1995, Singleton et al., 2001). Concentration of the bacteria and overnight adhesion to the plates greatly improved bacterial plate coverage. Furthermore, it was demonstrated that immobilisation improved significantly using live bacterial cultures as opposed to those previously UV irradiated, indicating that bacterial immobilisation onto the precoated surfaces is an active process. It was expected that the bacteria would adhere to collagen as the bacteria express collagen-binding adhesins on the cell surface (Foster and Hook, 1998). Furthermore, there have been numerous reports in the literature regarding the use of poly-lysines (D- or L-) to promote cell attachment to surfaces whereby the negatively charged bacterial cell wall is attracted to the positively charged poly- L- or D- lysine. Poly-L-lysine was used for subsequent bacterial immobilisation onto tissue culture plates prior to panning due to the unavailability of collagen I coated plates, even though this had initially given slightly better bacterial adhesion.

DNA sequencing of bacterial clones selected at random following panning against MRSA revealed that no predominant peptide sequence was isolated and neither were any obvious repeating subunits found. The variety of peptide sequences isolated and lack of consensus sequence observed may simply reflect the diversity of the bacterial target. A lack of overall consensus sequence was also observed by Brown et al (2000) following sequencing 100 clones derived from panning of the FliTrx™ library against a tumour-derived endothelial cell line. However although no obvious consensus was observed, this group did identify some recurring repeat sequences of 3-mer or more (17) that were predominately of a positive-positive-hydrophobic sequence.

Determination of the surface target to which the individual peptides bind is difficult to determine but possible surface targets could include peptidoglycan, teichoic acid or surface proteins that are all abundant bacterial cell wall components. If panning was performed against a single target it seems reasonable to assume that a greater degree of homology may be observed from the isolated peptide sequences. Consensus sequences are often obtained from epitope mapping of antibodies and would be expected to result in a higher frequency of consensus sequences obtained because sequences are selected for the antibody binding site only. However, Yacoby et al (2006) used a phage display peptide library displaying random 12-mer disulphide constrained peptides to pan against

live *S. aureus* in 4 rounds from a display library with a diversity of approximately 10^9 clones and identified repeated peptide sequences. Similarly, Dane et al (2006) used fluorescent bacterial display libraries of a diversity of $2x10^9$ and identified several consensus groups following screening against a breast cancer cell line by affinity selection by flow cytometry after screening of 70 clones. Therefore, a natural continuation of this work is to screen further clones from the MRSA panning, as the data may then yield a more obvious consensus sequence or repeated sequences.

Arginine was the most frequently isolated amino acid from all of the sequence data obtained, suggesting that this positively charged arginine residue may have been selected for from the diverse library by binding to the negatively charged bacteria. Arginine rich peptides were also identified by Brown et al (2000), following panning against tumour derived endothelial cells whereby most repeating sequences were basic in charge. However, lysine is also a positively charged amino acid that was not particularly prevalent in MRSA or *S. aureus* derived peptide sequences, although it was one of the most frequently occurring in *S. epidermidis* derived peptides. It would be anticipated that if it was simply the charge of the amino acids in the peptides that was an important determinant of individual peptide binding to bacteria then lysine and arginine residues would be seen at an equal frequency. However, six different codons code for the amino acid arginine whereas only two code for lysine, which may account for why less lysine residues were identified than arginine in the selected peptide sequences. Additionally, negatively charged residues were also isolated in individual sequences. Collectively all 20 different amino acids (not including selenocysteine and pyrrolysine) were represented within the sequences further suggesting that the displayed peptides could be against a diverse range of targets present on the bacterial surface rather than against a few predominately negatively charged moieties.

Numerous in-frame stop codons were identified in DNA sequences following panning against bacteria. Other studies selecting potential binding clones from the FliTrx™ library have also identified the presence of stop codons within sequences (Dinglasan et al., 2005, Yoshida et al., 2002); although do not identify the actual proportion. Therefore it may be expected that other studies performed using this library may have also identified stop codons within sequences that were unreported within the literature.

Following sequencing, two peptide sequences (peptide 19 and peptide12) that shared the greatest sequence homology with the other peptides with proposed binding to MRSA (Fig 3.4), but were not overly similar to each other in sequence, were selected and synthesised. The peptide binding ability against a range of bacteria, including the strain of MRSA that the library was panned against and also two other MRSA strains for comparison was determined by flow cytometry. Assessment of the binding ability of the two different peptides was difficult to determine due to the relatively high degree of binding of streptavidin or biotin alone to bacteria. This adhesive/'sticky' nature of the cell surface of MRSA may be due to the numerous surface proteins expressed by the bacteria (such as collagen, fibronectin and fibrinogen binding proteins) that help contribute to the pathogenic potential of MRSA that promote attachment leading to colonisation and invasion (Foster and Hook, 1998).

Peptide display technology can identify peptides with a range of affinities. Display systems vary in the amount of each ligand that is expressed, and in the original display vehicle (FliTrx™ library), peptides are expressed as a multivalent construct. Increasing the valency of the interaction is likely to cause an increase in the strength of binding; whereby selection from the FliTrx™ library may be based either on selection of strong binders based on high affinity, or, selection of modest/low affinity binders selected due to strong binding based on an avidity effect (Lu et al., 1995). Therefore selection using this library may possibly adopt a conformation to bind and therefore peptide binding may be improved by adopting a multivalent display approach as opposed to single peptides where weak/low affinity binding may be observed. Therefore, attempts were made to optimise the methodology by preincubating the peptide and streptavidin to form a peptide:streptavidin complex. One advantage of this would be to exclude the binding potential of streptavidin and another advantage would be the multimerisation of the peptides as four individual peptides would saturate the biotin-binding sites on the streptavidin molecule and therefore increase the avidity towards the target. De et al (2005) identified that tetramerisation of the peptide increased target binding affinity suggesting this effect by arguing that multivalent display showed greater similarity to the original phage expression (3-5 copies) during selection. However, in this instance, even though a multivalent approach to improve binding was attempted, removal from the overall display structure used in panning and potentially low binding affinity may have contributed to a limited binding effect. Although no peptide binding to any strain

of bacteria was observed compared with the control, flow cytometry analysis did indicate that binding of peptides was increased following peptide incubation with live bacteria cultures than those that had been previously UV-irradiated. This suggests that binding is an active process requiring the presence of live bacteria within the sample for maximum peptide binding or may indicate non-specific peptide uptake by live bacteria as the negative control also increased.

Further attempts to identify binding were undertaken by blocking the bacterial surface with unconjugated streptavidin and biotin to saturate any non-specific binding prior to testing of peptide binding. This appeared to improve binding presumably by increasing protein-protein interactions due to aggregation at the bacterial surface and may not necessarily reflect a true increase in peptide binding. This additional step of blocking the bacteria may have changed the surface of the bacteria to improve binding or possibly altered the target. Additionally, although preincubation steps were performed at a molar ratio of 5:1 in order to saturate the biotin binding sites on the streptavidin, if there were free binding sites on the streptavidin this may have contributed to an increase in mean fluorescence observed. Further attempts to characterise peptide binding utilising an anti-biotin antibody for secondary detection to try to utilise a different mechanism than streptavidin for detection were also unsuccessful. However, bacteria labelled with streptavidin PE:Cy5 only as a negative control to determine peptide binding may not be an appropriate control due to the ‘sticky’ bacterial surface. Similarly, an IgG anti-biotin antibody will bind non specifically to the surface of bacteria to a certain extent due to surface expression of protein A that enables the binding of numerous isotypes of IgG antibodies (such as the anti-biotin Cy5 used for detection) (Roberts and Gaston, 1987). Nonetheless, although there were difficulties associated with selecting an appropriate negative control for binding assessment and extensive optimisation to improve peptide binding, there was neither any difference in binding potential of the two different peptides or between cyclic and linear constructs indicating that no biotinylated peptide showed any particular affinity towards any bacterial strain investigated. All future similar studies based on target selection should therefore concentrate on using direct labelling or increasing valency to mimic the original selection construct to assess peptide binding when using flow cytometry.

Direct labelling of the peptides with a FITC fluorophore demonstrated binding of the cyclic construct against all three strains of MRSA tested. In all FITC-peptide binding studies, the cysteine constrained cyclic construct bound greater than the linear version in binding studies against bacteria, and in particular against MRSA. This 'better binding' would be expected as this conformation reflects its structure when originally panning to select for peptides ligands of interest. Previously, conformationally constrained peptides have been demonstrated to bind the selected target three times greater than linear peptides (Giebel et al., 1995, Oneil et al., 1992). Interestingly, the cyclic peptide bound most successfully to the strain of MRSA that it was panned against originally and therefore lends weight to the possibility that this technique could be suitable to identify a range of peptides against different pathogens. Furthermore, no binding to keratinocytes was observed, suggesting no binding potential towards eukaryotic cell types that can permit the selective targeting of pathogens without harmful effects to the host. The cyclic peptide also showed some binding to *S. aureus* and *S. epidermidis*. Peptides with specificity for MRSA may be expected to be effective against non-resistant *S. aureus* due to a similar bacterial cell surface and may suggest an enhanced role of isolated peptides for bacterial targeting. Some binding ability may also be expected against *S. epidermidis* due to homology amongst members of the *Staphylococci*, although may bind less, possibly due to slight differences and targets on the bacterial surface. No binding was observed against *E. coli*, a Gram-negative bacteria used as a control, suggesting that the peptide is not directed towards a target that is expressed on all prokaryotic cell types. However, interestingly binding of the cyclic construct was observed against *P. aeruginosa*, also Gram-negative, suggesting that this peptide sequence may have other useful applications rather than just targeting of MRSA or other *Staphylococcal* sp. This may be particularly useful as *P. aeruginosa* is also a frequent human pathogen that is becoming increasingly difficult to treat due to increasing resistance (Valencia et al., 2004).

Visualisation of peptide binding using peptides directly conjugated to a fluorophore appears to be the most suitable approach for characterising binding by flow cytometry and future work could investigate binding of the other selected clones utilising the same methodology. However, although flow cytometry is an efficient system for peptide screening, it may not be the optimal technique for characterising peptide binding. For example, the peptide may bind highly specifically to a single target that is not expressed

sufficiently highly on the bacterial surface and therefore the unique targets to MRSA may be undetectable, whereas a peptide that binds to a non-specific target on the cell surface that is highly expressed may appear to be the 'best binder'/peptide of choice. In order to be detectable using flow cytometry it is generally considered that approximately 8,000 targets/cell must be present. This argument could also be true for selecting peptides with perceived good binding properties by other techniques such as ELISA. Therefore, panning and a consensus sequence and subsequent binding analysis may not necessarily be a reflection of the 'best binders' that can be identified from a random peptide library.

Screening of display libraries has previously enabled successful identification of proteins that have specific binding properties to a range of different targets, including bacteria. Ideally, the optimal target would be an abundant and yet specific marker on the bacterial cell surface. Additionally, the target antigen should be exclusively expressed on bacteria, a marker that cannot be changed by resistance and whereby expression is not dependent on factors such as growth phase. Future work should include screening of more clones identified from the panned library using the direct binding assay to identify other peptides that display good MRSA specificity.

The screening technique described here allows for peptides to be selected against a target that is a relatively high-throughput and inexpensive system in order to identify new ligands that can be utilised in novel detection and drug delivery applications. The development of novel cell-specific reagents with excellent binding specificity that allows identification and targeting of bacteria may offer future potential in the treatment of wounds in addition to the usual culture methods and antimicrobial therapy. The panning technique described in this chapter is a versatile technique that could additionally be utilised to screen many other bacterial pathogens/numerous targets, such as *Pseudomonas* or *Streptococcal* species.

CHAPTER FOUR

Expression and purification of novel peptide-containing thioredoxin proteins

4.1 Introduction

The production of recombinant proteins is a common procedure that is well described within the literature. Such proteins can be expressed in a wide range of hosts, including bacteria, yeast, mammalian and insect cells, using a range of expression vectors and promoters. Selection of the optimal host and promoter for protein production is usually dependent on the target protein (Terpe, 2006). Production of recombinant proteins in *E. coli* is most probably the commonest procedure. This system has numerous advantages including rapid bacterial growth, high density expression, ease of handling, relatively low expense (media, strains and purification), a fully mapped genome, numerous strains/vectors and a long history of published data (Baneyx, 1999). Depending on the expression system, recombinant proteins may accumulate in the cytoplasm, in the periplasmic space, or be secreted into the culture medium. Typically total protein can accumulate between 1 and 20% of total cellular protein (LaVallie et al., 2000). One disadvantage of protein production in bacteria is that production can frequently result in the formation of inclusion bodies (insoluble misfolded intermediates) that then requires additional solubilisation and refolding of the protein (Baneyx and Mujacic, 2004). In addition to the expression of prokaryotic proteins, the expression of eukaryotic proteins in prokaryotic cell systems is frequently performed. However, one disadvantage of using the bacterial expression system is the lack of post-translational modifications, for example, glycosylation, and this may prevent the use of *E. coli* expression systems in some cases (Terpe, 2006).

In this chapter, a selection of the previously identified peptide sequences of interest (Chapter 3) were cloned in-frame within the entire thioredoxin sequence into the pPROTet *E. coli* expression system vector (Clontech). Thioredoxin is a small disulphide containing redox protein that has a conserved active site loop composed of a Cys-Gly-Pro-Cys (CGPC) motif (Stefankova et al., 2005). Thioredoxin has the potential to reduce substrate proteins and is itself maintained in a reduced state by thioredoxin reductase and NADPH (Kern et al., 2003). Thioredoxin across species have the same structure: a central core consisting of five beta strands flanked by four alpha helices and

a disulphide group active site (Kern et al., 2003). The pPROTet bacterial expression vector is one of the PRO™ bacterial expression system based on vectors developed by Lutz and Bujard (1997), allowing for tightly regulated expression of a protein without compromising the yield of protein induced (up to 10% of total protein). The pPROTet vector contains the P_{Ltet0-} promoter that is induced in response to the addition of anhydrotetracycline (aTc), Col E1 (a high copy replication origin with a 2,500 fold range of inducibility) and a chloramphenicol resistance gene to select for transformants.

Furthermore, one thioredoxin insert containing a peptide sequence of interest was also expressed as a GFP fusion protein construct for subsequent direct characterisation of peptide binding. Recombinant protein expression frequently employs the use of an affinity tag fused to the protein of interest to enable protein purification and detection (Terpe, 2003). In the system described here, the pPROTet vector contains a 6xHis-Asn affinity tag for subsequent purification using immobilised metal affinity chromatography (IMAC). Placement of polyhistidine tag for optimal affinity purification is recombinant protein specific but has been frequently placed either at N- or C- termini (Terpe, 2003). Following expression in *E. coli*, protein production was optimised and the protein extracted and purified for subsequent analysis (see Chapter 5).

4.2 Methods

4.2.1 PCR amplification of thioredoxin inserts containing different specific random peptide sequences and GFP

PCR was performed to amplify the DNA of the entire thioredoxin sequence each containing different peptide sequences of interest either with or without an additional 15 lysine residue linker (section 2.9.2, 2.9.2.1). Additionally following transformation of the GFP expression vector into *E. coli* JM109 (section 2.10) and selection of positive transformants (section 2.10), GFP was amplified by PCR with and without its natural stop codon (section 2.10). Following amplification all PCR products were purified either directly (section 2.9.3) or by gel extraction (section 2.10.1). Following purification an aliquot of each PCR product was visualised by agarose gel electrophoresis (section 2.9.3.1) and the concentration determined spectrophotometrically (section 2.6.1).

4.2.1.1 Digestion of PCR products from thioredoxin or GFP and the pPROTet expression vector

Following purification, double digestion reactions were performed to digest the amplified thioredoxin and GFP coding DNA and pPROTet bacterial expression vector using restriction enzymes previously described prior to ligation (section 2.9.4 and section 2.10.2 respectively). The digested PCR products and pPROTet vector were purified by gel extraction from a low melting point agarose gel. A test gel was performed following clean-up to ensure recovery of purified DNA of the correct size (section 2.9.3.1).

4.2.1.2 Ligation of thioredoxin or GFP products into pPROTet vector and *E. coli* transformation

Ligation reactions were performed in order to ligate individual thioredoxin insert fragments into the pPROTet vector at a molar ratio of 25:1 alongside control ligation reactions that contained cut plasmid DNA but no insert (section 2.9.5). Ligation reactions (1 µl) were visualised by agarose gel electrophoresis prior to transformation into *E. coli* JM109 (section 2.9.6). Additionally, PCR products, coding for GFP both with and without a stop codon, were ligated into the pPROTet vector at a molar ratio of 5:1 alongside control reactions containing no insert DNA (section 2.10.3). An aliquot of each GFP/pPROTet ligation reaction was transformed into *E. coli* DH10B competent cells (section 2.10.4). Transformed cells were then plated onto LB agar plates supplemented with antibiotic to select for positive thioredoxin/pPROTet or GFP/pPROTet transformants.

4.2.1.3 Confirmation of positive transformants

Colony PCR was performed to determine that the thioredoxin insert was successfully present and in the correct orientation within the vector (section 2.9.7). Following amplification, PCR products were visualised by agarose gel electrophoresis (section 2.9.7). Positive transformants were amplified by bacterial culture and glycerol stocks prepared (section 2.9.8). Plasmid DNA was extracted and ethanol precipitated prior to DNA sequencing in order to confirm the presence of the insert (section 2.9.9).

Furthermore, competent cells only and competent cells transformed with the empty expression vector were analysed by colony PCR following transformation to determine the presence and size of natural *E. coli* thioredoxin (section 2.9.6). For GFP transformants, single colonies were selected and the presence of GFP was confirmed by confocal microscopy analysis of individual transformants (section 2.10.4). Following confirmation of successful transformation of GFP, individual colonies were amplified and glycerol stocked (section 2.10.4).

4.2.2.3 Generation and verification of thioredoxin/GFP/pPROTet vectors

Plasmid DNA was extracted from positive bacterial cultures transformed with GFP/pPROTet plasmids (section 2.10.4). Double digestion reactions with *Sal*I and *Bam*HI restriction enzymes were performed in order to digest both purified GFP/pPROTet plasmid vector DNA and amplified thioredoxin PCR products (amplified without the lysine linker) (section 2.10.5). The digested DNA products were both purified by gel extraction (section 2.10.5). Ligation reactions were performed to join digested and cleaned GFP/pPROTet plasmid DNA at a 10:1 insert to vector molar ratio with each thioredoxin insert, alongside control reactions containing no insert DNA (section 2.10.6). Each thioredoxin/GFP/pPROTet ligated vector was transformed into *E. coli* GC10 competent cells (section 2.10.6). Plasmid DNA was isolated from individual transformants and PCR performed to confirm the presence of thioredoxin and GFP inserts (section 2.10.7). Isolated plasmid DNA was ethanol precipitated and the DNA sequenced using pPROTetFor primer and either GFPRev(WS or NS) or pPROTetRev primers (Table 2.2).

4.2.3 Determination of optimal protein induction and expression

Each bacterial culture was grown to an OD_{500} of 0.5. Cultures were then divided and induced with varying concentrations of aTc (section 2.11). Following induction an aliquot of each culture was removed at various time points and bacteria were pelleted by centrifugation. This method was also repeated following induction taking aliquots at the same time points, but bacterial cultures were diluted to an OD_{500} of 0.5 prior to centrifugation so that equivalent amounts of bacteria were present in each sample (section 2.11). SDS-PAGE was performed using 10% (w/v) resolving gels or 4-20%

(w/v) gradient gels (section 2.12). Following electrophoresis, each gel was either stained with Coomassie (section 2.12.1) or further analysed by Western blotting (section 2.12.2, 2.12.2.1, 2.12.2.2).

4.2.3.2 Shake-flask protein expression, purification and quantification

Bacterial cultures were amplified until an OD_{500} of 0.5 was obtained and following induction protein samples were prepared and purified by column purification (section 2.13.1, 2.13.2, 2.13.3). Eluted protein samples were concentrated in MWCO spin columns and buffer exchanged (section 2.13.4). Protein samples were quantified by Bradford assay (section 2.13.5) and further characterised by SDS-PAGE and Western blotting (section 2.13.6).

4.3 Results

4.3.1 Amplification of peptide sequences

Plasmid DNA encoding peptide sequences containing no stop codons were amplified by PCR using primers specific to amplify the full thioredoxin gene (Table 2.2; ThioFor and ThioRev) whereby the individual peptide sequences are situated within the middle of the thioredoxin sequence. Subsequently the ThioFor primer was modified to incorporate a 15 lysine linker on the N-terminal primer to facilitate subsequent conjugation to the photosensitiser (Table 2.2; ThioLysineFor). PCR was performed to amplify the 435 bp insert (thioredoxin containing insert plus linker) from plasmid DNA derived following panning and DNA sequencing. A representative example of an agarose gel of the thioredoxin inserts with and without the lysine linker following amplification and purification is shown in Fig 4.1 (lanes 1-3 and 5-7 respectively). For all subsequent cloning and DNA sequencing analysis, different modified thioredoxins containing unique peptides (either as DNA sequences or recombinant proteins) will be referred to based on the peptide sequence number identified in Figure 3.4 (Chapter 3).

Colony PCR was performed on competent cells alone and competent cells transformed with an empty expression vector using combinations of primers detailed in Table 2.2 (section 2.9.1; Chapter 2). Colony PCR performed on competent cells alone (Fig 4.2;

top row lanes 1-3) and cells transformed with an empty expression vector (i.e. no cloned thioredoxin or GFP; Fig 4.2; bottom row lanes 1-3), using PCR primers specific for thioredoxin, produced a product of approximately 350 bp corresponding to natural *E. coli* thioredoxin (Stefankova et al., 2005).

PCR using primers specific for the empty expression vector produced a PCR product of approximately 270 bp corresponding to the empty vector (Fig 4.2; bottom row lanes 14-16) that was not present in competent cells only (Fig 4.2; top row lanes 9-11) demonstrating no DNA corresponding to the expression vector was present in competent cells alone. Amplification using primer combinations of both thioredoxin and expression vector of competent cells only (Fig 4.2; top row lanes 5-7) and competent cells transformed with an empty expression vector (Fig 4.2; bottom row lanes 5-7, 9-11) were blank signifying no template DNA.

Furthermore, competent cells only (Fig 4.3 - Panel A) and competent cells transformed with an empty expression vector (Fig 4.3 - Panel B) were analysed by Western blot to ascertain the molecular weight of natural *E. coli* thioredoxin which was observed to be approximately 12 kDa (predicted Mw = 11.9 kDa). Following 2 h amplification, a small increase in the concentration of thioredoxin was observed (Fig 4.3- Panels A and B; lane 2) compared to initial concentrations (Fig 4.3 - Panels A and B; lane 1). However, when the optical density of the bacteria were diluted to starting values, no increase in thioredoxin was observed (Fig 4.3 - Panels A and B; lane 5). Additionally, no thioredoxin was observed in the supernatant of bacterial cultures (Fig 4.3 - Panels A and B; lanes 3 and 7). Furthermore, induction of bacterial cultures with 0.1 ng/ml aTc for 2 h (conditions determined to be optimal for protein expression) demonstrated no increase in thioredoxin concentration (Fig 4.3- Panels A and B; lane 8) when normalised to pre induction absorbance starting values (Fig 4.3 - Panels A and B; lane 5). However, as expected, a small increase was observed following 2 h amplification without normalisation (Fig 4.3 - Panels A and B; lane 6). Although the membrane was reprobed with an antibody specific for the 6xHN tag, visualisation was not possible due to the small size (4.6 kDa) of the product without an inserted cloned sequence for protein expression.

4.3.2 Cloning of peptides into pPROTet

Thioredoxin inserts of interest (n=9) and the expression vector pPROTet were digested and the ligation reactions optimised to determine the optimal insert to vector ratio for ligation. The optimal ligation ratio was determined to be 25:1 insert to vector respectively, as preliminary investigation using 5:1 and 10:1 demonstrated inconsistent ligation reactions (i.e. no ligated vector). Additionally, the optimal host *E. coli* strain for transformation was found to be JM109; as this resulted in successful transformations of all ligated vectors. Transformation of vectors into other competent strains (GC10 and BL21) to attempt to improve subsequent protein production were largely unsuccessful, mainly due to bad batches of commercial cells whereby approximately 15 independent transformations were attempted and no transformants were selected. A typical representative gel showing successful ligation prior to transformation is shown in Figure 4.4 (lanes 4-8) for thioredoxin 5, 11 12, 14 and 19/pPROTet ligated vectors; note the multiple bands indicative of ligated product.

Successful transformants were analysed by colony PCR to ensure the presence of the insert, in the correct orientation, using a forward primer specific for the expression vector and a reverse primer corresponding to thioredoxin to produce a band corresponding to 549 bp. On average, 6 clones for each recombinant protein of interest were analysed in duplicate. Following colony PCR screening to determine the presence of the insert each transformant was subsequently amplified in liquid culture and stored in glycerol for future use. A typical representative agarose gel of samples following colony PCR is shown in Fig 4.5. Additionally, DNA sequencing was performed in both directions on a selection of clones following transformation in order to confirm that thioredoxin inserts had been successfully cloned downstream of the $P_{\text{Ltet0-1}}$ and in-frame of the start codon in the right orientation. DNA sequences were translated using the ExPASy proteomics server of the Swiss Institute of Bioinformatics (http://www.expasy.ch/) (Bioinformatics, 2009).

4.3.3 Amplification of GFP and cloning of GFP and thioredoxin into pPROTet

GFP containing its natural stop codon and also a substitution to code for an alternative amino acid (to allow read through and possibly adopt more favourable protein folding

for comparison) were amplified by PCR. Following digestion, PCR products were cleaned-up and cloned in-frame into the pPROTet expression vector. Successful transformants were confirmed positive for GFP by confocal microscopy (Fig 4.6) and those of the highest relative fluorescence selected for future cloning. Plasmid DNA of positive clones were digested and ligated with thioredoxin inserts containing different peptide sequences (without the additional lysine linker; Fig 2.1). Following transformation of thioredoxin/GFP/pPROTet ligated vectors and overnight incubation, all thioredoxin/GFP (with stop)/pPROTet colonies appeared visibly green on the plate whereas thioredoxin/GFP (without stop)/pPROTet had a mixture of green and white colonies (approximately 50:50). Plasmid DNA was extracted from transformants and analysed for the presence of GFP and thioredoxin by PCR (Fig 4.7). Analysis by gel electrophoresis indicated that thioredoxin was only present in the colonies containing the expression vector with GFP with no natural stop codon and only in white colonies selected (Fig 4.7; lanes 5-8) whereas no thioredoxin was amplified from green colonies selected with the substituted stop codon (Fig 4.7; lanes 1-4). Additionally, no thioredoxin was present in vectors that retained GFP's natural stop codon (Fig 4.7; lanes 9-12).

Colony PCR of selected positive transformants (white colonies containing thioredoxin 5/GFP (no stop)/pPROTet) using different primer combinations specific for thioredoxin, GFP and the expression vector produced PCR products of the expected size (Fig 4.8). Furthermore, DNA sequencing of two randomly selected white colonies containing thioredoxin 5/GFP (no stop)/pPROTet was performed. Full sequencing was performed in both directions to verify the DNA coding sequence. Thioredoxin and GFP had been successfully cloned in-frame into the expression vector. No mutations were found in one transformant whereas sequencing of the other transformant demonstrated the presence of numerous premature stop codons resulting in protein termination and therefore no GFP coded for with the construct. This was due to a deletion in the sequence that resulted in the wrong amino acid being coded for (threonine (ACG) rather than aspartic acid (GAC)) resulting in a frameshift mutation so that the following DNA sequence coded for the wrong amino acids until a premature stop codon was reached. Furthermore DNA sequencing of two thioredoxin 5/GFP (with stop)/pPROTet clones indicated the vector had no thioredoxin.

4.3.4 Protein expression of thioredoxin inserts in pPROTet

Protein expression, induced by varying concentrations of aTc, was analysed by SDS-PAGE and Western blotting. Gels stained with Coomassie reagent demonstrated various bands indicating the presence of numerous proteins isolated from the bacterial pellets (Fig 4.9 lanes 1-7). Stained gels also indicated that 2 h induction had the greatest amount of protein present as indicated by the presence of darker bands (Fig 4.9 lane 2) compared with other incubation times (Fig 4.9 lane 1, 3-7), although it was not possible to visualise the exact protein band of interest from the gel. No thioredoxin protein was determined to be secreted into the supernatant as indicated by the presence of no bands following a Western blot probing for thioredoxin as determined from two repeat experiments.

Optimal protein expression was determined by Western blotting over a range of inducer concentrations and different durations of induction. Western blot analysis showed that induction with 0.1 ng/ml of aTc for 2 h was optimal for thioredoxin 19 protein (P19) production (predicted MW = 19.6 kDa), giving a band corresponding to approximately 26 kDa when probing for thioredoxin with an anti-thioredoxin antibody (Fig 4.10; lane 2). A two hour induction was also demonstrated to be optimal for protein production using different concentrations of inducer (e.g. 0.1, 1, 10 & 100 ng/ml). Furthermore, in addition to optimal P19 protein expression, these conditions were shown optimal for recombinant thioredoxin protein production that contained a different peptide (peptide12) and therefore were subsequently used for all protein expression. Following determination of optimal conditions, the membranes were stripped and reprobed for the 6xHN tag (Fig 4.11) and demonstrated a band corresponding to the same molecular weight indicating production of 6xHN tagged thioredoxin proteins (lane 2; ~26 kDa).

4.3.4.1 Extraction and purification of thioredoxin proteins

Preliminary attempts at protein extraction and purification were probably unsuccessful due to the limited amount of bacterial lysis following sonication for 3 x 10 sec and 3 x 30 sec to disrupt the bacteria and release the protein. However, the protocol was optimised to improve bacterial lysis by using a One Shot cell disruptor to achieve maximal lysis. Samples from using the sonication method always appeared very

translucent in colour whereas, One Shot derived lysates were noticeably more yellow in colour and of greater viscosity. Proteins were initially analysed using native SDS-PAGE to confirm the presence of thioredoxin. This method was initially optimised so that proteins were analysed using a precast 10% (w/v) resolving gel to ascertain the size of the product and further optimised to use 4-20% (w/v) gradient gels due to the relatively small size of the expected product, to allow better visualisation as the product was situated at the bottom of the gel.

The protein purification process was analysed by SDS-PAGE and Western blotting. Staining with Coomassie reagent produced very faint single bands observed following elution and concentration/buffer exchange but was not able to be clearly photographed. A typical representative Western blot to analyse thioredoxin 12 (P12) purification probing for thioredoxin (predicted MW = 19.4 kDa) with an anti-thioredoxin antibody is shown in Figure 4.12. Bacteria were analysed before and after induction (Fig 4.12; lanes 1+2 respectively), and following lysis to extract the protein (clarified sample - Fig 4.12; lane 3) whereby a protein band corresponding to approximately 26 kDa was observed. A small amount of thioredoxin protein did not bind to the resin during the purification process as indicated by the very faint band present in lane 4 in Figure 4.12. Eluted protein fractions (Fig 4.12; lane 5) were concentrated (Fig 4.12; lane 6) and were still present following buffer exchange (Fig 4.12; lanes 7+8) prior to conjugation to the photosensitiser. Additionally, the same membrane was reprobed for the 6xHN tag and produced faint bands of the same size and position as the thioredoxin probe (Fig 4.13: lanes 5-8 although most prominent in lane 6).

Following purification, concentration and buffer exchange the final concentration of the purified proteins were determined spectrophotometrically. The final concentration of P12 was determined to be 219 μg/ml, P19 was 175 μg/ml and thioredoxin 5 protein (P5) was calculated to be 299 μg/ml. However, the initial concentration of aliquots of P12 and P19 were also determined prior to volume concentration and buffer exchange of eluted proteins in the MWCO spin columns, and indicated that there was only a 26.8% and 25.9% recovery of each protein respectively resulting in a lower than expected yield. Further analysis indicated that there was no protein present in the buffer exchange flow-through from the column, thus the remaining protein had probably adhered to the membrane of the spin column.

4.3.4.2 Extraction and purification of thioredoxin/GFP proteins

Samples were analysed by SDS-PAGE and Coomassie staining (Fig 4.14). Coomassie staining of samples show that more thioredoxin 5/GFP protein (P5/GFP) had been produced following induction (Fig 4.14; lane 2) compared with starting values (Fig 4.14; lane 1) and a similar effect was demonstrated following induction of P5 only (Fig 4.14; lanes 5+6). However, it was not possible to visualise bands following protein concentration and buffer exchange for thioredoxin 5/GFP (Fig 4.14; lanes 3+4). However, multiple bands were detected in P5 following buffer exchange (Fig 4.14; lane 8) that were not observed in the concentrated sample (Fig 4.14; lane 7) indicating that a pure product was not obtained on this occasion.

Protein expression and purification of P5/GFP was analysed by Western blotting by probing for thioredoxin (Fig 4.15). Bacterial lysates following One Shot extraction were analysed before and after induction with 0.1 ng/ml aTc for 2 h (Fig 4.15; lanes 1+2 respectively) and indicated protein had been produced. Following protein purification and concentration, aliquots were analysed and a band corresponding to approximately 40 kDa was observed (Fig 4.15; lane 3) which remained following buffer exchange (Fig 4.15; lane 4) (predicted weight = 44.1 kDa). Additionally, P5/GFP production was compared to thioredoxin P5 production before and after induction (Fig 4.15; lanes 5+6 respectively and following concentration and buffer exchange (Fig 4.15; 7+8 respectively) in order to compare the relative size of extracted proteins with and without GFP. The concentration of the P5/GFP fusion protein was determined spectrophotometrically to be 414 μg/ml. These purified recombinant proteins are further characterised and discussed in Chapter 5.

4.4 Discussion

Selected clones P5, P12 and P19, identified through panning of the library (Chapter 3) for binding specificity to MRSA, were chosen for further analysis and cloned in-frame into an expression vector for protein production. In addition, one construct (P5) was cloned in-frame as a GFP fusion protein. This resulting fusion construct thus permits binding to MRSA through the thioredoxin containing peptide region and also GFP as a potential diagnostic tool for the rapid identification of MRSA.

It was considered that because the peptides of interest were small, 12-mer, and that the downstream application involved conjugation to a photosensitiser or GFP, that each peptide should be produced within the entire thioredoxin protein for stability, especially as they were initially selected in this format. The CGPC active site loop of *E. coli* thioredoxin is surface exposed that is situated at the end of a beta-strand and beginning of an alpha-helix (Kern et al., 2003). Therefore, because each peptide is situated within the active site loop of thioredoxin, it is predicted that the peptides will remain surface exposed in a similar construct to the original library (described by Lu et al., 1995).

The methodology for cloning of thioredoxin into the expression vector followed a now commonly used PCR cloning procedure whereby restriction enzyme sites were incorporated into the forward and reverse primers for successive cloning into the vector cut with the same enzymes, described by Scharf et al (1986). Additionally primers were designed to add extra base pairs before the restriction site because not all restriction enzymes are efficient at cutting at the ends of DNA (Kaufman and Evans, 1990). Furthermore, the cloning strategy was designed to perform double digestions of vector and insert DNA with different restriction enzymes to prevent self-ligation of the cut vector (without requiring dephosphorylation) and that restriction enzymes used for double digests of DNA (either thioredoxin or GFP) had compatible buffers and temperatures. Amplification of DNA by PCR was successful in identifying DNA bands of the correct size corresponding to thioredoxin and additionally following reamplification with the 15 lysine residue linker. Although the original amplified thioredoxin sequence did include lysine residues (accounting for 10/122 codons of the thioredoxin sequence, not including any lysine residues present in the peptide sequence), the addition of a 15 lysine linker was considered an important step in facilitating the subsequent conjugation of thioredoxin proteins to the photosensitiser.

An important step was the ability to differentiate natural *E. coli* thioredoxin from cloned thioredoxin because each different recombinant thioredoxin would subsequently be cloned into an expression vector for protein production in *E. coli*. The DNA from *E. coli* not containing recombinant protein (i.e. no individual peptides/additional lysine linker) was amplified by PCR from the bacterial strain used for protein production and visualisation of the amplified DNA demonstrated that the competent cells (alone or with an empty expression vector) were able to code for natural thioredoxin (Fig 4.2). This is

not surprising due to the ubiquitous nature of thioredoxin (Arner and Holmgren, 2000). Furthermore, DNA bands observed were of the predicted size for natural *E. coli* thioredoxin (i.e. no peptide and no lysine linker) that were smaller than DNA bands observed containing the inserted peptide and/or lysine linker. Visualisation of natural *E. coli* thioredoxin was further characterised by Western blotting and determined to be approximately 12 kDa (Fig 4.3). This is in agreement with the published literature whereby thioredoxin have a molecular weight of approximately 12 kDa (Stefankova et al., 2005).

All attempts at cloning thioredoxin only into the pPROTet expression vector were successful indicating that this system could be used to screen many different thioredoxin containing peptides with different MRSA binding specificities. However, it is unclear why restriction enzymes *Sal*I and *Bam*HI did not digest GFP (with stop)/pPROTet plasmids to obtain a linearised vector to allow insertion of thioredoxin inserts. This is in contrast to GFP (no stop)/pPROTet plasmids whereby partial cutting was achieved, in order to permit thioredoxin ligation, and resulted in a mixture of colonies that did and did not contain the thioredoxin insert. An extended digestion of the plasmids by addition of supplemental restriction enzymes during the incubation period may facilitate more efficient cutting in future investigations. However, because successful cloning of thioredoxin into GFP (no stop)/pPROTet was only observed in white colonies following transformation and not green colonies from the same vector or any colony from thioredoxin/GFP (with stop)/pPROTet vectors, it enabled a fast screening method to be developed for the selection of the required positive transformants. DNA sequencing of thioredoxin 5/GFP (no stop)/pPROTet constructs resulted in the correct sequence of one construct, but a premature stop codons in the other indicating that correct translation would not occur.

An advantage of this expression system for protein expression is that it involved expression of *E. coli* thioredoxin (a prokaryotic protein). Therefore no detrimental effect based on differences in codon usage between eukaryotes and prokaryotes was likely to occur; an effect that can often impact on eukaryotic protein production in prokaryotic hosts (Baneyx, 1999). Additionally, *E. coli* hosts can sometimes have difficulty in expressing eukaryotic proteins which may require modifications of proteins such as

glycosylation or other post translational modifications thus leading to non functional products (Terpe, 2006).

Protein production using the pPROTet bacterial expression system was optimised to increase the yield of recombinant protein by determining the optimal concentration of the inducer and the time of induction. In this system it was determined that optimal protein production was achieved following 2 h incubation after induction with 0.1 ng/ml aTc (Fig 4.9, Fig 4.10 & Fig 4.11). In theory, the longer the incubation following induction, the more protein should be produced but conversely longer periods of induction may allow for greater accumulation of inclusion body formation. Nonetheless, in this instance, 2 h incubation following induction with a range of inducer concentrations (0.1-100 ng/ml) was observed to be optimal for protein expression and therefore suggests that time of induction rather than concentration of inducer was a more important factor. However, 2 h induction was also shown to be optimal for protein expression even with no induction. This observation is difficult to explain, due to the proposed tight regulation of the expression vector, which should not allow any induction without the addition of aTc to the culture medium. A similar induction time was also employed by Tao et al (2000) who demonstrated that induction for 2.5 h was sufficient for small scale protein production. However, contrary to results indicated here, this group did not see any increased expression in the absence of induction (Tao et al., 2000). Membranes containing positive samples that were reprobed for the 6xHN tag, demonstrated a band that was only observed following 2 h incubation further supporting that 2 h incubation was the optimum time (Fig 4.11). The presence of a protein band of the same size following probing for thioredoxin and the 6xHN tag determined that the correct protein had been successfully induced.

Interestingly, Western blot analysis probing for thioredoxin produced at band at approximately 26 kDa whereas the predicted molecular weight was 19.6 kDa. However, analysis of thioredoxin/GFP fusion protein by Western blotting resulted in a slightly smaller size than predicted. Size determination using SDS-PAGE is not only determined by the protein size but also by charge and may also be slightly altered by other factors such as running conditions, gel concentration and pH. Western blotting of thioredoxin indicated the presence of multiple bands in addition to the band of interest. Oxidised and reduced thioredoxin have been demonstrated to interact with unfolded proteins and

have been suggested (along with thioredoxin reductase) to have chaperone-like properties (Kern et al., 2003). Therefore multiple bands may be due to the chaperoning function/protein interactions of natural thioredoxin protein with other proteins that were not separated by lysis in SDS loading buffer and therefore appear as protein dimers on the blot. However, this is considered unlikely as the interaction of thioredoxin and proteins was hypothesised by Kern et al (2003) to be due to weak hydrophobic interactions and unlike thioredoxin reductase, thioredoxin was not demonstrated to be able to form stable complexes with unfolded proteins in HPLC gel filtration experiments. However, thioredoxin binding to proteins was suggested to involve the active site (Lennon et al., 2000) and in this system novel peptides within the active site may have contributed to protein binding properties. A more likely explanation of the presence of multiple bands is the non-specific reactivity of the primary or secondary antibody. Therefore the use of a monoclonal thioredoxin antibody (instead of a polyclonal thioredoxin antibody) may reduce this.

Although sonication is a routine method employed to release proteins from cells, in this system protein release was greatly improved by using a One Shot cell disruptor. It is possible that the extraction process is not fully optimised and a variety of other approaches could be utilised to improve yield. Nonetheless, although protein extraction was improved, full extraction and recovery is unlikely in any system where proteins accumulate in the cytoplasm whereby some protein will nearly always remain in the bacterial debris as insoluble inclusion bodies. It is possible to solubilise proteins with a denaturing agent and refold the protein, although there is no certainty that the protein will refold *in vitro* in a biologically active form (Baneyx, 1999). Therefore native protein extraction of thioredoxin/thioredoxin GFP was preferable even if only a relatively small percentage is obtained compared with extraction under denaturing conditions.

In this expression system, although the formation of inclusion bodies cannot be completely excluded, because this system was largely expressing bacterial thioredoxin it was unlikely to be affected by substantial problems with insolubility. Thioredoxin has been used often as a fusion partner to enhance the solubility of passenger proteins and therefore is unlikely to form inclusion bodies. Both the N- and C- termini of thioredoxin are available for fusion (Katti et al., 1990) although thioredoxin is more frequently

placed at the N-termini when used as a fusion partner (Terpe, 2003). Therefore if thioredoxin fusions are typically used to improve the solubility of passenger proteins then the production of thioredoxin only in a soluble form seems achievable. Thioredoxin fusion proteins have been successful in improving solubility of numerous proteins. For example, thioredoxin fusion was employed to produce functional mammalian cytokines/growth factors at high levels that had previously only been formed as inclusion bodies (Lavallie et al., 1993). It has been suggested that improvement of passenger protein folding is due to rapid and correct folding of the fusion protein (e.g. thioredoxin, but also maltose-binding protein and glutathione-S-transferase) thus promoting downstream correct structure configuration in downstream folding units (Baneyx, 1999). Each purified protein (P5, P12 and P19) resulted in fairly similar yield obtained indicating that the induction time and inducer concentration used here were desirable for the generic expression of such protein constructs. Furthermore, purified thioredoxin/GFP fusion proteins gave approximately double the concentration of thioredoxin only recombinant proteins. The GFP fusion protein was approximately double the molecular weight of thioredoxin only proteins and therefore the number of moles of recombinant protein appears consistent suggesting favourable protein production even with the additional GFP protein sequence in the construct.

Purification of thioredoxin proteins was successful by affinity chromatography utilising the polyhistidine tag present at the N-terminus of the protein. Histidine tags present a low metabolic burden to bacteria and tags present at the N-terminus may improve the yield of recombinant protein due to efficient initialisation of translation (Waugh, 2005). Protein activity is unlikely to be affected by the presence of the tag and cleavage of the tag is not always necessary depending on the downstream application (Terpe, 2003) although this possibility cannot be excluded (Waugh, 2005, Terpe, 2003). Cleavage of the affinity tag from the recombinant thioredoxin proteins is possible utilising enterokinase although in this system cleavage of the tag was not performed as it was considered unlikely that this would inhibit peptide binding.

All of the recombinant proteins (P5, P12, P19 and P5/GFP) could be expressed suggesting that no recombinant thioredoxin proteins were toxic to the host. Although determination of the optimal inducer concentration and time of induction were performed in order to increase the yield of recombinant protein produced and also the

method of extracting the protein changed to improve yield, ultimately only a small amount of each protein was produced for further characterisation of protein binding to MRSA. Production using JM109 competent cells may have limited the protein produced. Although this strain is used in many applications such as routine subcloning, it is not an ideal for protein production. However, attempts were made to produce protein in strains that are more optimal for protein production (i.e. BL21 and GC10) but was not possible due to multiple unsuccessful transformations. One solution to achieve the desired amount of recombinant protein would be to scale up from shake flask expression to fermentation under more controlled conditions, or ultimately a different expression system, such as a yeast model, could be employed to attempt to improve protein yield. However, the limited amount of recombinant protein produced was mainly due to only a small recovery of purified protein following concentration in the MWCO spin column. Although some protein can be expected to be lost in this procedure, this recovery was a lot lower than anticipated. The protein was not lost in the column flow through and therefore it can only be assumed that the protein remained firmly bound to the membrane, although the reason behind this is unclear. In summary, despite considerable technological difficulties this system was successfully used to produce a selection of functional recombinant thioredoxin proteins containing different individual peptides cloned into a vector for expression in *E. coli.* Furthermore, the expression of these proteins was optimised in terms of yield, to develop a system for the production of recombinant proteins for subsequent analysis.

CHAPTER FIVE

Characterisation of recombinant protein binding potential and conjugation to a porphyrin photosensitiser for photodynamic therapy

5.1 Introduction

The continued evolution of bacterial resistance both generally and more specifically within chronic wounds has led to the requirement for novel modes of bacterial targeting and elimination, particularly methodologies whereby bacterial resistance cannot be easily gained. Photodynamic therapy (PDT) has been demonstrated to have an antimicrobial effect and subsequently shown not to be affected by microorganisms acquiring resistance (Wainwright and Crossley, 2004); however, its effects were not fully utilised mostly due to the discovery of highly efficient broad spectrum antibiotics (mainly during the 1950's). PDT involves the accumulation of a photosensitiser, either intracellularly or at the cell surface, and subsequent activation with an appropriate wavelength of light, in the presence of oxygen to produce reactive oxygen species (e.g. singlet oxygen) that causes bacterial killing (Wainwright, 1998). Since its discovery, PDT has been demonstrated to be an effective treatment against a wide range of Gram-positive and Gram-negative bacteria and also against viruses, fungi, parasites and yeast (Jori and Brown, 2004). However clinically, PDT has recently been utilised as a treatment for age-related macular degeneration and a few forms of cancer (Brown et al., 2004, Bressler and Bressler, 2000).

One approach for effective antimicrobial PDT could involve targeting specific pathogens within a wound. This would require existing or novel biomolecules that are effective against specific pathogenic bacteria, whilst avoiding other commensal bacteria or eukaryotic cell types. These biomolecules could then be covalently conjugated to a photosensitiser that has bactericidal activity against the target without its activity being affected by conjugation. One group of porphyrin photosensitisers containing a single reactive isothiocyanate group (NCS) were developed previously (Sutton et al., 2002, Clarke and Boyle, 1999). Conjugation of the porphyrin photosensitiser to the biomolecule of interest is achieved through reaction of the NCS group and the amine group contained in lysine residues forming a covalent bond between the two molecules under mild conditions without unwanted byproducts (Staneloudi et al., 2007). Recently,

isothiocyanate porphyrins have been conjugated to monoclonal antibodies (Hudson et al., 2005) and single chain Fv fragments (Staneloudi et al., 2007) highlighting their potential for use in targeted therapy.

Ideally, like other antibacterial agents now in general use, all new molecules developed that are involved in selective bacterial targeting/elimination should have pathogenic bacterial specificity with little or no specificity for host cell types. Furthermore, in addition to targeted PDT, new molecules with a high degree of bacterial specificity may also have potential utility as a novel approach of bacterial identification (Carnazza et al., 2008), offering a rapid diagnostic approach that could be used in conjunction with the current culture methods currently employed.

In this study, the purified P12 protein from the previous chapter with potential binding ability to MRSA was conjugated to a photosensitiser and the cytotoxic effects of the bioconjugate (P12 conjugate) against MRSA was characterised in comparison to any effects on *E. coli* and keratinocytes. Cell toxicity was also compared with the unconjugated porphyrin. In addition, two further recombinant proteins (P5 and P19) were characterised for the specificity of binding to MRSA in comparison with Gram-negative species and a keratinocyte cell line. One of these proteins was subsequently expressed as a GFP fusion protein and assessed for use as a rapid MRSA diagnosis tool.

5.2 Methods

5.2.1 Bioconjugation and visualisation of recombinant protein P12 and porphyrin

The capped and uncapped porphyrins used in this study were dissolved in anhydrous DMSO to a 5 mM stock concentration. Purified P12 was conjugated to the porphyrin at a molar ratio of 5:1, purified through a PD10 column to remove unbound porphyrin, and characterised spectrophotometrically (section 2.14.2). The P12 conjugate and capped porphyrin were separated by gel electrophoresis and illuminated by UV light and Coomassie stained for visualisation of porphyrin and conjugated protein respectively (section 2.14.2).

5.2.2 Cytotoxicity assays

Cytotoxicity assays were performed against MRSA, *E. coli* (section 2.15) and a human keratinocyte cell line (section 2.15.1). Bacteria or keratinocytes were incubated with either the P12 conjugate or capped porphyrin alone, either at the same porphyrin concentration as the P12 conjugate or a 10-fold excess of capped porphyrin for comparison. Cells only and media only were used as controls to determine any effect of light alone. Unbound P12 conjugate or porphyrin was removed by washing, and then cells plated in triplicate onto two separate plates. One plate was irradiated at 633 nm whilst the other acted as a dark control to determine any dark toxicity. Following overnight incubation, bacterial proliferation was determined by measuring absorbance at 630 nm. MRSA cultures from the irradiated plate were serially diluted and plated out onto agar. Following overnight incubation, the number of cfu/ml was determined (section 2.15). Keratinocyte cell proliferation was determined by MTT assay (section 2.15.1).

5.2.3 Assessment of binding of unconjugated proteins by flow cytometry

The binding ability of purified recombinant proteins P5 and P19 to MRSA, *E. coli* and a keratinocyte cell line was determined by flow cytometry (section 2.16). Having incubated either keratinocytes or bacterial cultures with P5 or P19 proteins, binding was assessed by incubation with an anti-thioredoxin antibody followed by washing and detection with a secondary antibody prior to flow cytometry (section 2.16).

5.2.4 Binding assessment of P5/GFP by flow cytometry

The binding of P5/GFP to MRSA, *E. coli* and keratinocytes was determined directly by flow cytometry. A range of concentrations of P5/GFP were incubated with bacteria or keratinocytes to demonstrate protein binding. Cells were washed in PBS to remove any unbound protein prior to flow cytometric analysis (section 2.16.1).

5.3 Results

5.3.1 Conjugation and cytotoxicity assays of the conjugated P12 protein

A pilot study undertaken with P12 was performed to test conjugation and the cytotoxic potential of the P12 conjugate to assess the validity of the approach. Following conjugation of the porphyrin to P12, the degree of loading was calculated to be 0.22 moles of porphyrin per mole P12. It was not possible to visualise the porphyrin under UV light, and subsequent SDS-PAGE followed by Coomassie staining to detect the protein, observed only a very weak band at approximately 20 kDa that could not be observed photographically and was not repeated due to the limited sample size.

Incubation of MRSA with the P12 conjugate demonstrated a 66% reduction in cell growth following irradiation (Fig 5.1; purple bar - irradiation) compared with non irradiated control cells (Fig 5.1; blue bar - no irradiation). In comparison, incubation with the same concentration of unconjugated capped porphyrin resulted in only a 20% reduction in cell growth (Fig 5.1: yellow bar - irradiation) whereas a 10-fold excess of the porphyrin alone demonstrated a 91% reduction (Fig 5.1; green bar - irradiation). It should be noted that a 24% reduction was observed following irradiation with red light alone (Fig 5.1; blue bar - irradiation), a similar effect to that observed with the lower concentration of capped porphyrin alone. In contrast, non-irradiated MRSA incubated with the P12 conjugate, capped porphyrin or 10-fold excess of porphyrin demonstrated an increase in cell growth (6, 36% and 20% respectively) (Fig 5.1; purple, yellow and green bars - no irradiation) in comparison to the non-irradiated control. Bacterial colonies plated out onto agar following overnight incubation showed a similar trend of cell growth as determined by calculating cfu/ml. Bacteria incubated with the P12 conjugate resulted in a count of 2.01×10^8 cfu/ml, a 78% reduction compared with bacteria irradiated with red light only (9.33×10^8 cfu/ml). A similar trend was observed with the unconjugated porphyrin alone resulting in a 17% reduction (7.79×10^8 cfu/ml) compared with bacteria following no treatment except irradiation with red light. MRSA incubated with a 10-fold excess of porphyrin and showed no growth following overnight incubation indicating that no viable bacteria were present following treatment.

Irradiation of *E. coli* following incubation with the P12 conjugate, capped porphyrins or bacteria only showed approximately a 10% decrease in bacterial growth in comparison with untreated *E. coli* alone (Fig 5.2). Similarly, non-irradiated *E. coli* showed 2-3% reduction in growth compared to the control samples. Keratinocytes incubated with the conjugated P12 protein and irradiated demonstrated a 13% reduction in cell viability compared with untreated, non irradiated keratinocytes (Fig 5.3). However, this effect is also observed (14% reduction) following incubation with the P12 conjugate without irradiation. The capped porphyrin without irradiation resulted in a 16% decrease, a similar effect to the conjugated protein, when neither was irradiated whereas, a 10-fold excess of porphyrin demonstrated a small increase in cell growth (6%) compared to the control cells (Fig 5.3). Incubation of keratinocytes with the capped porphyrin demonstrated a 29% decrease in cell growth following irradiation whereas, a 10-fold excess of porphyrin resulted in a 98% decrease in cell growth, a similar response to that seen against MRSA.

5.3.2 Investigation of thioredoxin proteins binding by flow cytometry

The binding of P5 and P19 to MRSA, *E. coli* and keratinocytes was characterised by flow cytometry to determine any MRSA specific binding of purified proteins. The FACS profiles used to determine non-specific binding of detection antibodies to MRSA to enable subsequent analysis of P5 and P19 are shown in Figure 5.4. The FSC/SSC (Fig 5.4; Panel A) was used to identify the MRSA population gate for subsequent analysis of control reagent (primary and secondary antibodies) and test reagent (P5 and P19) binding. Control experiments were performed to assess the non-specific binding of the primary and secondary antibodies used for detection. Negligible binding of the anti-thioredoxin primary antibody was observed (Fig 5.4; Panel B; mean = 2.6) in comparison to bacteria alone (mean = 1.1). However an increase in mean fluorescence was observed following incubation with the secondary antibody alone (Fig 5.4; Panel C; mean = 129.1). In addition incubation of both primary and secondary antibodies without recombinant protein resulted in a further increase in mean fluorescence (Fig 5.4; Panel D; mean = 568.6) thus indicating the binding potential of the detection antibodies alone.

FACS analysis to determine binding of P5 and P19 indicated two distinct fluorescent peaks upon analysis (Fig 5.4b; Panels A and B respectively) that were not observed with

detection antibodies alone. Although the second larger peak observed is attributable to non-specific antibody binding (as determined from analysis of Fig 5.4; Panels C and D), the smaller peak of lower fluorescence (determined by the marker M1) was not observed due to non-specific binding of detection reagents. This was presumed to be attributable to recombinant protein binding to bacteria and binding assessed as the percentage of events in M1 in comparison to the events in M1 of both detection antibodies. A small amount of P5 binding was observed (Fig 5.4b; Panel A; gated marker = 20.5%) in comparison to detection antibodies (Fig 5.4; Panel D; gated marker = 7.0%). A further increase in binding of P19 was also observed (Fig 5.4b; Panel B; gated marker = 30.5%) in comparison to detection antibodies only controls.

The non-specific binding of detection antibodies against *E. coli* was also assessed (Fig 5.5) to allow characterisation of P5 and P19 binding. The main bacterial population was determined by FSC/SCC (Panel A). Similar to MRSA, the primary antibody showed little specificity against *E. coli* (Panel B; mean = 1.6) in comparison to unlabelled bacteria (mean = 1.2). A small degree of non-specific binding of the secondary antibody was observed (Panel C; mean = 5.0). A similar effect was seen following incubation with both primary and secondary antibodies alone (Panel D; mean = 6.8). Binding of P5 and P19 to *E. coli* was also assessed following comparison as a percentage of the gated marker (M1) in comparison to the percentage of *E. coli* that was dual labelled with both antibodies. The gated marker for *E. coli* was set at the same percentage of 'bacteria only' used as a negative control for analysis of MRSA (0.06%). Binding of P5 was slightly increased (Fig 5.5b; Panel A; gated marker = 68.9%) in comparison to *E. coli* labelled with both detection antibodies alone (Fig 5.5; Panel D; gated marker = 66.1%). A similar binding effect of P19 against *E. coli* was also observed (Fig 5.5b; Panel B; gated marker = 69.0) indicating minor binding of P5 and P19 to *E. coli*.

Binding of P5 and P19 to keratinocytes was assessed by flow cytometry and is shown in Fig 5.6. Panel A (Fig 5.6) demonstrates a typical FSC/SSC profile used to identify the keratinocyte cell population. The primary antibody alone showed no particular specificity for keratinocytes (Fig 5.6; Panel B; mean = 5.7). An increase in binding was observed following incubation with the secondary antibody alone (Fig 5.6; Panel C; mean = 17.2) and further increased following dual labelling with both primary and secondary antibodies (Fig 5.6; Panel D; mean = 21.9). The gated marker (M1) for

keratinocytes was set at 0.03% of the unlabelled negative control cells (a similar percentage to conditions used for bacterial binding analysis (0.06%)). Binding of keratinocytes was determined based on differences in the percentage of the gated marker of recombinant protein binding in comparison to cells dual labelled with detection antibodies only. A small amount of P5 binding to keratinocytes was observed (Fig 5.6b; Panel A; gated marker = 20.4%) in comparison to both detection antibodies alone (Fig 5.6; Panel D; gated marker = 13.0%). Similar to P5, a small level of P19 binding was also observed (Fig 5.6b; Panel B; gated marker = 18.6%), albeit to a slightly lesser extent.

5.3.3 Assessment of a thioredoxin/GFP fusion protein binding by flow cytometry

The binding of P5/GFP fusion protein was assessed by flow cytometry. A range of concentrations of P5/GFP (40-398 µg/ml) was assessed for binding against MRSA, *E. coli* and keratinocytes (Fig 5.7). The main cell populations of MRSA, *E. coli* and keratinocytes were determined by FSC/SSC analysis shown in Panels A, C and E respectively (Fig 5.7). Binding of P5/GFP protein to MRSA (Fig 5.7; Panel B), *E. coli* (Fig 5.7; Panel D) and keratinocytes (Fig 5.7; Panel F) was assessed as any increase in mean fluorescence in comparison to unlabelled cells. The data showed a very small increase in binding with increasing concentration of protein. Mean fluorescence values demonstrating this increase are shown in Table 5.1.

Table 5.1: Mean fluorescence (MF) values after incubation of P5/GFP with MRSA, *E. coli* and keratinocytes for determination of binding

Concentration of P5/GFP	MF of MRSA	MF of *E. coli*	MF of keratinocytes
Cells alone	1.5	1.7	4.4
40 µg/ml P5/GFP	1.6	1.7	4.6
200 µg/ml P5/GFP	1.7	1.9	4.8
398 µg/ml P5/GFP	1.9	2.0	4.9

5.4 Discussion

The use of PDT for the topical treatment of infected/chronic wounds has previously been suggested (Zolfaghari et al., 2009, Embleton et al., 2005, Lambrechts et al., 2005, Embleton et al., 2002, Karrer et al., 1999, Griffiths et al., 1997). A range of photosensitisers have been shown to have bactericidal photodynamic action to eliminate bacteria that could potentially play a successful role in treatment of wounds. The development of photosensitisers with antimicrobial action, that can be conjugated in a defined manner to novel or existing biomolecules to enhance specificity for the target organism/s that increase the cytotoxic effectiveness of the photosensitiser whilst minimising damage to surrounding eukaryotic cells would enhance the overall effectiveness of PDT for wound management.

5.4.1 Conjugation of recombinant protein P12 to a porphyrin photosensitiser and cytotoxicity assays

In this chapter one of the peptides (peptide12) that had previously been shown to bind preferentially to MRSA by flow cytometry in Chapter 1 was cloned within the full thioredoxin protein sequence into a bacterial expression vector and following subsequent expression and purification (Chapter 2) conjugated to an isothiocyanate porphyrin. Previous work investigating porphyrins as photosensitisers has also showed the feasibility of conjugation of isothiocyanate porphyrins to biomolecules such as BSA (Sutton et al., 2002) and monoclonal antibodies (Hudson et al., 2005). This group of porphyrins has also been conjugated to scFvs displaying colorectal tumour cell reactivity and demonstrated a selective photocytotoxic effect against colorectal cell lines as an alternative to whole IgG molecules thereby offering enhanced tumour penetration and faster clearance from the bloodstream (Staneloudi et al., 2007). The purified proteins investigated here are approximately the same size as a scFv protein investigated by Staneloudi et al (2007) therefore demonstrating the feasibility of this approach. The current study has shown that it was possible to conjugate the recombinant protein of interest with proposed binding specificity to MRSA to the desired porphyrin, via coupling of the NCS group of the porphyrin that covalently binds to lysine residues on the protein. Following bioconjugation, attempts were made to visualise the P12 conjugate and capped porphyrin by SDS-PAGE and visualised by irradiation with UV

light. However, the P12 conjugate and the capped porphyrin were not readily detectable under UV light presumably due to the relatively low concentration of the P12 conjugate separated on the gel.

In this pilot study it was demonstrated that the conjugated P12 protein caused a decrease in growth of MRSA following irradiation with red light in comparison to non treated control cells (Fig 5.1). A reduction in cell growth following incubation and irradiation with an equal concentration of unconjugated capped porphyrin was also observed however, this reduction was to a lesser extent than PDT using the P12 conjugate. This may suggest that the conjugated P12 protein enhanced the efficacy of PDT over use of photosensitiser alone and therefore indicates some degree of cellular specificity of the conjugate. Conjugation of photosensitisers to biomolecules, such as antibodies, for enhanced killing of *S. aureus* strains including MRSA in comparison to the photosensitiser alone has previously been demonstrated to improve specificity towards the potential pathogenic bacteria (Embleton et al., 2002, Embleton et al., 2004, Gross et al., 1997). Further to this, antibodies directed towards other potential pathogens such as *P. ginivalis* (Bhatti et al., 2000) and *P. aeruginosa* (Berthiaume et al., 1994), have also been utilised as targeting moieties suggesting that this approach can improve photodynamic inactivation. Interestingly, Berthiaume et al (1994) found that the non conjugated photosensitiser had no effect using an *in vivo* model targeting *P. aeruginosa*, whereas the specific targeting moiety resulted in a 75% reduction in the number of viable bacteria. Furthermore, groups have demonstrated that antibody conjugated photosensitisers were able to selectively kill bacteria in a mixed bacterial suspension (Bhatti et al., 2000, Embleton et al., 2002). Therefore, it may be possible to use similar approach to identify and develop novel biomolecules against MRSA that are an alternative to antibody based biomolecules, with varying specificities for different bacteria as targeting vehicles to deliver the photodynamic agents.

However, although targeted therapy appears promising, investigations have looked at photosensitisers used without targeted biomolecules with very effective results (Maisch et al., 2005). In addition, Bertoloni et al (2000) demonstrated that a very low binding capacity of haematoporphyrin (less than 1% tightly bound to bacteria) was still sufficient to cause a cytotoxic effect. Therefore, although targeted photosensitisers are an attractive target worthy of investigation, some photosensitisers are effective even

without the requirement of cell-specific reagents. In this study, incubation of the bacteria with a 10-fold excess of the photosensitiser resulted in highly efficient killing of MRSA (Fig 5.1), suggesting that the use of this photosensitiser alone may be effective against a wider range of Gram-positive pathogens. However, because a similar killing effect was also observed against keratinocytes, it may suggest that this particular photosensitiser is not suitable for use on its own for PDT as surrounding tissue may also be damaged, whereas conjugation resulted in killing of MRSA with limited damage to keratinocytes.

Interestingly, in this study a reduction in bacterial growth was also observed following treatment with the red light alone, similar to the effect seen following PDT with the lower concentration of capped porphyrin thus indicating that light alone can apparently cause a certain reduction in cell growth. Therefore, the reduction in bacterial growth observed following treatment with the lower concentration of capped porphyrin and irradiation may suggest that this is due to the irradiation effect and that a greater concentration of porphyrin is required to affect cell growth. This also indicates that targeted treatment with the same concentration of P12 conjugated porphyrin rather than free porphyrin was effective at eliminating bacteria and suggests that lower doses of targeted therapy may be required than using the porphyrin alone. Additionally, a greater reduction in bacterial growth observed following incubation of MRSA with the P12 conjugate or high concentration of capped porphyrin may also indicate that in this case red light alone may just accentuate the killing effect following these treatments. In contrast to the current investigation, Grinholc et al (2008) demonstrated that no cytotoxic effect of light alone was observed following photodynamic inactivation of 40 different clinical strains of MRSA and 40 separate strains of MSSA. However, Griffiths et al (1997) found that there was an effect of light alone on 3 of the 16 different EMRSA investigated that resulted in a reduction of bacterial viability and therefore susceptibility to light alone appears to be strain dependent. Additionally, the effect of light alone has been demonstrated to have a damaging effect on wound healing in *S. aureus* infected burn wounds in mice, whereby wounds took 6.2 days more to heal in the irradiation group than the dark, although this was probably due to the high light dose (either 211 Jcm^{-2} or 423 Jcm^{-2}) used in comparison to other studies (Lambrechts et al., 2005).

Determination of cell viability as a measure of absorbance or by determining the number of cfu/ml gave similar results and further supported the binding potential of the conjugated P12 protein suggesting that the conjugate or high concentration of porphyrin were more successful in treatment than the lower concentration of capped porphyrin that was equivalent to the conjugate. The slight difference in bacterial viability between methods is presumably because that although bacteria may be present in the sample that can be measured by absorbance, the bacteria are not necessarily truly viable, i.e. capable of dividing, and therefore do not form visible colonies on plates.

Growth of MRSA was enhanced following incubation with the low and high concentrations of capped porphyrin alone (36% and 20% respectively) following no irradiation and slightly increased following incubation with the P12 conjugate (6%) suggesting that neither the conjugate nor porphyrin has cellular toxicity in the absence of activation on its own. Similar effects on bacterial proliferation without irradiation were observed by Karrer et al (1999) whereby an increase in growth of *S. aureus* was observed following incubation with varying concentrations 5-aminolevulinic acid and no irradiation in a dose-dependent manner however, growth of *S. epidermidis* was noted to decrease. Additionally in 80 different *S. aureus* strains, Grinholc et al (2008) demonstrated very limited toxicity of the photosensitiser (less than 0.2 $\log_{10}$ reduction in viable count) when not activated by light. Although limited toxicity of the photosensitiser used in this and previous studies may be advantageous in that it suggests that bacterial elimination can be controlled with targeted irradiation with the light source, bacterial cytotoxicity of the unirradiated photosensitiser may not necessarily be a disadvantage as long as the damage is pathogen and not host cell specific. However, in this study incubation with the P12 conjugate or porphyrin without irradiation enhanced bacterial proliferation whereas a certain degree of dark toxicity against keratinocytes was observed and therefore only short incubation times prior to irradiation should be applied to maximise bacterial killing whilst minimising damage to the host.

There was no cytotoxic effect on *E. coli* following incubation and irradiation with either the P12 conjugate or either concentration of photosensitiser as demonstrated by a very small decrease in viability compared to the non-treated control cells (Fig 5.2). Similarly, cells treated and not exposed to light showed a smaller reduction in growth, thus indicating that the compounds have little cytotoxic effects. Furthermore, it may suggest

that the P12 conjugate may have some level of MRSA specificity due to the small reduction in bacterial growth following treatment and also that the capped porphyrin alone has little effect in *E. coli*. However this effect is more likely due to differences in the bacterial cell walls whereby Gram-positive bacteria are more susceptible to photodynamic therapy than Gram-negative bacteria, particularly with anionic or neutral photosensitisers (O'Riordan et al., 2005). However, although the photosensitiser used in this case was cationic and therefore should be more effective than an anionic or neutral photosensitiser, in this instance no killing was observed, even using a 10-fold excess of porphyrin that was sufficient to kill 91% of MRSA and therefore higher concentrations could be investigated to attempt to eliminate *E. coli*.

The decrease in MRSA bacterial growth observed following PDT with the P12 conjugate was greater than the cell knockdown observed in keratinocytes (66% vs. 13% respectively) and therefore may suggest a preferential targeting of the conjugate. The small decrease in cell growth following incubation with the P12 conjugate was also observed following incubation of the conjugate without irradiation suggesting the same amount of light and dark toxicity of the conjugate and therefore may be independent of light treatment and the generation of reactive oxygen species. Eukaryotic species are known to be more resistant to PDT than prokaryotic cells, e.g. Zeina et al (2002) demonstrated that sufficient conditions required to kill skin flora (such as *S. aureus*) did not induce a great cytotoxic effect in keratinocytes *in vitro* whereby the kill rate was up to 200 times slower than prokaryotic cells. Additionally treatment of keratinocytes under the same conditions that induce prokaryotic death was not sufficient to induce a genotoxic effect as determined by comet assay to detect DNA damage (Zeina et al., 2003). Similarly, Embleton et al (2005) demonstrated that a phage conjugate did not affect the viability of human epithelial cells *in vitro* following treatment whilst retaining specificity for EMRSA-16, suggesting that targeting with biomolecules can offer an advantage in PDT. However, in this investigation, treatment with the low concentration of porphyrin alone (1.25 μM) had a slightly greater cytotoxic effect, albeit a small difference (~9%), against keratinocytes compared to MRSA. This further suggests the requirement of targeted PDT with biomolecules to reduce damage to host cells.

The low concentration of the capped porphyrin demonstrated a greater decrease in keratinocyte proliferation than the P12 conjugate, even though both contained the same

concentration of porphyrin, therefore suggesting that the conjugated P12 protein caused less cellular damage than the porphyrin only and therefore possibly indicates some degree of specificity for MRSA in comparison with *E. coli* or keratinocytes. However, a 10-fold excess of the photosensitiser demonstrated a large reduction in cell proliferation. This effect was similar to that observed in MRSA treatment, indicating the high cytotoxic potential of the porphyrin alone against these cell types, although not observed when used against *E. coli*. In contrast to MRSA and *E. coli*, the effect of light alone was demonstrated to have a slight increase on cell proliferation in keratinocytes. Maisch et al (2007) demonstrated using a porcine skin model that irradiation of the epidermis with light alone did not demonstrate a significant increase in apoptotic cells. Therefore if treatment with light can decrease bacterial growth whilst boosting eukaryotic growth then this may also be advantageous for antimicrobial PDT that may be further enhanced by the use of specific targeting agents.

One obvious drawback in this pilot investigation was the limited concentration of purified protein produced in order to test the photodynamic potential of the conjugated protein. Future experiments that investigate the effect of increasing the P12 conjugate concentration and light dose and also determine these effects on different growth phases of bacteria could improve the effectiveness of PDT using this biomolecule. In order to achieve greater specificity and potentially more effective killing, the resulting bioconjugate should demonstrate that, following conjugation, the biomolecule retains or improves its target binding affinity and additionally the photosensitiser remains fully active. However, due to the limited concentration of the extracted purified protein, it was not possible to determine the binding ability of P12 before and after conjugation to determine any gross loss (or gain) of binding specificity. Although it is desirable to determine that no loss of binding specificity of the protein occurred, the results here indicate that the P12 conjugate was bound to the MRSA as indicated by the photocytotoxic effect of the conjugate against MRSA compared with controls. However, previous investigations had demonstrated that the individual peptide sequence when conjugated to FITC was able to bind MRSA and therefore it is reasonable to assume that the peptide of interest situated within the entire protein sequence that is surface accessible should retain the same binding affinity, especially because it had been selected for this display format. If the increased yield of protein could be achieved then not only could the characterisation of the conjugate in a dose-dependent manner be

investigated but also the initial toxicity of the protein prior to conjugation. However, toxicity of thioredoxin itself seems unlikely because this protein is ubiquitously expressed (Arner and Holmgren, 2000). However, it is theoretically possible that the individual peptide sequence expressed within the active site of thioredoxin could potentially have toxic properties, although in this case it would be expected that significant dark toxicity would be observed. Furthermore, toxicity of the bacteria expressing the peptide during the panning would perhaps also be expected; hence no such peptides would be generated.

In addition to investigating the photodynamic potential of the P12 conjugate and capped photosensitiser against MRSA, it would be interesting to investigate the effect of the compounds against other *Staphylococcal* species, including a non-resistant strain of *S. aureus* and *S. epidermidis*. Grinholc et al (2008) and Szpakowska et al (2001) both demonstrated that MRSA resistance to photodynamic therapy was higher than MSSA strains, which may suggest that factors conferring drug resistance to bacteria may be associated with increased resistance to photodynamic therapy. Four strains of MRSA out of 40 investigated were resistant, whereas no MSSA strains showed resistance; with a broad range of intermediately resistant, sensitive and highly sensitive strains across both MRSA and MSSA strains. These data suggests a strain-dependent nature of the photodynamic effect, that was hypothesised to be associated with the ability to produce biofilms (Grinholc et al., 2008). However, although drug-resistant strains have been observed to be potentially less susceptible to photodynamic therapy, a range of different photosensitisers should be investigated in these cases to explore the effects of different classes of photodynamic compounds.

5.4.2 Characterisation of recombinant protein binding specificity

In addition to new methods of targeting bacteria for treatment regimens, novel biomolecules that recognise and bind specific pathogens might have an important alternative function in the rapid diagnosis of different bacterial species, possibly from wounds or to determine carriage, as an alternative to the usual culture techniques. Two novel proteins (P5 and P19) similar in structure were assessed for binding ability to MRSA and also to *E. coli* and keratinocytes for comparison. Assessment of binding of the unconjugated proteins by flow cytometry was characterised using antibodies that

specifically recognise the protein of interest (thioredoxin) and appropriate secondary reagents for detection. Characterisation of P5 and P19 binding to MRSA suggested that both proteins were bound to MRSA, with P19 appearing to bind MRSA slightly better than P5. A very small amount of P5 and P19 binding against *E. coli* was observed whereby both proteins demonstrated the same, small level, of binding which therefore may possibly be due to non specific interaction. However, flow cytometry data should be interpreted with caution due to non-specific binding of the antibodies used for detection. MRSA express protein A on their surface that enables binding of many isotypes of IgG antibodies via the Fc region of the molecule (Roberts and Gaston, 1987) making analysis of true binding ability difficult to interpret. However, expression of protein A has previously been exploited for targeted PDT towards the surface of bacteria (Embleton et al., 2002, Embleton et al., 2004, Gross et al., 1997). The photodynamic effect was negated by incubation of bacteria with natural IgG, by blocking the binding site in a strain of *S. aureus* Cowen I, a strain with naturally high expression of protein A on the surface (Gross et al., 1997). Therefore, in order to assess binding potential accurately one possible approach could be to coat the bacteria with non-specific antibodies to block the non-specific binding sites of the primary and secondary antibodies. In this investigation blocking by incubation of bacteria with milk proteins and BSA was not sufficient enough to exclude non-specific binding of the antibodies used for detection. Therefore future binding experiment must involve more effective blocking of the bacterial Fc receptors. Ideally, this would involve blocking with purified IgG from the host species of the secondary antibody, so in this case bacteria could be blocked with purified sheep IgG. Alternatively, incubation with non specific antibodies, for example, those derived from human serum, provided that the serum donor has not been exposed to MRSA and raised antibodies against it, should be effective in blocking non-specific binding. Another simple strategy to assess binding more effectively would be to use the primary antibody directly conjugated to the fluorphore for detection and measure the mean fluorescence following incubation with the purified protein and subtract the mean fluorescence observed from the antibody and cells only.

Although P5 and P19 have very similar homology, differences in binding of the two have been observed against the different cell types. This suggests that it is the differences in the peptides displayed in the active site that affect the binding ability of

each protein. Overall, it appeared that P19 had greater binding ability against the prokaryotic cell types than P5. However, P5 showed a greater specificity for keratinocytes. The ideal biomolecule should show good binding of prokaryotes with little specificity for eukaryotic cells and therefore future investigation should focus on screening a range of recombinant proteins identified from panning and sequencing for binding potential to MRSA. Although P19 appears to bind greater to MRSA than P5 and therefore may have some utility in bacterial targeting, the conjugation of the photosensitiser to P19 may affect the ability of the recombinant protein to bind to the bacterial target due to the presence of a lysine residue within the peptide sequence that may interrupt binding. Conversely, if the binding potential was retained (whereby the binding properties were due to a different part of the displayed peptide), then the killing ability may be enhanced in this instance, by bringing the photosensitiser in closer proximity to the bacterial cell wall. However, this is very speculative and requires further investigation to identify the advantages/disadvantages of lysine residues within the peptide sequence.

One protein (P5) was expressed as a GFP fusion protein to investigate the feasibility of developing novel cell specific reagents for rapid diagnosis that circumvents the utilisation for antibodies for detection. Binding experiments were performed starting at approximately 4-fold the typical concentration of antibodies routinely utilised for detection (0.5 μg) within our laboratory as a starting concentration, and subsequently increasing the concentration of P5/GFP (40-398 μg/ml). However, results indicated a very small level of initial binding with very slight increases in binding observed as concentration of the fusion protein increased in a dose-dependent manner similar to that of an antibody titre. Therefore, it could be concluded that this compound does not have the same specificity as an antibody and therefore may not be useful for rapid diagnosis of pathogens. Alternatively, considering that P5 was shown to bind previously, loss of binding ability may suggest that the GFP is blocking the protein binding site and therefore modification to the structure of the fusion protein is required for this biomolecule to be effective as a diagnostic tool.

The continued development of bacterial resistance and the limited discovery of new antimicrobials have led to novel methodologies for eradication of bacteria to be required, of which PDT represents a promising approach. Numerous photosensitisers

and a range of light sources can provide inexpensive tools for the treatment of bacterial infection (Wainwright, 1998). The pilot data presented here suggest that it may be possible to utilise recombinant proteins with bacterial binding properties for targeted PDT that may have enhanced bacterial killing properties than the photosensitiser alone. Furthermore, more screening of other recombinant proteins identified from panning against MRSA may identify new proteins with greater MRSA specificity. Therefore it seems feasible to identify other proteins with different binding properties to a range of bacteria that, following demonstration of clear binding, may then be conjugated to either a photosensitiser for targeted PDT or a fluorescent tag for rapid diagnosis of pathogenic bacteria.

CHAPTER SIX
General discussion

6.1 Summary

This thesis has identified a selection of 12-mer peptides with binding specificity for MRSA that have potential as new detection and targeting moieties. Similar to phage technology, microbial display has developed a large number of potential applications including high throughput screening of peptide, antibody and enzyme libraries, live vaccine development/antibody production, epitope mapping, development of bioadsorbents and diagnostic tools/biosensors (Benhar, 2001, Chen and Georgiou, 2002, Lee et al., 2003). Peptides can have similar binding affinities to those of antibodies and furthermore, the small size of peptides and rapid clearance from the blood may be advantageous in comparison with antibodies for *in vivo* studies (Zitzmann et al., 2005). Additionally, the removal of the peptides from the display vehicle would result in straightforward production as peptides are easy to produce, and may also result in longer shelf life than within the display format (De et al., 2005). Furthermore, not only can peptides be produced in large quantities, peptides are amenable to modifications, and may be able to access some binding sites easier than monoclonal antibodies due to their smaller size (Zhou et al., 2004).

In this study the FliTrx ^{TM} bacterial display random peptide library, containing an estimated 1.77×10^8 individual peptides, developed by Lu et al (1995), was screened to identify MRSA-specific peptides. Following selection, through panning, and DNA sequencing, peptides of interest were synthesised. Peptide binding to various bacterial strains and a keratinocyte cell line were performed in order to characterise peptide binding ability and specificity to both pathogen and mammalian cell types. Direct binding of FITC-labelled peptides was observed against all strains of MRSA tested, with greater binding observed using the cyclic construct, presumably because this conformation more closely replicated the original selection format than the linear construct. Furthermore, no binding to keratinocytes was observed indicating selective targeting of MRSA over mammalian cell types. Display technologies provide a very useful technology in the isolation of cell specific ligands because no knowledge of the target is required prior to selection (Bishop-Hurley et al., 2005, Zhou et al., 2004). The

panning and characterisation of peptide binding described here has shown that the process of screening bacteria to identify peptides with pathogen-specific properties is feasible and therefore represents an adaptable system that could be used to further identify many different pathogen-specific peptides.

The continuous increase in bacterial resistance has necessitated the development of alternative treatments that target resistant pathogens. These novel agents need bacterial specificity for pathogen elimination that is independent of pathogen resistance status and little or no cross reactivity for host cells or commensal bacteria. Antimicrobial PDT represents an alternative treatment that has been reported to be effective against both sensitive and drug resistant strains of *S. aureus* (Griffiths et al., 1997, Grinholc et al., 2008, Maisch et al., 2005, Szpakowska et al., 2001). Furthermore, conjugation of different photosensitisers to various biomolecules has previously demonstrated the feasibility of targeted antimicrobial PDT strategies directed against both MRSA and other pathogenic organisms (Hope et al., 2009, Embleton et al., 2004, Hamblin et al., 2002a, Bhatti et al., 2000, Gross et al., 1997, Berthiaume et al., 1994). Therefore, PDT shows promise as an effective topical treatment of chronic wounds, that may be useful either alone or in conjunction with antibiotics to reduce bacterial bioburden and aid wound healing.

The synthesis of high purity (>95%) peptides with modifications such as cyclisation and addition of detection molecules (e.g. biotin or FITC) can be relatively expensive on a small scale. Therefore, a further aim of this thesis was to develop a system to produce native recombinant thioredoxin proteins each containing different peptide sequences of interest previously derived from panning. An *E. coli* based expression and purification system (Clontech) was optimised for successful production of recombinant proteins containing the peptides of interest. In this thesis recombinant proteins were characterised for binding specificity and one protein was conjugated to a porphyrin photosensitiser to determine the cytotoxic effect of the bioconjugate. This pilot study successfully demonstrated the rapid and simple conjugation of the porphyrin to recombinant proteins. The use of the targeted photosensitiser (P12 conjugate) resulted in a greater decrease in MRSA growth than treatment with an equal concentration of the unconjugated capped porphyrin suggesting that direct targeting of pathogens may enhance treatment. This preliminary work strongly supports the concept of an increase

in effectiveness of PDT and therefore it is possible that optimising experimental conditions could further enhance the killing potential of the conjugate. Previously, Embleton et al (2002) demonstrated not only a dose dependent increase in bacterial cell death following an increase in either light dose or photosensitiser concentration separately, however in both cases the IgG conjugated photosensitiser was more effective in treatment than the photosensitiser alone (Embleton et al., 2002). Additionally this group showed a similar effect using a different targeting moiety (phage 75) to deliver the same photosensitiser to varying strains of MRSA (Embleton et al., 2005); demonstrating that targeting of photosensitisers is efficacious.

For successful use a number of factors need to be considered. Photodynamic therapy of wounds may require multiple doses of treatment to eliminate all of the bacteria from the site. Treatment also requires sufficient light and generation of sufficient reactive oxygen species to eradicate bacteria, even those penetrating deeper layers as bacterial regrowth may occur if not all of the microbes are eradicated. Using an animal model for treatment of burn wounds in mice, Lambrechts et al (2005) suggested that future experiments targeting the photosensitiser specifically to the bacteria in the wound may improve efficacy of this treatment and prevent bacterial re-growth that was observed following the experimental PDT, whilst minimising host damage. Furthermore, other groups have demonstrated that repeated PDT exposure on bacterial survivors following previous treatments could still decrease bacterial numbers and that resistant populations unaffected by treatment did not arise (Embleton et al., 2004, Griffiths et al., 1997), further suggesting PDT as a new method of treating pathogens where resistance is not able to develop. Therefore, investigations into the optimal treatment frequencies/dosages to eliminate bacteria completely from wounds are clearly warranted.

6.2 Future work

In this thesis, removal of the peptide of interest from the display vehicle was shown to retain binding against MRSA. However, it may be considered that synthesis following removal from the original structure may not necessarily assume the exact conformation for binding as the original fusion (Lu et al., 1995). Future work should include increasing the valency of peptides by developing multiple peptide display constructs to

attempt to further improve binding by displaying peptides in a more similar conformation to the original selection format.

Sequencing against MRSA, *S. aureus* and *S. epidermidis* identified no obvious consensus sequence which may suggest the identification of peptides that bind to more than one target and therefore may have a range of binding abilities. Future work should involve further large scale DNA sequencing (200+ sequences) of panned clones to identify any consensus or repeated sequences/subunits and then synthesis of the consensus sequence peptide if found. Additionally, further synthesis of the other identified peptides and assessment of binding specificity may identify a range of peptides from MRSA specific, to *Staphylococcal* specific to prokaryotic specific or broad binding to all cells types.

Previous studies have already demonstrated the utility of incorporating negative panning steps to identify peptides with affinity for cancer cell types over normal tissue (Brown et al., 2000, Dane et al., 2006, Li et al., 2008). In order to search for truly prokaryotic markers, future panning studies should incorporate more subtractive panning steps performed throughout selected rounds by panning against eukaryotic cells prior to selection against prokaryotes. Additionally to identify MRSA specific clones, negative panning could first be performed against *S. aureus* in each round prior to MRSA selection. Additionally to negative panning steps, more stringent wash conditions and continuous panning cycles until very few clones are selected may improve specificity of isolated sequences.

Future studies could also involve screening of many other bacterial targets in order to identify peptides against a range of pathogens involved in chronic wounds. Panning could be performed either against intact pathogenic bacteria or against a single target known to be present on the cell surface. However, it may be more advantageous to pan against intact bacteria thus panning against a range of cellular targets, albeit unknown, to identify a series of biomolecules rather than a single target in order to hinder target modification or bacterial adaptation to lose or decrease expression of the target over time.

Furthermore, it would be interesting to compare peptides isolated from this display system with a different display system, e.g. a phage system. Although numerous successes in identifying ligands derived from both display systems have been described, few direct comparisons between the systems have been reported. Lunder et al (2005) compared a commercially available phage and bacterial library and reported that the phage system outperformed the bacterial system following panning against a single purified target (streptavidin). However, it would be interesting to compare the differences between display systems following panning against a more diverse target, such as eukaryotic or prokaryotic cells.

Even though the expression and purification system for recombinant protein production was optimised to improve yield, one limitation of this study was the amount of recombinant protein recovered and therefore alternative systems to produce recombinant proteins need to be identified. However, the associated added cost of using a different expression system should be taken into account. The cytotoxicity assays performed here represent pilot data demonstrating the feasibility of using biomolecules conjugated to photosensitiser for targeted antimicrobial PDT. Future work should be based on investigating the potential of all of the other recombinant thioredoxins successfully cloned into the expression vector (7 against MRSA, 3 against *S. aureus* and 2 against *S. epidermidis*). Additionally varying the concentrations of the conjugate, varying the light dose/frequency, and characterisation of killing potential for other photosensitisers will allow determination of the optimal killing conditions of the conjugate for maximal bacterial death. Finally, investigation into conjugation of the peptides or recombinant proteins to other antimicrobial compounds to improve the efficacy of these compounds may be useful, and also specific targeting could provide a platform to use more potent drugs that currently cannot be used because of damage to the host.

It would be interesting to investigate the differences in the photodynamic action of both the conjugate and photosensitiser alone against a non-resistant strain of *S. aureus*. Previous work on a similar topic by Embleton et al (2004) using an antibody directed against MRSA was shown to also be effective against MSSA and showed some potential against *S. epidermidis*. It was hypothesised that this was due to some antigens being shared and therefore some cross-reactivity with the antibody conjugate was also

observed. In this thesis, although originally the conjugate was derived from panning against MRSA, it may be expected to be effective against non-resistant *S. aureus* and possibly have some activity against *S. epidermidis*. This thesis demonstrated that FITC-labelled peptide derived from panning against MRSA also showed various levels of binding to *S. aureus* and *S. epidermidis*. It may therefore be reasonable to assume that the recombinant protein conjugated to the porphyrin studied here would have some level of cross-reactivity with *Staphylococci* but may also be shown to cross-react with all Gram-positive species to some degree, therefore further testing against these bacteria and other Gram-positive pathogens such as *Streptococci* is warranted. Additionally, as the FITC-labelled peptide was shown to bind *P. aeruginosa*, cytotoxicity assays should be performed against this pathogen in order to assess the utility of the conjugate against this Gram-negative species. However, although very unlikely, it is also possible that the conjugate is MRSA strain specific and therefore will only be effective against MRSA; thus investigation into different bacterial strain targeting would clearly be advantageous to at least begin to elucidate the protein binding target on the bacterial surface. It would also be of interest to determine whether the original peptide sequence conjugated directly to the photosensitiser performs as well or better/worse then the peptide embedded within the full thioredoxin protein.

Cytotoxicity assays targeting bacteria, as part of a biofilm or in animal models rather than in suspension would also be worthy of future investigation. Lambrechts et al (2005) demonstrated that a substantially higher concentration of photosensitiser was required to kill *S. aureus in vivo* than *in vitro* (500 μM and 1.6 μM respectively). Similarly the light dose required was also higher (211 J cm^{-2} *in vivo* and 0.6 J $^{-2}$ *in vitro*). Additionally, Maisch et al (2007) used a 100-fold higher concentration of photosensitiser to treat bacteria in an *ex vivo* porcine skin model than this group had previously used in *in vitro* studies (Maisch et al., 2005). Furthermore, testing the conjugate at different phases of bacterial growth (i.e. lag, exponential and stationary phase) at different concentrations needs investigating. For example, Embleton et al (2002) demonstrated that bacteria exposed to their IgG-conjugated photosensitiser in both the exponential and stationary growth phase were substantially reduced following photodynamic therapy, whereas the susceptibility of bacteria in the lag phase was unaffected. Other studies have shown that *S. aureus* was more resistant in the stationary phase (Nitzan et al., 1989). In contrast others have failed to show an effect of growth

phase on bacterial photosensitisation potential (Embleton et al., 2004, Embleton et al., 2005, Griffiths et al., 1997, Wilson and Pratten, 1995), which suggests that the effect on growth phase appears to be due to the photosensitiser and/or the targeting moiety. Nonetheless, it may be of interest to investigate if there is a growth phase dependent binding effect of the protein which may help to establish if the target on the bacteria is up or down regulated in each growth phase, which may help to characterise the target on the bacterial surface.

To summarise, although PDT shows increasing promise in treatment for eradicating pathogenic bacteria *in vitro,* further investigations *in vivo* are required that investigates the contribution of host factors, bacterial synergy/mixed populations and biofilm formations. The use of different photosensitisers/concentrations, bacterial strains/concentration, light sources, duration/intensity of light, type of dosage, recovery times, viability measurement, host factors, incubation times, *in vitro* vs. *in vivo* studies and general study design (i.e. investigating different strain susceptibility or measuring total bacterial eradication) often make antimicrobial studies difficult to compare. Nonetheless, although it appears to be a multifaceted process, antimicrobial PDT has emerged as a potential powerful tool to treat a range of bacterial pathogens, including those with developing resistant traits that are now difficult to treat with conventional treatments.

6.3 Conclusions

The increasing prevalence of drug resistant bacterial isolates and the bacterial ability to acquire further resistance has led to new and alternative methods of bacterial targeting and detection being urgently required. These new methods employed should be pathogen specific, that are not susceptible to bacterial resistance mechanisms thus rendering the new drugs ineffective, that are able to be used and modified over time to improve efficacy. Although PDT on its own has shown some success, by adopting a targeted antimicrobial PDT approach to select for pathogenic bacteria, indiscriminate killing of host cells and commensal bacteria can be avoided (Bhatti et al., 2000).

This thesis has described a system to identify and produce different proteins that could be utilised for targeted PDT against a range of pathogenic bacteria identified within

chronic wounds for localised treatment with limited damage to the host. Not only does PDT represents a very attractive candidate independently but also identification of novel proteins with pathogenic selectively can only help to enhance this potential. PDT may also provide a very cost effective treatment modality compared to some conventional expensive antimicrobial therapies and requires relatively little infrastructure. Furthermore, novel biomolecules with specific pathogen selectively may have even further applications in addition to targeted PDT as potential rapid diagnostic agents. I believe that targeted antimicrobial PDT represents a truly exciting approach as an alternative treatment of pathogenic organisms that are resistant to conventional therapy, offering great potential to improve treatment times, reduce costs and increase patient quality of life. A collaborative effort should be made between biologists, chemists, microbiologists and clinicians to ensure the development of new biomolecules with enhanced selectively that make their way into general practice.

REFERENCES

AGTERBERG, M., ADRIAANSE, H., VANBRUGGEN, A., KARPERIEN, M. & TOMMASSEN, J. (1990) Outer-Membrane PhoE Protein of Escherichia-Coli K-12 as an Exposure Vector - Possibilities and Limitations. *Gene*, 88, 37-45.

ALOUINI, Z. & JEMLI, M. (2001) Destruction of helminth eggs by photosensitized porphyrin. *Journal of Environmental Monitoring*, 3, 548-551.

AMEMIYA, K., NAKATANI, T., SAITO, A., SUZUKI, A. & MUNAKATA, H. (2005) Hyaluronan-binding motif identified by panning a random peptide display library. *Biochimica Et Biophysica Acta-General Subjects*, 1724, 94-99.

ANWAR, H., DASGUPTA, M. K. & COSTERTON, J. W. (1990) Testing the susceptibility of bacteria in biofilms to antibacterial agents. *Antimicrobial Agents and Chemotherapy*, 34, 2043-2046.

ARNER, E. S. J. & HOLMGREN, A. (2000) Physiological functions of thioredoxin and thioredoxin reductase. *European Journal of Biochemistry*, 267, 6102-6109.

AZZAZY, H. M. E. & HIGHSMITH, W. E. (2002) Phage display technology: clinical applications and recent innovations. *Clinical Biochemistry*, 35, 425-445.

BANEYX, F. (1999) Recombinant protein expression in Escherichia coli. *Current Opinion in Biotechnology*, 10, 411-421.

BANEYX, F. & MUJACIC, M. (2004) Recombinant protein folding and misfolding in Escherichia coli. *Nature Biotechnology*, 22, 1399-1408.

BARRETT, J. F. (2004) MRSA: status and prospects for therapy? An evaluation of key papers on the topic of MRSA and antibiotic resistance. *Expert Opinion on Therapeutic Targets*, 8, 515-519.

BENHAR, I. (2001) Biotechnological applications of phage and cell display. *Biotechnology Advances*, 19, 1-33.

BERTHIAUME, F., REIKEN, S. R., TONER, M., TOMPKINS, R. G. & YARMUSH, M. L. (1994) Antibody-targeted photolysis of bacteria in-vivo. *Bio-Technology*, 12, 703-706.

BERTOLONI, G., LAURO, F. M., CORTELLA, G. & MERCHAT, M. (2000) Photosensitizing activity of hematoporphyrin on Staphylococcus aureus cells. *Biochimica Et Biophysica Acta-General Subjects*, 1475, 169-174.

BERTOLONI, G., ROSSI, F., VALDUGA, G., JORI, G., ALI, H. & VANLIER, J. E. (1992) Photosensitizing activity of water-soluble and lipid-soluble phthalocyanines on prokaryotic and eukaryotic microbial-cells. *Microbios*, 71, 33-46.

BERTOLONI, G., ROSSI, F., VALDUGA, G., JORI, G. & VANLIER, J. (1990) Photosensitizing activity of water-soluble and lipid-soluble phthalocyanines on Escherichia-coli. *Fems Microbiology Letters*, 71, 149-155.

BHATTI, M., MACROBERT, A., HENDERSON, B., SHEPHERD, P., CRIDLAND, J. & WILSON, M. (2000) Antibody-targeted lethal photosensitization of Porphyromonas gingivalis. Antimicrobial Agents and Chemotherapy, 44, 2615-2618.

BIOINFORMATICS, S. I. O. (2009) ExPASy Proteomics Server. Swiss Institute of Bioinformatics.

BISHOP-HURLEY, S. L., SCHMIDT, F. J., ERWIN, A. L. & SMITH, A. L. (2005) Peptides selected for binding to a virulent strain of Haemophilus influenzae by phage display are bactericidal. *Antimicrobial Agents and Chemotherapy*, 49, 2972-2978.

BISLAND, S. K., CHIEN, C., WILSON, B. C. & BURCH, S. (2005) Pre-clinical in vitro and in vivo studies to examine the potential use of photodynamic therapy in the treatment of osteomyelitis. *Optical Methods for Tumor Treatment and Detection: Mechanisms and Techniques in Photodynamic Therapy XIV*, 5689, 26-38.

BJARNSHOLT, T., KIRKETERP-MOLLER, K., JENSEN, P. O., MADSEN, K. G., PHIPPS, R., KROGFELT, K., HOIBY, N. & GIVSKOV, M. (2008) Why chronic wounds will not heal: a novel hypothesis. *Wound Repair and Regeneration*, 16, 2-10.

BLISS, J. M., BIGELOW, C. E., FOSTER, T. H. & HAIDARIS, C. G. (2004) Susceptibility of Candida species to photodynamic effects of photofrin. *Antimicrobial Agents and Chemotherapy*, 48, 2000-2006.

BOEHNCKE, W. H., ELSHORST-SCHMIDT, T. & KAUFMANN, R. (2000) Systemic photodynamic therapy is a safe and effective treatment for psoriasis. *Archives of Dermatology*, 136, 271-272.

BOWLER, P. G., DUERDEN, B. I. & ARMSTRONG, D. G. (2001) Wound microbiology and associated approaches to wound management. *Clinical Microbiology Reviews*, 14, 244-+.

BOWLER, P. G. & DAVIES, B. J. (1999) The microbiology of infected and noninfected leg ulcers. *International Journal of Dermatology*, 38, 573-578.

BRADFORD, M. M. (1976) Rapid and sensitive method for quantitation of microgram quantities of protein utilizing principle of protein-dye binding. *Analytical Biochemistry*, 72, 248-254.

BREKKE, O. H. & LOSET, G. A. (2003) New technologies in therapeutic antibody development. *Current Opinion in Pharmacology*, 3, 544-550.

BRESSLER, N. M. & BRESSLER, S. B. (2000) Photodynamic therapy with verteporfin (visudyne): Impact on ophthalmology and visual sciences. *Investigative Ophthalmology & Visual Science*, 41, 624-628.

BROOK, I. & FRAZIER, E. H. (1998) Aerobic and anaerobic microbiology of chronic venous ulcers. *International Journal of Dermatology*, 37, 426-428.

BROWN, S. B., BROWN, E. A. & WALKER, I. (2004) The present and future role of photodynamic therapy in cancer treatment. *Lancet Oncology*, 5, 497-508.

BROWN, C. K., MODZELEWSKI, R. A., JOHNSON, C. S. & WONG, M. K. K. (2000) A novel approach for the identification of unique tumor vasculature binding peptides using an E-coli peptide display library. *Annals of Surgical Oncology*, 7, 743-749.

BUCHLI, P. J., WU, Z. N. & CIARDELLI, T. L. (1997) The functional display of interleukin-2 on filamentous phage. *Archives of Biochemistry and Biophysics*, 339, 79-84.

BUSSOW, K., NORDHOFF, E., LUBBERT, C., LEHRACH, H. & WALTER, G. (2000) A human cDNA library for high-throughput protein expression screening. *Genomics*, 65, 1-8.

CALZAVARA-PINTON, P. G., VENTURINI, M. & SALA, R. (2005) A comprehensive overview of photodynamic therapy in the treatment of superficial fungal infections of the skin. *Journal of Photochemistry and Photobiology B:Biology*, 78, 1-6.

CARBON, C. (1999) Costs of treating infections caused by methicillin-resistant Staphylococci and vancomycin-resistant Enterococci. *Journal of Antimicrobial Chemotherapy*, 44, 31-36.

CARNAZZA, S., FOTI, C., GIOFFRE, G., FELICI, F. & GUGLIELMINO, S. (2008) Specific and selective probes for Pseudomonas aeruginosa from phage-displayed random peptide libraries. *Biosensors & Bioelectronics*, 23, 1137-1144.

CHAN, Y. & LAI, C. H. (2003) Bactericidal effects of different laser wavelengths on periodontopathic germs in photodynamic therapy. *Lasers in Medical Science*, 18, 51-55.

CHANG, S., SIEVERT, D. M., HAGEMAN, J. C., BOULTON, M. L., TENOVER, F. C., DOWNES, F. P., SHAH, S., RUDRIK, J. T., PUPP, G. R., BROWN, W. J., CARDO, D., FRIDKIN, S. K. & VANCOMYCIN-RESISTANT, S. (2003) Infection with vancomycin-resistant Staphylococcus aureus containing the vanA resistance gene. *New England Journal of Medicine*, 348, 1342-1347.

CHARBIT, A., MOLLA, A., SAURIN, W. & HOFNUNG, M. (1988) Versatility of a Vector for Expressing Foreign Polypeptides at the Surface of Gram-Negative Bacteria. *Gene*, 70, 181-189.

CHEN, W. & GEORGIOU, G. (2002) Cell-surface display of heterologous proteins: From high-throughput screening to environmental applications. *Biotechnology and Bioengineering*, 79, 496-503.

CHOW, J. W. (2000) Aminoglycoside resistance in enterococci. *Clinical Infectious Diseases,* 31, 586-589.

CLARKE, O. J. & BOYLE, R. W. (1999) Isothiocyanatoporphyrins, useful intermediates for the conjugation of porphyrins with biomolecules and solid supports. *Chemical Communications*, 2231-2232.

CONNER-KERR, T. A., SULLIVAN, P. K., GAILLARD, J., FRANKLIN, M. E. & JONES, R. M. (1998) The effects of ultraviolet radiation on antibiotic-resistant bacteria in vitro. *Ostomy Wound Management*, 44, 50-6.

DANE, K. Y., CHAN, L. A., RICE, J. J. & DAUGHERTY, P. S. (2006) Isolation of cell specific peptide ligands using fluorescent bacterial display libraries. *Journal of Immunological Methods*, 309, 120-129.

DANIELSEN, L., BALSLEV, E., DORING, G., HOIBY, N., MADSEN, S. M., AGREN, M., THOMSEN, H. K., FOS, H. H. S. & WESTH, H. (1998) Ulcer bed infection - Report of a case of enlarging venous leg ulcer colonized by Pseudomonas aeruginosa. *Acta Pathologica, Microbiologica et Immunologica Scandinavica*, 106, 721-726.

DAVIS, E. (1996) Don't deny the chance to heal!. 2nd joint Meeting of the Wound healing Society and the European Tissue Repair Society. Boston.

DE HAARD, H. J., VAN NEER, N., REURS, A., HUFTON, S. E., ROOVERS, R. C., HENDERIKX, P., DE BRUINE, A. P., ARENDS, J. W. & HOOGENBOOM, H. R. (1999) A large non-immunized human Fab fragment phage library that permits rapid isolation and kinetic analysis of high affinity antibodies. *Journal of Biological Chemistry*, 274, 18218-18230.

DE, J., CHANG, Y. C., SAMLI, K. N., SCHISLER, J. C., NEWGARD, C. B., JOHNSTON, S. A. & BROWN, K. C. (2005) Isolation of a Mycoplasma-specific binding peptide from an unbiased phage-displayed peptide library. *Molecular Biosystems*, 1, 149-157.

DI POTO, A., SBARRA, M. S., PROVENZA, G., VISAI, L. & SPEZIALE, P. (2009) The effect of photodynamic treatment combined with antibiotic action or host defence mechanisms on Staphylococcus aureus biofilms. *Biomaterials*, 30, 3158-3166.

DINGLASAN, R. R., PORTER-KELLEY, J. M., ALAM, U. & AZAD, A. F. (2005) Peptide mimics as surrogate immunogens of mosquito midgut carbohydrate malaria transmission blocking targets. *Vaccine*, 23, 2717-2724.

DISSEMOND, J. (2009) Methicillin resistant Staphylococcus aureus (MRSA): Diagnostic, clinical relevance and therapy. *Journal Der Deutschen Dermatologischen Gesellschaft*, 7, 544-551.

DONG, J., LIU, C., ZHANG, J., XIN, Z. T., YANG, G., GAO, B., MAO, C. Q., LIU, N. L., WANG, F., SHAO, N. S., FAN, M. & XUE, Y. N. (2006) Selection of novel nickel-binding peptides from flagella displayed secondary peptide library. *Chemical Biology & Drug Design*, 68, 107-112.

DZIDIC, S., SUSKOVIC, J. & KOS, B. (2008) Antibiotic resistance mechanisms in bacteria: Biochemical and genetic aspects. *Food Technology and Biotechnology*, 46, 11-21.

EL ZOEIBY, A., SANSCHAGRIN, F., DARVEAU, A., BRISSON, J. R. & LEVESQUE, R. C. (2003) Identification of novel inhibitors of Pseudomonas aeruginosa MurC enzyme derived from phage-displayed peptide libraries. *Journal of Antimicrobial Chemotherapy*, 51, 531-543.

ELSTON, D. M. (2007) Community-acquired methicillin-resistant Staphylococcus aureus. *Journal of the American Academy of Dermatology*, 56, 1-16.

EMBLETON, M. L., NAIR, S. P., HEYWOOD, W., MENON, D. C., COOKSON, B. D. & WILSON, M. (2005) Development of a novel targeting system for lethal photo sensitization of antibiotic-resistant strains of Staphylococcus aureus. *Antimicrobial Agents and Chemotherapy*, 49, 3690-3696.

EMBLETON, M. L., NAIR, S. P., COOKSON, B. D. & WILSON, M. (2004) Antibody-directed photodynamic therapy of methicillin resistant Staphylococcus aureus. *Microbial Drug Resistance*, 10, 92-97.

EMBLETON, M. L., NAIR, S. P., COOKSON, B. D. & WILSON, M. (2002) Selective lethal photosensitization of methicillin-resistant Staphylococcus aureus using an IgG-tin(IV) chlorin e6 conjugate. *Journal of Antimicrobial Chemotherapy*, 50, 857-864.

ESTEY, E. P., BROWN, K., DIWU, Z. J., LIN, J. X., LOWN, J. W., MILLER, G. G., MOORE, R. B., TULIP, J. & MCPHEE, M. S. (1996) Hypocrellins as photosensitizers for photodynamic therapy: A screening evaluation and pharmacokinetic study. *Cancer Chemotherapy and Pharmacology*, 37, 343-350.

FERRO, S., RICCHELLI, F., MANCINI, G., TOGNON, G. & JORI, G. (2006) Inactivation of methicillin-resistant Staphylococcus aureus (MRSA) by liposome-delivered photo sensitising agents. *Journal of Photochemistry and Photobiology B:Biology*, 83, 98-104.

FILIUS, P. M. G. & GYSSENS, I. C. (2002) Impact of increasing antimicrobial resistance on wound management. *American Journal of Clinical Dermatology*, 3, 1-7.

FOSTER, T. J. & HOOK, M. (1998) Surface protein adhesins of Staphylococcus aureus. *Trends in Microbiology*, 6, 484-488.

FRANCISCO, J. A., CAMPBELL, R., IVERSON, B. L. & GEORGIOU, G. (1993) Production and fluorescence-activated cell sorting of Escherichia-coli expressing a functional antibody fragment on the external surface. *Proceedings of the*

National Academy of Sciences of the United States of America, 90, 10444-10448.

FRANCISCO, J. A., EARHART, C. F. & GEORGIOU, G. (1992) Transport and anchoring of beta-lactamase to the external surface of Escherichia-coli. *Proceedings of the National Academy of Sciences of the United States of America*, 89, 2713-2717.

FREUDL, R., MACINTYRE, S., DEGEN, M. & HENNING, U. (1986) Cell-Surface Exposure of the Outer-Membrane Protein OmpA of Escherichia-Coli K-12. *Journal of Molecular Biology*, 188, 491-494.

FRIEDBERG, J. S., TOMPKINS, R. G., RAKESTRAW, S. L., WARREN, S. W., FISCHMAN, A. J. & YARMUSH, M. L. (1991) Antibody-targeted photolysis - bacteriocidal effects of sn (iv) chlorin e6- dextran-monoclonal antibody conjugates. *Temporal Control of Drug Delivery*, 618, 383-393.

FUCHS, P., WEICHEL, W., DUBEL, S., BREITLING, F. & LITTLE, M. (1996) Separation of E-coli expressing functional cell-wall bound antibody fragments by FACS. *Immunotechnology*, 2, 97-102.

GAD, F., ZAHRA, T., FRANCIS, K. P., HASAN, T. & HAMBLIN, M. R. (2004a) Targeted photodynamic therapy of established soft-tissue infections in mice. *Photochemical & Photobiological Sciences*, 3, 451-458.

GAD, F., ZAHRA, T., HASAN, T. & HAMBLIN, M. R. (2004b) Effects of growth phase and extracellular slime on photodynamic inactivation of gram-positive pathogenic bacteria. *Antimicrobial Agents and Chemotherapy*, 48, 2173-2178.

GEORGIOU, G., STATHOPOULOS, C., DAUGHERTY, P. S., NAYAK, A. R., IVERSON, B. L. & CURTISS, R. (1997) Display of heterologous proteins on the surface of microorganisms: From the screening of combinatorial libraries to live recombinant vaccines. *Nature Biotechnology*, 15, 29-34.

GIEBEL, L. B., CASS, R. T., MILLIGAN, D. L., YOUNG, D. C., ARZE, R. & JOHNSON, C. R. (1995) Screening of cyclic peptide phage libraries identifies ligands that bind streptavidin with high affinities. *Biochemistry*, 34, 15430-15435.

GJODSBOL, K., CHRISTENSEN, J. J., KARLSMARK, T., JORGENSEN, B., KLEIN, B. M. & KROGFELT, K. A. (2006) Multiple bacterial species reside in chronic wounds: a longitudinal study. *International Wound Journal*, 3, 225-31.

GOLD, H. S. & MOELLERING, R. C. (1996) Drug therapy - Antimicrobial-drug resistance. *New England Journal of Medicine*, 335, 1445-1453.

GRELLIER, P., SANTUS, R., MOURAY, E., AGMON, V., MAZIERE, J. C., RIGOMIER, D., DAGAN, A., GATT, S. & SCHREVEL, J. (1997) Photosensitized inactivation of Plasmodium falciparum- and Babesia divergens-infected erythrocytes in whole blood by lipophilic pheophorbide derivatives. *Vox Sanguinis*, 72, 211-220.

GREY, J. E., ENOCH, S. & HARDING, K. G. (2006) ABC of wound healing - Venous and arterial leg ulcers. *British Medical Journal*, 332, 347-350.

GRIFFITHS, M. A., WREN, B. W. & WILSON, M. (1997) Killing of methicillin-resistant Staphylococcus aureus in vitro using aluminium disulphonated phthalocyanine, a light-activated antimicrobial agent. J*ournal of Antimicrobial Chemotherapy*, 40, 873-876.

GRINHOLC, M., SZRAMKA, B., KURLENDA, J., GRACZYK, A. & BIELAWSKI, K. P. (2008) Bactericidal effect of photodynamic inactivation against methicillin-resistant and methicillin-susceptible Staphylococcus aureus is strain-dependent. *Journal of Photochemistry and Photobiology B:Biology*, 90, 57-63.

GROSS, S., BRANDIS, A., CHEN, L., ROSENBACH-BELKIN, V., ROEHRS, S., SCHERZ, A. & SALOMON, Y. (1997) Protein-A-mediated targeting of Bacteriochlorophyll-IgG to Staphylococcus aureus: A model for enhanced site-specific photocytotoxicity. *Photochemistry and Photobiology*, 66, 872-878.

GUIOTTO, A., CHILIN, A., MANZINI, P., DALLACQUA, F., BORDIN, F. & RODIGHIERO, P. (1995) Synthesis and antiproliferative activity of furocoumarin isosters. *Farmaco*, 50, 479-488.

GUNNERIUSSON, E., SAMUELSON, P., UHLEN, M., NYGREN, P. A. & STAHL, S. (1996) Surface display of a functional single-chain Fv antibody on Staphylococci. *Journal of Bacteriology*, 178, 1341-1346.

GURRAN, C., HOLLIDAY, M. G., PERRY, J. D., FORD, M., MORGAN, S. & ORR, K. E. (2002) A novel selective medium for the detection of methicillin-resistant Staphylococcus aureus enabling result reporting in under 24 h. J*ournal of Hospital Infection*, 52, 148-151.

HALBERT, A. R., STACEY, M. C., ROHR, J. B. & JOPP-MCKAY, A. (1992) The effect of bacterial colonization on venous ulcer healing. *Australasian Journal of Dermatology*, 33, 75-80.

HALL, C. E. (2008) The synthesis of cationic porphyrins for use in photodynamic antimicrobial chemotherapy (PACT). Chemistry. Hull, Hull.

HAMBLIN, M. R. & HASAN, T. (2004) Photodynamic therapy: a new antimicrobial approach to infectious disease? *Photochemical & Photobiological Sciences*, 3, 436-450.

HAMBLIN, M. R., ZAHRA, T., CONTAG, C. H., MCMANUS, A. T. & HASAN, T. (2003) Optical monitoring and treatment of potentially lethal wound infections in vivo. *Journal of Infectious Diseases*, 187, 1717-1725.

HAMBLIN, M. R., O'DONNELL, D. A., MURTHY, N., RAJAGOPALAN, K., MICHAUD, N., SHERWOOD, M. E. & HASAN, T. (2002a) Polycationic photosensitizer conjugates: effects of chain length and Gram classification on the photodynamic inactivation of bacteria. *Journal of Antimicrobial Chemotherapy*, 49, 941-951.

HAMBLIN, M. R., O'DONNELL, D. A., MURTHY, N., CONTAG, C. H. & HASAN, T. (2002b) Rapid control of wound infections by targeted photodynamic therapy monitored by in vivo bioluminescence imaging. *Photochemistry and Photobiology*, 75, 51-57.

HERRICK, S. E., SLOAN, P., MCGURK, M., FREAK, L., MCCOLLUM, C. N. & FERGUSON, M. W. J. (1992) Sequential-changes in histologic pattern and extracellular-matrix deposition during the healing of chronic venous ulcers. *American Journal of Pathology*, 141, 1085-1095.

HIRAMATSU, K., CUI, L., KURODA, M. & ITO, T. (2001) The emergence and evolution of methicillin-resistant Staphylococcus aureus. *Trends in Microbiology*, 9, 486-493.

HIRAMATSU, K., ITO, T. & HANAKI, H. (1999) Mechanisms of methicillin and vancomycin resistance in Staphylococcus aureus. *Baillieres Clinical Infectious Diseases*, 5, 221-242.

HIRAMATSU, K., HANAKI, H., INO, T., YABUTA, K., OGURI, T. & TENOVER, F. C. (1997) Methicillin-resistant Staphylococcus aureus clinical strain with reduced vancomycin susceptibility. *Journal of Antimicrobial Chemotherapy*, 40, 135-136.

HONGCHARU, W., TAYLOR, C. R., CHANG, Y. C., AGHASSI, D., SUTHAMJARIYA, K. & ANDERSON, R. R. (2000) Topical ALA-photodynamic therapy for the treatment of acne vulgaris. *Journal of Investigative Dermatology*, 115, 183-192.

HOPE, C. K., PACKER, S., WILSON, M. & NAIR, S. P. (2009) The inability of a bacteriophage to infect Staphylococcus aureus does not prevent it from specifically delivering a photosensitizer to the bacterium enabling its lethal photosensitization. *Journal of Antimicrobial Chemotherapy*, 64, 59-61.

HOWELL-JONES, R. S., WILSON, M. J., HILL, K. E., HOWARD, A. J., PRICE, P. E. & THOMAS, D. W. (2005) A review of the microbiology, antibiotic usage and resistance in chronic skin wounds. *Journal of Antimicrobial Chemotherapy*, 55, 143-149.

HUANG, W. Z., PETROSINO, J. & PALZKILL, T. (1998) Display of functional beta-lactamase inhibitory protein on the surface of M13 bacteriophage. *Antimicrobial Agents and Chemotherapy*, 42, 2893-2897.

HUDSON, R., CARCENAC, M., SMITH, K., MADDEN, L., CLARKE, O. J., PELEGRIN, A., GREENMAN, J. & BOYLE, R. W. (2005) The development and characterisation of porphyrin isothiocyanate-monoclonal antibody conjugates for photoimmunotherapy. *British Journal of Cancer*, 92, 1442-1449.

INFORMATION, N. C. F. B. (2009) Genbank. National Institutes of Health.

INVITROGEN (2009) FliTrx™ Random Peptide Display Library (Version G).

ITO, I., MITSUOKA, N., SOBAJIMA, J., UESUGI, H., OZAKI, S., OHYA, K. & YOSHIDA, M. (2004) Conformational difference in HMGB1 proteins of human neutrophils and lymphocytes revealed by epitope mapping of a monoclonal antibody. *Journal of Biochemistry*, 136, 155-162.

JAYARAMAN, R. (2009) Antibiotic resistance: an overview of mechanisms and a paradigm shift. *Current Science,* 96, 1475-1484.

JEVONS, M. P. (1961) 'Celbenin'-resistant Staphylococci. *British Medical Journal* 1, 124-5.

JORI, G. & BROWN, S. B. (2004) Photosensitized inactivation of microorganisms. *Photochemical & Photobiological Sciences*, 3, 403-405.

KAC, G., BUU-HOI, A., HERISSON, E., BIANCARDINI, P. & DEBURE, C. (2000) Methicillin-resistant Staphylococcus aureus nosocomial acquisition and carrier state in a wound care center. *Archives of Dermatology*, 136, 735-739.

KARRER, S., SZEIMIES, R. M., ERNST, S., ABELS, C., BAUMLER, W. & LANDTHALER, M. (1999) Photodynamic inactivation of staphylococci with 5-aminolaevulinic acid or photofrin. *Lasers in Medical Science*, 14, 54-61.

KATTI, S. K., LEMASTER, D. M. & EKLUND, H. (1990) Crystal-structure of thioredoxin from Escherichia-coli at 1.68A resolution. *Journal of Molecular Biology*, 212, 167-184.

KAUFMAN, D. L. & EVANS, G. A. (1990) Restriction endonuclease cleavage at the termini of PCR products. *Biotechniques*, 9, 304-306.

KERN, R., MALKI, A., HOLMGREN, A. & RICHARME, G. (2003) Chaperone properties of Escherichia coli thioredoxin and thioredoxin reductase. *Biochemical Journal*, 371, 965-972.

KHAN, A. S., THOMPSON, R., CAO, C. & VALDES, J. J. (2003) Selection and characterization of peptide memitopes binding to ricin. *Biotechnology Letters*, 25, 1671-1675.

KISHIMOTO, J., FUKUMA, Y., MIZUNO, A. & NEMOTO, T. K. (2005) Identification of the pentapeptide constituting a dominant epitope common to all eukaryotic heat shock protein 90 molecular chaperones. *Cell Stress & Chaperones*, 10, 296-311.

KOMERIK, N., WILSON, M. & POOLE, S. (2000) The effect of photodynamic action on two virulence factors of gram-negative bacteria. *Photochemistry and Photobiology*, 72, 676-680.

KREITNER, M., WAGNER, K.-H., ALTH, G., EBERMANN, R., FOISSY, H. & ELMADFA, I. (2003) Finding optimal photosensitisers for the decontamination of foods by the photodynamic effect. *Forum of Nutrition*, 56, 367-9.

KUZNETSOVA, N. A., MAKAROV, D. A., KALIYA, O. L. & VOROZHTSOV, G. N. (2007) Photosensitized oxidation by dioxygen as the base for drinking water disinfection. *Journal of Hazardous Materials*, 146, 487-491.

LAMBRECHTS, S. A. G., DEMIDOVA, T. N., AALDERS, M. C. G., HASAN, T. & HAMBLIN, M. R. (2005) Photodynamic therapy for Staphylococcus aureus infected burn wounds in mice. *Photochemical & Photobiological Sciences*, 4, 503-509.

LAVALLIE, E. R., LU, Z. J., DIBLASIO-SMITH, E. A., COLLINS-RACIE, L. A. & MCCOY, J. M. (2000) Thioredoxin as a fusion partner for production of soluble recombinant proteins in Escherichia coli. *Applications of Chimeric Genes and Hybrid Proteins, Pt A*, 326, 322-340.

LAVALLIE, E. R., DIBLASIO, E. A., KOVACIC, S., GRANT, K. L., SCHENDEL, P. F. & MCCOY, J. M. (1993) A thioredoxin gene fusion expression system that circumvents inclusion body formation in the Escherichia-coli cytoplasm. *Bio-Technology*, 11, 187-193.

LEE, S. Y., CHOI, J. H. & XU, Z. H. (2003) Microbial cell-surface display. *Trends in Biotechnology*, 21, 45-52.

LEE, J. S., SHIN, K. S., PAN, J. G. & KIM, C. J. (2000) Surface-displayed viral antigens on Salmonella carrier vaccine. *Nature Biotechnology*, 18, 645-648.

LENNON, B. W., WILLIAMS, C. H. & LUDWIG, M. L. (2000) Twists in catalysis: Alternating conformations of Escherichia coli thioredoxin reductase. *Science*, 289, 1190-1194.

LI, W. H., LEI, P., YU, B., WU, S., PENG, J. L., ZHAO, X. P., ZHU, H. F., KIRSCHFINK, M. & SHEN, G. X. (2008) Screening and identification of a novel target specific for hepatoma cell line HepG2 from the FliTrx bacterial peptide library. *Acta Biochimica et Biophysica Sinica*, 40, 443-451.

LIM, T. S., MWIPATAYI, B. P., MURRAY, R., SIEUNARINE, K., ABBAS, M. & ANGEL, D. (2006) Microbiological profile of chronic ulcers of the lower limb: A prospective observational cohort study. *Anz Journal of Surgery*, 76, 688-692.

LIN, H. Y., CHEN, C. T. & HUANG, C. T. (2004) Use of merocyanine 540 for photodynamic inactivation of staphylococcus aureus planktonic and biofilm cells. *Applied and Environmental Microbiology*, 70, 6453-6458.

LIVERMORE, D. M. (2000) Antibiotic resistance in staphylococci. International *Journal of Antimicrobial Agents*, 16, S3-S10.

LU, Z. J., MURRAY, K. S., VANCLEAVE, V., LAVALLIE, E. R., STAHL, M. L. & MCCOY, J. M. (1995) Expression of thioredoxin random peptide libraries on the Escherichia-coli cell-surface as functional fusions to flagellin - a system designed for exploring protein-protein interactions. *Bio-Technology*, 13, 366-372.

LUNDER, M., BRATKOVIC, T., DOLJAK, B., KREFT, S., URLEB, U., STRUKELJ, B. & PLAZAR, N. (2005) Comparison of bacterial and phage display peptide libraries in search of target-binding motif. *Applied Biochemistry and Biotechnology*, 127, 125-131.

LUTZ, R. & BUJARD, H. (1997) Independent and tight regulation of transcriptional units in Escherichia coli via the LacR/O, the TetR/O and AraC/I-1-I-2 regulatory elements. *Nucleic Acids Research*, 25, 1203-1210.

MA, X. X., ITO, T., TIENSASITORN, C., JAMKLANG, M., CHONGTRAKOOL, P., BOYLE-VAVRA, S., DAUM, R. S. & HIRAMATSU, K. (2002) Novel type of staphylococcal cassette chromosome mec identified in community-acquired methicillin-resistant Staphylococcus aureus strains. *Antimicrobial Agents and Chemotherapy*, 46, 1147-1152.

MACRAE, F. (2006) A bright new future for MRSA testing. Clinical Laboratory International.

MADSEN, S. M., WESTH, H., DANIELSEN, L. & ROSDAHL, V. T. (1996) Bacterial colonization and healing of venous leg ulcers. *Acta Pathologica, Microbiologica et Immunologica Scandinavica*, 104, 895-899.

MAISCH, T. (2007a) Anti-microbial photodynamic therapy: useful in the future? *Lasers in Medical Science*, 22, 83-91.

MAISCH, T., BOSL, C., SZEIMIES, R. M., LOVE, B. & ABELS, C. (2007b) Determination of the antibacterial efficacy of a new porphyrin-based photosensitizer against MRSA ex vivo. *Photochemical & Photobiological Sciences*, 6, 545-551.

MAISCH, T., BOSL, C., SZEIMIES, R. M., LEHN, N. & ABELS, C. (2005) Photodynamic effects of novel XF porphyrin derivatives on prokaryotic and eukaryotic cells. *Antimicrobial Agents and Chemotherapy*, 49, 1542-1552.

MAJANDER, K., KORHONEN, T. K. & WESTERLUND-WIKSTROM, B. (2005) Simultaneous display of multiple foreign peptides in the FliD capping and FliC filament proteins of the Escherichia coli flagellum. *Applied and Environmental Microbiology*, 71, 4263-4268.

MANIATIS, T., FRITSCH, E. F. & SAMBROOK, J. (1982) Molecular Cloning, A Laboratory Manual. , New York, Cold Spring Harbor Laboratory.

MCCAFFERTY, J., JACKSON, R. H. & CHISWELL, D. J. (1991) Phage-Enzymes - Expression and Affinity-Chromatography of Functional Alkaline-Phosphatase on the Surface of Bacteriophage. *Protein Engineering*, 4, 955-961.

MENEZES, S., CAPELLA, M. A. M. & CALDAS, L. R. (1990) Photodynamic-action of methylene-blue - repair and mutation in Escherichia-coli. *Journal of Photochemistry and Photobiology B:Biology*, 5, 505-517.

MERCHAT, M., BERTOLINI, G., GIACOMINI, P., VILLANUEVA, A. & JORI, G. (1996) Meso-substituted cationic porphyrins as efficient photosensitizers of

gram-positive and gram-negative bacteria. *Journal of Photochemistry and Photobiology B:Biology*, 32, 153-157.

MERSICH, C. & JUNGBAUER, A. (2008) Generation of bioactive peptides by biological libraries. *Journal of Chromatography B-Analytical Technologies in the Biomedical and Life Sciences*, 861, 160-170.

MINNOCK, A., VERNON, D. I., SCHOFIELD, J., GRIFFITHS, J., PARISH, J. H. & BROWN, S. B. (1996) Photoinactivation of bacteria. Use of a cationic water-soluble zinc phthalocyanine to photoinactivate both gram-negative and gram-positive bacteria. *Journal of Photochemistry and Photobiology B-Biology*, 32, 159-164.

MULLEN, L. M., NAIR, S. P., WARD, J. M., RYCROFT, A. N. & HENDERSON, B. (2006) Phage display in the study of infectious diseases. *Trends in Microbiology*, 14, 141-147.

NAGAI, K., DAVIES, T. A., JACOBS, M. R. & APPELBAUM, P. C. (2002) Effects of amino acid alterations in penicillin-binding proteins (PBPs) 1a, 2b, and 2x on PBP affinities of penicillin, ampicillin, amoxicillin, cefditoren, cefuroxime, cefprozil, and cefaclor in 18 clinical isolates of penicillin-susceptible, -intermediate, and -resistant pneumococci. *Antimicrobial Agents and Chemotherapy,* 46, 1273-1280.

NAKAJIMA, H., SHIMBARA, N., SHIMONISHI, Y., MIMORI, T., NIWA, S. & SAYA, H. (2000) Expression of random peptide fused to invasin on bacterial cell surface for selection of cell-targeting peptides. *Gene*, 260, 121-131.

NAZ, R. K., ZHU, X. L. & KADAM, A. L. (2000) Identification of human sperm peptide sequence involved in egg binding for immunocontraception. *Biology of Reproduction*, 62, 318-324.

NGAMPASUTADOL, J., RICE, P. A., WALSH, M. T. & GULATI, S. (2006) Characterization of a peptide vaccine candidate mimicking an oligosaccharide epitope of Neisseria gonorrhoeae and resultant immune responses and function. *Vaccine*, 24, 157-170.

NIGAM, Y., BEXFIELD, A., THOMAS, S. & RATCLIFFE, N. A. (2006) Maggot therapy: The science and implication for CAM - Part I - History and bacterial resistance. *Evidence-Based Complementary and Alternative Medicine*, 3, 223-227.

NISSIM, A., HOOGENBOOM, H. R., TOMLINSON, I. M., FLYNN, G., MIDGLEY, C., LANE, D. & WINTER, G. (1994) Antibody Fragments from a Single Pot Phage Display Library as Immunochemical Reagents. *Embo Journal,* 13, 692-698.

NITZAN, Y., SALMON-DIVON, M., SHPOREN, E. & MALIK, Z. (2004) ALA induced photodynamic effects on Gram positive and negative bacteria. *Photochemical & Photobiological Sciences*, 3, 430-435.

NITZAN, Y., GUTTERMAN, M., MALIK, Z. & EHRENBERG, B. (1992) Inactivation of gram-negative bacteria by photosensitized porphyrins. *Photochemistry and Photobiology*, 55, 89-96.

NITZAN, Y., SHAINBERG, B. & MALIK, Z. (1989) THE MECHANISM OF Photodynamic inactivation of staphylococcus-aureus by deuteroporphyrin. *Current Microbiology*, 19, 265-269.

NOBLE, W. C., VIRANI, Z. & CREE, R. G. A. (1992) Co-transfer of vancomycin and other resistance genes from Enterococcus-faecalis nctc-12201 to Staphylococcus-aureus. *Fems Microbiology Letters*, 93, 195-198.

O'BRIEN, F. G., PEARMAN, J. W., GRACEY, M., RILEY, T. V. & GRUBB, W. B. (1999) Community strain of methicillin-resistant Staphylococcus aureus involved in a hospital outbreak. *Journal of Clinical Microbiology*, 37, 2858-2862.

O'MEARA, S., AL-KURDI, D. & OVINGTON, L. G. (2008) Antibiotics and antiseptics for venous leg ulcers. Cochrane Database of Systematic Reviews.

O'NEIL, K. T., HOESS, R. H., JACKSON, S. A., RAMACHANDRAN, N. S., MOUSA, S. A. & DEGRADO, W. F. (1992) Identification of novel peptide antagonists for GPIIb/IIIa from a conformationally constrained phage peptide library. *Proteins-Structure Function and Genetics*, 14, 509-515.

O'RIORDAN, K., AKILOV, O. E. & HASAN, T. (2005) The potential for photodynamic therapy in the treatment of localized infections. *Photodiagnosis and Photodynamic Therapy 2*, 247-262.

OLSEN, M. J., STEPHENS, D., GRIFFITHS, D., DAUGHERTY, P., GEORGIOU, G. & IVERSON, B. L. (2000) Function-based isolation of novel enzymes from a large library. *Nature Biotechnology*, 18, 1071-1074.

ORENSTEIN, A., KLEIN, D., KOPOLOVIC, J., WINKLER, E., MALIK, Z., KELLER, N. & NITZAN, Y. (1997) The use of porphyrins for eradication of Staphylococcus aureus in burn wound infections. *Fems Immunology and Medical Microbiology*, 19, 307-314.

RAAB, O. (1900) Ueber die Wirkung fluorizierender Stoffe auf Infusorien. *Zeitschrift Biologie*, 39, 524-546.

REICHENBERG, J. & DAVIS, M. (2005) Venous ulcers. *Seminars in Cutaneous Medicine and Surgery*, 24, 216-226.

ROBERTS, J. I. S. & GASTON, M. A. (1987) Protein-A and coagulase expression in epidemic and non-epidemic staphylococcus-aureus. *Journal of Clinical Pathology*, 40, 837-840.

RUCKLEY, C. V. (1997) Socioeconomic impact of chronic venous insufficiency and leg ulcers. *Angiology*, 48, 67-69.

SANGER, F., NICKLEN, S. & COULSON, A. R. (1977) DNA sequencing with chain-terminating inhibitors. *Proceedings of the National Academy of Sciences of the United States of America*, 74, 5463-5467.

SANTUS, R., GRELLIER, P., SCHREVEL, J., MAZIERE, J. C. & STOLTZ, J. F. (1998) Photodecontamination of blood components: advantages and drawbacks. *Clinical Hemorheology and Microcirculation*, 18, 299-308.

SCHARF, S. J., HORN, G. T. & ERLICH, H. A. (1986) Direct cloning and sequence-analysis of enzymatically amplified genomic sequences. *Science*, 233, 1076-1078.

SCHRAIBMAN, I. G. (1990) The significance of beta-hemolytic Streptococci in chronic leg ulcers. *Annals of the Royal College of Surgeons of England*, 72, 123-124.

SEGALLA, A., BORSARELLI, C. D., BRASLAVSKY, S. E., SPIKES, J. D., RONCUCCI, G., DEI, D., CHITI, G., JORI, G. & REDDI, E. (2002) Photophysical, photochemical and antibacterial photosensitizing properties of a novel octacationic Zn(II)-phthalocyanine. *Photochemical & Photobiological Sciences*, 1, 641-8.

SHARMA, M., VISAI, L., BRAGHERI, F., CRISTIANI, I., GUPTA, P. K. & SPEZIALE, P. (2008) Toluidine blue-mediated photodynamic effects on staphylococcal biofilms. *Antimicrobial Agents and Chemotherapy*, 52, 299-305.

SIDHU, S. S., WEISS, G. A. & WELLS, J. A. (2000) High copy display of large proteins on phage for functional selections. *Journal of Molecular Biology*, 296, 487-495.

SINGLETON, D. R., MASUOKA, J. & HAZEN, K. C. (2001) Cloning and analysis of a Candida albicans gene that affects cell surface hydrophobicity. *Journal of Bacteriology*, 183, 3582-3588.

SMITH, G. P. (1985) Filamentous Fusion Phage - Novel Expression Vectors That Display Cloned Antigens on the Virion Surface. *Science*, 228, 1315-1317.

SOMERS, V. A., BRANDWIJK, R. J., JOOSTEN, B., MOERKERK, P. T., ARENDS, J. W., MENHEERE, P., PIETERSE, W. O., CLAESSEN, A., SCHEPER, R. J., HOOGENBOOM, H. R. & HUFTON, S. E. (2002) A panel of candidate tumor antigens in colorectal cancer revealed by the serological selection of a phage displayed cDNA expression library. *Journal of Immunology*, 169, 2772-2780.

SOUKOS, N. S., XIMENEZ-FYVIE, L. A., HAMBLIN, M. R., SOCRANSKY, S. S. & HASAN, T. (1998) Targeted antimicrobial photochemotherapy. *Antimicrobial Agents and Chemotherapy*, 42, 2595-2601.

SOUSA, C., KOTRBA, P., RUML, T., CEBOLLA, A. & DE LORENZO, V. (1998) Metalloadsorption by Escherichia coli cells displaying yeast and mammalian metallothioneins anchored to the outer membrane protein LamB. *Journal of Bacteriology*, 180, 2280-2284.

STANELOUDI, C., SMITH, K. A., HUDSON, R., MALATESTI, N., SAVOIE, H., BOYLE, R. W. & GREENMAN, J. (2007) Development and characterization of novel photosensitizer : scFv conjugates for use in photodynamic therapy of cancer. *Immunology*, 120, 512-517.

STEFANKOVA, P., KOLLAROVA, M. & BARAK, I. (2005) Thioredoxin - Structural and functional complexity. *General Physiology and Biophysics*, 24, 3-11.

STEPHENS, P., WALL, I. B., WILSON, M. J., HILL, K. E., DAVIES, C. E., HILL, C. M., HARDING, K. G. & THOMAS, D. W. (2003) Anaerobic cocci populating the deep tissues of chronic wounds impair cellular wound healing responses in vitro. *British Journal of Dermatology*, 148, 456-466.

STRAUSS, A. & GOTZ, F. (1996) In vivo immobilization of enzymatically active polypeptides on the cell surface of Staphylococcus carnosus. *Molecular Microbiology*, 21, 491-500.

SUTTON, J. M., CLARKE, O. J., FERNANDEZ, N. & BOYLE, R. W. (2002) Porphyrin, chlorin, and bacteriochlorin isothiocyanates: Useful reagents for the synthesis of photoactive bioconjugatest. *Bioconjugate Chemistry*, 13, 249-263.

SZPAKOWSKA, M., LASOCKI, K., GRZYBOWSKI, J. & GRACZYK, A. (2001) Photodynamic activity of the haematoporphyrin derivative with rutin and arginine substituents (HpD-Rut(2)-Arg(2)) against Staphylococcus aureus and Pseudomonas aeruginosa. *Pharmacological Research*, 44, 243-246.

TAO, J. S., WENDLER, P., CONNELLY, G., LIM, A., ZHANG, J. S., KING, M., LI, T. C., SILVERMAN, J. A., SCHIMMEL, P. R. & TALLY, F. P. (2000) Drug target validation: Lethal infection blocked by inducible peptide. *Proceedings of the National Academy of Sciences of the United States of America*, 97, 783-786.

TASCHNER, S., MEINKE, A., VON GABAIN, A. & BOYD, A. P. (2002) Selection of peptide entry motifs by bacterial surface display. *Biochemical Journal*, 367, 393-402.

TELENTI, A., IMBODEN, P., MARCHESI, F., LOWRIE, D., COLE, S., COLSTON, M. J., MATTER, L., SCHOPFER, K. & BODMER, T. (1993) Detection of rifampicin-resistance mutations in Mycobacterium-tuberculosis. *Lancet,* 341, 647-650.

TERPE, K. (2006) Overview of bacterial expression systems for heterologous protein production: from molecular and biochemical fundamentals to commercial systems. *Applied Microbiology and Biotechnology*, 72, 211-222.

TERPE, K. (2003) Overview of tag protein fusions: from molecular and biochemical fundamentals to commercial systems. *Applied Microbiology and Biotechnology*, 60, 523-533.

THAI, T. R., KEAST, D. H., CAMPBELL, K. E., WOODBURY, M. G. & HOUGHTON, P. E. (2005) Effect of ultraviolet light C on bacterial colonization in chronic wounds. *Ostomy Wound Management*, 51, 32-+.

TOMMASSEN, J., AGTERBERG, M., JANSSEN, R. & SPIERINGS, G. (1993) Use of the Enterobacterial Outer-Membrane Protein PhoE in the Development of New Vaccines and DNA Probes. *Zentralblatt Fur Bakteriologie-International Journal of Medical Microbiology Virology Parasitology and Infectious Diseases*, 278, 396-406.

TRENGOVE, N. J., STACEY, M. C., MCGECHIE, D. F. & MATA, S. (1996) Qualitative bacteriology and leg ulcer healing. *Journal of Wound Care*, 5, 277-80.

TRIAS, J. & GORDON, E. M. (1997) Innovative approaches to novel antibacterial drug discovery. *Current Opinion in Biotechnology*, 8, 757-762.

TRIPP, B. C., LU, Z. J., BOURQUE, K., SOOKDEO, H. & MCCOY, J. M. (2001) Investigation of the 'switch-epitope' concept with random peptide libraries displayed as thioredoxin loop fusions. *Protein Engineering*, 14, 367-377.

TSAI, T., YANG, Y. T., WANG, T. H., CHIEN, H. F. & CHEN, C. T. (2009) Improved Photodynamic Inactivation of Gram-Positive Bacteria Using Hematoporphyrin Encapsulated in Liposomes and Micelles. *Lasers in Surgery and Medicine*, 41, 316-322.

UENO, T., MISAWA, S., OHBA, Y., MATSUMOTO, M., MIZUNUMA, M., KASAI, N., TSUMOTO, K., KUMAGAI, I. & HAYASHI, H. (2000) Isolation and characterization of monoclonal antibodies that inhibit hepatitis C virus NS3 protease. *Journal of Virology*, 74, 6300-6308.

VALENCIA, I. C., KIRSNER, R. S. & KERDEL, F. A. (2004) Microbiologic evaluation of skin wounds: Alarming trend toward antibiotic resistance in an inpatient dermatology service during a 10-year period. *Journal of the American Academy of Dermatology*, 50, 845-849.

VON TAPPEINER, H. (1904) Zur Kenntnis der lichtwirkenden (fluoreszierenden) Stoffe. *Deutsche Medizinische Wochenschrift*, 1, 579-580.

WAINWRIGHT, M. & CROSSLEY, K. B. (2004) Photosensitising agents - circumventing resistance and breaking down biofilms: a review. *International Biodeterioration & Biodegradation*, 53, 119-126.

WAINWRIGHT, M., PHOENIX, D. A., NICKSON, P. B. & MORTON, G. (2002) The use of new methylene blue in Pseudomonas aeruginosa biofilm destruction. *Biofouling*, 18, 247-249.

WAINWRIGHT, M. (1998a) Photodynamic antimicrobial chemotherapy (PACT). *Journal of Antimicrobial Chemotherapy*, 42, 13-28.

WAINWRIGHT, M., PHOENIX, D. A., LAYCOCK, S. L., WAREING, D. R. A. & WRIGHT, P. A. (1998b) Photobactericidal activity of phenothiazinium dyes against methicillin-resistant strains of Staphylococcus aureus. *Fems Microbiology Letters*, 160, 177-181.

WAKAYAMA, Y., TAKAGI, M. & YANO, K. (1980) Photosensitized inactivation of Escherichia-coli-cells in toluidine blue-light system. *Photochemistry and Photobiology*, 32, 601-605.

WALL, I. B., DAVIES, C. E., HILL, K. E., WILSON, M. J., STEPHENS, P., HARDING, K. G. & THOMAS, D. W. (2002) Potential role of anaerobic cocci in impaired human wound healing. *Wound Repair and Regeneration*, 10, 346-353.

WALSH, C. (2003) Antibiotics: actions, origins, resistance, Washington DC, ASM Press.

WAUGH, D. S. (2005) Making the most of affinity tags. *Trends in Biotechnology*, 23, 316-320.

WERNERUS, H. & STAHL, S. (2004) Biotechnological applications for surface-engineered bacteria. *Biotechnology and Applied Biochemistry*, 40, 209-228.

WESTERLUND-WIKSTROM, B. (2000) Peptide display on bacterial flagella: Principles and applications. *International Journal of Medical Microbiology*, 290, 223-230.

WESTERLUND-WIKSTROM, B., TANSKANEN, J., VIRKOLA, R., HACKER, J., LINDBERG, M., SKURNIK, M. & KORHONEN, T. K. (1997) Functional expression of adhesive peptides as fusions to Escherichia coli flagellin. *Protein Engineering*, 10, 1319-1326.

WHITE, R. J. & CUTTING, K. F. (2006) Critical colonization - The concept under scrutiny. *Ostomy Wound Management*, 52, 50-56.

WILLATS, W. G. T. (2002) Phage display: practicalities and prospects. *Plant Molecular Biology*, 50, 837-854.

WILSON, M., BURNS, T. & PRATTEN, J. (1996) Killing of Streptococcus sanguis in biofilms using a light-activated antimicrobial agent. *Journal of Antimicrobial Chemotherapy*, 37, 377-381.

WILSON, M. & PRATTEN, J. (1995) Lethal photosensitization of staphylococcus-aureus in-vitro - effect of growth-phase, serum, and preirradation time. *Lasers in Surgery and Medicine*, 16, 272-276.

WILSON, M. & YIANNI, C. (1995) Killing of methicillin-resistant staphylococcus-aureus by low-power laser-light. *Journal of Medical Microbiology*, 42, 62-66.

XIN, Z. T., LIU, C., DONG, B., GAO, Y. P., SHAO, N. S., LIU, W., ZHANG, J., DONG, J., LING, S. G. & XUE, Y. N. (2004) A subtractive fluorescence-activated cell-sorting strategy to identify mimotopes of HBV-preS protein from bacterially displayed peptide library. *Journal of Immunological Methods*, 293, 13-21.

XIN, Z. T., LIU, C., GAO, Y. P., MAO, C. Q., ZHAO, A., ZHANG, H., SHAO, N. S., LING, S. G. & XUE, Y. N. (2003) Identification of mimotopes by screening of a

bacterially displayed random peptide library and its use in eliciting an immune response to native HBV-preS. *Vaccine*, 21, 4373-4379.

YACOBY, I., SHAMIS, M., BAR, H., SHABAT, D. & BENHAR, I. (2006) Targeting antibacterial agents by using drug-carrying filamentous bacteriophages. *Antimicrobial Agents and Chemotherapy*, 50, 2087-2097.

YANG, W. H., LUO, D. F., WANG, S. X., WANG, R., CHEN, R., LIU, Y., ZHU, T., MA, X. Y., LIU, R. H., XU, G., MENG, L., LU, Y. P., ZHOU, J. F. & MA, D. (2008) TMTP1, a novel tumor-homing peptide specifically targeting metastasis. *Clinical Cancer Research*, 14, 5494-5502.

YOSHIDA, H., BAIK, S. H. & HARAYAMA, S. (2002) An effective peptide screening system using recombinant fluorescent bacterial surface display. *Biotechnology Letters*, 24, 1715-1722.

ZANIN, I. C. J., LOBO, M. M., RODRIGUES, L. K. A., PIMENTA, L. A. F., HOFLING, J. F. & GONCALVES, R. B. (2006) Photosensitization of in vitro biofilms by toluidine blue O combined with a light-emitting diode. *European Journal of Oral Sciences*, 114, 64-69.

ZEINA, B., GREENMAN, J., CORRY, D. & PURCELL, W. M. (2003) Antimicrobial photodynamic therapy: assessment of genotoxic effects on keratinocytes in vitro. *British Journal of Dermatology*, 148, 229-232.

ZEINA, B., GREENMAN, J., CORRY, D. & PURCELL, W. M. (2002) Cytotoxic effects of antimicrobial photodynamic therapy on keratinocytes in vitro. *British Journal of Dermatology*, 146, 568-573.

ZEINA, B., GREENMAN, J., PURCELL, W. M. & DAS, B. (2001) Killing of cutaneous microbial species by photodynamic therapy. *British Journal of Dermatology*, 144, 274-278.

ZHAO, S. M. & LEE, E. Y. C. (1997) A protein phosphatase-1-binding motif identified by the panning of a random peptide display library. *Journal of Biological Chemistry*, 272, 28368-28372.

ZHENG, X., SALLUM, U. W., VERMA, S., ATHAR, H., EVANS, C. L. & HASAN, T. (2009) Exploiting a Bacterial Drug-Resistance Mechanism: A Light-Activated Construct for the Destruction of MRSA. *Angewandte Chemie-International Edition*, 48, 2148-2151.

ZHOU, X., CHANG, Y. C., OYAMA, T., MCGUIRE, M. J. & BROWN, K. C. (2004) Cell-specific delivery of a chemotherapeutic to lung cancer cells. *Journal of the American Chemical Society*, 126, 15656-15657.

ZITZMANN, S., KRAMER, S., MIER, W., MAHMUT, M., FLEIG, J., ALTMANN, A., EISENHUT, M. & HABERKORN, U. (2005) Identification of a new prostate-specific cyclic peptide with the bacterial FliTrx system. *Journal of Nuclear Medicine*, 46, 782-785.

ZOLFAGHARI, P. S., PACKER, S., SINGER, M., NAIR, S. P., BENNETT, J., STREET, C. & WILSON, M. (2009) In vivo killing of Staphylococcus aureus using a light-activated antimicrobial agent. Bmc Microbiology, 9. DOI:10.1186/1471-2180-9-27

Fig 1.1: Potential microbial factors contributing to wound non-healing/infection

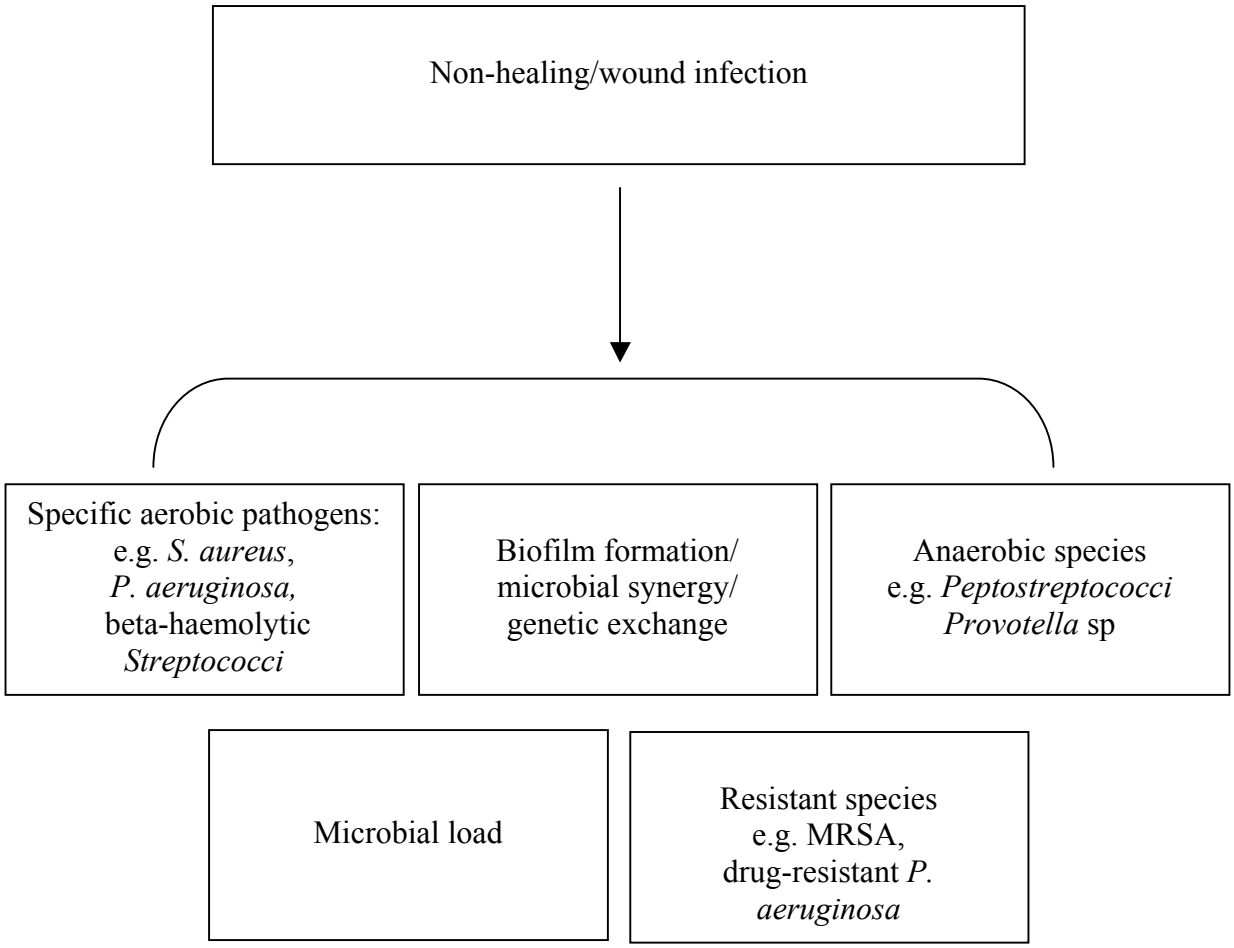

Fig 1.1: Microbial factors that can contribute to the wound non-healing/ infection phenotype

Fig 1.2: Structure of *S. aureus* cell wall peptidoglycan

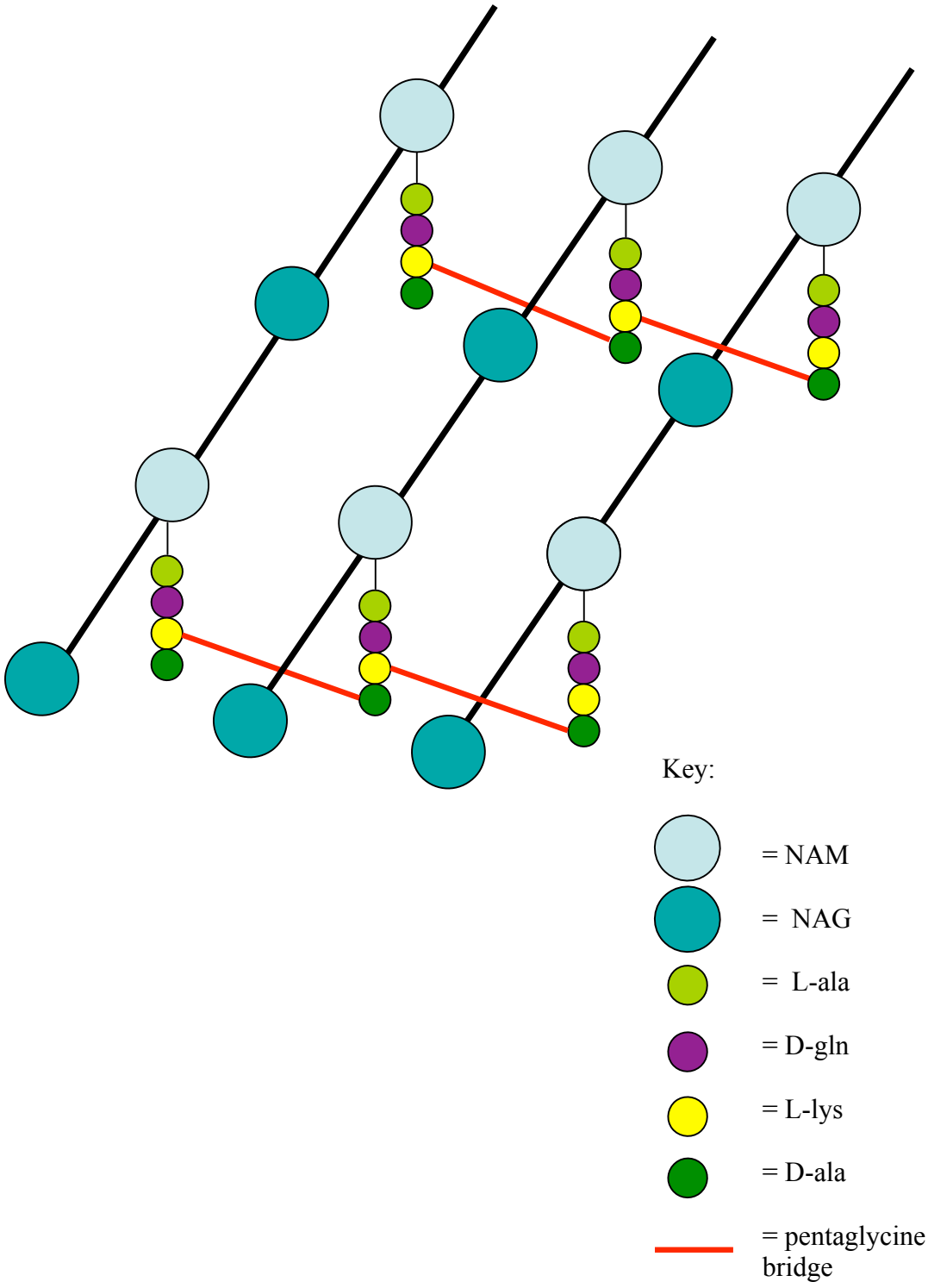

Fig 1.2: Schematic representation of peptidoglycan structure. Peptidoglycan consists of two joined amino sugars NAM and NAG with L-ala-D-gln-L-lys-D-ala peptides attached to the NAM linking strands by a pentaglycine bridge

Fig 1.3: Structure of *S. aureus* cell wall

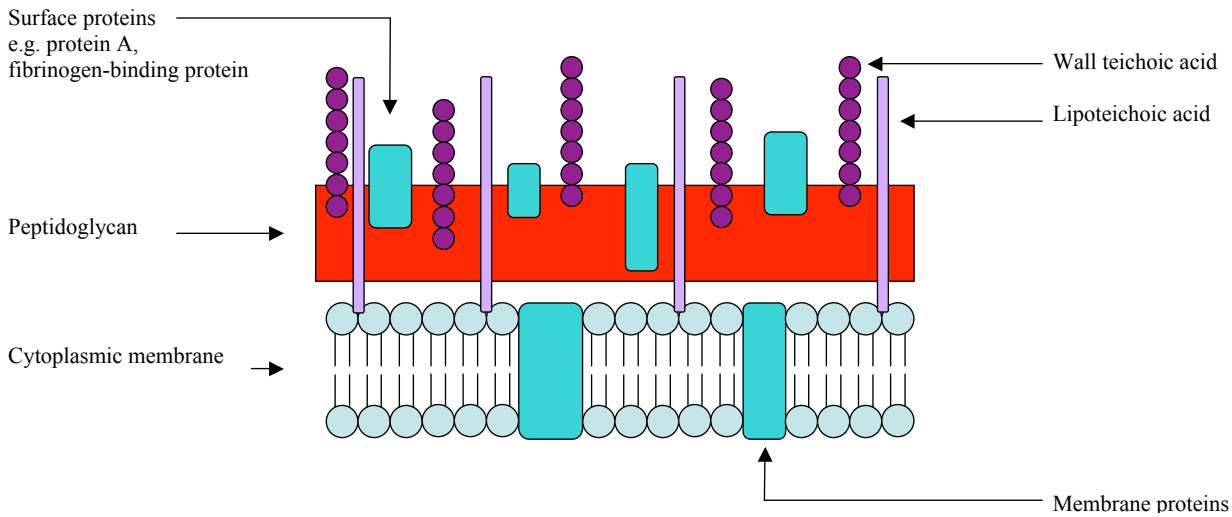

Fig 1.3: Schematic representation of *S. aureus* cell wall composed of peptidoglycan, teichoic acid, lipoteichoic acid and wall associated proteins

Fig 1.4: Diagrammatic representation of virulence factors possessed by *S. aureus* that enable host colonisation and infection

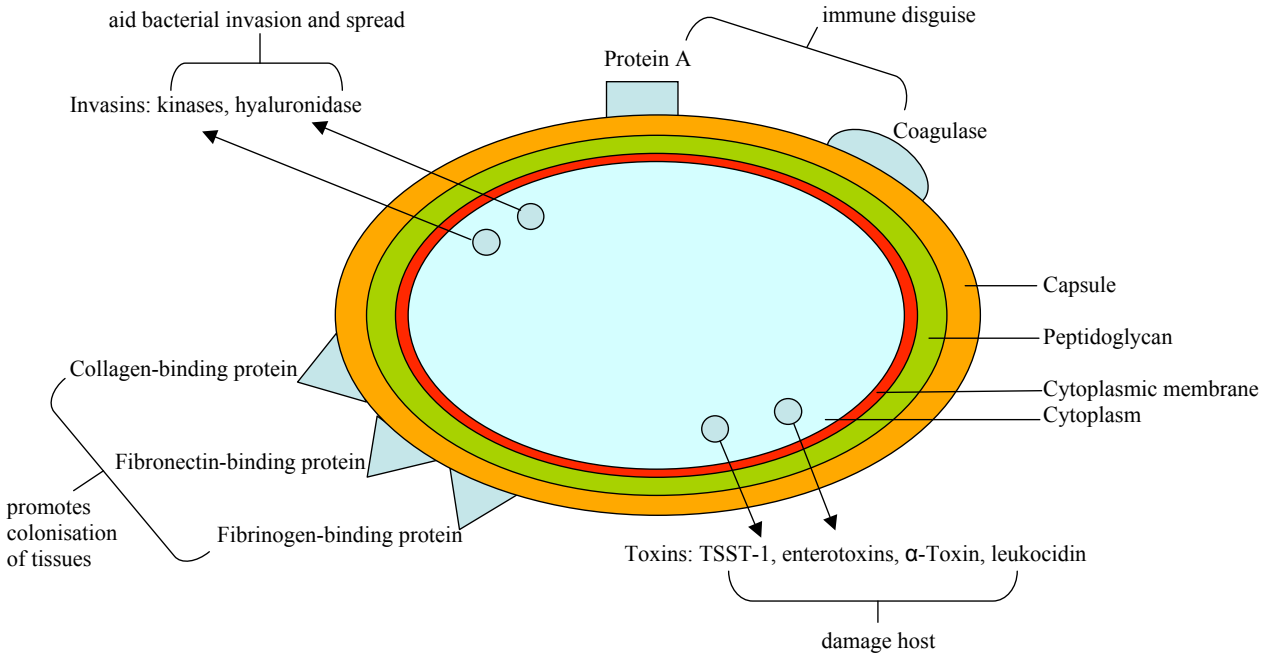

Fig 1.4: Summary of virulence factors possessed by *S. aureus* that enable host colonisation and infection

Fig 1.5: Schematic representation of the flagella filament

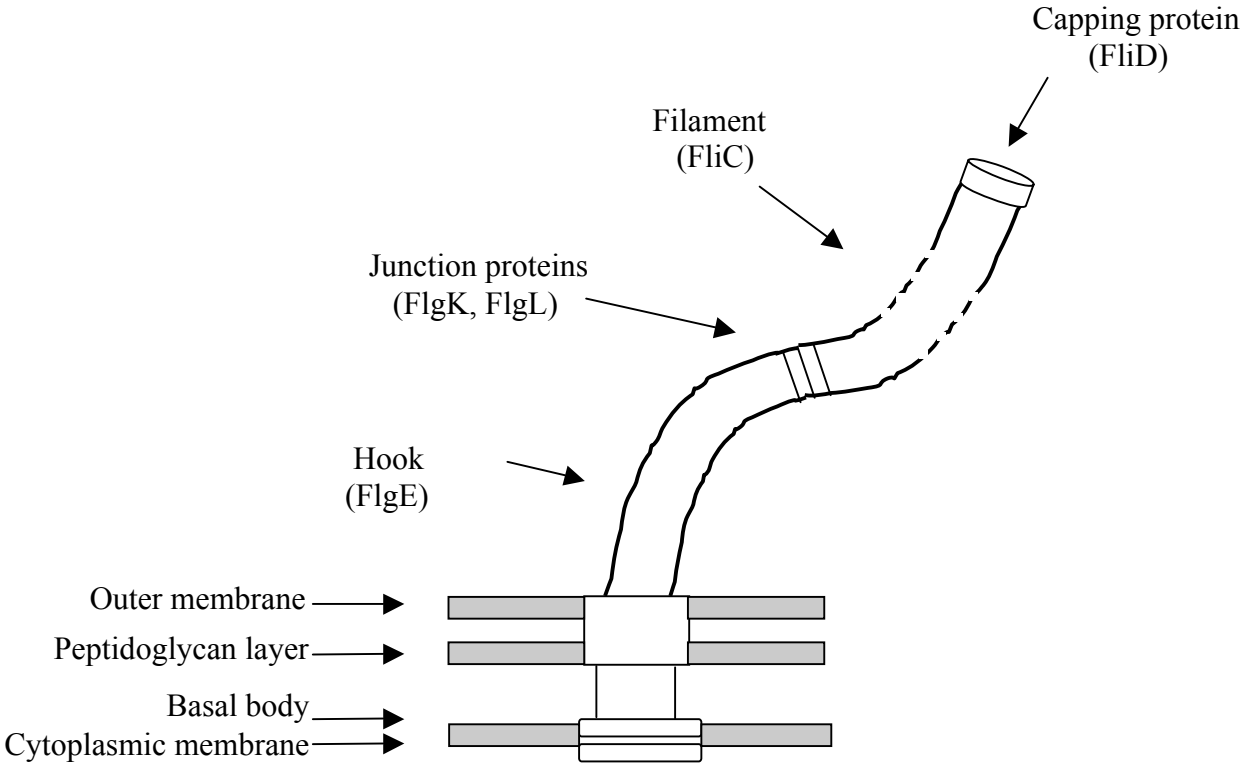

Adapted from Westerlund-Wikstrom, (2000)

.Fig 1.6: Structure of the FliTrx™ peptide library

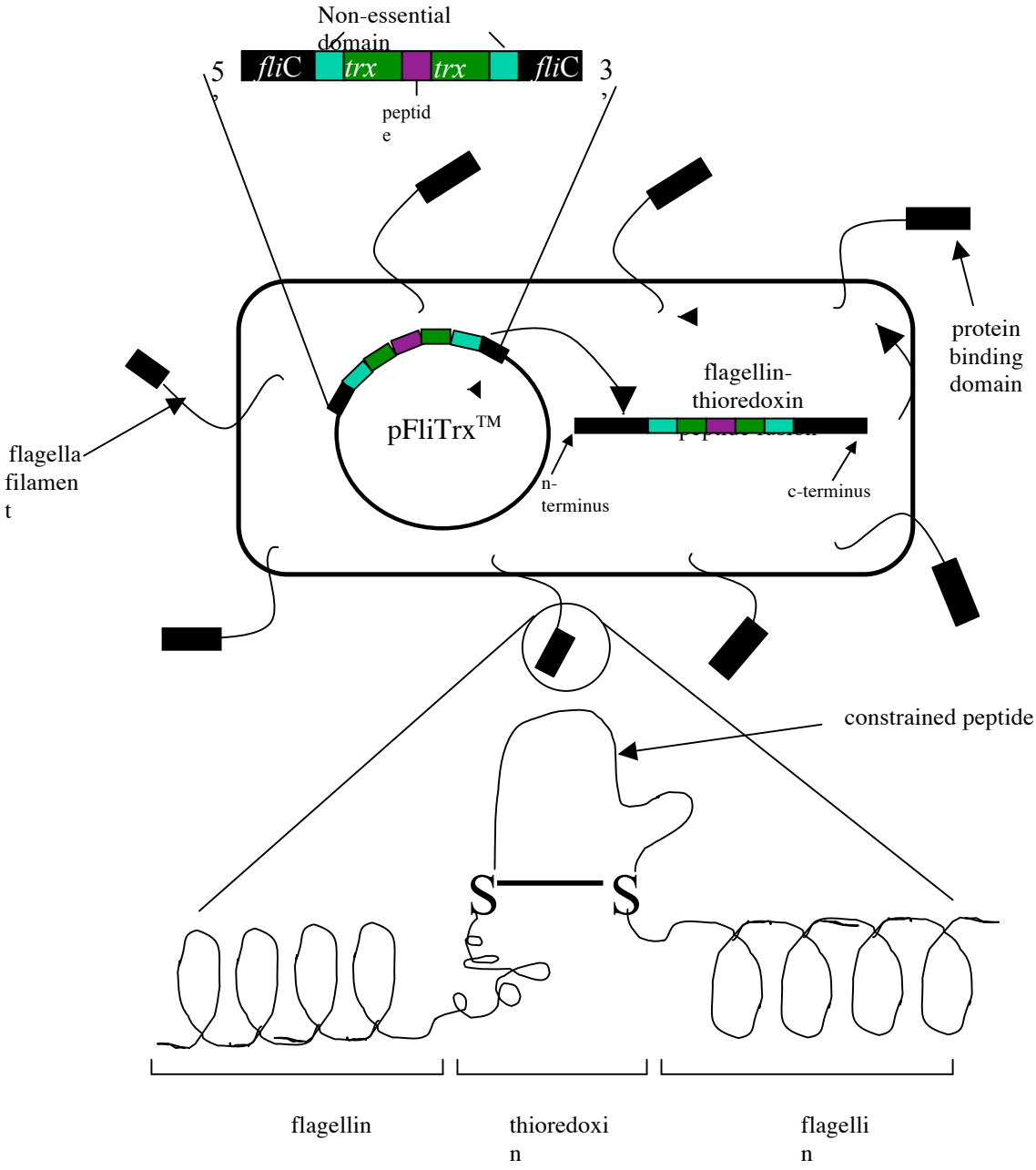

Adapted from the FliTrx™ Random Peptide Display Library protocol (Invitrogen 2009)

Fig 1.7: Expression of the FliTrx™ peptide library

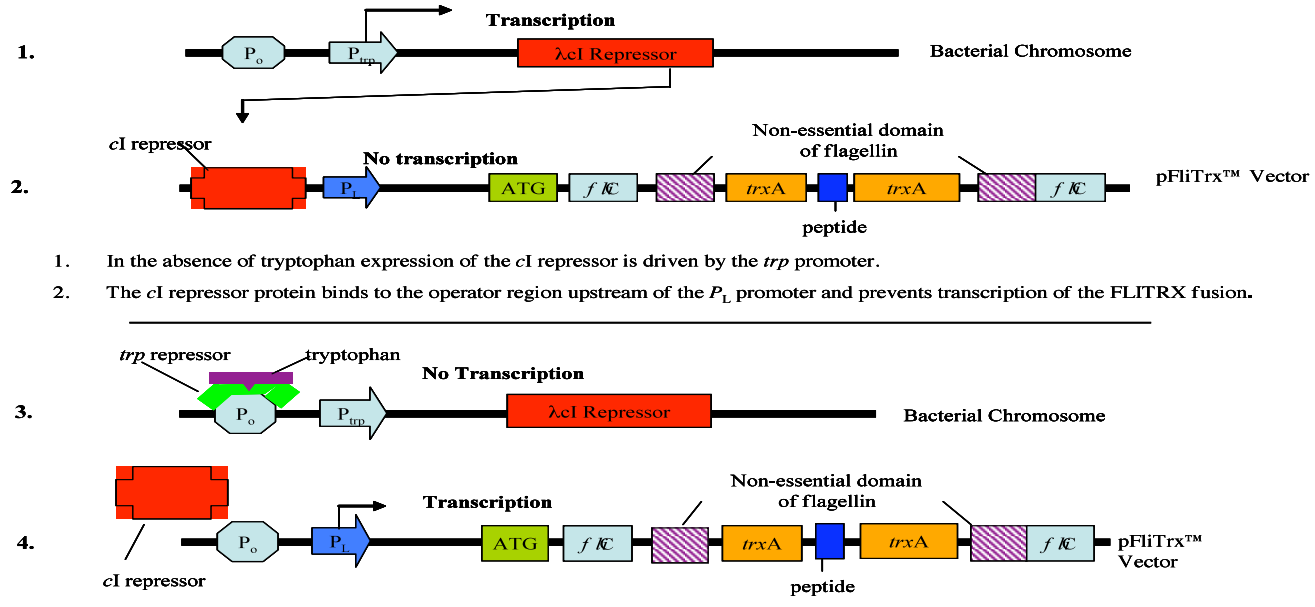

1. In the absence of tryptophan expression of the *c*I repressor is driven by the *trp* promoter.
2. The *c*I repressor protein binds to the operator region upstream of the P_L promoter and prevents transcription of the FLITRX fusion.
3. Tryptophan is added to the medium and a tryptophan-*trp* repressor complex is formed. This complex binds tightly to the *trp* operator blocking expression of the *c*I repressor.
4. The *c*I repressor dissociates from the P_L operator, allowing transcription of the flagellin/thioredoxin peptide fusion.

Adapted from the FliTrx™ Random Peptide Display Library protocol (Invitrogen, 2009)

Table 1.1: Applications of the FliTrx™ random peptide library

Application	a) Target against which peptides were selected b) Number of panning rounds and clones sequenced c) Key findings	Reference
Epitope mapping	a) 30 anti-human heat shock protein 90 monoclonal antibodies b) 5 rounds of panning, unknown number of clones sequenced c) Identification of common epitopes between immunogenic sites	Kishimoto et al., 2005
Epitope mapping	a) Anti-human high-mobility-group-box monoclonal antibodies b) 5 rounds of panning, 352 clones sequenced c) Identified linear and conformational epitopes	Ito et al., 2004
Epitope mapping	a) 6C5-H4CA monoclonal antibody b) 5 rounds of panning, unknown number of clones sequenced c) Identified peptides that may be involved in hydrophobic cell attachment of *Candida albicans* to host tissue	Singleton et al., 2001
Epitope mapping	a) Anti-human interleukin 8 monoclonal antibody b) 4 rounds of panning, 100 clones sequenced c) Identified peptides with reversible antibody binding mediated by metals or pH	Tripp et al., 2001
Epitope mapping	a) Monoclonal antibodies against non-structural protein 3 of Hepatitis C virus b) 3 rounds of panning, 23 clones sequenced c) Modified panning method to use magnetic cell sorting	Ueno et al., 2000
Receptor-ligand	a) Human umbilical cord hyaluronan b) 5 rounds of panning, 40 clones sequenced c) Peptides synthesised and peptide affinity measured	Amemiya et al., 2005
Receptor-ligand	a) Ricin b) 5 rounds of panning, 4 clones sequenced c) Synthesised peptide specific for ricin offering an alternative to antibody based detection currently utilised	Khan et al., 2003

Enzyme-substrate	a) Recombinant protein phosphatase 1 b) 6 rounds of panning, 104 clones sequenced c) Identified a consensus peptide binding motif for protein binding to protein phosphatase 1	Zhao and Lee, 1997
Bioremediation	a) Identified nickel binding peptides b) 4 rounds of panning, 10 clones sequenced c) Generated secondary libraries to select for peptides with up to 8-fold stronger affinity than identified from the original panned library. Identification of common epitopes between immunogenic sites	Dong et al., 2006
Vaccine development	a) Anti-gonococcal lipooligosaccharide (2C7 epitope) b) 5 rounds of panning, 14 clones sequenced c) Synthesised cyclic, linear and multiple peptide display constructs	Ngampasutadol et al., 2006
Vaccine development	a) Anti-hepatitis B virus-preS protein polyclonal antibody b) 4 rounds of panning, 13 clones sequenced c) Modified panning method to use flow cytometry	Xin et al., 2004
Vaccine development	a) Human zona pellucida protein b) 5 rounds of panning, 18 clones sequenced c) Identified testis-specific peptides that inhibited sperm binding	Naz et al., 2000

Fig 1.8: Schematic representation of antimicrobial PDT

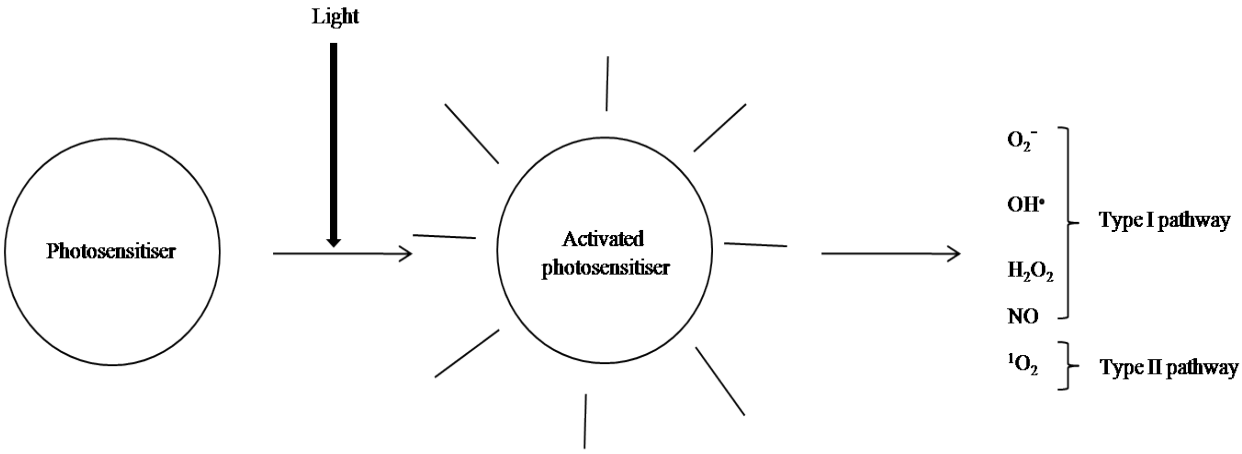

Fig 1.8: Diagrammatic representation of antimicrobial PDT (adapted from O'Riordan *et al*, 2005). Following irradiation of the photosensitiser (porphyrin) by light of an appropriate wavelength (600-650 nm) to an excited state, the photosensitiser produces toxic species that damage DNA and/or membrane sites.

Table 1.2: Different classes of antimicrobial photosensitisers

Class of compound	Name	Site of action	Reference
Natural compounds	Furanocoumarins	Intercalation of DNA	Guiotto et al., 1995
	Perylenequinonoin hypericin	Inhibitor of protein kinase C	Estey et al., 1996
Phenothiazines	Methylene blue	DNA interaction	Menezes et al., 1990
	Acridine	DNA interaction	Wainwright, 1998a
	Toluidine blue	Plasma membrane	Wakayama et al., 1980
Cyclic tetrapyrroles	Phthalocyanines/ Porphyrins	Membrane/cytosolic sites	Bertoloni et al., 1992

(Adapted from Maisch 2007a)

Table 1.3: Photosensitisers shown to be effective against drug resistant and drug sensitive strains of *S. aureus*

Photosensitiser	Bacterial strain/s tested	Findings	Group
Protoporphyrin diarginate	40 clinical MRSA and 40 clinical methicillin sensitive *S. aureus* (MSSA) strains and 1 reference strain	PDT effect was strain dependent MRSA resistance to PDT was higher than MSSA strains	Grinholc et al., 2008
Haematoporphyrin	2 strains of MRSA	Photosensitiser showed dose-dependent effect Plasma membrane is the major target of PDT whereas, DNA damage is secondary	Bertoloni et al., 2000
Haematoporphyrin derivatives (HpD-Rut_2-Arg_2)	17 MRSA and 11 MSSA	Higher photosensitiser concentration required for MRSA than MSSA to achieve bactericidal effect	Szpakowska et al., 2001
XF73 (porphyrin based)	MRSA and MSSA	Time and dose-dependent effects of the photosensitiser observed in an *ex vivo* porcine skin model and no damage of surrounding tissue	Maisch et al., 2007b
5-phenyl-10,15,20-tris(*N* -methyl-4-pyridyl)-porphyrin chloride	Bioluminescent *S. aureus*	Treatment of third degree burn wounds in mice infected with *S. aureus* was effective but bacterial regrowth was also observed	Lambrechts et al., 2005

3 porphyrin based photosensitisers (XF70, XF73, CTP1)	2 strains of MRSA, 1 strain of MSSA and 1 strain of methicillin resistant *S. epidermidis*	Greater than 99.9% bactericidal activity of two photosensitisers against all *Staphylococci* tested, independent of resistance profile No toxicity against eukaryotic cells was observed at similar concentrations	Maisch et al., 2005
Deuteroporphyrin-hemin complex	Multidrug resistant *S. aureus*	Bactericidal effect *in vitro* without photosensitisation Greater than 99% reduction of *S. aureus* in infected burn wounds in an animal model	Orenstein et al., 1997
5-aminolevulinic acid or Photofrin®	*S. aureus* and *S. epidermidis*	Photofrin® effective but showed dark toxicity and a limited effect observed with 5-aminolevulinic acid	Karrer et al., 1999
5-aminolevulinic acid	MRSA and *S. epidermidis*	5-aminolevulinic acid induced the endogenous porphyrin biosynthesis pathway resulting in a significant decrease in viability	Nitzan et al., 2004
Methylene blue or 5-aminolevulinic acid	Bioluminescent biofilm-producing *S. aureus*	Both compounds effective *in vitro* against bacterial suspensions 3 dosages of light investigated: single acute, fractionated or metronomic ALA partially inhibited biofilms in an *in vivo* animal model of osteomyelitis and may be a potential treatment of microbial bone infection	Bisland et al., 2005
Methylene blue	EMRSA-16	A 25-fold and 14-fold reduction in viable bacteria in excision and superficial wounds respectively in an *in vivo* murine wound model without damage to host tissue	Zolfaghari et al., 2009
Methylene blue	*S. aureus* and *S. epidermidis*	Both strains were more susceptible to treatment than *C. albicans*	Zeina et al., 2001

Free chlorin$_{e6}$, polylysine- chlorin$_{e6}$ and methylene blue	Wild-type and mutant *S. aureus* and *S. epidermidis*	PDT was affected by growth phase and production/absence of extracellular slime layer Greater sensitivity of non-biofilm producing strains	Gad et al., 2004a
Polylysine- chlorin$_{e6}$ and chlorin$_{e6}$	Bioluminescent *S. aureus*	Light dose dependent effect using an *in vivo* murine model targeting established soft tissue infections, however bacterial regrowth occurred	Gad et al., 2004b
Toluidine blue	MRSA and *S. epidermidis*	Light dose dependent inactivation of cells and disruption of biofilm structure Enhanced PDT against *S. epidermidis* but not *S. aureus* biofilms following the treatment of biofilms with EDTA	Sharma et al., 2008
Toluidine blue	MRSA	Dose dependent effect for light and photosensitiser concentration whereas varying the incubation of the photosensitiser prior to irradiation had little effect	Wilson and Yianni, 1995
5 phenothiazinium dyes	4 strains of MRSA 1 strain of *S. aureus*	2 of the compounds (DMMB and NMB) were bactericidal at lower concentrations than vancomycin against EMRSA-15 and -16	Wainwright et al., 1998b
Merocyanine 540	*S. aureus*	Lower light doses required to kill planktonic cultures of *S. aureus* than cells present as a biofilm due to limited penetration of light	Lin et al., 2004
Aluminium disulphonated phthalocyanine	EMRSA 1-16	All strains were susceptible with a photosensitiser concentration and light dose-dependent effect Not dependent on growth phase or preincubation time	Griffiths et al., 1997
Aluminium disulphonated phthalocyanine	MRSA	Bactericidal effect was not dependent on growth phase Killing was decreased when serum was added to the medium	Wilson and Pratten, 1995

Table 1.4: Conjugated photosensitisers for targeting of MRSA and *S. aureus*

Photosensitiser	Bacterial strain/s tested	Conjugate/Findings	Reference
5-(4'-carboxybutylamino)-9-diethylaminobenzo [a]phenothiazinium chloride	Four strains of MRSA, *S. aureus*	Conjugated to a cephalosporin derivative Cleavage of the cephalosporin β-lactam ring by MRSA expressing β-lactamase releases the quenched photosensitiser to an activated state Strain dependent susceptibility that was inversely correlated to bacterial susceptibility to penicillin G (corresponding to greater β-lactamase activity and hydrolysis of the photosensitiser)	Zheng et al., 2009
Tin (IV) chlorin$_{e6}$ conjugate	EMRSA-16, *S. aureus*, *E. coli*	Conjugated to bacteriophage Φ11 Both strains of *S. aureus* were susceptible even though the phage was not able to infect EMRSA-16 No effect against *E. coli*	Hope et al., 2009
Tin (IV) chlorin$_{e6}$ conjugate	EMRSA-1, -3, -15, -16, -17, VISA, community-acquired hypervirulent strain, MSSA	Conjugated to *S. aureus* bacteriophage 75 All strains susceptible and not growth phase dependent No effect on epithelial cells	Embleton et al., 2005
Tin (IV) chlorin$_{e6}$ conjugate	EMRSA-1, -3, -15, -16, MSSA, *S. epidermidis, E. coli*	Conjugated to a polyclonal anti-MRSA antibody Effective against all MRSA strains at all growth phases Specificity for EMRSA-16 in mixed suspension with *E. coli* and *S. epidermidis*, although some kill observed against *S. epidermidis*	Embleton et al., 2004
Tin (IV) chlorin$_{e6}$ conjugate	EMRSA-1, -3, -15, -16, *S. aureus* and *S. sanguis*	Conjugated to IgG Strain variability effect and growth phase dependent	Embleton et al., 2002
Bacteriochlorophyll	*S. aureus* Cowen I	Conjugated to rabbit IgG Conjugate more effective than a non-targeted serine conjugate	Gross et al., 1997

Table 1.5: Photosensitisers conjugated to biomolecules for targeting of bacteria

Photosensitiser	Bacterial strain/s tested	Conjugate/Findings	Reference
Chlorin $_{e6}$	*P. aeruginosa*	Conjugated to poly-L-lysine Light dose dependent response using an *in vivo* murine wound model and wounds healed faster than treatment with a topical antimicrobial agent.	Hamblin et al., 2003
Chlorin $_{e6}$	Non pathogenic bioluminescent *E. coli*	Conjugated to poly-L-lysine Light dose dependent reduction following treatment with the conjugate in a wound infection murine model with little damage to host tissue.	Hamblin et al., 2002b
Tin (IV) chlorin $_{e6}$	*Actinomyces viscosus* and *Porphyromonas gingivalis*	Conjugated to poly-L-lysine Greater than 99% killing of bacterial species with little damage to an oral epithelial cell line	Soukos et al., 1998
Tin (IV) chlorin $_{e6}$	*P. aeruginosa*	Conjugated to an anti- *P. aeruginosa* antibody Greater than 75% decrease in viable bacteria using a specific conjugate whereas bacterial growth observed using a non-specific conjugate in an *in vivo* murine skin model infected with *P. aeruginosa*	Berthiaume et al., 1994
Tin (IV) chlorin $_{e6}$	*P. aeruginosa*	Conjugated to a monoclonal antibody against *P. aeruginosa* Selective killing of *P. aeruginosa* in a mixed suspension of *S. aureus*	Friedberg et al., 1991
Toluidine blue	*Porphyromonas gingivalis*	Conjugated to a monoclonal antibody against *Porphyromonas gingivalis* lipopolysaccharide. Demonstrated *Porphyromonas gingivalis* specificity in mixed cultures with *Streptococcus sanguis* or human dermal fibroblasts	Bhatti et al., 2000

Table 2.2: Primer sequences

Primer	Sequence
ThioFor	*GGT GGA* GTC GAC[1] ATG AGC GAT AAA AAT ATT CAC CTG (1 = *Sal*I)
ThioRev	*TCC ACC* GGA TCC[2] CAG GTT AGC GTC GAG GAA CTC (2 = *Bam*HI)
ThioLysineFor	*GGT GGA* GTC GAC[1] AAA AAA AAG AAA AAA AAG AAA AAA AAG AAA AAA AAG AAA AAA AAG ATG AGC GAT AAA AAT ATT CAC CTG (1 = *Sal*I)
pPROTetFor	5 - TGA GCA CAT CAG CAG GAC GCA – 3’
pPROTetRev	5’ - GGA GAG CGT TCA CCG ACA AAC – 3’
GFPFor	5’ - *GGA GGC* CTG CAG[3] ATG GTG AGC AAG GGC GCC GAG CTG - 3’ (3 = *Pst*I)
GFPRev(WS)	5’ - *CTA CTA* CGA TCG[4] TCA CTT GTA CAG CTC ATC CAT GCC - 3’ (4 = *Pvu*I)
GFPRev(NS)	5’ - *TCC ACC G*CG ATC G[4]GA CTT GTA CAG CTC ATC CAT GCC - 3’ (4 = *Pvu*I)

Fig 2.1: Diagrammatic representation of the overall cloning procedure

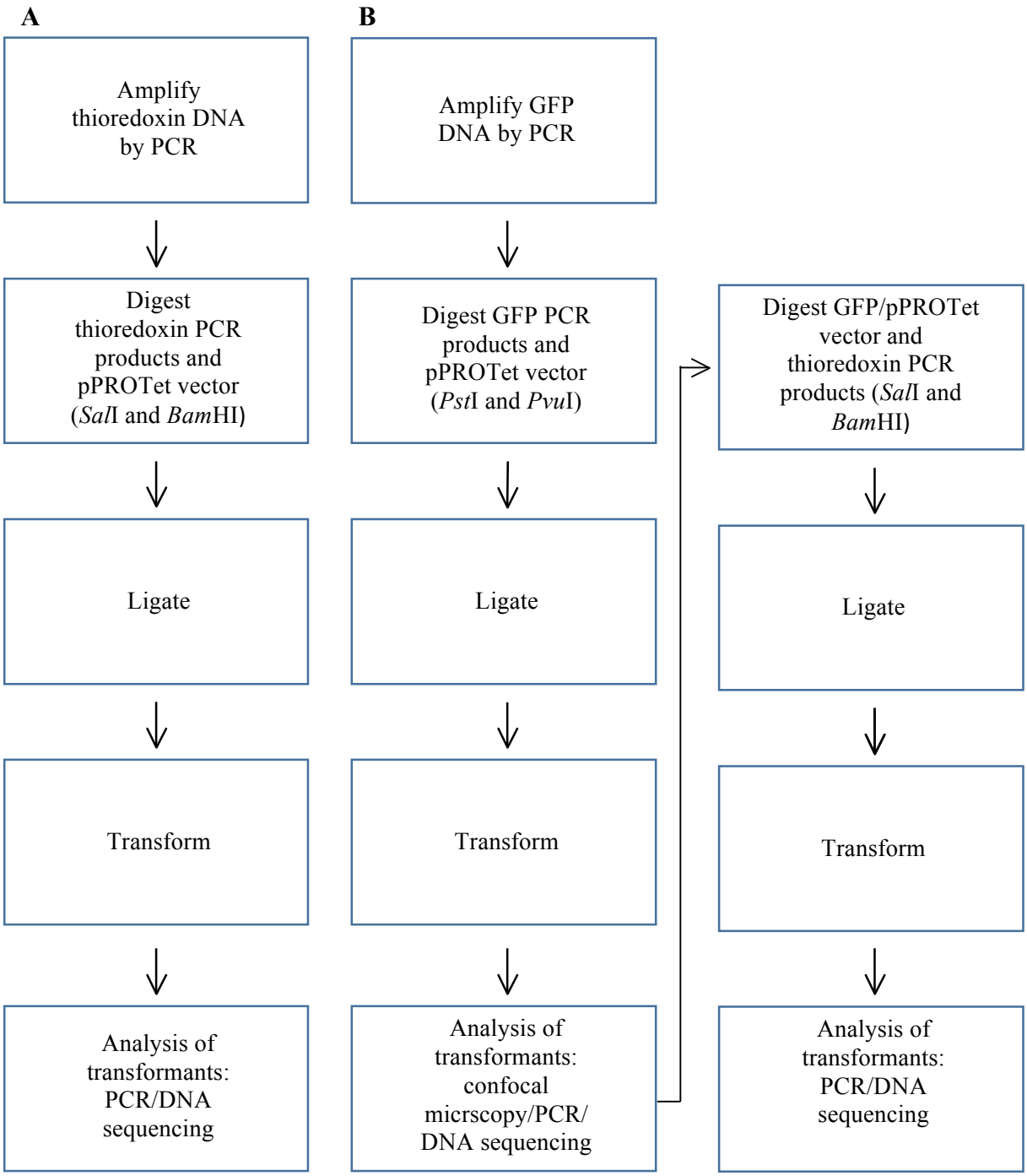

Fig 2.1: Flow diagram demonstrating overall process to clone thioredoxin containing peptides (A) and also as a GFP fusion construct (B) into the *E. coli*

expression vector.

Fig 2.2: Diagrammatic representation of the thioredoxin/pPROTet and thioredoxin/GFP/pPROTet final vector constructs

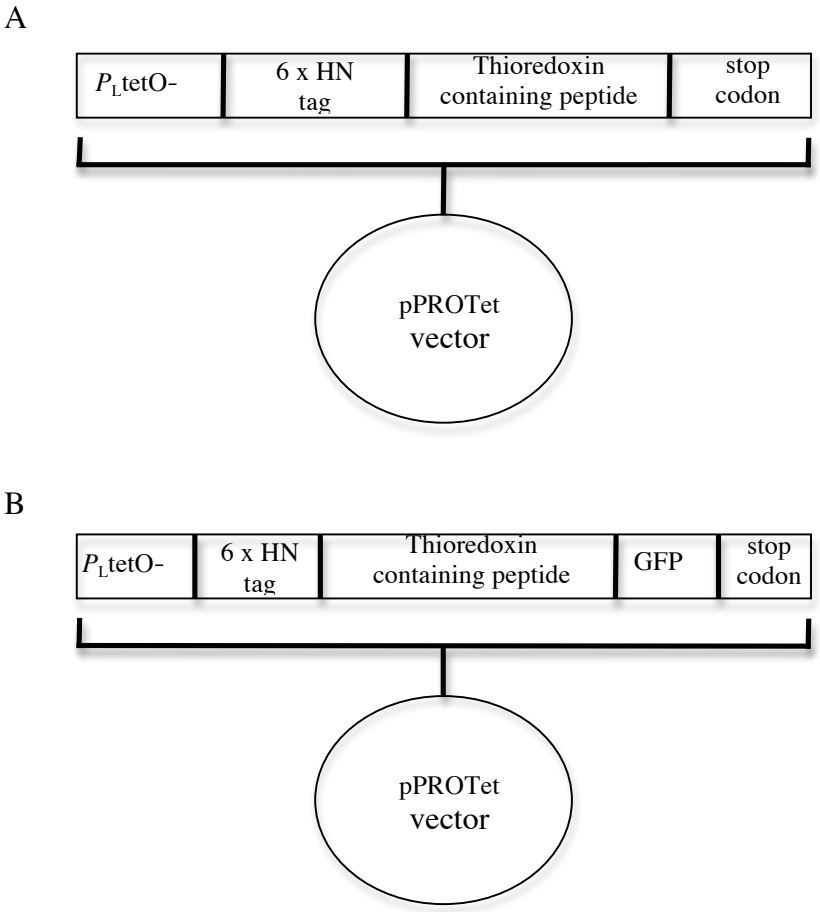

Fig 2.2: Overall final vector cloning construct for thioredoxin/pPROTet (A) and thioredoxin/GFP/pPROTet (B).

Fig 3.1: Typical confocal microscopy images of live/dead stained MRSA cultures with and without UV irradiation

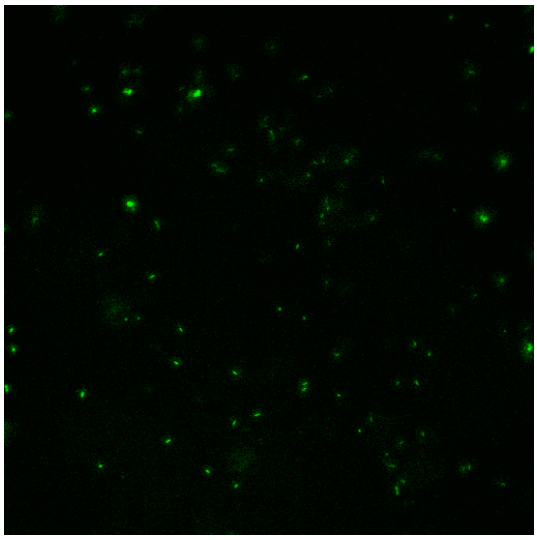

Live MRSA culture

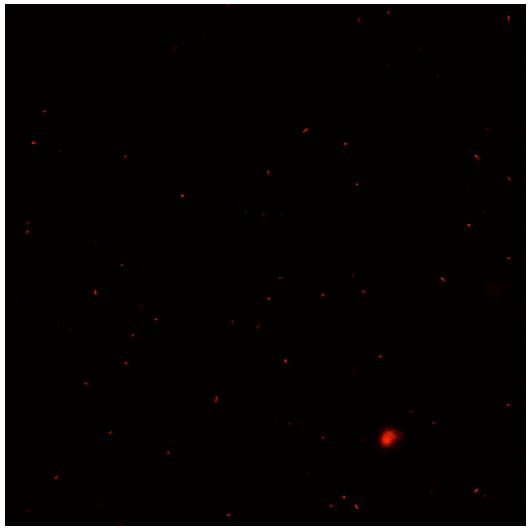

UV irradiated MRSA culture

Fig 3.1: MRSA cultures were grown to late log phase. One aliquot was subjected to UV irradiation for 5 min using a 15 W 254 nm UV lamp for comparison against an identical, non-irradiated sample. The samples were stained with SYTO 9 and PI and analysed using a confocal microscope, equipped with a x60 magnification objective. Results shown are typical of three repeat experiments on independent cultures of MRSA and indicated that >90% cell death was achieved.

Fig 3.2: Bacterial immobilisation and washing procedure on different substrates using live and dead bacterial cultures

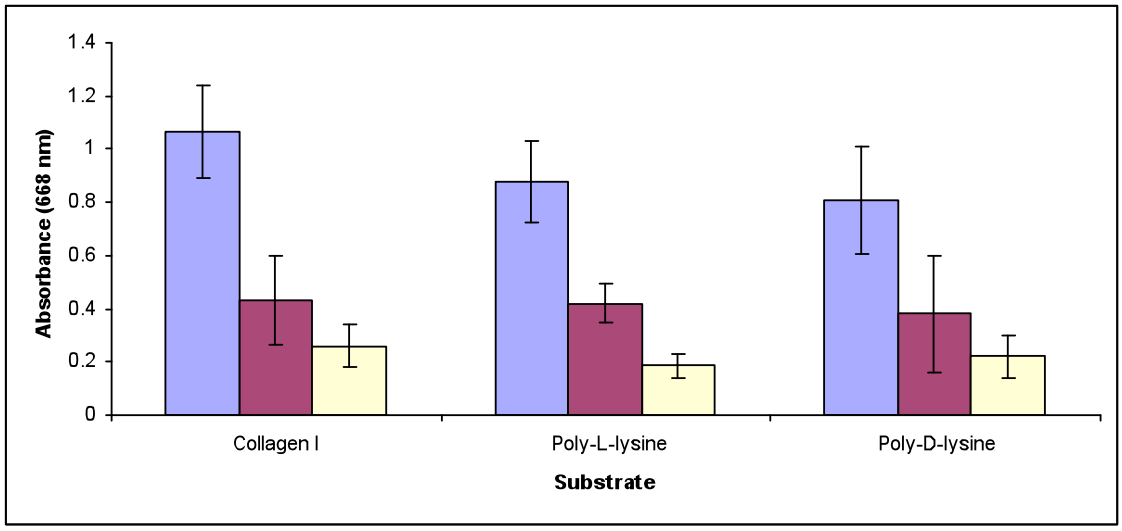

Fig 3.2: Bacterial adhesion investigations were performed using 6-well plates coated with either collagen I, poly-L-lysine or poly-D-lysine. Bacterial cultures (40 ml) were grown to late log phase and concentrated using centrifugation. Bacteria were killed by UV irradiation for 5 min using a 15 W 254 nm lamp. Live and dead/non-viable bacterial cultures (2 ml) were added to each plate and left to adhere overnight at 4°C. The plates were washed and vortexed as per the panning protocol and the bacteria that remained adhered to the plate were stained with methylene blue. The bacteria were destained with ethanol and the absorbance measured at 668 nm to ascertain the relative amount of bacteria that remained attached to the plate. The blue bars represent live bacteria that had remained adhered to the plate whereas the purple bars represent UV-inactivated bacteria. The yellow bars represent control wells that contained no bacteria. The error bars represent the standard deviation from 4 repeat plates.

Fig 3.3: Photograph of immobilised bacteria

Live **Dead** **Dead**

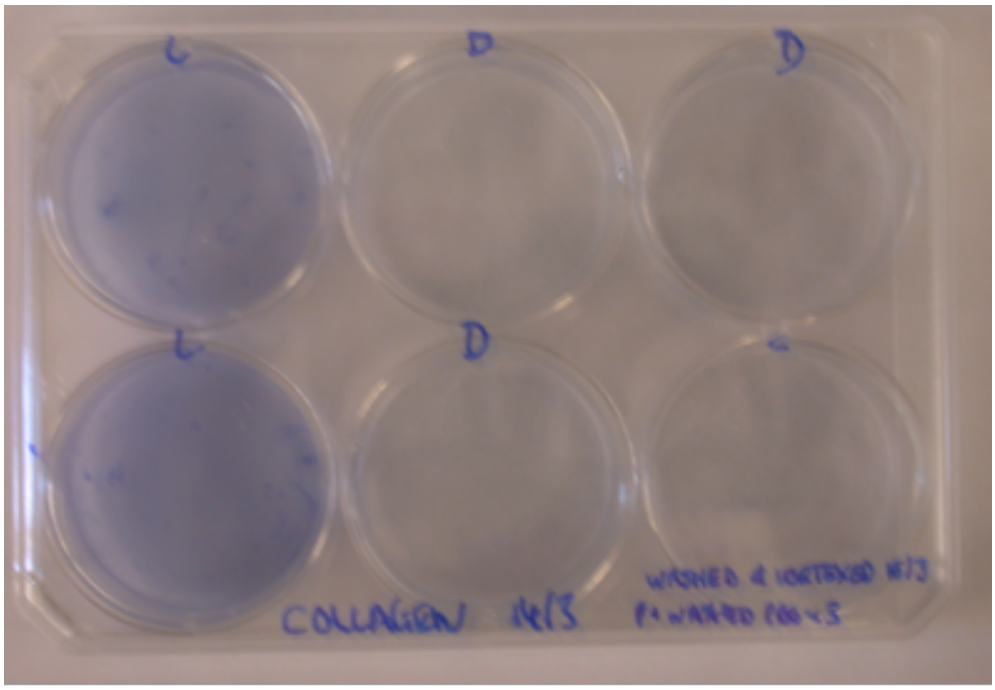

Control

Fig 3.3: Photograph following bacterial immobilisation onto a collagen I plate. Live and dead/non-viable bacteria were applied to the wells and left to adhere overnight at 4ºC. Following washing, the plates were stained with methylene blue.

Fig 3.4: Peptide sequences derived from panning against MRSA

1.	His	Gly	Ile	Arg	Ala	Leu	Leu	Leu	Leu	Glu	Gly	Asp
2.	Val	Ala	Glu	Tyr	Asn	Thr	Arg	Glu	Gln	-	Arg	Arg
3.	Met	Leu	Val	Gly	Ser	Ser	Ala	Leu	Gly	Gln	Ser	Ser
4.	Arg	-	Pro	Arg	Gly	Thr	Leu	Ile	Val	Cys	Ile	Ser
5.	Leu	Pro	Thr	Ala	Val	Asp	Ser	Gln	Gly	Ala	Ile	Arg
6.	Gln	Trp	Glu	Ser	Val	Asp	Phe	Ala	Asp	Val	Asp	Val
7.	Ser	Ala	Glu	Arg	-	Gln	Ala	Arg	Asp	Asn	Arg	Ala
8.	Cys	Ile	His	Gly	Gln	Val	Ala	Ala	Arg	Arg	Pro	Leu
9.	Cys	Thr	Ala	-	Trp	Arg	Asn	Asn	Cys	Asp	Ser	Asp
10.	Gln	Asp	Val	Phe	Asp	Asp	Arg	Pro	Arg	-	Thr	Asn
11.	Glu	Trp	Gly	Trp	Ile	Val	Pro	Cys	Trp	Arg	Cys	Ala
12.	Gly	Ser	Gly	Arg	Glu	His	Ala	Arg	Gly	Val	Arg	Gly
13.	Ser	Gly	Gly	Ser	Tyr	Met	-	Arg	Thr	Gly	Glu	Pro
14.	Arg	Ser	Gly	Gly	Ala	Gln	Ser	Val	Pro	Ser	Arg	Gly
15.	Asp	Ala	Val	Ala	Gln	His	Val	-	Arg	Gly	Ala	Lys
16.	Glu	Arg	Arg	Arg	Glu	Thr	Ser	Glu	Arg	-	Arg	-
17.	Phe	Val	Ile	Arg	Arg	Leu	Ala	Ala	-	Tyr	Pro	His
18.	Lys	Gly	Glu	Leu	Val	Gly	-	Ile	-	Pro	Glu	Leu
19.	Arg	Arg	Asn	Ala	Asn	Leu	Gly	Lys	Gln	Ala	Arg	Arg
20.	-	Glu	Gln	Val	Val	Arg	Leu	Thr	Pro	Asp	Leu	Val

- = stop codon

Fig 3.4: PCR products were sequenced in both directions and the amino acid configuration of the 36 bp peptides sequences were determined. Amino acid sequences are depicted as amino acid three letter abbreviations.

Fig 3.5: Peptide sequences selected from panning against *S. aureus*

1.	Arg	Arg	Val	Leu	Arg	Gly	Gly	Ala	Leu	Ser	Val	Gly
2.	Arg	Val	Val	Ile	Arg	Gly	Asn	Gly	Gly	Asp	Lys	Val
3.	Gln	Pro	Gly	Val	Cys	Val	Ala	Tyr	Leu	Arg	Pro	Val
4.	Lys	Leu	Tyr	-	Arg	Arg	Gly	Gln	Glu	Val	Asp	Lys
5.	Glu	Ser	Leu	Cys	Arg	Leu	Glu	Leu	Ile	Val	Gly	Leu
6.	Arg	Arg	Arg	Pro	Ser	Arg	Arg	Asp	Ile	Leu	Ala	Val
7.	Asp	Val	Thr	Val	Gly	Tyr	Thr	Leu	Glu	Gly	Asp	Arg
8.	Ala	Gly	Cys	Thr	Ser	Pro	Ser	Thr	Asp	Gly	Glu	Val
9.	Ala	Leu	Leu	Thr	Val	Lys	Leu	Phe	Ser	Ser	Gly	Arg

- = stop codon

Fig 3.5: The amino acid sequences of the randomly selected clones were determined following DNA sequencing in both directions of the amplified PCR products.

Fig 3.6: Peptide sequences derived from panning against *S. epidermidis*

1.	Phe	Pro	Arg	Gly	Lys	Gly	Arg	Pro	Arg	Thr	Arg	Ser
2.	Arg	Gly	Gln	Arg	Met	Gly	Leu	Lys	Ile	Arg	Pro	Glu
3.	Ala	Ser	Thr	Leu	Val	Ala	Ser	Arg	Trp	Leu	Arg	Tyr
4.	Ser	Arg	Thr	Lys	Pro	Ser	Arg	Ala	Lys	Ile	Ser	Glu
5.	Glu	Ser	Cys	Gln	Pro	Arg	Ser	Arg	Arg	Gln	Leu	Gly
6.	Leu	Thr	Arg	Gly	Leu	Ala	Arg	Leu	Arg	Val	Leu	-
7.	Arg	Arg	Ser	Gly	Thr	Gly	Leu	Cys	Ala	Gly	Arg	Arg
8.	Ala	Lys	Ser	Arg	Pro	Ala	Ser	Leu	Ser	Pro	Arg	Arg
9.	Thr	Ala	Gly	Ile	Lys	Gly	Arg	Arg	Pro	Ala	Lys	Lys
10.	Cys	Ser	Val	Gly	Ser	Arg	Arg	Phe	Asn	Gly	Arg	Lys
11.	Lys	Met	Tyr	Lys	Ser	Gln	Leu	Arg	Ser	Asn	Arg	Gly

- = stop codon

Fig 3.6: PCR products were sequenced in both directions and the amino acid sequence determined.

Fig 3.7: Flow cytometric analysis to investigate binding of biotinylated peptides to MRSA

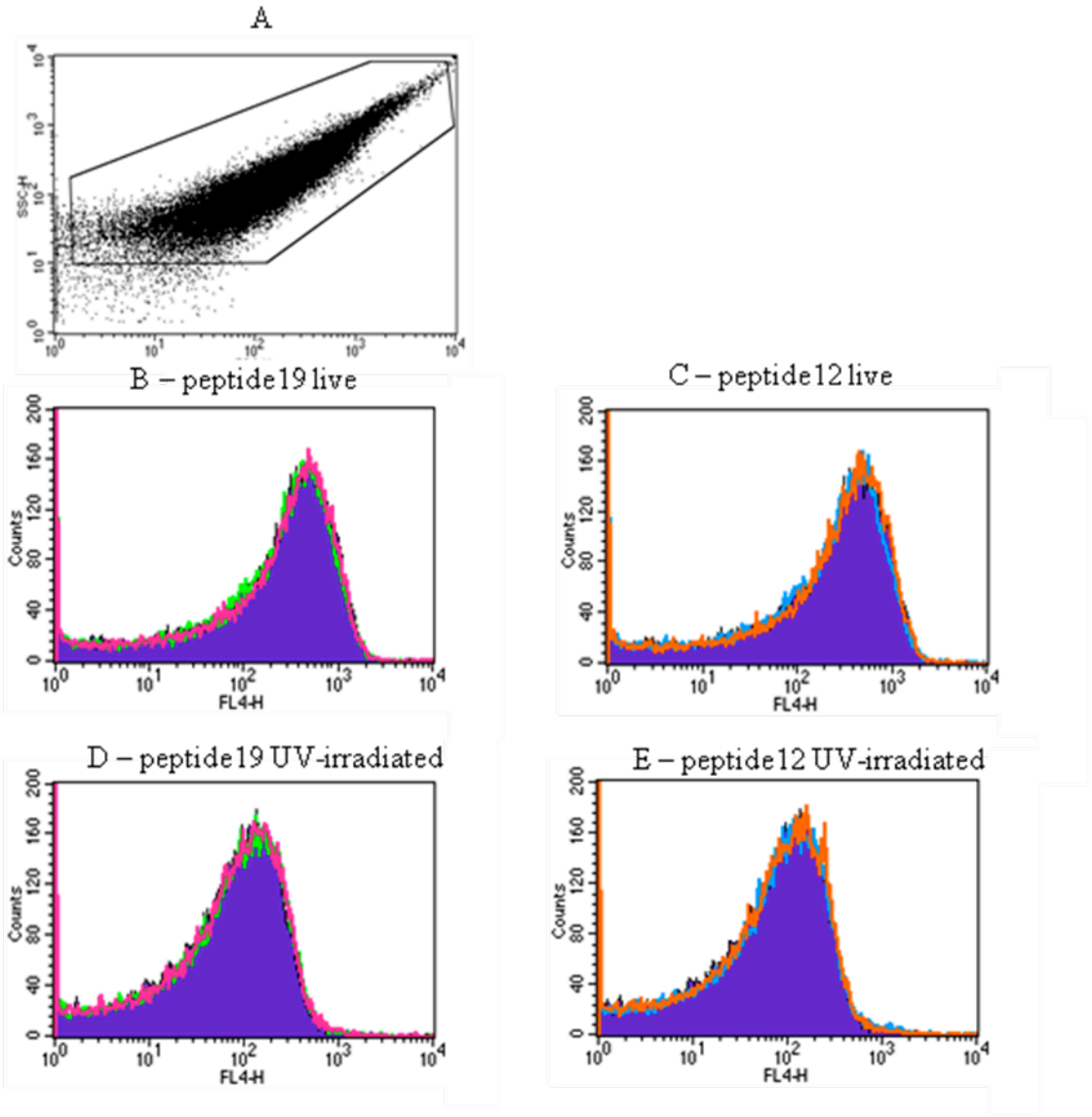

Fig 3.7: Flow cytometry profiles for binding assessment of two different biotinylated peptides as both cyclic and linear constructs to live and UV-inactivated MRSA. Panel A represents FSC/SSC used to determine the bacterial population of MRSA1 for analysis. Panels B and C represent profiles used to characterise binding of peptide19 cyclic (green line) and linear (pink line) and peptide12 cyclic (blue line) and linear (orange line) to live MRSA1. Panels D and E characterise peptide binding against the same strain except that MRSA1 had been UV-inactivated. The purple filled line denotes MRSA incubated with streptavidin PE:Cy5 only as a negative control. Flow cytometry analysis was based on counting 50,000 events. Similar results were obtained characterising binding of the peptides against two different strains of MRSA (MRSA2 & MRSA3), *S. aureus* and *S. epidermidis*.

Fig 3.8: Assessment of biotinylated peptide binding to MRSA1 by flow cytometry

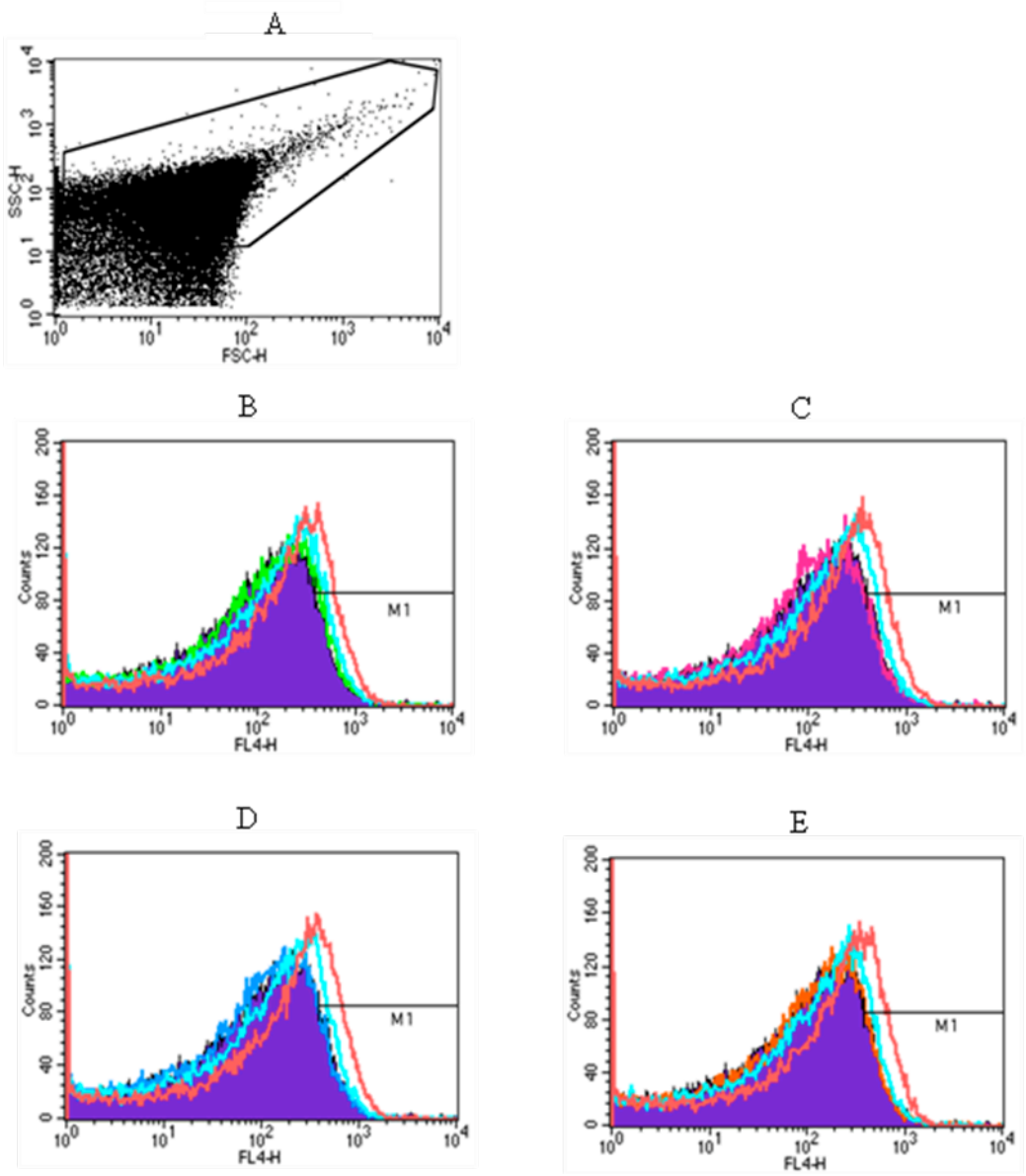

Fig 3.8: Flow cytometry profiles characterising binding of biotinylated peptides to MRSA. The bacterial population of MRSA1 was gated to determine the main bacterial population for analysis (Panel A). Panels B and C represent profiles characterising cyclic (green) and linear (pink) constructs of peptide19 binding to MRSA1. Panels D and E demonstrate cyclic (blue) and linear (orange) peptide12 binding to MRSA1. The turquoise line represents bacteria preincubated with biotin complexed with unconjugated streptavidin (5:1) prior to incubation with peptides. The peach line represents preincubation of bacteria with biotin complexed with unconjugated streptavidin (50:1) prior to peptide incubation. The purple filled line represents MRSA1 incubated with streptavidin PE:Cy5 only as a negative control. For analysis, 50,000 events were counted. Similar results were obtained characterising binding of the peptides against a different strain of MRSA (MRSA2).

Table 3.1: Mean fluorescence intensities for assessment of biotinylated peptide binding to MRSA1

Peptide19 (cyclic) – Panel C	**Mean fluorescence**	**Gated marker (%)**
Control	140.4	8.2
Peptide:streptavidin PE:Cy5	147.0	9.2
Unconjugated streptavidin:biotin + peptide:streptavidin PE:Cy5	168.2	12.2
Unconjugated streptavidin:10Xbiotin + peptide:streptavidin PE:Cy5	215.6	20.3
Peptide19 (linear) – Panel D	**Mean fluorescence**	**Gated marker (%)**
Control	140.4	8.2
Peptide:streptavidin PE:Cy5	129.4	6.5
Unconjugated streptavidin:biotin + peptide:streptavidin PE:Cy5	161.5	11.2
Unconjugated streptavidin:10Xbiotin + peptide:streptavidin PE:Cy5	218.2	21.0
Peptide12 (cyclic) – Panel E	**Mean fluorescence**	**Gated marker (%)**
Control	140.4	8.2
Peptide:streptavidin PE:Cy5	131.0	6.7
Unconjugated streptavidin:biotin + peptide:streptavidin PE:Cy5	162.6	11.0
Unconjugated streptavidin:10Xbiotin + peptide:streptavidin PE:Cy5	223.7	21.5
Peptide12 (linear) – Panel F	**Mean fluorescence**	**Gated marker (%)**
Control	140.4	8.2
Peptide:streptavidin PE:Cy5	139.5	7.6
Unconjugated streptavidin:biotin + peptide:streptavidin PE:Cy5	158.4	10.7
Unconjugated streptavidin:10Xbiotin + peptide:streptavidin PE:Cy5	220.1	21.3

In all cases 50,000 cells were analysed. A marker (M1) was set based on the distribution of the control plot.

Fig 3.9: Characterisation of biotinylated peptide binding to MRSA using an anti-biotin detection antibody

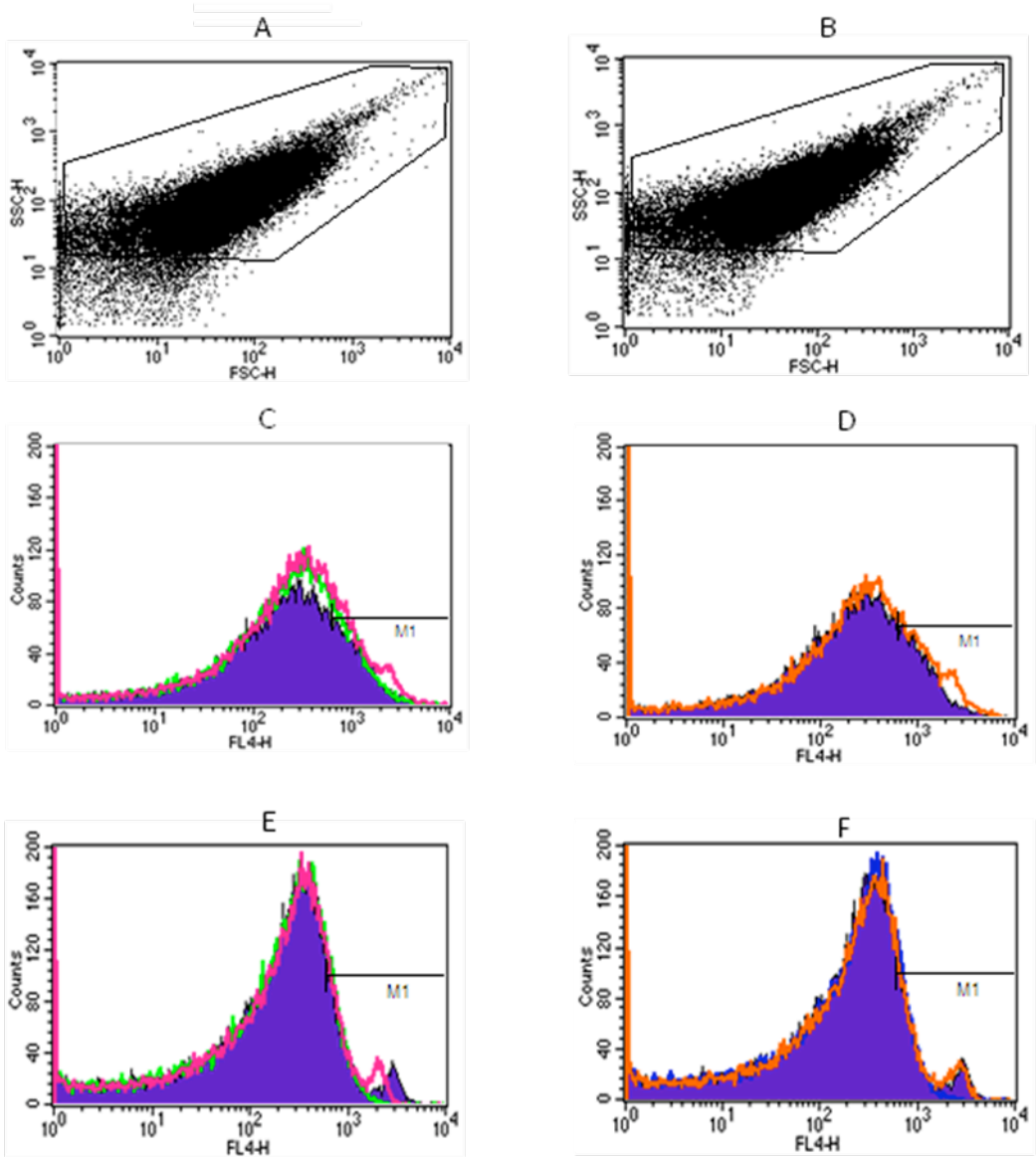

Fig 3.9: Flow cytometry profiles for assessment of biotinylated peptide binding to strains of MRSA characterised using an anti-biotin antibody. Panels A and B represents FSC/SSC used to determine bacterial populations of MRSA1 and MRSA2 respectively for analysis. Panel C represents a flow cytometry profile used to characterise peptide19 cyclic (green) and linear (pink) constructs to MRSA1 in comparison to the negative control (purple filled line). Panel D represents binding of peptide12 cyclic (blue) and linear (orange) constructs to MRSA1 in relation to the negative. For flow cytometry analysis 50,000 events were counted. Panels E and F are the same as C and D except that peptide binding was characterised against MRSA2.

Fig 3.10a: Characterisation of FITC-labelled peptide binding by flow cytometry

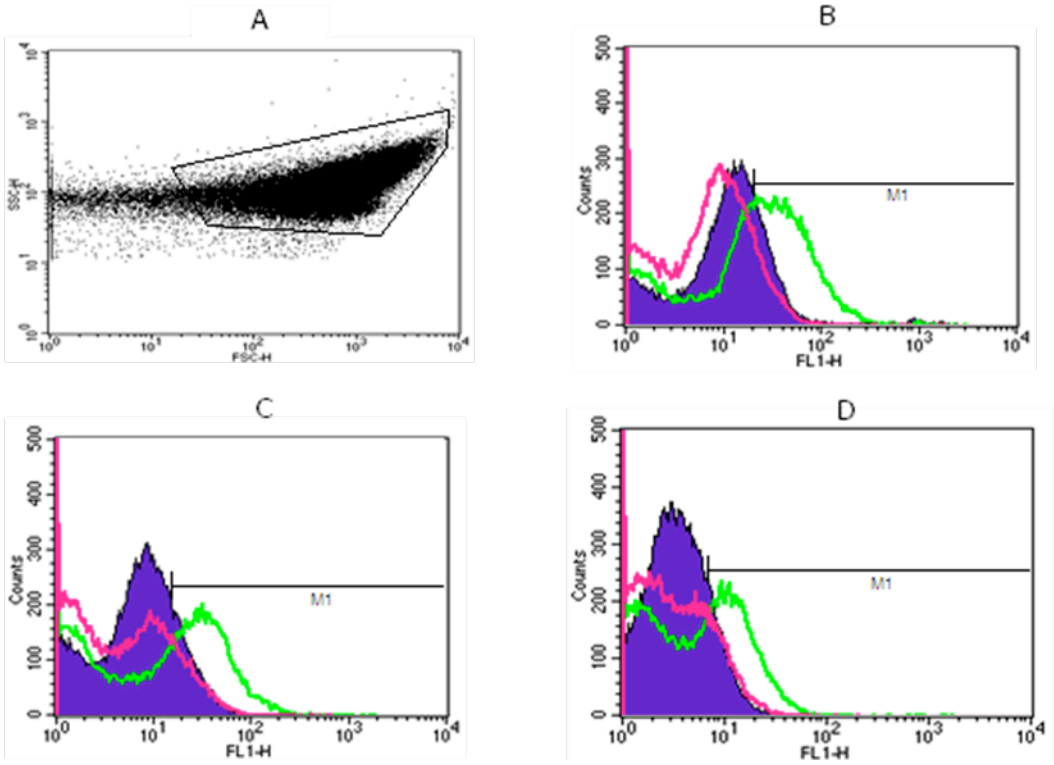

Fig 3.10a: Flow cytometry profiles for assessment of FITC-labelled peptide binding to MRSA. The main bacterial population for analysis was determined by FSC/SSC (Panel A). Binding of cyclic peptide12 (green) and linear peptide12 (pink) was characterised against MRSA1, -2 and -3 (Panels B-D respectively) in comparison to bacteria only as a negative control (purple filled line). Each profile was based upon counting 100,000 events.

Fig 3.10b: Assessment of FITC-labelled peptide binding by flow cytometry

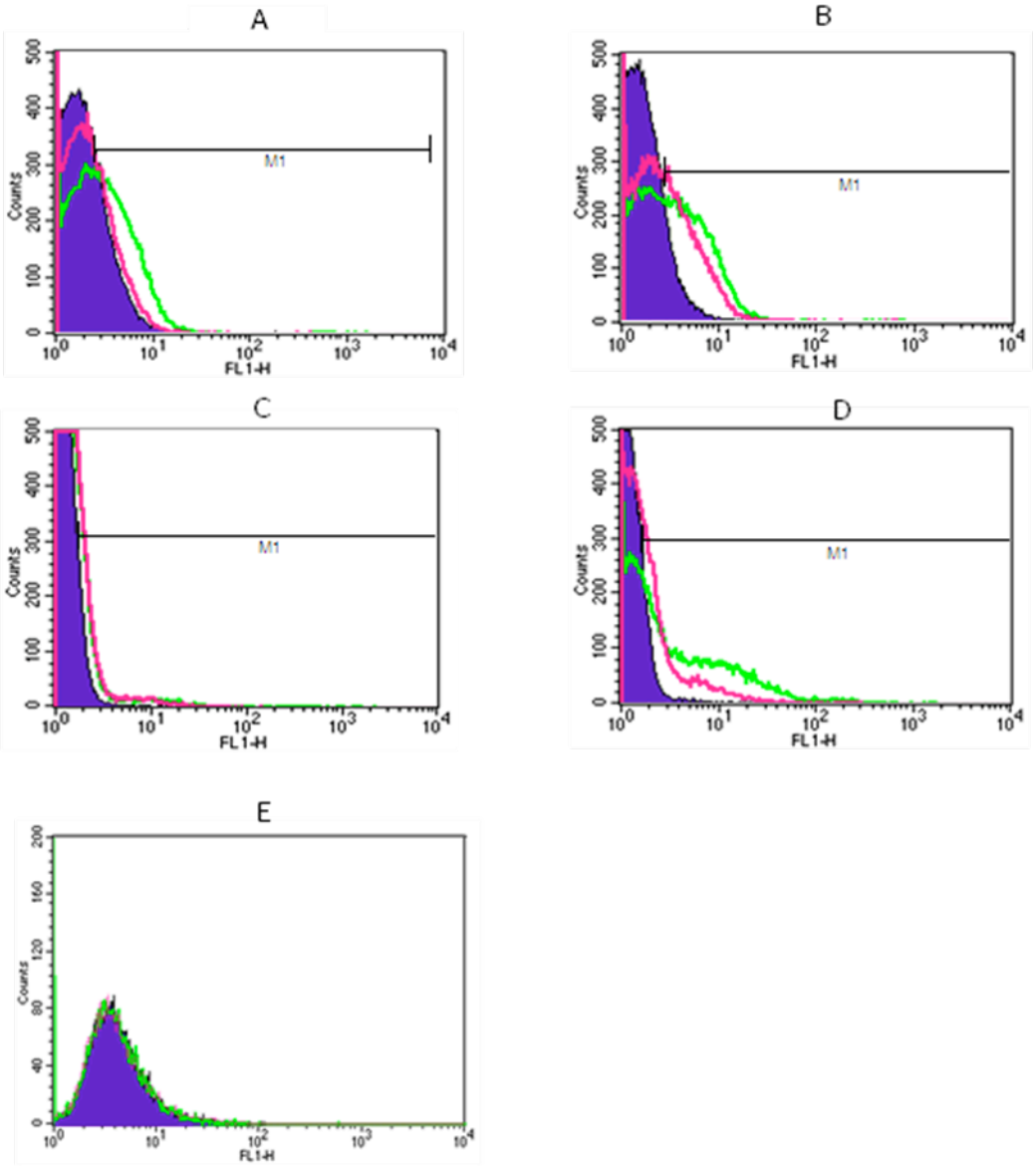

Fig 3.10b: Flow cytometry profiles for assessment of FITC-labelled peptide binding to *S. aureus*, *S. epidermidis*, *E. coli*, *P. aeruginosa* and a keratinocyte cell line (Panels A-E respectively). Cell populations for analysis were determined based on FSC/SSC as previously described in Figure 3.10a. Binding of cyclic peptide12 (green) and linear peptide12 (pink) was characterised in comparison to an unlabelled cell population (purple filed line). Flow cytometry analysis was based on counting 100,000 events for bacterial populations and 10,000 events for keratinocytes. Note that the keratinocyte profile (Panel E) has been drawn so that the cell count has been adjusted to 200.

Fig 4.1: Typical agarose gel depicting individual thioredoxin inserts following DNA amplification

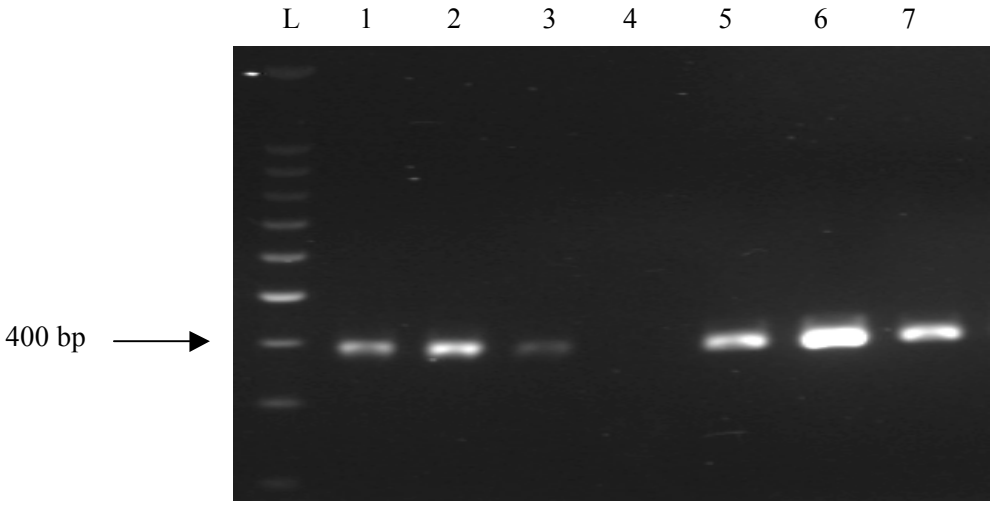

Fig 4.1: Gel electrophoresis was performed to visualise amplified DNA following PCR using primers designed to amplify the thioredoxin moiety containing peptide sequences 5, 12 and 19 (lanes 1-3 respectively) or with an additional 15 lysine residue linker (lanes 5-7 respectively). PCR was performed using ThioFor or ThioLysineFor primers and ThioRev primers. PCR products (3 µl) were visualised on a 2% (w/v) gel. Thioredoxin containing the peptides of interest produce an expected DNA fragment of 390 bp (lanes 1-3) whereas those with the additional lysine linker are expected to be 435 bp (lanes 5-7). A 100 bp ladder was used to determine the size of the bands observed (lane L). Lane 4 is the negative control containing no template DNA and therefore indicates there was no contamination of reagents.

Fig 4.2: Amplification of natural *E. coli* thioredoxin

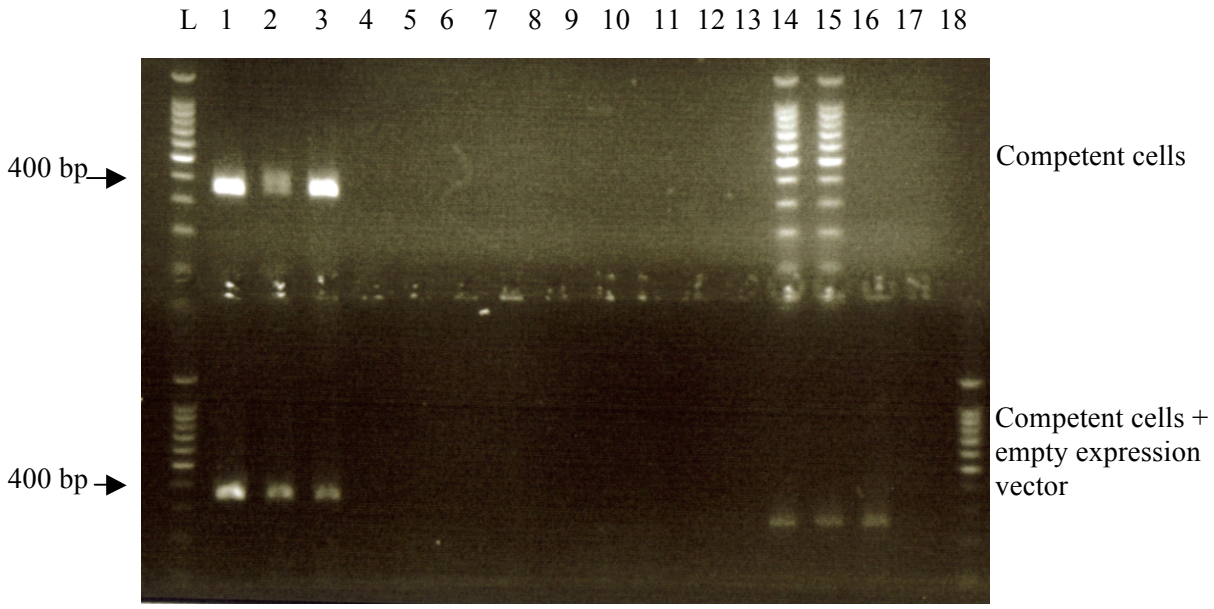

Fig 4.2: Gel electrophoresis to visualise amplified DNA following colony PCR of competent cells alone (top row) and competent cells transformed with an empty pPROTet expression vector (bottom row). PCR products (5 µl) were visualised on a 2% (w/v) gel.

Lane order (top):	Expected product
L, 14, 15 = 100 bp ladder	
1-3 = PCR product (ThioFor and ThioRev primers)	354 bp
5-7 = PCR product (pPROTetFor and ThioRev primers)	none
9-11 = PCR product (pPROTetFor and pPROTetRev primers)	none
4, 8, 12 = negative controls	none
13, 16-18 = empty lanes	none

Lane order (bottom):	Expected product
L, 18 = 100 bp ladder	
1-3 = PCR product (ThioFor and ThioRev primers)	354 bp
5-7 = PCR product (ThioLysineFor and pPROTetRev primers)	none
9-11 = PCR product (pPROTetFor and ThioRev primers)	none
14-16 = PCR product (pPROTetFor and pPROTetRev primers)	267 bp
4, 8, 12, 17 = negative controls	none
13 = empty lanes	none

Fig 4.3: Induction of competent cells only and competent cells transformed with an empty expression vector

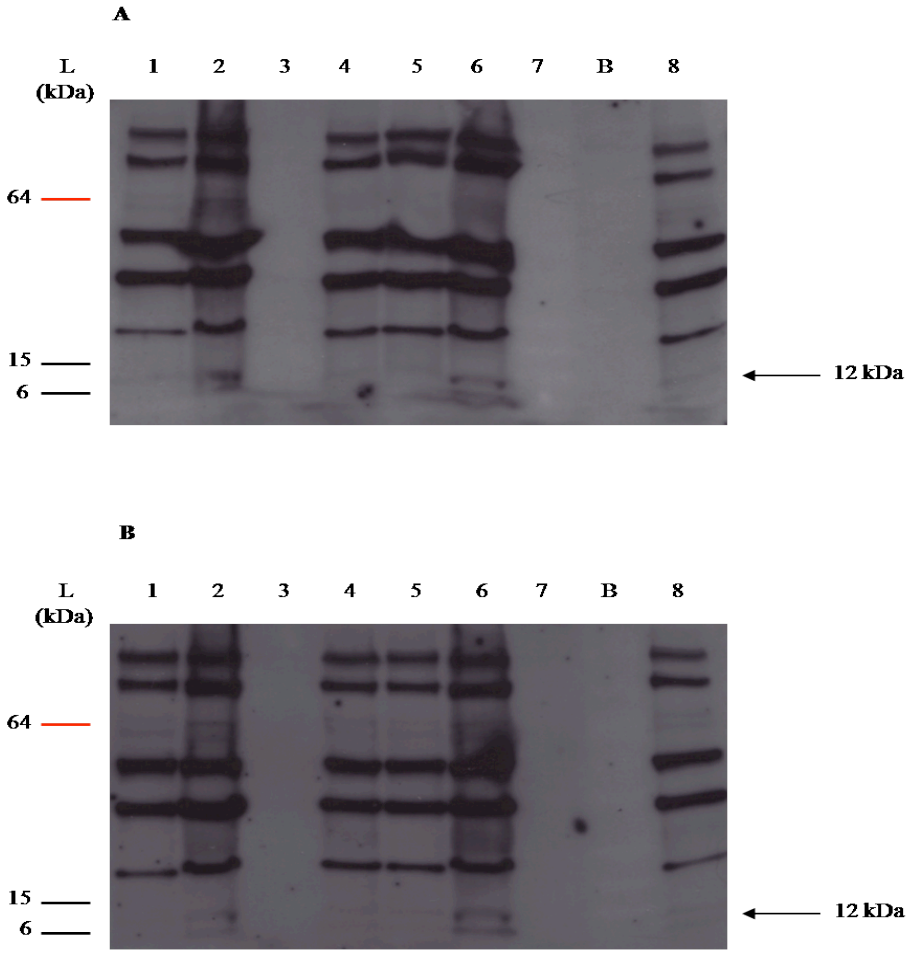

Fig 4.3: Competent cells only (Panel A) and competent cells transformed with an empty expression vector (Panel B) were analysed by Western blotting probing for thioredoxin (1:1000 dilution) to ascertain the size of natural *E. coli* thioredoxin. Bacteria were grown to an optical density of OD_{500} = 0.5 (lane 1) and amplified for a further 2 hr (lane 2). Following 2 hrs, cells were normalised to the same optical density as starting values (lane 4). Bacterial aliquots (1 ml) were lysed and an aliquot (12 µl) loaded onto a 4-20% (w/v) gradient gel. Additionally, following centrifugation to pellet the bacteria, the supernatant (30 µl) was also analysed for the presence of thioredoxin (lanes 3, 7). Bacterial cultures were also induced by the addition of 0.1 ng/ml aTc for 2 hr (lane 6) and compared to initial starting concentrations (lane 5) and also to normalised values (lane 8). Similar to non-induced samples, bacteria (1 ml) were lysed and 12 µl loaded onto a gradient gel. Lane B is blank. Faint bands were observed corresponding to natural *E. coli* thioredoxin (predicted molecular weight = ~12 kDa) in lanes 2 and 6 (Panels A and B) following incubation for 2 hr both with and without the addition of aTc that were not observed preinduction or following 2 hr incubation following normalisation to starting concentrations.

Fig 4.4: Typical representative agarose gel to visualise ligation reactions

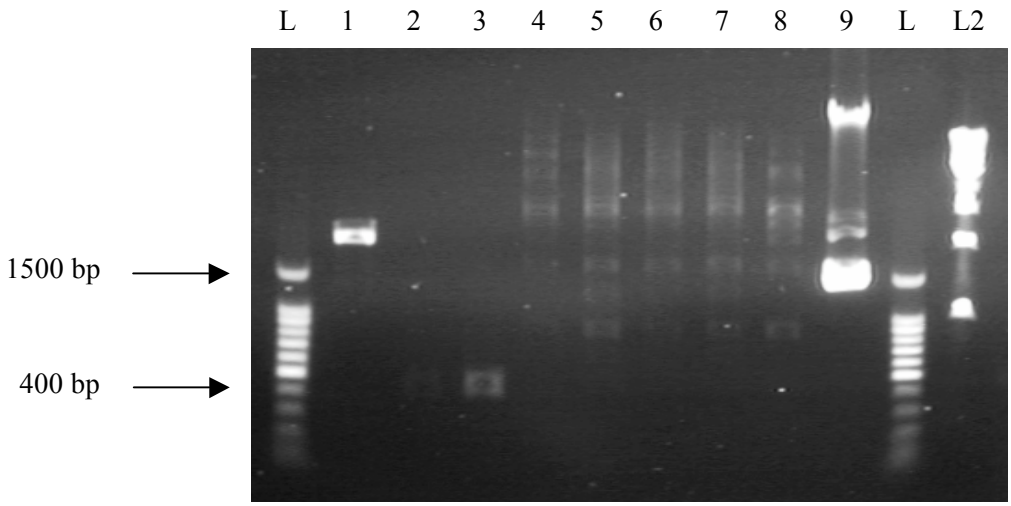

Fig 4.4: Ligated vector (1 µl) visualised by gel electrophoresis prior to transformation using a 0.7% (w/v) gel. Thioredoxin 5, 11 12, 14 and 19/pPROTet ligated vectors (lanes 4-8 respectively) were visualised and compared against an aliquot (1 µl) of *Bam*HI and *Sal*I digested pPROTet vector (lane 1; 2.15 kb). PCR products (3 µl) of amplified thioredoxin DNA containing peptides 5 and 12 respectively (ThioLysineFor and ThioRev primers) were visualised in lanes 2 and 3 respectively (435 bp) for comparison. The uncut pPROTet vector (0.5 µl) is shown in lane 9. A 100 bp ladder (lane L) and 1 kb ladder (L2) were used to determine the size of the bands.

Fig 4.5: A typical agarose gel electrophoresis image following colony PCR

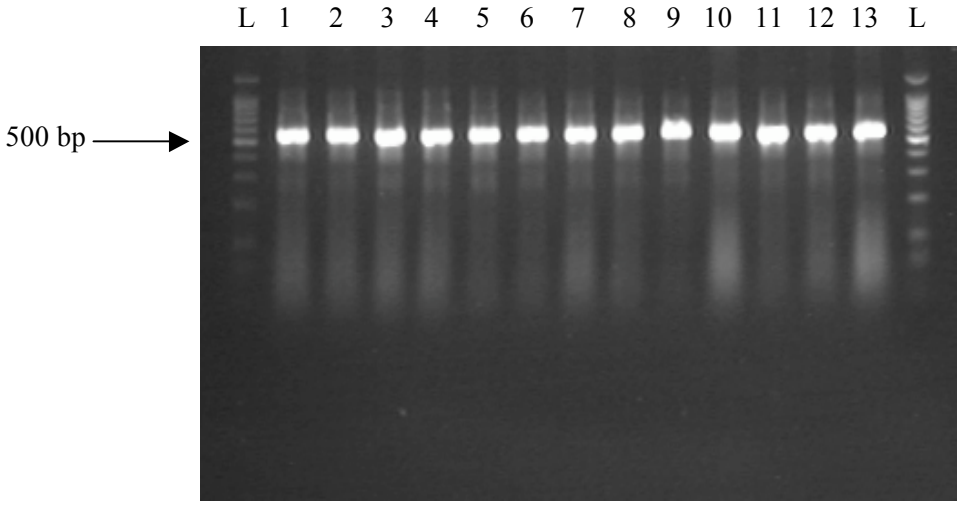

Fig 4.5: Amplification of DNA by colony PCR following successful transformation, using pPROTetFor and ThioRev primers. DNA from randomly selected colonies following transformation containing the thioredoxin 5, 12 and 19/pPROTet ligated vectors was amplified and PCR products (5 µl) were visualised by agarose gel electrophoresis (lanes 1-4 = thioredoxin 5/pPROTet, 5-8 = thioredoxin 12/pPROTet and 9-13 = thioredoxin 19/pPROTet respectively) on a 2% (w/v) gel. The expected size of PCR products was 549 bp. A 100 bp ladder (lane L) was used to determine the size of the observed bands.

Fig 4.6: Typical confocal microscopy image to confirm successful cloning of GFP/pPROTet into *E. coli*

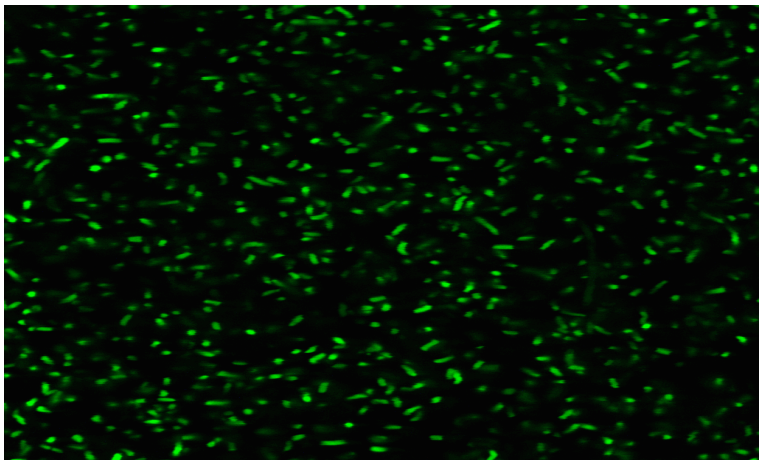

Fig 4.6: Transformants were selected and analysed using a confocal microscope, equipped with a x60 magnification objective to confirm successful transformation of GFP/pPROTet.

Fig 4.7: PCR analysis of thioredoxin and GFP inserts following transformation

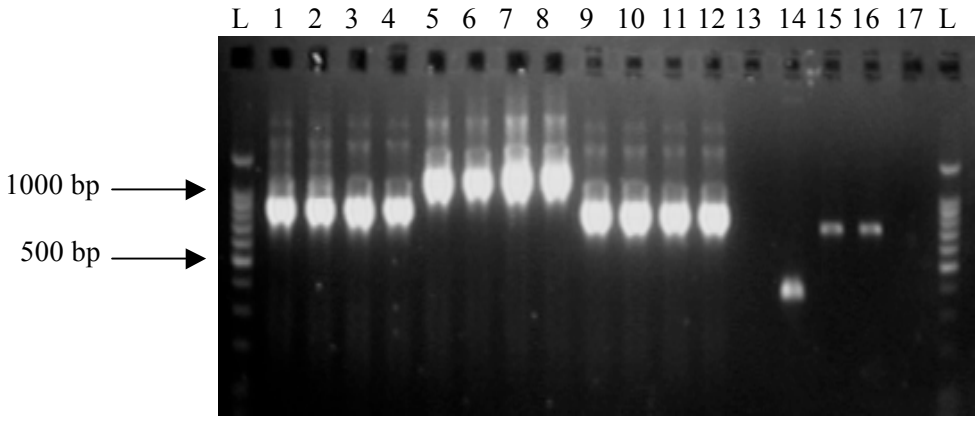

Fig 4.7: Amplification of DNA from plasmid preparations following transformation of thioredoxin 5/GFP/pPROTet ligated vector. Plasmid DNA was extracted from transformants from both green and white colonies. Plasmid DNA was amplified using the pPROTetFor and either GFPRev(WS or NS) primer or pPROTet reverse primers to determine the presence of GFP and thioredoxin. PCR products (5 µl) were analysed in duplicate by agarose gel electrophoresis to visualise the product on a 2% (w/v) gel. Note lane 13 appears blank whereby the digested and cleaned PCR products were not of sufficient concentration to be visualised.

Lane order:

L = 100 bp ladder

1-4 = Green colonies containing thioredoxin 5/GFP (no stop) expression vector (pPROTetFor and GFPRev(NS) primers) (expected product = 876 bp)

5, 6 = White colonies containing thioredoxin 5/GFP (no stop) expression vector (pPROTetFor and GFPRev(NS) primers) (expected product = 1236 bp)

7, 8 = White colonies containing thioredoxin 5/GFP (no stop) expression vector (pPROTetFor and pPROTetRev primers) (expected product = 1335 bp)

9-12 = Green colonies containing thioredoxin 5/GFP (with stop) expression vector (pPROTetFor and GFPRev(WS) primers) (expected product = 876 bp)

13,14 = Thioredoxin containing peptide3 following digestion and clean up and peptide5 prior to digestion and purification respectively (ThioFor and ThioRev primers) (expected product = 390 bp)

15 = GFP (with stop) PCR product (GFPFor and GFPRev(WS) primers) (expected product = 744 bp)

16 = GFP (no stop) PCR product (GFPFor and GFPRev(NS) primers) (expected product = 744 bp)

17 = negative control

Fig 4.8: Colony PCR of thioredoxin 5/GFP (no stop) expression vector (white colony)

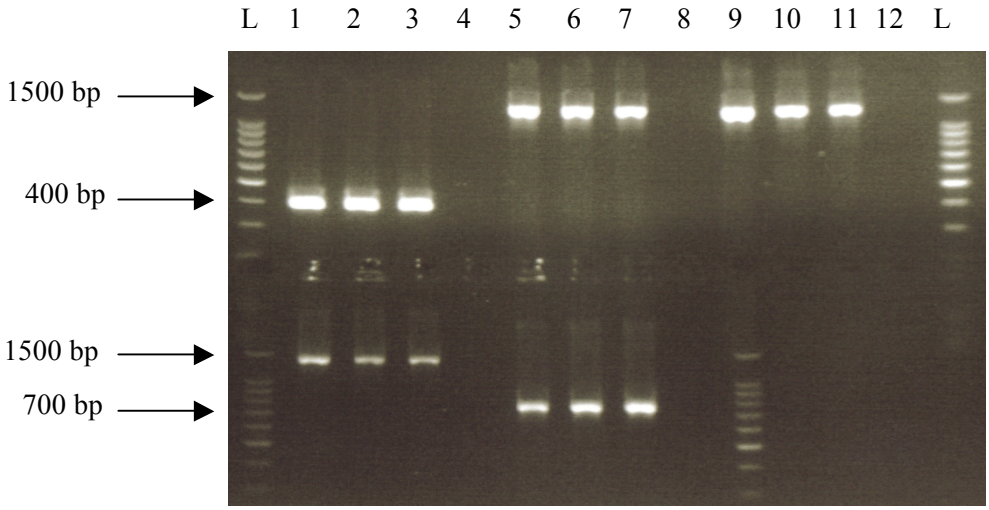

Fig 4.8: Agarose gel electrophoresis to visualise PCR products (5 µl) amplified by colony PCR from positive transformants using different primer combinations. PCR products were visualised on a 2% (w/v) gel. Colony PCR was performed on three different colonies randomly selected following transformation.

Lane order (top):	Expected product
L = 100 bp ladder	
1-3 = PCR product (ThioFor and ThioRev primers)	390 bp
5-7 = PCR product (pPROTetFor and GFPRev(NS) primers)	1236 bp
9-11 = PCR product (ThioFor and pPROTetRev primers)	1209 bp
4, 8, 12 = negative control	

Lane order (bottom):	Expected product
L = 100 bp ladder	
1-3 = PCR product (pPROTetFor and pPROTetRev primers)	1335 bp
5-7 = PCR product (GFPFor and GFPRev(NS) primers)	744 bp
4, 8 = negative control	

Fig 4.9: Typical representative gel stained with Coomassie reagent to determine optimal protein induction

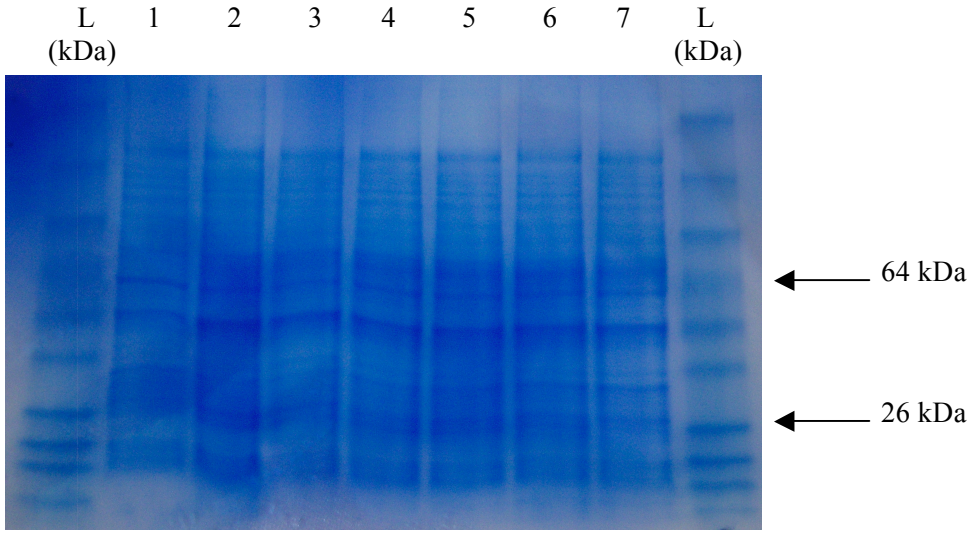

Fig 4.9: Coomassie stained gel to determine optimal expression of recombinant protein. Bacteria were induced with 0.1 ng/ml aTc when an OD_{500} of 0.5 was reached and amplified for 0, 2, 4, 6, 7 and 24 hours respectively (lanes 1-6). Following induction, bacterial cultures were normalised so that the final absorbance was the same as pre-induction absorbance values to give the same concentration of bacteria. An aliquot (1 ml) of each bacterial culture was lysed in SDS-sample buffer and loaded onto a 4-20% (w/v) precast gradient gel. Lane 7 demonstrates bacteria after 24 hours following no induction, that was normalised to pre-induction absorbance values. Protein size was determined against prestained protein ladders (15 µl; lane L).

Fig 4.10: Typical representative Western blot to determine optimal expression conditions

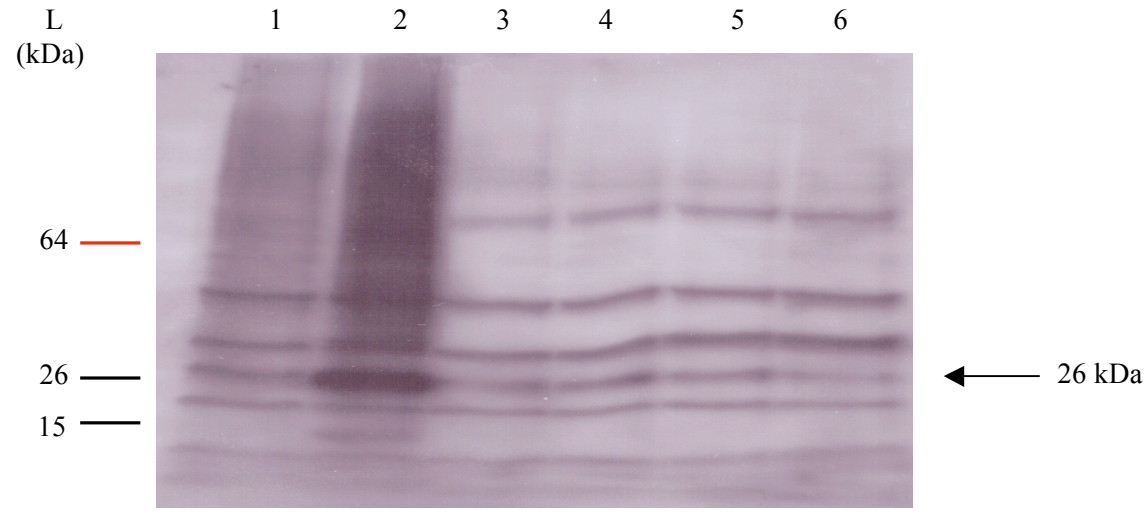

Fig 4.10: The optimal expression of recombinant thioredoxin protein 19 was analysed by Western blotting probing for thioredoxin using the same samples that had previously been stained with Coomassie reagent. Bacteria were amplified and induced with aTc when an OD_{500} of 0.5 was reached, and then incubated for 0-24 h to determine the optimum incubation time. Following induction, the absorbance of bacterial cultures were normalised to preinduction values, i.e. the same concentration of bacteria/ml were lysed. Bacterial cultures (1 ml) were lysed in SDS-sample buffer and aliquots (12 µl) loaded onto 4-20% (w/v) precast gels. Following transfer the membrane was incubated with an anti-thioredoxin antibody (1:1000 dilution). Lanes 1-6 indicate bacterial samples that were incubated for 0, 2, 4, 6, 7 and 24 hr respectively following normalisation to preinduction concentrations. Recombinant thioredoxin produced an observed band at approximately 26 kDa. A prestained protein ladder (15 µl) was used to determine the size of the proteins (lane L). Representative of 2 repeats.

Fig 4.11: Reprobe of Western blot to confirm the presence of the protein of interest

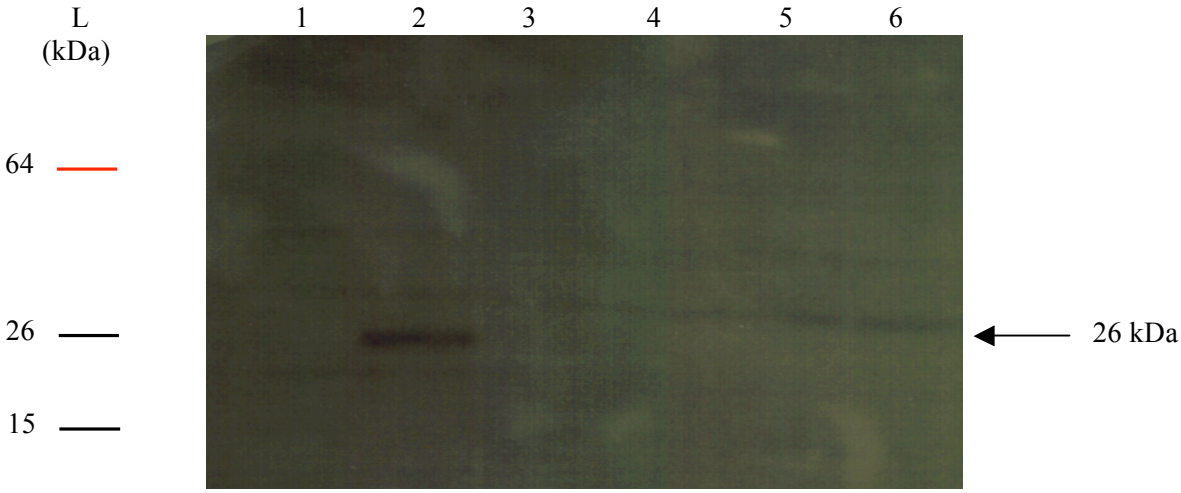

Fig 4.11: Following the Western blot confirming the presence of thioredoxin the same nitrocellulose membrane was stripped and reprobed for the 6xHN tag to confirm that the protein of interest had been induced and that the protein was of the correct size. Protein size was determined against a prestained protein ladder (Lane L). Bacterial cultures were induced for 0, 2, 4, 6, 7 and 24 hours (lanes 1-6 respectively). The membrane was incubated with an anti-6xHN tag antibody (1:1000 dilution). A single band was observed at 26 kDa following 2 h induction (lane 2); this was not observed in any other lane. Representative of 2 repeats.

Fig 4.12: Western blot analysis of extracted and purified proteins

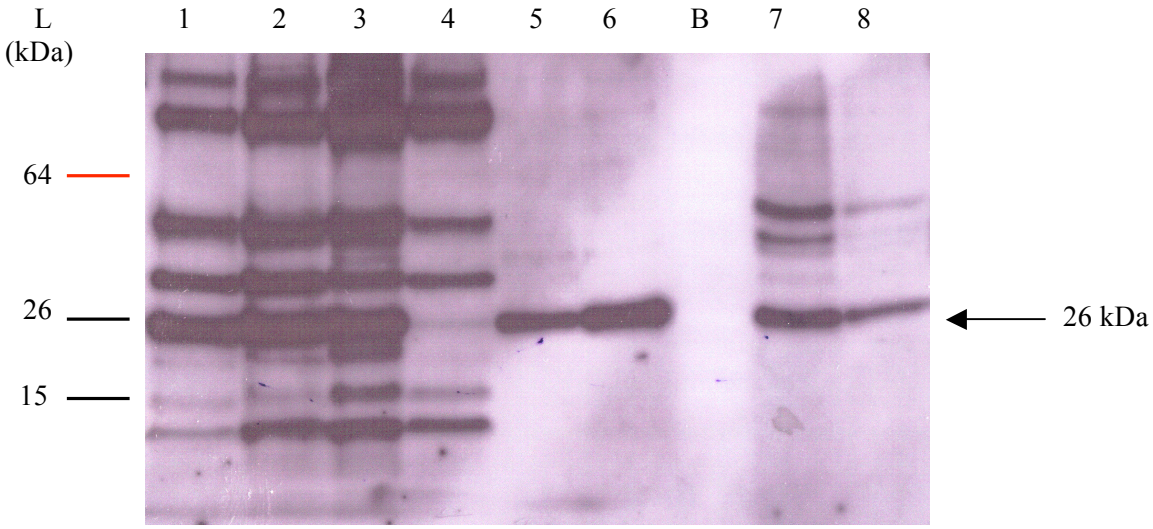

Fig 4.12: The extraction and purification process was analysed by Western blotting. Samples were separated on a 4-20% (w/v) precast gradient gel and following transfer were probed for thioredoxin (1:1000 dilution). Bacteria were induced by addition of 0.1 ng/ml aTc for 2 hr (lane 2) and compared to pre-induction (lane 1). Pre and post induction bacterial aliquots (1 ml) were lysed in SDS-sample buffer and 12 µl were applied to the gel. Lane 3 (12 µl loaded) is the clarified sample following extraction by lysis and centrifugation to pellet unwanted debris. Lane 4 represents protein that did not bind to the column (12 µl). Eluted protein is shown in lane 5, concentrated eluted protein in lane 6 and following buffer exchange in lanes 7 and 8 (all 30 µl loaded), observed as bands of approximately 26 kDa. The sizes of proteins were compared to a prestained protein ladder (L). Representative of 2 repeats. Lane B is blank.

Fig 4.13: Reprobe of Western blot to determine the presence of thioredoxin with 6xHN tagged protein

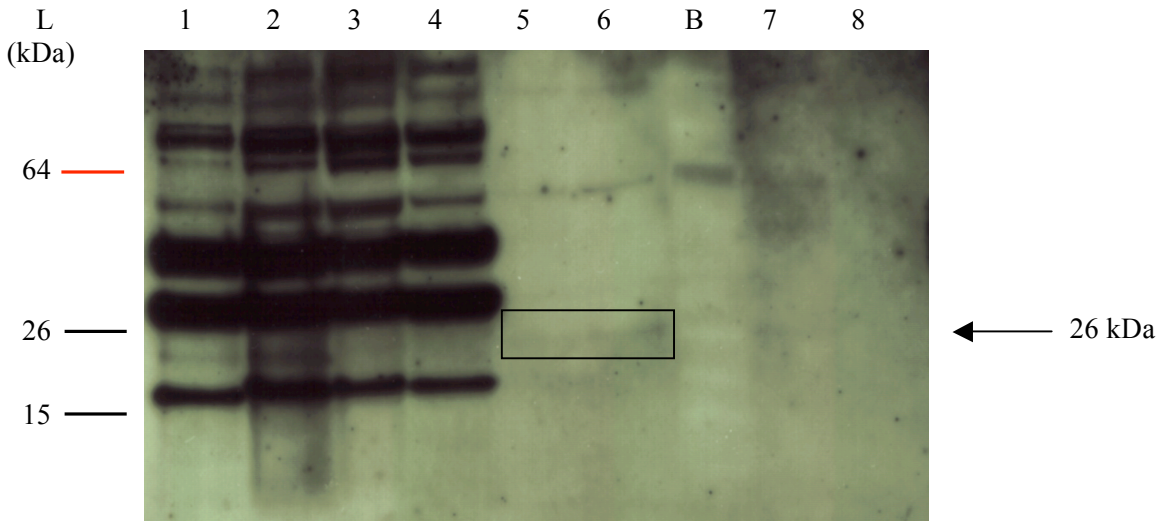

Fig 4.13: Following probing for thioredoxin, the membrane was stripped and reprobed for the 6xHN tag (1:1000 dilution) to confirm purification of the protein of interest. Bacteria were induced by addition of 0.1 ng/ml aTc for 2 hr (lane 2) and compared to pre-induction (lane 1). Lane 3 is the clarified sample following extraction by lysis. Lane 4 represents protein that did not bind to the column. Eluted protein is shown in lane 5, concentrated eluted proteins in lane 6 and following buffer exchange in lanes 7 and 8 observed as very faint bands at approximately 26 kDa. The sizes of proteins were compared to a prestained protein ladder (L). Lane B is blank. Representative of 2 repeats.

Fig 4.14: Coomassie staining of thioredoxin/GFP proteins

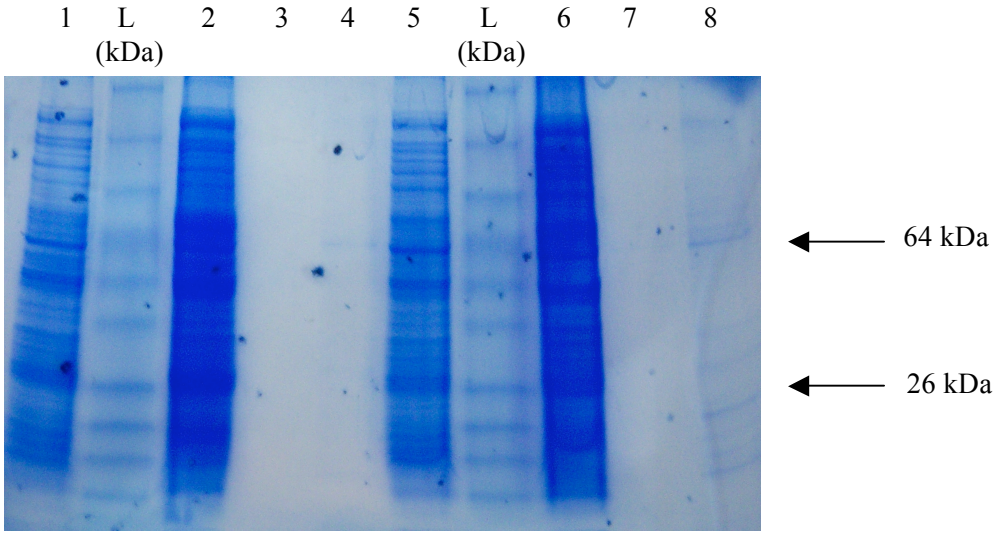

Fig 4.14: Protein expression of P5/GFP and P5 was analysed by staining with Coomassie reagent following separation using a 4-20% (w/v) precast gradient gel in order to visualise protein bands. Protein production was induced by addition of 0.1 ng/ml aTc for 2 h and analysed by lysing a bacterial aliquot (1 ml) in SDS-sample buffer and loading 12 µl onto a precast gel. Protein expression was analysed before and after induction for P5/GFP (lanes 1+2 respectively) and additionally for P5 (lanes 5+6 respectively). P5/GFP was concentrated (lane 3; 30 µl loaded) and buffer exchanged (lane 4; 30 µl loaded) and compared to P5 (lanes 7+8 respectively; 30 µl loaded). Protein size was determined against a prestained protein ladder (lane L; 15 µl).

Fig 4.15: Western blot analysis of thioredoxin/GFP proteins

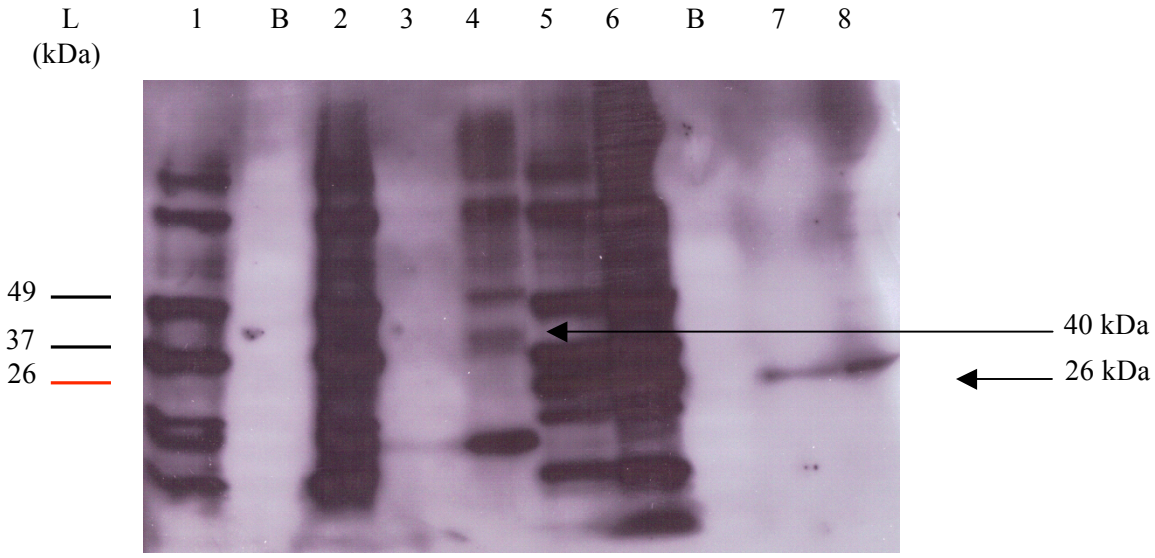

Fig 4.15: Protein expression of P5/GFP and P5 were analysed by Western blot probing for thioredoxin (1:1000 dilution) following separation on a 4-20% (w/v) precast gradient gel. Bacteria were induced for 2 hr with 0.1 ng/ml aTc when an OD_{500} of 0.5 was reached. Protein expression was analysed before and after induction for P5/GFP (lanes 1+2 respectively) and additionally for P5 (lanes 5+6 respectively). Pre and post induction samples were analysed by loading 12 µl isolated from an aliquot of each bacterial culture (1 ml). P5/GFP was concentrated (lane 3; 30 µl loaded) and buffer exchanged (lane 4; 30 µl loaded) and compared to P5 (lanes 7+8 respectively; 30 µl loaded). Lane B is blank.

Fig 5.1: Determination of the cytotoxic effect of the conjugated protein and capped porphyrin on MRSA with and without irradiation

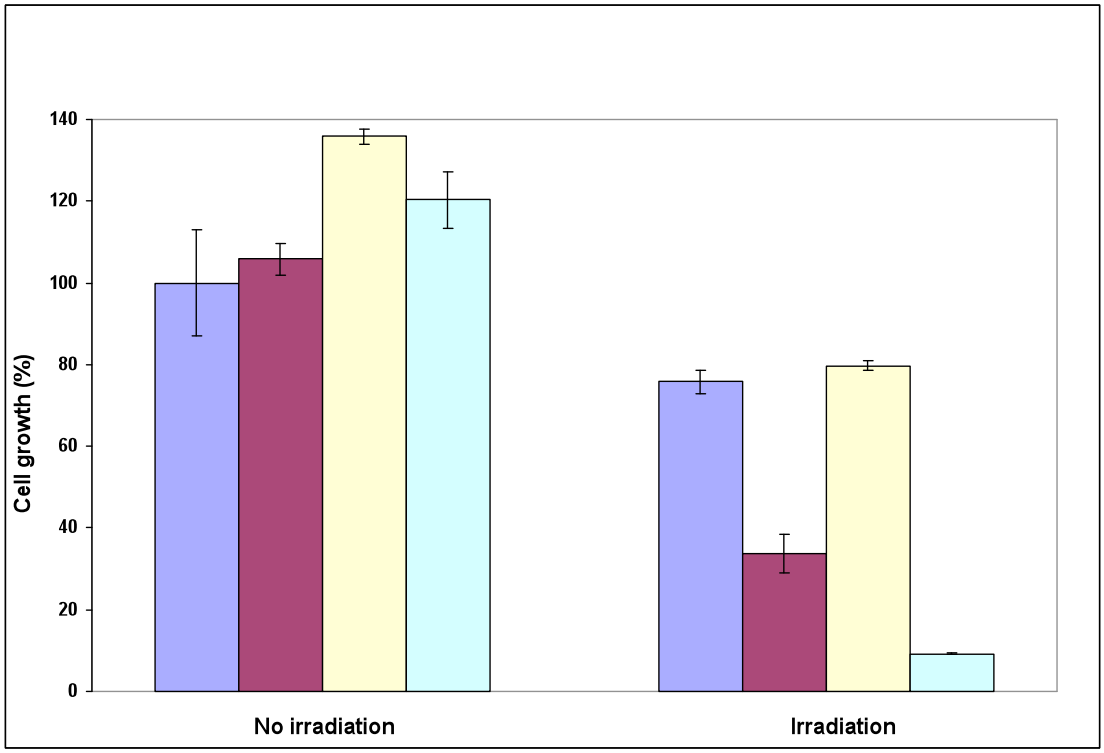

Fig 5.1: The cytotoxic effect of the conjugated protein and capped photosensitiser against MRSA was determined following irradiation with red light and non-irradiated bacteria as a dark control. Following overnight growth the absorbance was measured at 630 nm and bacterial survival calculated as percentage viability in comparison to the untreated, non-irradiated culture. Untreated bacteria are represented by the blue bars following irradiation and no irradiation. The purple bars indicate bacteria incubated with the P12 conjugate and the yellow bars indicate MRSA incubated with the same concentration of capped porphyrin as the P12 conjugate (1.25 μM - low concentration). The green bars represent bacteria incubated with a 10-fold excess of capped photosensitiser (12.5 μM - high concentration). The error bars represent the standard deviation from 3 repeat wells.

Fig 5.2: Determination of the cytotoxic effect of the P12 conjugate and capped porphyrin on *E. coli* following irradiation and no irradiation

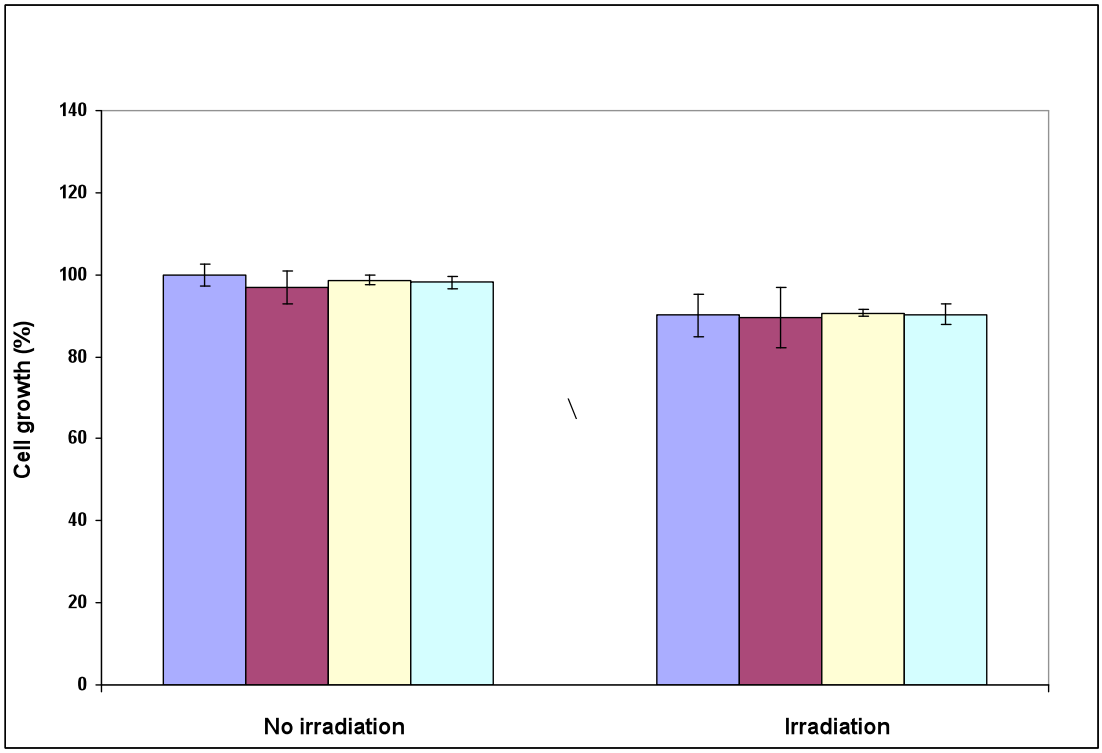

Fig 5.2: The P12 conjugate and capped photosensitisers were assessed for cytotoxic activity against *E. coli* following irradiation with red light and no irradiation as a control. Untreated control cells are represented by the blue bars and used to compare bacterial viability following incubation with the P12 conjugate (purple bars), low porphyrin concentration (1.25 μM - yellow bars) and high porphyrin concentration (12.5 μM - green bars). Following overnight incubation, absorbance was measured at 630 nm and used to calculate the percentage viability of bacteria. The error bars represent the standard deviation from 3 repeat wells.

Fig 5.3: Determination of the cytotoxic effect of the P12 conjugate and capped porphyrin on keratinocytes with and without irradiation

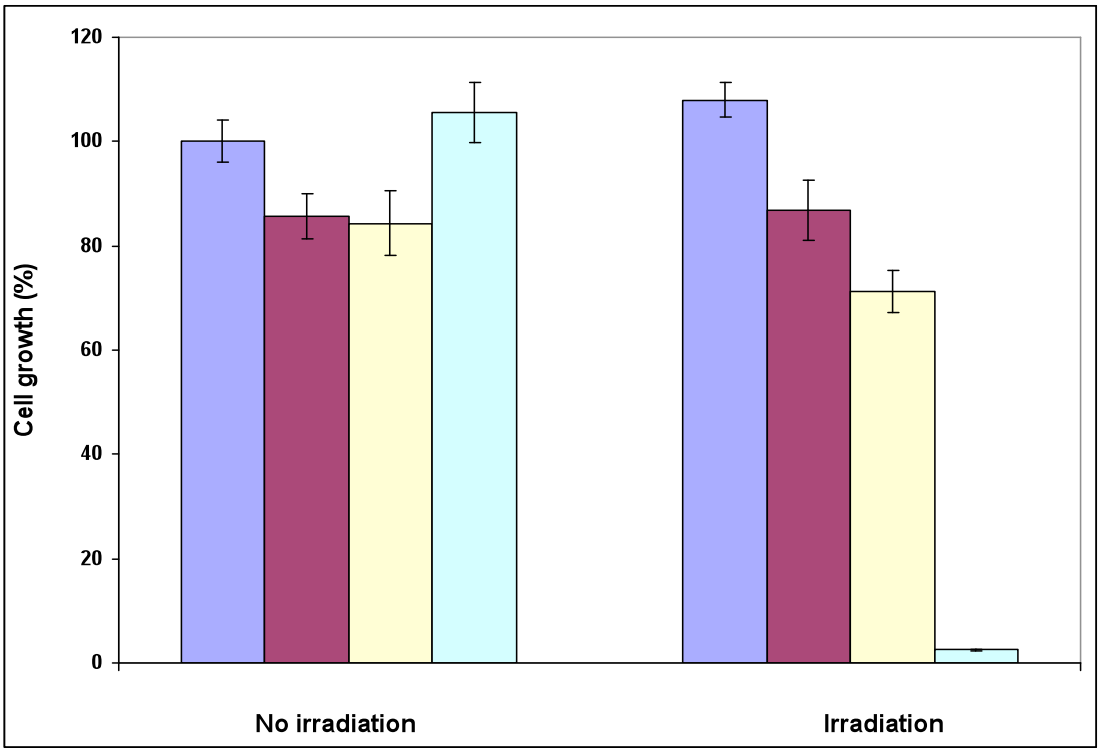

Fig 5.3: Conjugated protein P12 and capped photosensitiser were assessed for cytotoxic potential against a keratinocyte cell line. Cell growth was measured by MTT assay and compared to untreated control cells. Untreated keratinocytes are represented as blue bars. The purple bars indicate keratinocytes incubated with the P12 conjugate whereas the yellow and green bars indicate keratinocyte incubation with a low (1.25 μM) and high (12.5 μM) concentration of capped photosensitiser respectively. The error bars represent the standard deviation from 3 repeat wells.

Fig 5.4: Flow cytometric analysis to determine binding of detection antibodies to MRSA

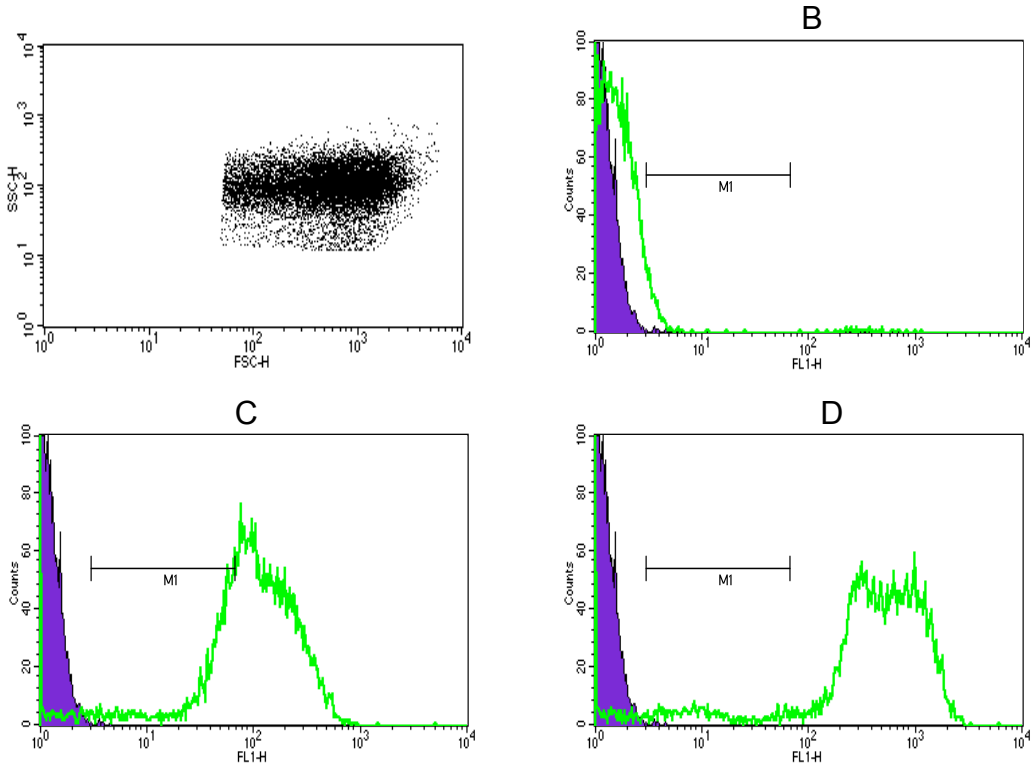

Fig 5.4: Flow cytometry profiles of control experiments to determine non-specific binding of detection antibodies to MRSA. Panel A represents FSC/SSC used to define bacterial populations for analysis. Panel B represents incubation with the anti-thioredoxin primary antibody alone. Panel C represents a bacterial population incubated with the secondary antibody only and Panel D represents binding of both the primary and secondary antibodies. The purple filled lines denote MRSA only used as a negative control. The green lines denote an increase in fluorescence following incubation with detection antibodies compared to the negative control.

Fig 5.4b: Flow cytometric analysis to determine P5 and P19 binding to MRSA

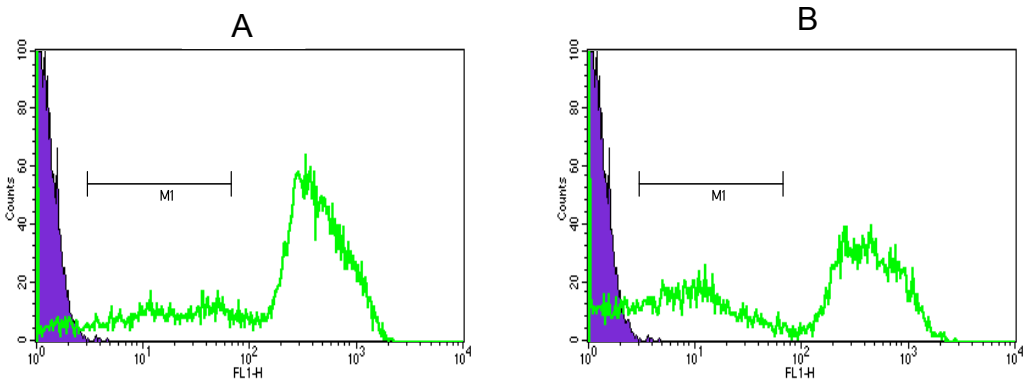

Fig 5.4b: Flow cytometry profiles assessing P5 and P19 binding to MRSA. Panels A and B represent profiles used to characterise binding of P5 and P19 respectively. Bacterial populations for analysis were determined based on FSC/SSC properties shown in Figure 5.4 (Panel A). The purple filled lines denote MRSA only as a negative control. The green lines denote an increase in fluorescence following protein binding compared to the negative control. The gated marker (M1) was used to identify recombinant protein binding to MRSA in comparison to bacteria dual labelled with both detection antibodies.

Fig 5.5: Analysis of binding specificity of detection antibodies against *E. coli*

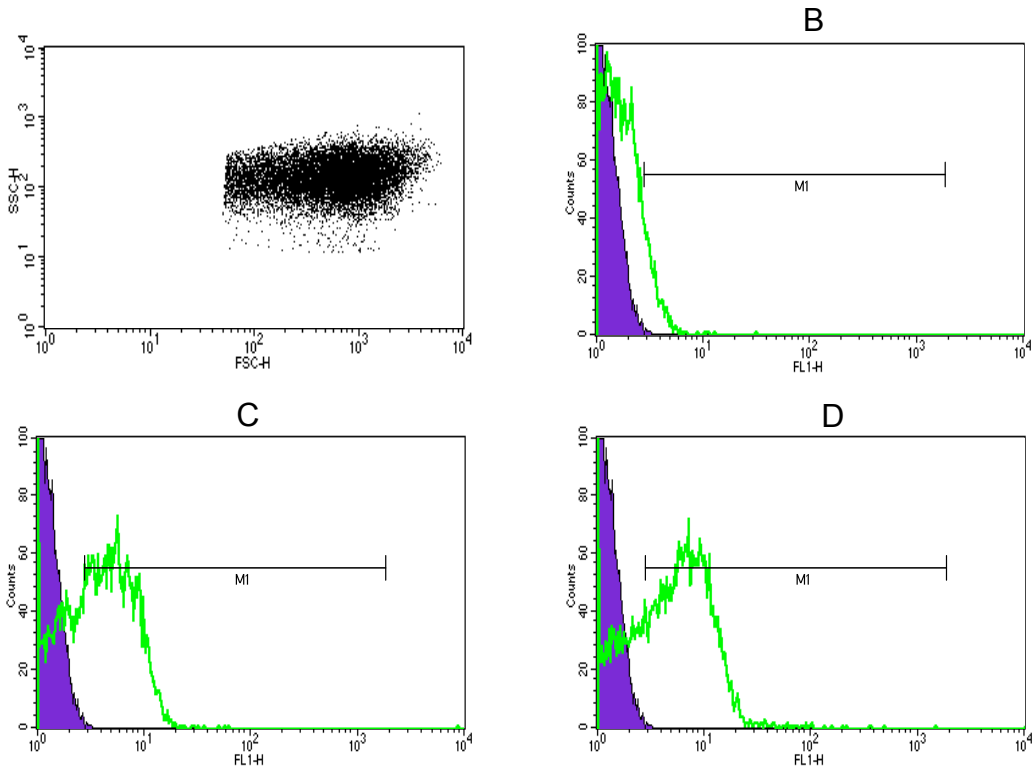

Fig 5.5: Flow cytometric analysis profiles of control experiments to assess detection antibody binding to *E. coli*. The bacterial population for analysis was determined by FSC/SSC as demonstrated in Panel A. Binding of the primary antibody alone (Panel B), secondary antibody only (Panel C) and primary and secondary antibodies (Panel D) is demonstrated by the green line denoting an increase in fluorescence in comparison to *E. coli* only as a negative control (filled purple line).

Fig 5.5b: Characterisation of binding specificity of P5 and P19 against *E. coli* by flow cytometry

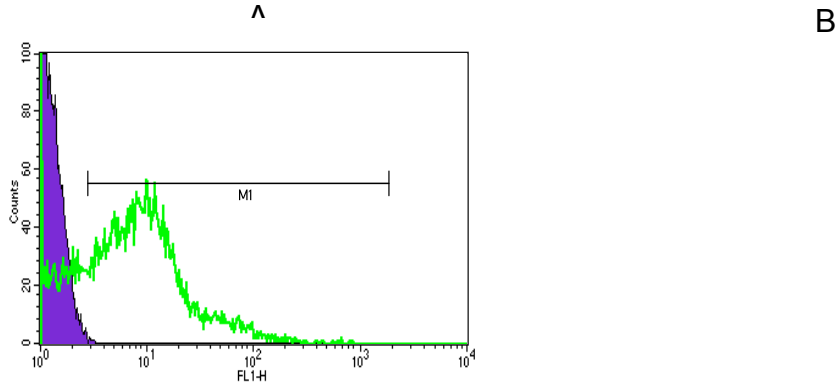

Fig 5.5b: Demonstration of P5 and P19 binding against *E. coli*. Panels A and B represent profiles used to characterise binding of P5 and P19 respectively. The bacterial population for analysis was determined based on FSC/SSC properties shown in Figure 5.5 (Panel A). The purple filled line denotes *E. coli* only used as a negative control whereas the green line denotes an increase in fluorescence compared to the negative control. The gated marker (M1) was used to identify recombinant protein binding to *E. coli*.

Fig 5.6: Assessment of detection antibody binding to keratinocytes by flow cytometry

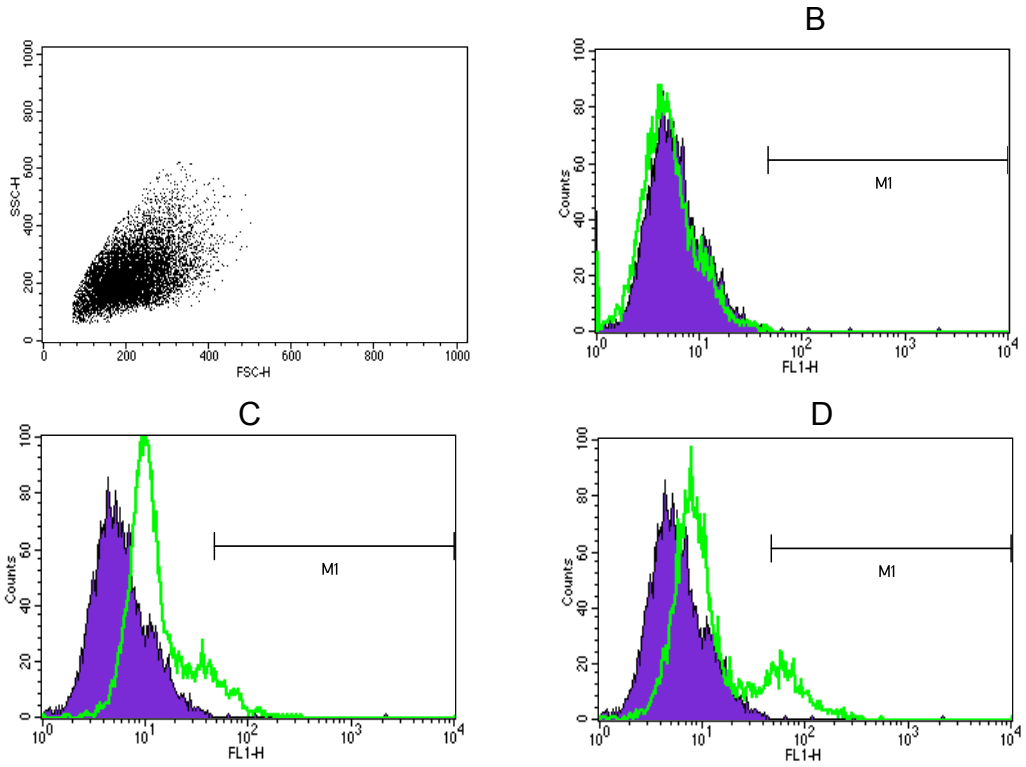

Fig 5.6: Flow cytometry profiles of control experiments to determine binding of detection antibodies to keratinocytes. Panel A represents FSC/SSC used to define the keratinocyte cell population for analysis. Panel B depicts keratinocyte incubation with the primary antibody alone whilst Panel C represents a cell population incubated with the secondary antibody only. Panel D represents the primary and secondary antibody incubated with cells. The purple filled line denotes keratinocytes only used a negative control whereas the green line denotes an increase in fluorescence following detection antibody binding compared to that of the negative control.

Fig 5.6b: Binding characterisation of P5 and P19 to keratinocytes

Fig 5.6b: FACS profiles assessing binding potential of P5 and P19 to keratinocytes. Keratinocyte populations for analysis were determined based on FSC/SSC properties shown in Figure 5.6 (Panel A). Panels A and B represent profiles used to characterise binding of P5 and P19 respectively. The purple filled line represents fluorescence of the untreated control cells. The green line demonstrates an increase in fluorescence compared to the negative control. The gated marker (M1) was used to identify recombinant protein binding to keratinocytes.

Fig 5.7: Characterisation of P5/GFP binding to MRSA, *E. coli* and keratinocytes by flow cytometry

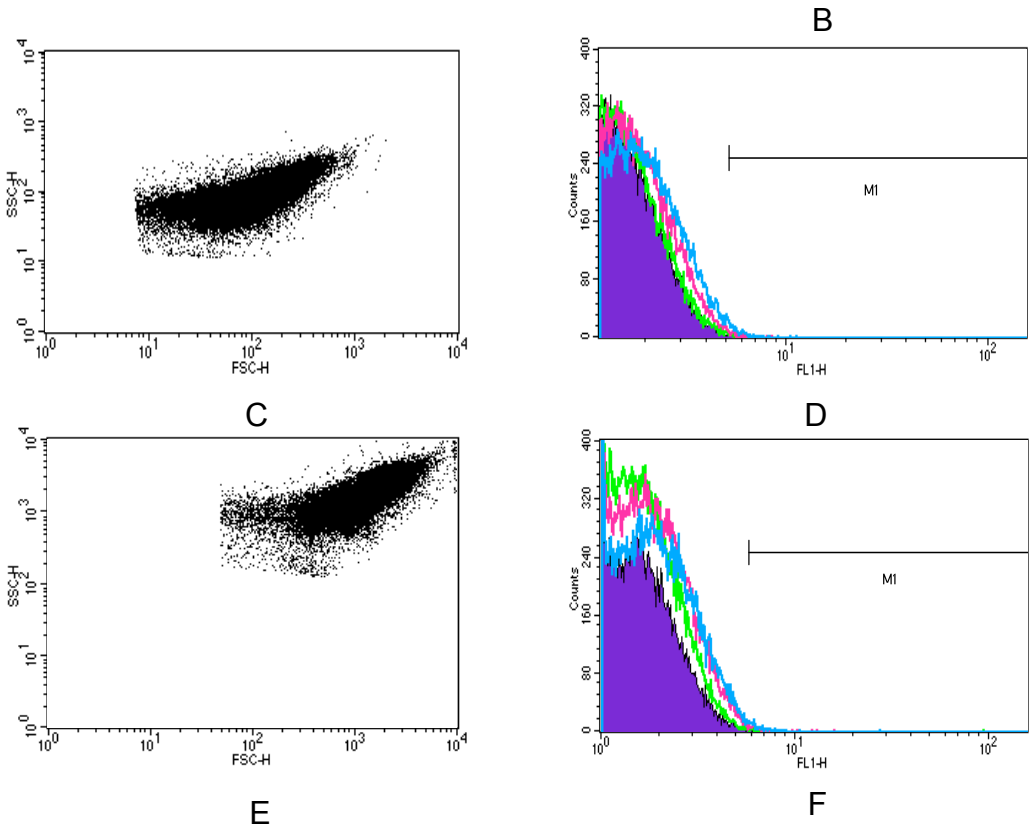

Fig 5.7: Binding of P5/GFP to MRSA, *E. coli* and keratinocytes was analysed by flow cytometry. Panels A, C and E represent FSC/SSC used to define the MRSA, *E. coli* and keratinocyte cell populations respectively for analysis. A range of concentrations of P5/GFP was incubated with MRSA, *E. coli* and keratinocytes separately and an increase in fluorescence characterising protein binding is demonstrated as the green (40 µg/ml), pink (200 µg/ml) and blue (398 µg/ml) lines respectively compared to control cells only (purple filled line).